AN EXPERIMENTAL INVESTIGATION OF THE EFFECT OF SUBDIVISION OF CONTACT AREA ON SURFACE TEMPERATURES GENERATED BY FRICTION

by

Craig Alan Rogers

Thesis submitted to the Faculty of the
Virginia Polytechnic Institute and State University
in partial fulfillment of the requirements for the degree of

MASTER OF SCIENCE

in

Mechanical Engineering

APPROVED:

M. J. Furey, Chairman

N. S. Eiss, Jr.

H. L. Wood

December, 1982

Blacksburg, Virginia

AN EXPERIMENTAL INVESTIGATION OF THE EFFECT OF SUBDIVISION OF THE CONTACT ON SURFACE TEMPERATURES GENERATED BY FRICTION

by

Craig Alan Rogers

(ABSTRACT)

An experimental investigation of surface temperatures generated by dry sliding friction was carried out with the use of an infrared radiometric microscope system that was developed at Virginia Polytechnic Institute and State University. The objective of this study was to investigate the effect of subdividing the apparent contact area on the surface temperature generated by friction.

Subdividing the geometric contact resulted in lowering the surface temperatures and followed the trend predicted by theory quite well. The study concluded that the surface temperatures predicted by the Archard and Jaeger theories correctly described the influence of nominal load and sliding velocity on the experimental surface temperatures.

A detailing description of the experimental apparatus, the radiation analysis used to convert the radiance output of the microscope to temperature, and the experimental procedure is included.

ACKNOWLEDGMENTS

I would like to express my sincere gratitude to those who have helped me with advice, constructive discussion and guidance. In particular, I thank Dr. Michael J. Furey, principal investigator and chairman of my graduate committee and the other members of my committee, Dr. N. S. Eiss, Jr. and Dr. H. L. Wood, for their suggestions and advice.

I am also grateful to the National Science Foundation for supporting this research.

I also acknowledge the tremendous assistance and cooperation of Steven C. Moyer on this project for his many useful comments, suggestions and assistance during the past year working together on this project.

A very special thanks is extended to my wife, Kathy, for her never ending love and support, and sacrifices which she chose to make. Together we dedicate this thesis to all our friends and family whose friendship and support have allowed us to reach this important goal in our lives.

TABLE OF CONTENTS

TABLE OF CONTENTS
(Continued)

LIST OF FIGURES

LIST OF FIGURES (Cont.)

LIST OF FIGURES (Cont.)

LIST OF FIGURES (Cont.)

LIST OF FIGURES (Cont.)

LIST OF FIGURES (Cont.)

LIST OF TABLES

1.0 INTRODUCTION

The study of surface temperatures caused by friction has been an area in which investigators have attempted to characterize a complex frictional process with relatively simple models and assumptions. The magnitude, duration, and distribution of such generated temperatures are extremely important as increasingly severe machine requirements have placed greater demands on materials and lubricants and also on the engineer's ability to utilize the total effectiveness of both material and lubricant. However, our knowledge of the heat generated by frictional processes and its characteristics is still lacking. It has become apparent that experimental methods to measure temperatures caused by friction in both lubricated and unlubricated systems must be advanced to present more physical data from which perhaps better and more rigorous theoretical work may be based.

There have been numerous theoretical and experimental studies of surface temperatures generated by friction in solid/solid contact. Yet, with all the studies, there are still several areas in which we have no data and basic questions still exist. It has been suggested that high temperatures may be the key to lubricant film failure. Heat generated by friction can also affect the physical and chemical behavior of the rubbing solids and/or any substance between these solids. There are two main theories concerning the cause of failure of nonreactive lubricants or nonconformal surfaces such as gears. One is that lubrication is successful only if the film thickness as predicted by elastohydrodynamic analysis is great enough to prevent metal-to-metal contact. Another

opinion, proposed by Blok [1,2], is the critical temperature hypothesis, which states that, for a given combination of material and nonreactive lubricant, failure occurs when a critical temperature in the contact zone is exceeded. This concept of a critical temperature for lubricant failure can also be seen in works of Al-Rubeye [3], Fein [4], Fohl and Vetz [5], Kelly [6], and Matveevskii [7].

The importance of surface temperatures is not only a factor in lubricant failure but may aid in our understanding of various wear mechanisms and other tribological phenomena. There are many tribological theories that use flash temperatures or heat generated at points of contact as working mechanisms, e.g., the oxidational wear mechanism proposed by Quinn [8], seizure models presented by Rozeanu [9], and the work on thermoeleastic transition and instability by Burton [10]. There is evidence that surface temperature is a key factor in the formation of certain effective antiwear films [13,14]. Examples of this [15] would include the thermal decomposition of the widely-used antiscuffing additive zinc dialkydithiophosphate [16]. Another concept proposed by Furey [17,18], using the key of temperatures, is the intentional "in situ" formation of thin, protective polymeric films on rubbing surfaces to reduce wear. According to this concept, the potential polymer forming compound is first dissolved, dispersed, or mixed at low concentrations in a carrier medium (e.g., a liquid hydrocarbon). Due to the conditions existing in the contact region, in particular the high surface temperatures generated by frictional contact and possibly the catalytic action of certain freshly-exposed surfaces, a very thin protective polymeric

film will form directly on and between the rubbing surfaces. Figure 1 [17] is a simplified representation of the basic concept.

In spite of all the experimental and theoretical studies that have been made of frictionally-generated surface temperatures, the topic is still far from being understood. The importance of this information is to aid our understanding of the mechanisms by which wear occurs and other tribological phenomena such as in materials processing and machining, surface grinding and polishing, frictional welding, the action of brakes, spark generation by friction, electrical contact behavior, drilling through hard materials, and other processes which simply involve sliding contact.

The experimental investigation that is presented here is a continuation of research at VPI&SU in which the overall objectives include: From a broad point of view, it was felt that there is a need to know more about the various ways in which energy can be delivered to the solid-solid contact regions. This of course involves the fundamental nature and causes of friction as an irreversible process. It was also felt that there is a need to know more about ways in which this energy can be distributed and absorbed in the contact zone, including not only conduction but also thermal effects associated with phase changes and chemical reactions. Past research has included carefully controlled designed experiments at various speeds and loads with several well-characterized solids sliding against sapphire. These have included a very pure and well-defined graphite commonly used as a base for electrical contact brushes as well as several polymers varying in

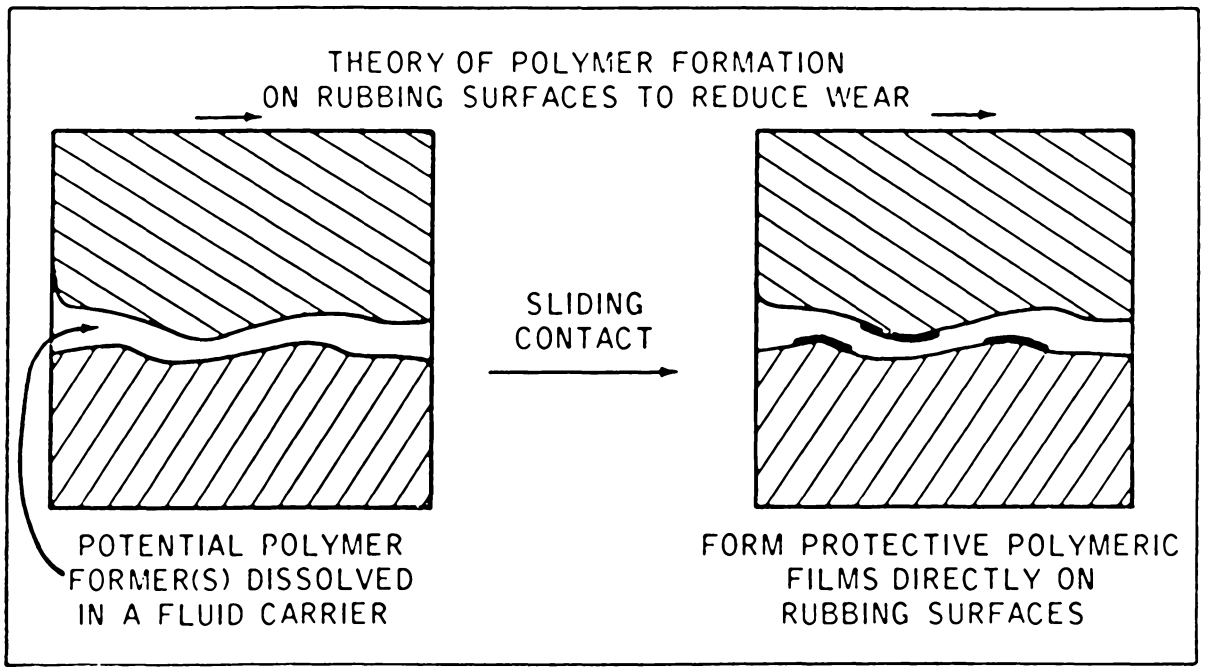

Figure 1. Simplified Diagram of the In-Situ Polymer-forming Concept [18]

structure and degree of crystallinity, e.g., polyethylene, polytetrafluoroethylene, polycaprolactam, polystyrene, and polymethylmethacrylate [16]. This study represents the first completed investigation with the use of a metal in contact with sapphire.

The following experimental results will be presented in an attempt to further our understanding of the factors and variables that are working as part of frictionally-generated surface temperatures. Not only does this thesis present general information, but it also presents data on a practical and important concept, that of the effect of subdivision of the apparent contact area on the temperatures produced. The specific goals of the present study were as follows:

1) To reliably measure surface tempertures of a metal (copper) in dry-sliding contact with sapphire through the use of an infrared radiometric microscope.
2) To experimentally determine the effect of subdivision of the contact area on surface temperatures generated by friction.
3) To experimentally determine the effect of load and sliding velocity on surface temperatures.
4) To compare the above results with the existing theories of Archard and Jaeger.
5) To modify the experimental apparatus to measure the radiance and friction data and store this data on magnetic tape.
6) To develop and implement a detailed infrared radiation analysis that will result in a more accurate and reliable method for interpreting the radiance data.

7) To develop more useful and general computer programs that will numerically and graphically show the effects of load, sliding velocity and subdivision of the contact area, independently, on surface temperatures. Both the Archard and Jaeger theories are to be incorporated.

2.0 LITERATURE REVIEW

2.1 Theoretical Review

The classical theoretical work on surface temperatures was developed by Blok [1] in 1937. Blok studied the problems of both stationary and moving sources of heat by assuming perfectly plane surfaces and that the bodies to which the heat is supplied have infinitely large heat capacity. Blok's theory was confined to the following approximate model of a band-shaped heat source with some distribution of heat flux, q, having an average denoted by q_{av}, and moving at a uniform speed v along a solid body bounded by a plane surface (Fig. 2) [39]. Blok then formulated an equation that approximates the maximum flash temperature, T_{max} when the speed, v, is relatively high.

$$\theta_{max} = A \frac{q_{av}}{b} \sqrt{w/v} \tag{1}$$

where w is the width of the heat source and v its velocity, b denotes the square root of the product of the specific heat, c', per unit volume and the thermal conductivity of the body, k. The quantity c' can be found from the expression $c' = \rho c$. Accordingly, $b = (kc')^{\frac{1}{2}} = (k\rho c)^{\frac{1}{2}}$. The factor A is a form factor which is a function of the heat flux distribution over the width of the heat source. For a uniform heat flux distribution, $q = q_{av}$ over the entire width, A is equal to $2/\sqrt{\pi} = 1.3$, and for a semielliptical distribution it is equal to 1.11.

In evaluating equation (1) to describe the case of meshing gear teeth or similar cases like cams and tappets, one must consider the

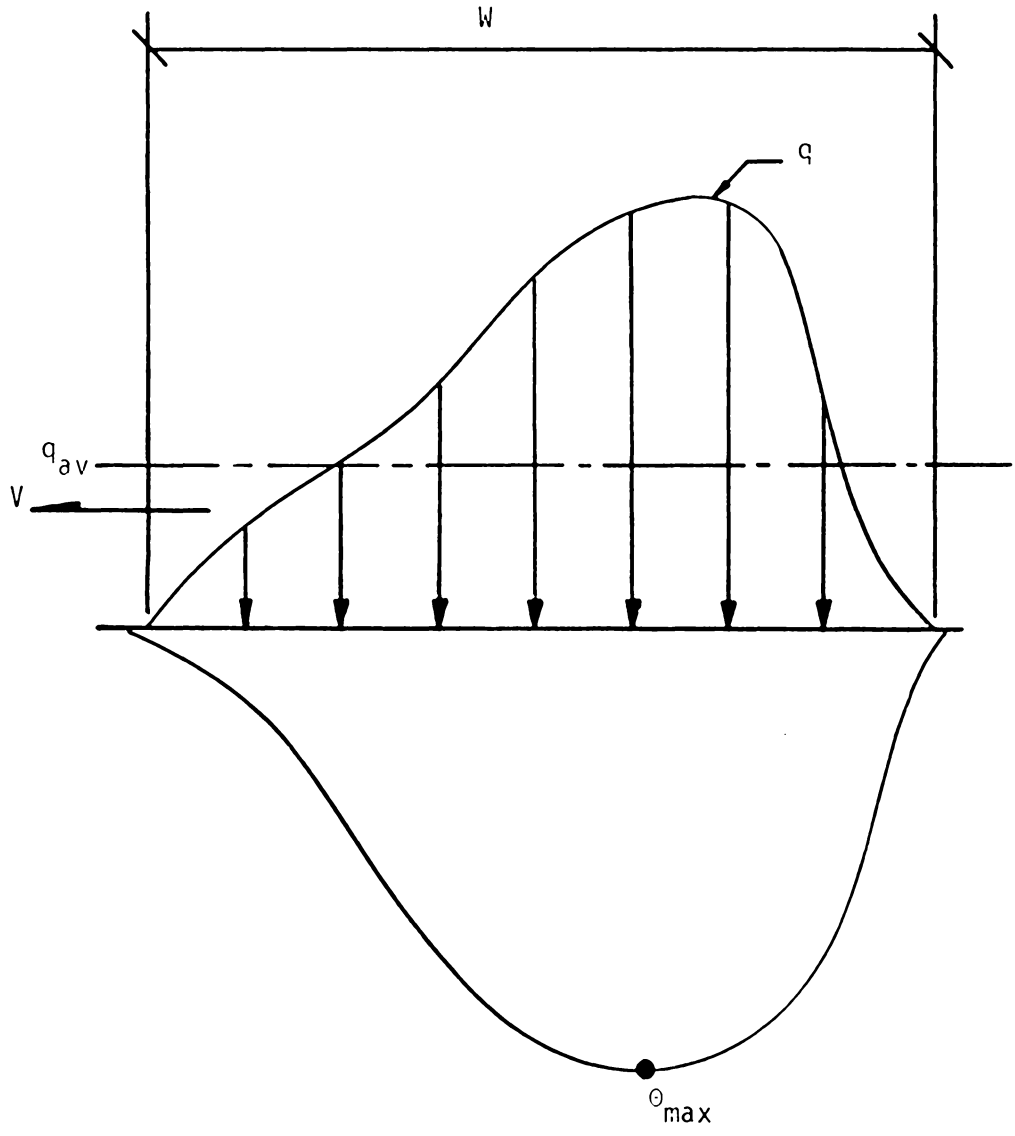

Figure 2. Blok's Model [1]

Jaeger [19] carried out a theoretical study much like Blok's, but was much more mathematically rigorous. In his paper an attempt is made, in connection with the problem of plane sliding, to set out fully the assumptions made and the numerical consequences of the mathematical theory in a form in which it is hoped can easily be used by experimenters to discuss particular models of sliding surfaces. The ultimate objective of his paper is the calculation of the temperature in a semi-infinite solid on which another body slides. Jaeger treats mathematically two of the most general and tractable cases of contact geometry, an infinite band source and a rectangular source which are defined as, (a) the band source of length 2ℓ in which heat is liberated uniformly at the rate of q per unit area per unit time over an infinite strip parallel to the y-axis and of length 2ℓ along the x-axis and in which the source moves with velocity v in the x-direction; (b) the rectangular source of sides 2ℓ parallel to the x-axis and 2b parallel to the y-axis in which heat is liberated uniformly at the rate of q per unit time per unit area over the rectangular. The center of the rectangle moves with velocity v along the x-axis.

STATIONARY SOURCES [19]

The temperature at time t, at the point (x,y,z), in the semi-infinite solid $z>o$ with no flow of heat over the surface $z=0$, due to heat supplied at the rate q per unit time per unit area over the square $-\ell< x'<\ell, -\ell<y'<\ell$, $z'=0$, commencing at zero time, when the solid is at zero temperature, is

$$\Theta = \frac{q\kappa}{4K(\pi\kappa)^{3/2}} \int_0^T \frac{dt'}{(T-t)^{3/2}} \int_{-\ell}^{\ell} dx' \int_{-\ell}^{\ell} dy' \exp\frac{(x-x')^2+(y-y')^2+z^2}{4\kappa(T-t')} \tag{5}$$

To find the steady state temperature evaluate the above equation when $t=\infty$

$$\Theta_{ss} = \frac{q}{2K\pi} \int_{-\ell}^{\ell} dx' \int_{-\ell}^{\ell} dy' \{(x-x')^2+(y-y')^2+z^2\}^{1/2} \tag{6}$$

The maximum temperature occurs at $x=y=z=0$ and is

$$\Theta_{max} = \frac{4\ell q}{K\pi} \log_e(1+\sqrt{2}) = 1.122 \frac{\ell q}{K} \tag{7}$$

The average temperature over the area of the source is

$$\Theta_{avg} = \frac{4\ell q}{K\pi} \{\log_e(\frac{1+\sqrt{2}-\sqrt{2}-1}{3})\} = 0.946 \frac{\ell q}{K} \tag{8}$$

The corresponding result for the maximum temperature for a circular source of radius ℓ is

$$\Theta_{max} = \frac{q\ell}{K} \tag{9}$$

THE CASE IN WHICH MOTION OF THE SOURCE HAS TAKEN PLACE FOR A FINITE TIME T. [19]

We consider a rectangular source with sides 2ℓ parallel to the x-axis and 2b parallel to the y-axis. Its center moves with velocity v along the x-axis in the plane z=0 of the semi-infinite medium with no loss of heat from the plane z=0. Suppose that at time t the center of the source has just reached the origin. Jaeger then derives an expression for the average temperature over the area of the source, starting from equation (1), i.e.,

$$\Theta_{av} = \frac{1}{4BL} \int_{-\ell}^{\ell} dX \int_{-B}^{B} \Theta dY \tag{10}$$

and is given by

$$\frac{\pi KV}{2q\kappa} \Theta_{av} = \frac{1}{4LB} \left(\frac{\pi}{2}\right)^{1/2} \int_{0}^{v^2T/2\kappa} u^{1/2} du \phi(B(2/u)^{1/2})$$

$$x\{\phi(\frac{2L+y}{(2u)^{1/2}} + \phi\frac{|2L-2u|}{(2u)^{1/2}} - 2\phi[(u/2)^2]\} \tag{11}$$

where $\phi(X) = \int_{0}^{X} \text{erf } x \, dx$

$$= X\text{erf} - \frac{1}{\pi^{1/2}} + \frac{1}{\pi^{1/2}} e^{-x^2} \tag{12}$$

effects of friction, load, contact area and many physical properties. First the relationship for the heat flux, q, is:

$$q = fpv_s \tag{2}$$

where f is the coefficient of friction and p is the pressure in the contact zone. Symbol v_s denotes the sliding velocity:

$$v_s = v_1 - v_2 \tag{3}$$

where v_1 and v_2 represent the velocities at which the contact zone moves along each surface. Equation (2) represents a heat flux being applied to a solid body. In order to derive an equation that is representative of a practical problem, Blok had to account for the heat source which is developed in the contact zone and therefore results in partitioning of the total heat developed between the two solids. Blok states that if the two velocities, v_1 and v_2 are high enough then the heat withdrawn by the two solids 1 and 2 are in proportion to $(b_1\sqrt{v_1})/(b_2\sqrt{v_2})$ and the inverse respectively. For the case of gear teeth or any situation where the two solids are identical or where their thermal contact coefficients b_1 and b_2 are equal or nearly equal, equation (1) can then be adapted to the case of meshing gear teeth or any solid on solid contact as follows:

$$\theta_{max} = \frac{1.11fW|\sqrt{v_1}\sqrt{v_2}|}{b\sqrt{w}} \tag{4}$$

where $W = wp_{av}$. If p_{av} represents the average contact pressure then W denotes the load per unit width of the contact.

It will be shown shortly that the factor $\frac{\pi KV}{2q_K}\Theta_{av}$ is an important and necessary quantity.

CALCULATION OF THE MAXIMUM AND AVERAGE STEADY STATE TEMPERATURE OVER THE AREA OF THE SOURCE

The objective of the above analysis is to arrive at an expression or expressions that would allow one to conveniently calculate the mean and average temperatures over the area of the source. The theory is divided into three regions based on a Peclet number criterion. The Peclet number, L, is the ratio of the time required for the temperature to penetrate into the surface a distance equal to the contact radius to the time required for the contact to move a distance equal to the contact radius [26].

$$L = \frac{Va}{2\kappa} = \frac{Va\rho c}{2\kappa} \tag{12.1}$$

For the square source, the derived expressions are

1) If L is large (L>5) the maximum temperature is:

$$\frac{4aL^{1/2}}{KV\pi^{1/2}} = \frac{2a}{K}\left(\frac{2\kappa\ell}{\pi V}\right)^{1/2} \tag{13}$$

and the average temperature over the area of the source is:

$$\frac{8q\kappa}{3KV\pi^{1/2}} = \frac{1.064a}{K}\left(\frac{\kappa\ell}{V}\right)^{1/2} \tag{14}$$

2) If L is small ($L < 0.1$) the maximum temperature is:

$$\frac{8q\kappa}{\pi KV} \log_e(1+\sqrt{2}) = 1.122 \frac{q\ell}{\kappa} \tag{15}$$

and the average temperature is

$$\frac{8q\kappa}{\pi KV} \{\log_e(1+\sqrt{2}) - \frac{\sqrt{2-1}}{3}\} = 0.946\frac{q\ell}{K} \tag{16}$$

3) For the intermediate values, $0.1 < L < 5$, in which the above formulae do not hold, the maximum temperature must be obtained from curves such as those of Fig. 3 and the average temperatures are most easily calculated from (11)[19]. This is obviously not an equation that one would want to tackle very often. Jaeger plotted its results where ($\pi KV/2\rho q$) times the average and maximum temperatures for the square source are plotted against L (see Fig. 3).

The above equations allow us to calculate the average and maximum surface temperatures assuming that heat input, q, is being received entirely by the one solid of interest. The practical case is one in which both bodies have finite conductivity and therefore both the slider and second substance conduct some portion of the generated heat. The practical situation is further complicated by the sequence of the slider being heated by the source and cooled by the oncoming cooler portions of the other substance. In order to account for the division of heat, it is assumed that, when a steady state has been attained, a fraction, α, of the heat q per unit time per unit area, generated from the frictional

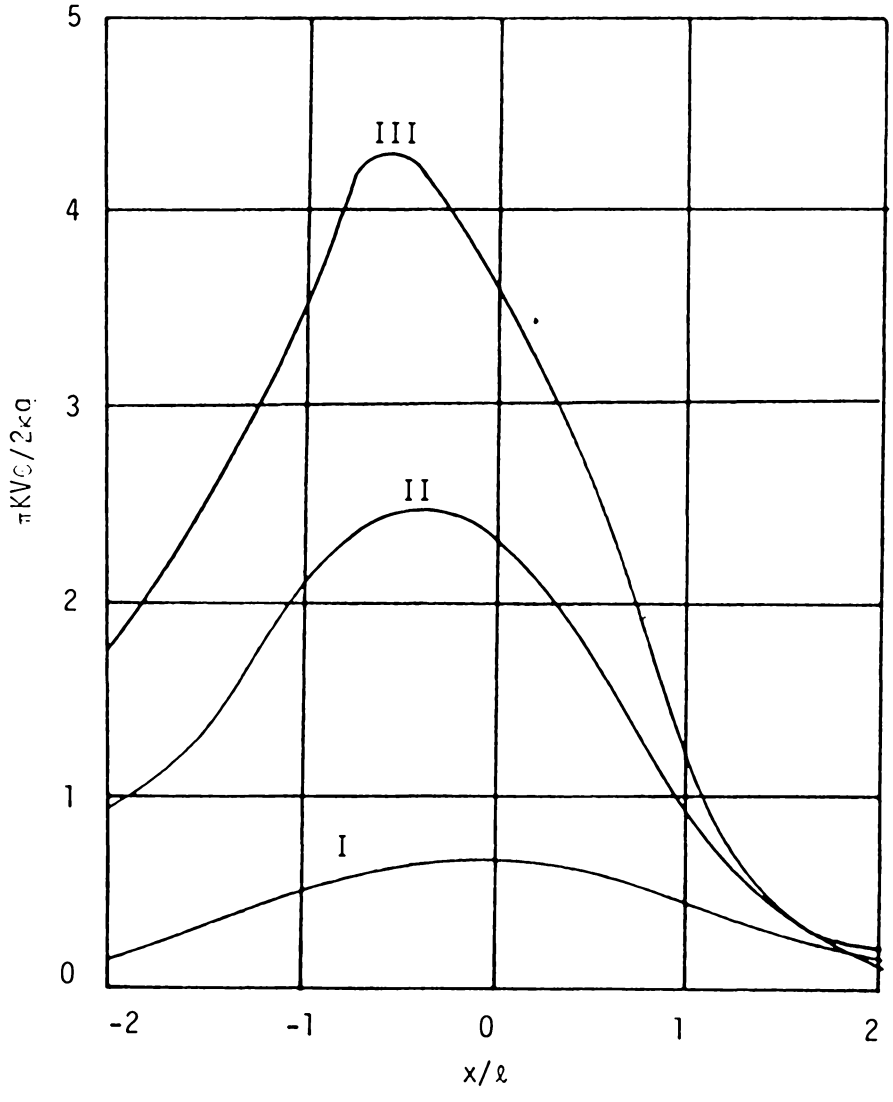

Figure 3. The Temperature for a Square Source at Points on the x-axis [19]

process passes to the substance 1 and the remaining fraction (1-α) to substance 2. The fraction of heat that is conducted into substance 1 is then calculated by the requirement that the surface temperature of substance 1 must equal that of substance 2. To do this, the equation for a moving heat source of quantity, q, in substance which must equal the average temperature calculated for substance 2 by means of the equation for a stationary source of (1-α)q.

To illustrate how to calculate the average surface temperatures using the above method, the following general example is provided [19].

Square-Load Against a Rotating Disk

The system consists of semi-infinite slider K_2,κ_2, with a square contact of sides 2ℓ moving with a velocity V on a semi-infinite medium K_1,κ_1. We assume a fraction α of the heat q generated per unit time per unit area goes to the medium and (1-α) to the slider.

If L for both bodies is small, the average temperature over the area of contact is given by the heat distribution criterion for each body which results in the expression

$$0.946\frac{\alpha q \ell}{K_1} = 0.946\frac{(1-\alpha) q \ell}{K_2} \tag{17}$$

Thus

$$\alpha = \frac{K_1}{K_1+K_2} \tag{18}$$

and the average temperature is

$$0.946 \frac{q}{K_1+K_2} \tag{19}$$

For the case in which L is large, applying the heat distribution criteria to (8) and (14) results in

$$1.06\alpha q \frac{}{K_1} \left(\frac{\kappa \ell}{v}\right)^{1/2} = 0.946 \frac{(1-\alpha)q\ell}{K_2} \tag{20}$$

Thus

$$\alpha = \frac{K_1(\ell v)^{1/2}}{1.125K_2\kappa_1^{1/2}} \tag{21}$$

and the average temperature over the area of contact is

$$\frac{1.06+q\ell\kappa^{1/2}}{1.125K\kappa^{1/2}+K_1(\ell v)^{1/2}} \tag{22}$$

For the intermediate values of L (0.1 L 5) the average temperature for the substance 1 must be obtained from Fig. 7 of Jaeger's paper [19] (see Fig. 4). If we let $y = (\pi KV/2\alpha q\kappa)\Theta_{av}$ be the ordinate of this curve with L as the abscissa and then using equation (14) for the Θ_{av} term, α can be solved for as:

$$\alpha = \frac{1.486\ell K_1 V}{1.486\ell K_1 V+\kappa_1 K_2 v} \tag{23}$$

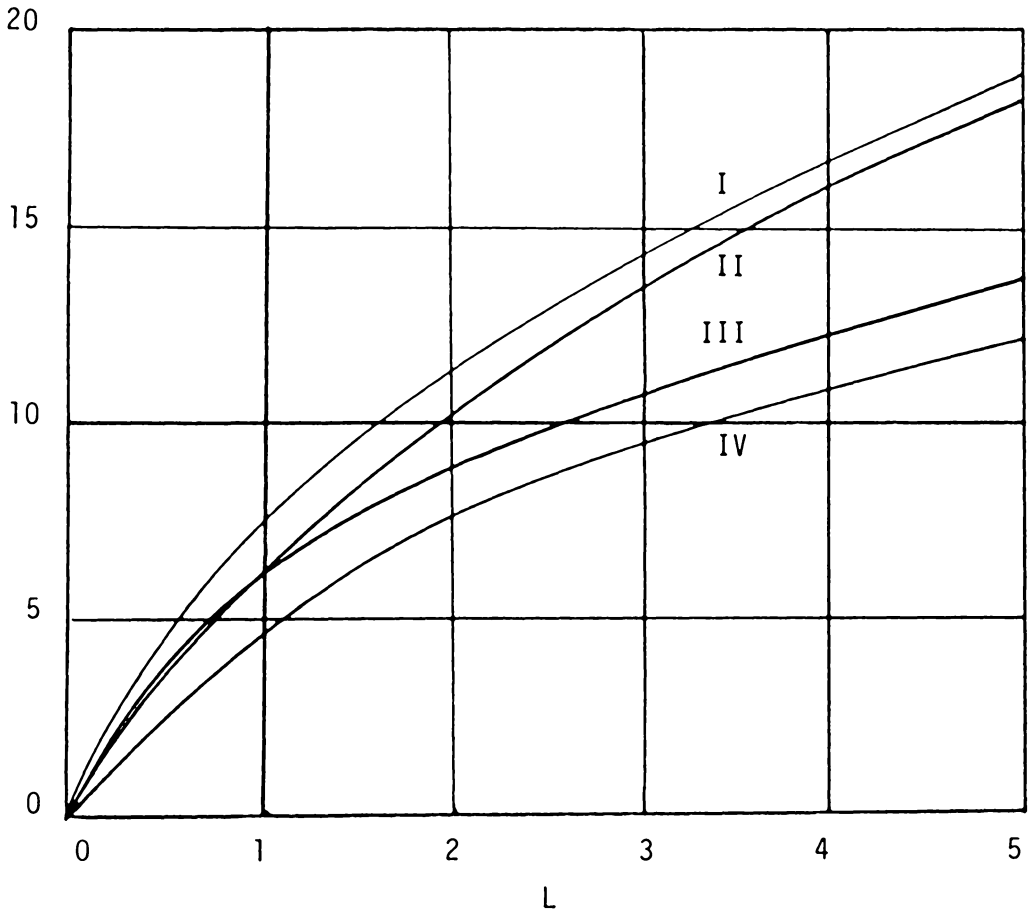

I Maximum Temperature of Band Source
II Maximum Temperature of Square Source
III Average Temperature of Band Source
IV Average Temperature of Square Source

Figure 4. Maximum and Average Temperatures vs. Peclet Number [19]

and the average temperature is

$$\frac{0.946\ell\kappa_1 v q}{1.486\ell K_1 V+\kappa_1\kappa_2 v} \tag{24}$$

Since Jaeger's work there have been many theoretical studies which have tried to reduce the mathematical complexities of Jaeger's treatment, e.g., Holm [20], Bowden and Tabor [21], Cook and Bhushan [22], Francis [23], Ling [24], and Archard [25]. Archard's formulation of flash temperature merely reduces the mathematical complexities of Jaeger's work and emphasizes the relevant physical considerations [25].

Archard's theory requires the solution of the equations for flow of heat into each body. The theory is based on two main assumptions, (a) the heat is generated at the area of true contact, considering a single area of contact as a plane heat source, and that (b) this heat is conducted away into the bulk of the rubbing members. The derived surface temperatures are expressed in terms of the rate of supply of heat, the size and speed of the heat source, and the thermal properties of the materials. Archard uses as a model (Fig. 5) a protuberance on the surface of body B which forms a circular area of contact which moves with a velocity V over the flat surface of body C. Body B therefore receives heat from a stationary heat source and body C from a moving heat source.

Archard's formulation, much like Jaeger's, subdivides the theory into three different sectors; a stationary or slow moving heat source, a

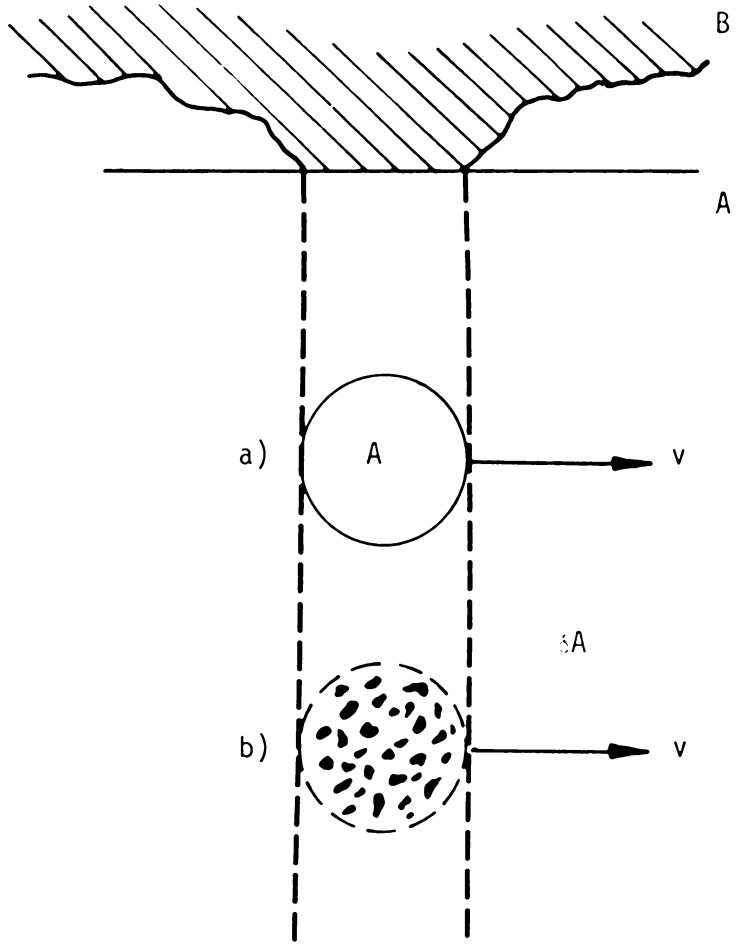

Figure 5. Archard Model [25]

high velocity heat source, and a transition zone between these two. These zones are defined by the Peclet number, where a stationary heat source is defined by a Peclet number of zero and a slow moving heat source has a Peclet number less than 0.1. A high speed moving heat source is defined by a Peclet number greater than 5. The transition zone occurs between the slow and high speed regimes or $0.1 < L < 5$.

For the stationary heat source, body B, the mean temperature rise above the bulk solid temperature is

$$\theta_m = \frac{Q_B}{4aK_B} \tag{26}$$

If Body A is moving slowly ($L < 0.1$), it can be treated as essentially a stationary heat source case also. Therefore

$$\theta_A = \frac{Q_A}{4aK_A} \tag{27}$$

where

Q_a = rate of frictional heat supplied to body A

K_a = thermal conductivity of body A

For large values of L, or a fast moving heat source, the surface temperature of the moving surface is given by

$$\theta = \frac{2Qx}{Ka^2 \rho cV} \tag{28}$$

where x is the distance from the leading edge of the contact. The average temperature over the circular contact in this case then becomes

$$\Theta_m = \frac{Q}{3.25 K_B a} \left(\frac{1}{2L}\right) \tag{29}$$

The above can be simplified graphically if we define

$$N = \frac{Q}{a^2 \rho c V} \tag{30}$$

Then for $L < 0.1$, equations (26) and (27) become

$$\Theta_m = 0.5\ NL \tag{31}$$

and for high speed moving surfaces ($L > 5$) equation (29) becomes

$$\Theta_m = 0.435 NL^{1/2} \tag{32}$$

For the transition region ($0.1 > L > 5$)

$$\Theta_m = 0.5 \alpha NL \tag{33}$$

where it has been shown that the factor α is a function of L ranging from about 0.85 at L=0.1 to 0.35 at L=5. α in the above equation can be solved for, much like it was in Jaeger's paper. From Jaeger

$$\text{let } y = \frac{\pi K_1 V \alpha}{2 q_K} \Theta_m \tag{34}$$

The average temperature for a stationary heat source is:

$$\Theta_m = 0.5\ NL;\ N = \frac{\pi q}{\rho c V} \tag{35}$$

Substituting Θ_m into equation (35) results in

$$y = \frac{\pi^2 La}{4} \tag{36}$$

Therefore

$$\alpha = \frac{4y}{\pi^2 L} \tag{37}$$

Equations (31), (32) and (33) can be plotted as shown in Fig. 6 as a function of L or velocity as the Peclet number is proportional to velocity.

To apply the results of the above derivations to a practical problem, the proportion of frictional heat supplied to each body must be taken into account. Archard's approach is to calculate the temperature of both bodies B and C assuming that all the heat is supplied to each one. To calculate the mean surface temperature the following relationship is used:

$$\frac{1}{\theta_m} = \frac{1}{\theta_A} + \frac{1}{\theta_B} \tag{38}$$

Even though the Archard model (Fig. 5) is very simple, he acknowledged the fact that most engineering materials and contacts will not have a continuous zone of contact but may instead be subdivided into a number of smaller contact areas each δA. The temperature calculations can be applied to deduce the temperature distribution for the general contact region A or for the individual contact areas δA. It is important to consider the relative importance of the temperatures deduced in these two ways.

Consider the contact areas δA of Fig. 5b as being fairly closely packed. At low sliding speeds the thermal resistance consists of the constriction resistance of the whole region A in series with the sum (in parallel) of the constriction resistances of the areas δA. In the

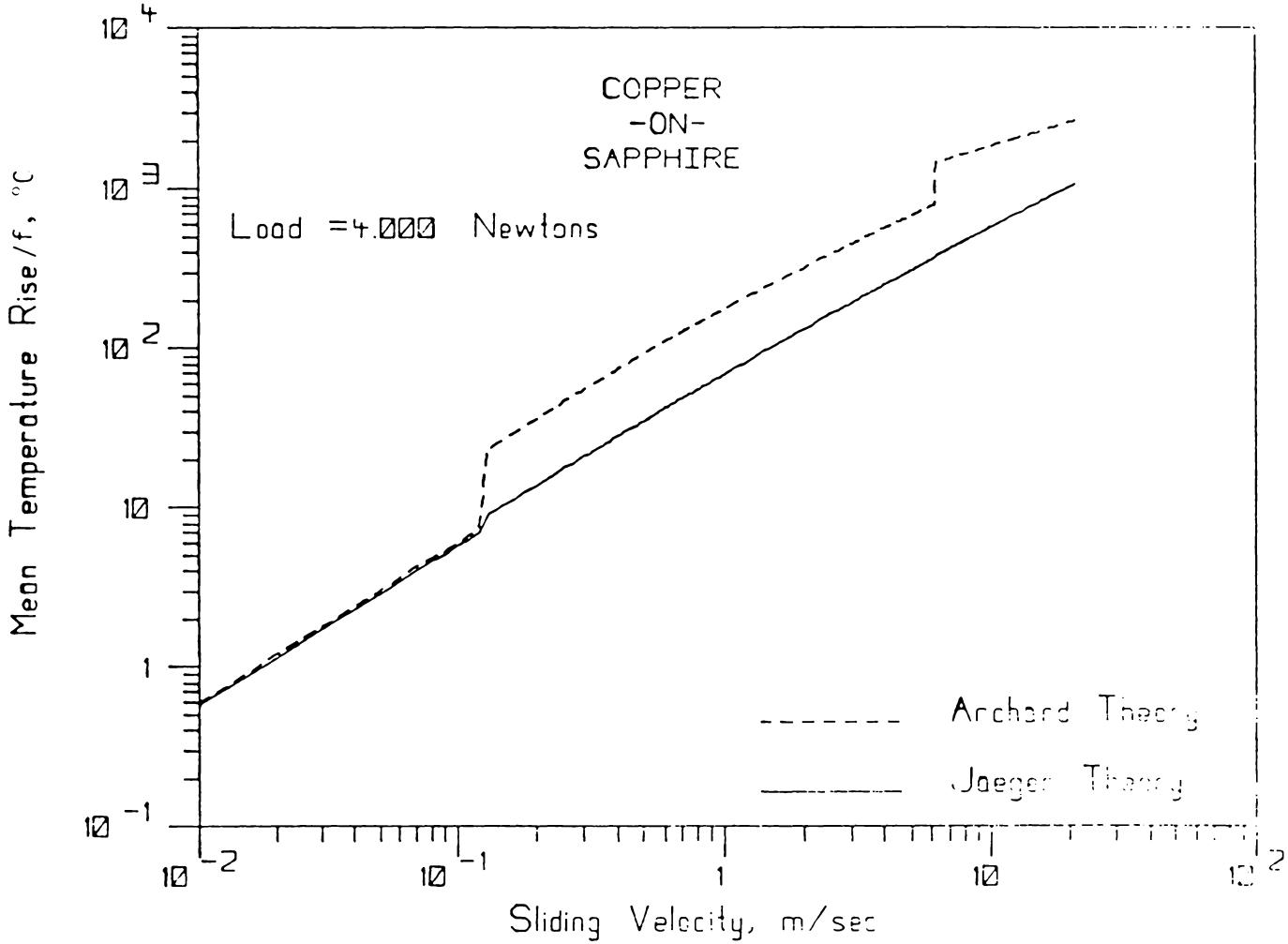

Figure 6. The Effect of Velocity on Surface Temperature, Load=4.0N

corresponding electrical example it has been shown [47] experimentally and theoretically that the aggregate resistance of a large number of small closely grouped constrictions, each δA, is very little greater than the resistance of one large constriction A. Therefore, to a first approximation, the surface temperature of the model of Fig. 5a. equals that of Fig. 5b.

There is another approach to this problem of subdivision of the contact area. If one assumes that each contact spot, δA, is independent of the others (which is to say that their temperature is not influenced by any of the material around them) then the analytical approach would be to distribute the load over all the contact areas. Assuming all the contacts are circular and equal in size, they therefore each carry the same load. From this point we can apply any theory to an individual contact. Figure 7 shows an example of the rapid decrease in the predicted surface temperature rise with this type subdivision of the contact zone. The effect of subdivision is rather dramatic (using these assumptions) compared to the first rationale where it was deduced that the mean temperature rise would not change.

The classical treatments of surface temperatures generated from friction are for the most part based on simplifying assumptions of the contact interface, such as a singular contact zone. There is an ever-increasing number of papers which are trying to rationalize and analyze some of the more complex physical occurrences in the contact zone. One of the very interesting concepts that deal with a more nearly real model of the contacting interfaces was proposed by Ling [41]. Ling's basic

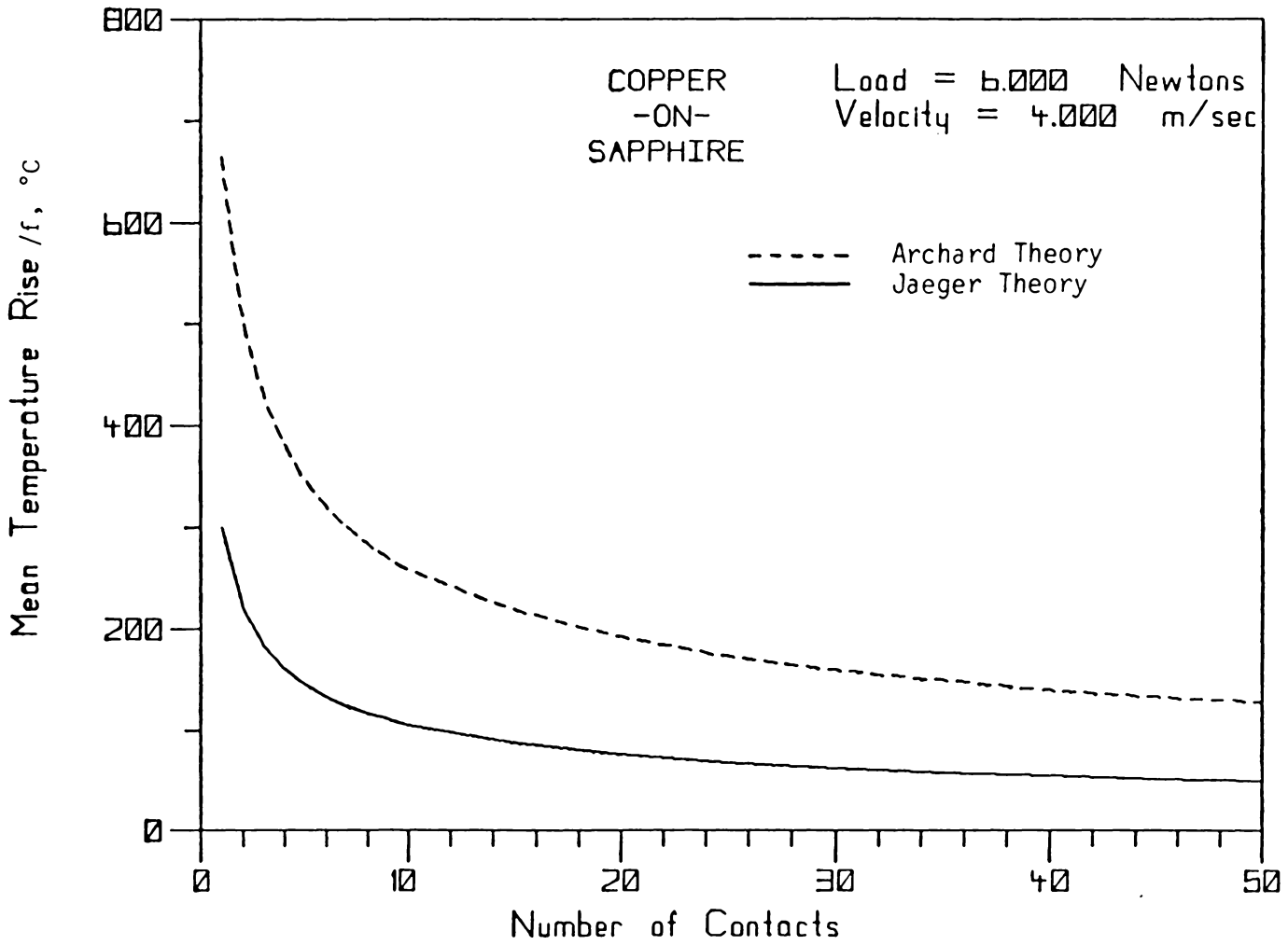

Figure 7. Theoretical Effect of Subdivision of Contact Area.

premise of concern is where the real area of contact is less than the geometric contact area and this contact area is created by a number of smaller contacts that are able to move and coalesce into larger areas.

To this end, he developed a simple stochastic model as follows: (1) a geometric contact area is given (Fig. 8); (2) given a load, W, based on existing friction theory, the fraction of geometric area in actual contact does not change with time; (3) the geometric area is subdivided into a number equal unit areas, (4) for a given time interval, suitable for the speeds of sliding and computational requirements, the distribution of units in contact are varied; (5) by random processes, n units are populated; (6) coalesence of units makes larger area of contact than the unit area, and (7) the same process is carried out for each succeeding time interval. After such a model is created, heat conduction analyses using basic solutions lead to a histogram of surface temperature transients and the following observations [41]:

(1) The average surface temperature of the stationary body differs in general from that of the moving one.

(2) The average surface temperatures of the stationary and the moving bodies, as well as the actual contact temperatures, are low relative to the maximum.

(3) The ratios of standard deviations of surface temperatures of the stationary and the moving bodies to the respective average surface temperatures are between 0.3 and 3.7 with the added observation that (a) the lower the speeds, the smaller the

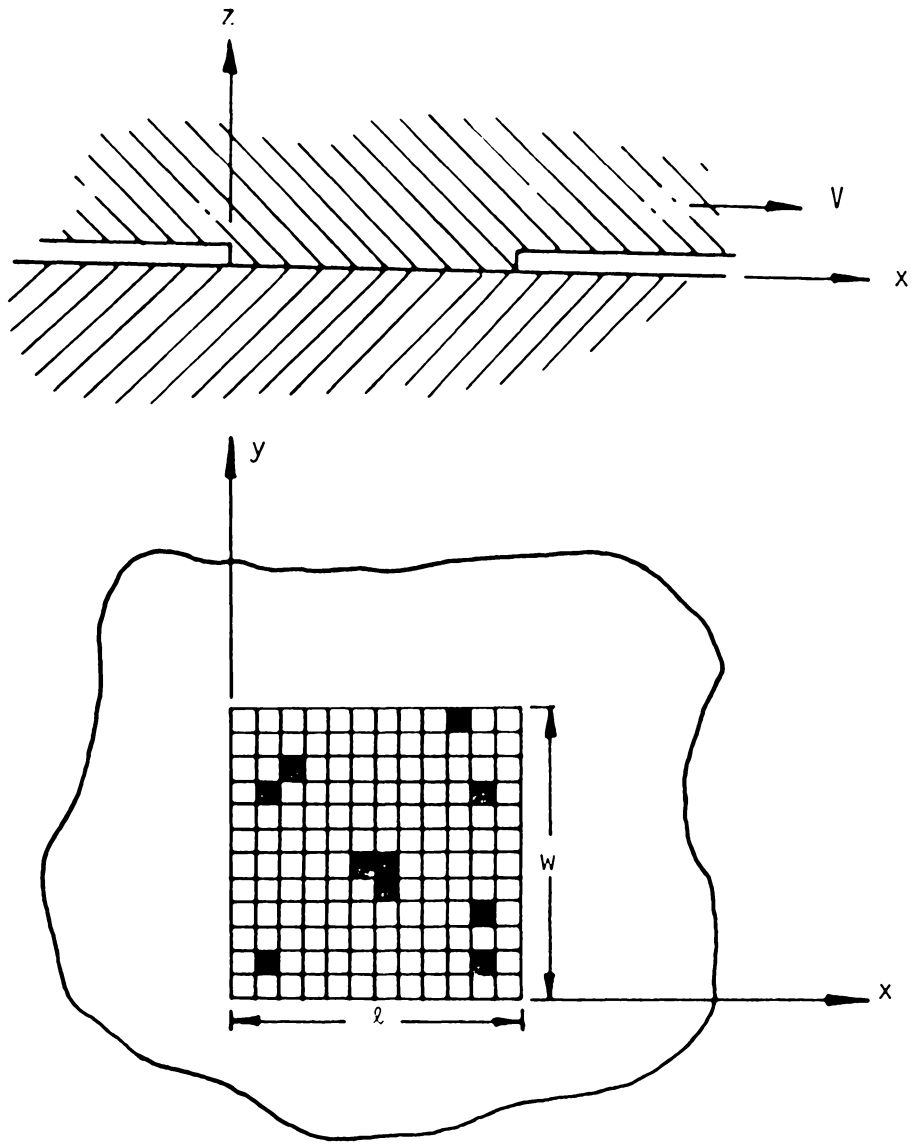

Figure 8. Ling's Model [24]

ratios, and (b) the larger the contact areas, the smaller the range level for the ratios and the lower the levels at which the ratios occur.

(4) The ratios of standard deviations of surface temperatures over contact areas to the average of contact surface temperatures are between 0 and 0.37.

(5) The spectral information on temperatures in insensitive to the particular program of heat-input distribution for a given percentage of contact, a fact which gives credence to the simplified stochastic process.

One of the main conclusions of Ling's work is that while the average temperature may be T = 0.06 (normalized temperature in which the maximum temperature equals 1.0), there is a significant peak average at T = 0.37. It is suggested that the former temperature may affect the general metallurgical state, while the latter may affect chemical actions [41].

Another of the simplifying assumptions that Jaeger, Archard and Blok used was that all the physical and thermal properties of the sliding bodies remained constant with time and temperature. Powell and Earles [27] have attacked this problem from a theoretical viewpoint with aid of experimentally-determined subsurface temperatures, friction coefficients and available temperature-dependent physical properties. The investigation centered around modifying the Jaeger-Archard theory to account for differences in subsurface temperature of the two bodies.

The main operating premise of Powell and Earle's work is that any frictional process is always accompanied by a dissipation of heat which raises the temperatures of the sliding surfaces and/or the surrounding environment. They state that there are actually two stages of temperature increase, a general rise which affects the whole of the surface, which is referred to as the subsurface temperature θ_s, and localized temperature flashes which are caused by the dissipation of frictional energy into small raised asperities on one or both surfaces and which are superimposed on the subsurface temperature. This two-stage concept differs from the Jaeger-Archard theory in that they assumed that the two sliding bodies were infinite heat sinks and that there was an insignificant amount of subsurface heating or that the temperature of each body at a distance equal to the width of an asperity contact was at ambient temperature.

In most real practical applications, the conditions are such that there will occur significant subsurface heating. The subsurface temperature rise in each body, θ_{SB} and θ_{SC} respectively, will depend on the relative ease with which heat can be conducted away on either side of the frictional contact. Since θ_{SB} and θ_{SC} will not generally be equal, matching of the total temperature $\theta_T = \theta_S + \theta_F$ on each body will produce new equations for both the distribution of heat and the flash temperature [27]. As an example, for conditions in which $L > 5.0$

$$\theta_T = \frac{Q_B}{4aK_B} + \theta_{SB} = \frac{0.31Q_C}{aK_C}\left(\frac{\kappa_C}{Va}\right)^{1/2} + \theta_{SC} \qquad (39)$$

giving

$$\alpha = \frac{1-4aK_B(\Theta_{sc}-\Theta_{sB})/\mu NV}{(1+0.88(K_B/K_c)L_c^{\frac{1}{2}}} \tag{40}$$

From (39), Θ_T may now be written in the form

$$\Theta_T = \frac{(1-\alpha)\mu NV}{4aK_B} + \Theta_{sB} = \frac{\alpha\mu NV}{aK_c}\left(\frac{K_c}{Va}\right)^{\frac{1}{2}} + \Theta_{sc} \tag{41}$$

giving

$$\Theta_{FB} = \Theta_T - \Theta_{sB} \text{ and } \Theta_{FC} = \Theta_T - \Theta_{sc} \tag{42}$$

Another of Powell and Earle's contributions was to show the significance of temperature-dependent physical and thermal properties when used in the classical flash temperature theories. Figure 9 shows how the physical and thermal properties may change with temperature. The other complication that they addressed was the effect of the number of contacts. Powell and Earle used the rationale in their study that subdividing the contact area distributes the normal load to each of the contacts in direct proportion to their area. Assuming that there is no 'driving force' between discrete areas of contact means that the surface temperature of each contact may be evaluated by using its area and the load which it supports.

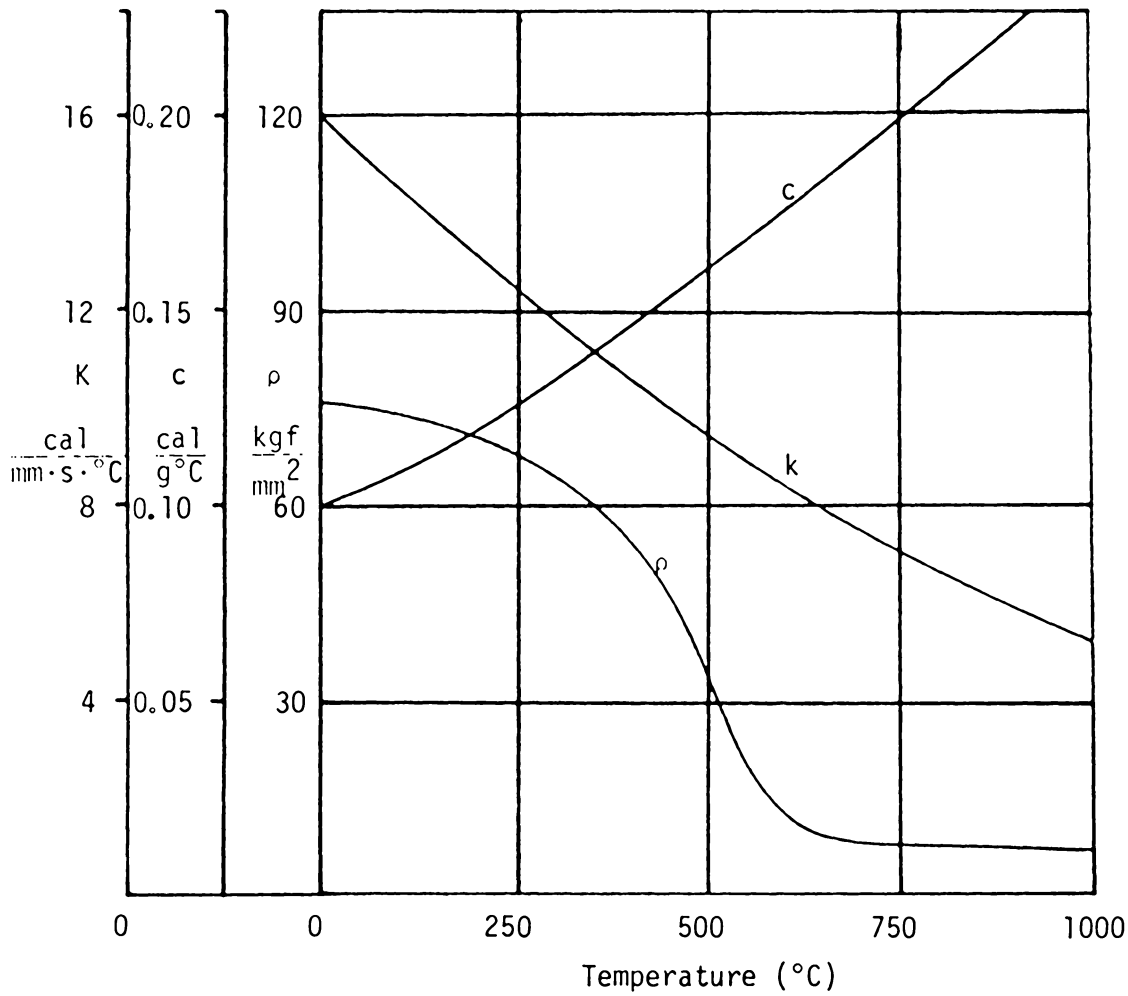

Figure 9. Temperature Dependence of the Physical Properties on SAE 1113 Steel [27]

There have been many other theoretical treatments of flash temperature and related topics. There are also a number of theories that use the classical flash temperature theories just presented as working foundations or the concept of surface temperature increase caused by friction for other concepts such as scuffing of gear teeth [42], the Quinn oxidational wear mechanism [8], and the "in-situ" formation of protective polymeric films on rubbing surfaces [17,18]. The classical theories of Jaeger, Blok and Archard have also been extended to supposedly explain the physical phenomena more accurately. Rozeanu and Pnueli [9] developed a model which establishes the existence of two temperature gradients in the material; a weak one in the bulk, and a very strong one at the surface. This model was created because a large number of friction failures, which could not be explained by the classical continuum model, are easily interpreted by the two gradient model.

2.2 Experimental Review

As has just been shown, there are numerous theoretical treatments of surface temperatures generated by friction. However, there are very few experimental studies that deal with this topic. Due to the meager experimental data it is difficult to accept or reject any of the theories as accurately defining and describing the problem properly. As stated by Ling and Simkins [49], the lack of rigorous experimental information on the junction condition is attributable to the difficulties with the measurement of temperature distribution of surface temperatures at the interface.

Several methods have been used to attempt to measure surface temperatures generated by friction. These have included embedded thermocouples, the dynamic or Herbert-Gottwein thermocouple [11], evidence of melting or metallurgical transformations [25], the recording of visible hot spots [44], special thin film transducers [43], infrared thermography and photon detectors [46].

Of these experimental techniques, the infrared detector is the most promising. The infrared method has been used in a few investigations to measure surface temperature but every one has its unique advantages or faults. Furey [16] briefly examines some of the similarities as well as the differences among these investigations. For example, earlier work was carried out with systems having a rather large target spot (e.g., 1 mm), thus making scanning of a contact region difficult or impossible. Furthermore, contact geometries ranged from simple to complex. While some studies were made using dry, unlubricated systems, others involved

lubricated systems -- including conditions of partial metallic contact as well as elastohydrodynamic lubrication. In some cases, the infrared detector "looked at" the region of contact during contact; in other cases, the detector viewed the region just after contact [30]. Often, (a) friction -- the cause of surface heating -- was not measured, (b) the load and speed range were limited, (c) the contact geometries were too complex or ill-defined, or (d) the system was complicated by the presence of a lubricant film. Thus, it was difficult to make a direct comparison of experimental results with the Blok/Jaeger/Archard theory.

The classic investigation of surface temperatures using infrared techniques was performed by Bowden and Thomas [46] in 1954. Their technique was to use a lead sulfide detector to investigate frictional hot spots caused by various metals in dry sliding contact against a glass disk. This investigation had limitations however, the infrared transmissivity of glass is relatively low, the target area was not given, and friction not measured. References to other early studies using infrared detectors to measure surface temperatures in more complex processes (e.g., braking, metal cutting) may be found in the paper by Godet et al [30] [16].

In 1973, a detailed study was begun at Virginia Polytechnic Institute and State University, under the direction of M. J. Furey, to investigate surface temperatures in an unlubricated system of pure sliding. The specific goals of the initial research program were: (a) to examine in detail the problem of surface temperatures generated by relative motion between solids, with emphasis being placed on an

advanced experimental investigation; (b) to carry out the major part of this study by the design, construction, calibration, and use of a sliding contact device which has as its main component a highly advanced infrared microscope (a Barnes Engineering Company, Model RM-2A) [35,36]; (c) to examine the surface temperature and tribological behavior of some simple and well-characterized sliding systems [37,38]; and (d) to study possible reasons for the discrepancies that appear to exist between theory and experiment [16].

In 1973, Winer, Sanborn, and Torchina reported on an investigation using an infrared microscope. They were also using a Barnes Engineering Company, Model RM-2A, infrared microscope, to measure oil film and surface temperatures under conditions of elastohydrodynamic (EHD) lubrication. In 1974, Wimer and Macpherson [50] also used a similar infrared technique for the measurement of gear tooth surface temperatures under lubricated conditions.

At the current time a new research investigation is underway at VPI&SU which is to use a sophisticated infrared microscope system to carry out further fundamental and predominantly experimental studies of surface temperatures produced in tribological processes. This includes (a) the extension of the infrared technique to other systems; (b) the continued careful examination of the relationships between friction, the real area of contact, and surface temperatures (thus radiance and emissivity); (c) experiments designed to test the importance of other thermal phenomena (e.g., melting) in the contact zone; (d) the application, development, and use of advanced instrumentation to improve upon

and expand our experimental capabilities; (e) an analysis of the rotating sapphire disc system to determine whether or not comparisons with existing surface temperature theories are indeed valid; and (f) a reexamination of the classical surface temperatures theories in the light of new experimental data [48].

At this point in our knowledge of surface temperatures and of the technology available to measure temperatures at interfaces, it appears that the infrared microscope or infrared detection technique is the most promising experimental technique. Even though the technique is relatively complex, the technique offers many advantages over most other methods.

3.0 EXPERIMENTAL TECHNIQUE

3.1 Apparatus [35, 36, 37, 38, 51]

A sliding point contact is formed by using a specimen which is loaded against a rotating, 1 mm thick, sapphire flat. As is shown in Figure 10, the infrared microscope is placed over the contact to directly measure the infrared radiation emitted from the contact, and, therefore, allow surface temperatures to be deduced.

The radiometric microscope [31] can be equipped with a 36X reflecting objective which allows spot size resolutions of 1.78×10^{-5} m (0.0007 in.) with a focal length of 5.3 mm and a numerical aperature of 0.65. A 15X reflecting objective with a spot size resolution of 3.45×10^{-5} m (0.0014 in.) and a numerical aperture of 0.28 is also available. The small target spot diameter of 1.78×10^{-5} m, makes scanning of a contact region possible. Figure 11 compares the target spot size of the 36X and 15X reflecting objective lens with contact wear spots of the copper specimens at a load of 2 Newtons and sliding velocity of 2 m/s against a sapphire disk for 15 sec. The radiation from this spot plus that from a related solid angle between this spot and the objective is focused onto a liquid nitrogen cooled indium antimonide detector. This detector has a spectral response of $1.8 - 5.5 \times 10^{-6}$ m (1.8 to 5.5 microns). This is illustrated in Fig. 12 which shows the spectral distribution of radiation emitted by a black body at various temperatures.

The microscope unit is modularized and conforms with conventional microscope configurations. The unique feature is its dual channel

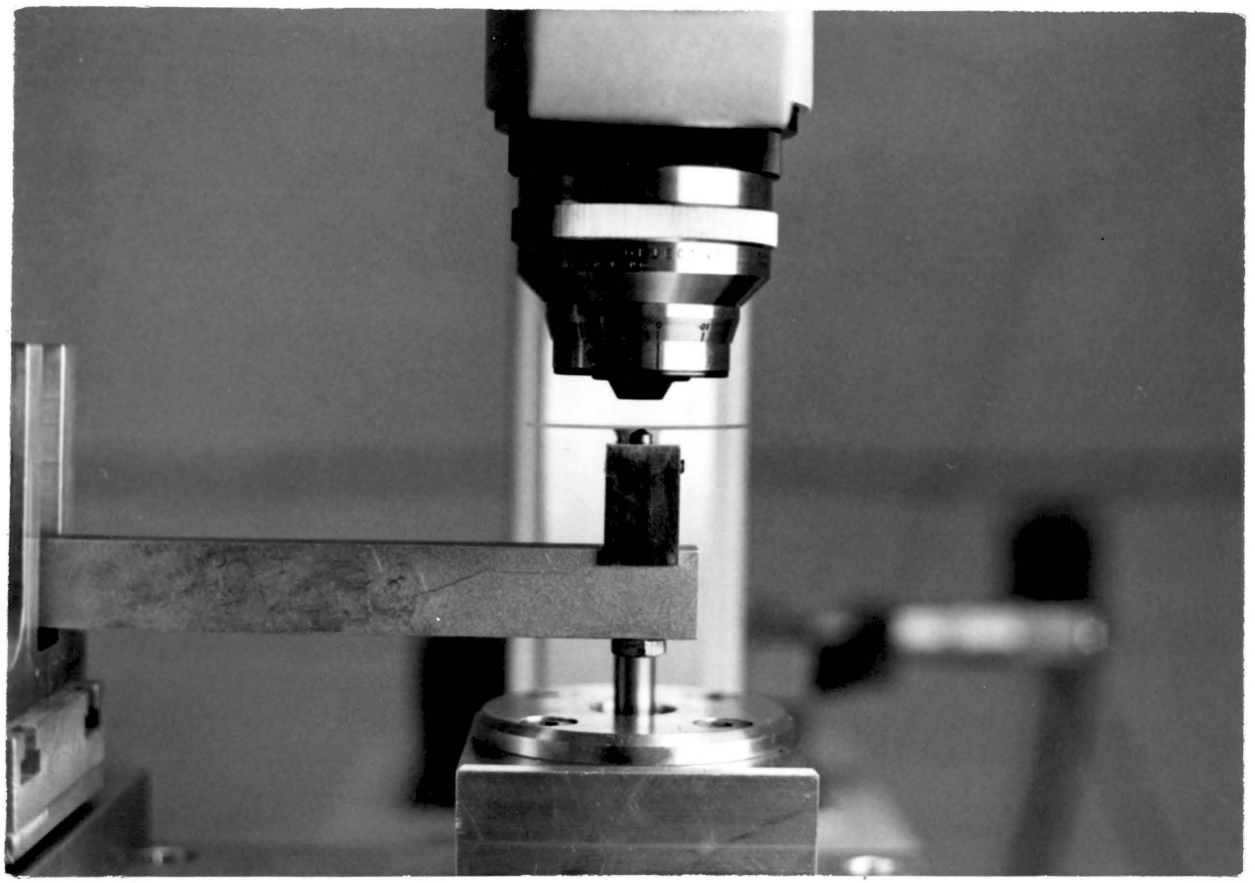

Figure 10. Basic Contact Geometry

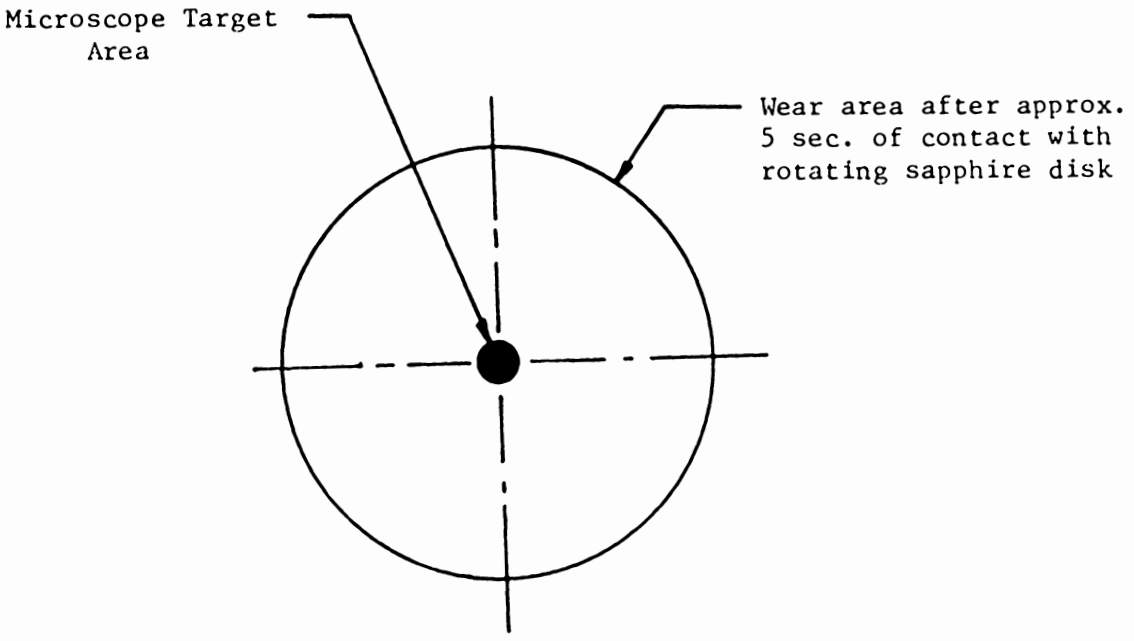

Figure 11. Comparison of Wear Area to Microscope Target Spot

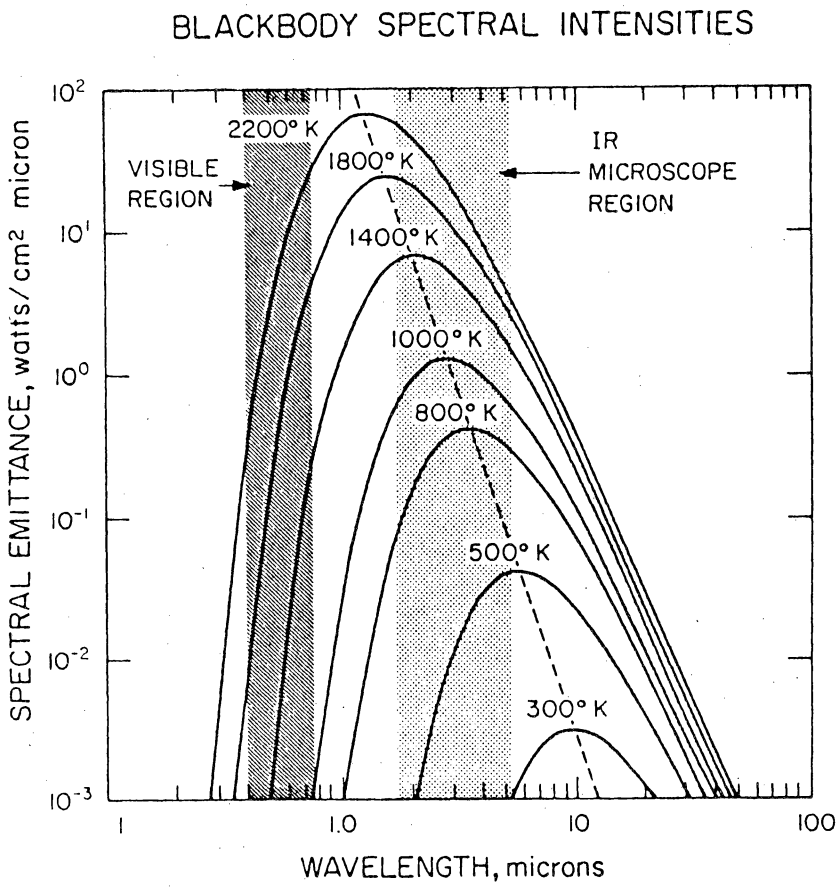

Figure 12. Spectral Range of the RM-2A Infrared Microscope [16]

design which allows for simultaneous visual observation of the surface and infrared temperature measurements. The visible channel is a wide field, medium-powered microscope of equal magnification. All power to the electrical subassemblies and the signals from these subassemblies are run through a single cable which connects the control unit with the microscope unit.

Figure 13 shows the major components of the Barnes Engineering Company RM-2A Infrared Radiometric Microscope. The radiation emitted by a target, both visible and infrared, enters the reflective objective, where it is optically collected and directed toward an infrared detector in the radiometer portion of the microscope unit. A germanium disk reflects the visible radiation to the visible channel and allows the infrared energy to pass to the detector in the infrared channel. The detector produces an electrical signal which is directly proportional to the infrared radiation level. This signal is amplified and sent to the control unit, where it is either amplified further and processed to display temperature directly, or coupled to an external recorder.

The tuning fork optical chopper, located just above the germanium dichroic, is designed so that target and reference radiation are alternately incident on the infrared detector. The optical chopper consists of a tuning fork with chopper blades attached to its tines. As the tuning fork resonates (which causes the blades to rotate), it alternately opens and closes the aperture to the detector. The chopper blades allow for continuous comparison of the radiation emitted from the

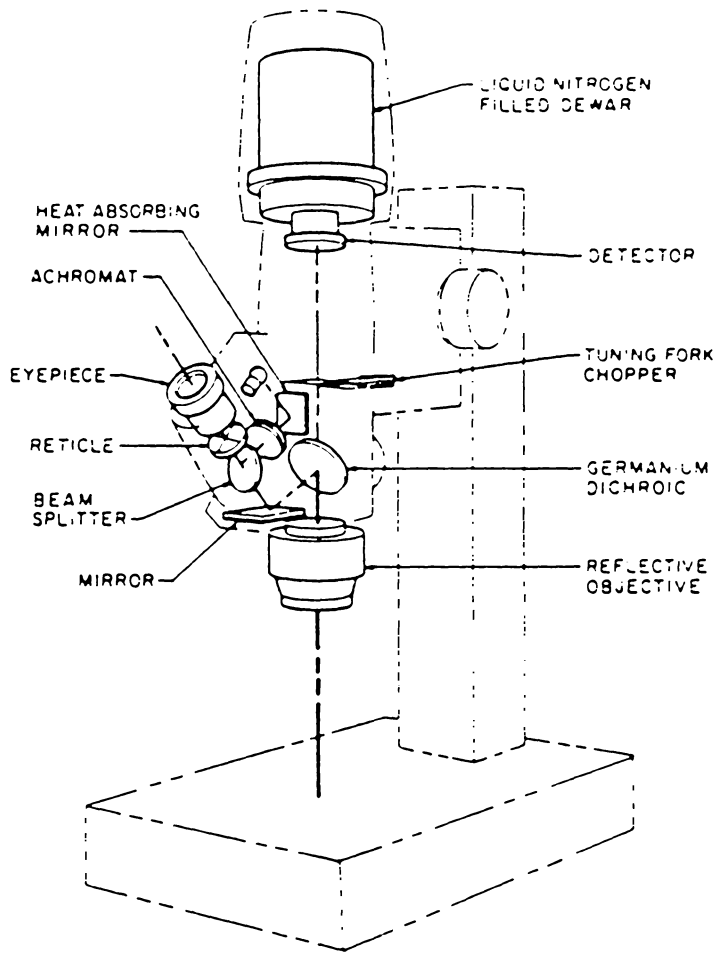

Figure 13. Optical Diagram of the RM-2A Infrared Microscope [51]

target to the ambient radiation which is the radiation emitted by the blades. The infrared detector, indium antimonide, produces an AC electrical output that is proportional to the difference between the radiation received during the opened and closed intervals of the chopping cycles. The detector is mounted within a stainless dewar for cooling to liquid nitrogen temperature, which is a constant 77°K.

The microscope unit also has a preamplifier (see Fig. 14) which amplifies the detector output signal to an amplitude and impedance level suitable for transmission through a cable to the control unit.

The control unit contains the main processing circuits. These circuits further amplify the electrical signal from the preamplifier in the microscope unit and produce a direct readout proportional to the target temperature. The preamplifier signal can either be processed by the control unit's circuits, or be made available directly at an output jack on the rear panel, thus bypassing these circuits. At the input to the first amplifier, in the control unit, is the emissivity control, by means of which the amplifier gain may be increased to compensate automatically for targets having emissivities less than unity.

As with any infrared instrument, the temperature resolution of the RM-2A radiometric microscope depends on the temperature being measured. Figure 15 shows the temperature resolution of the RM-2A with the electrical bandwidth set to 1 Hz. Since temperature resolution improves with decreasing bandwidth, the narrowest bandwidth consistent with the response time needed should always be used. Figure 16 shows how tem-

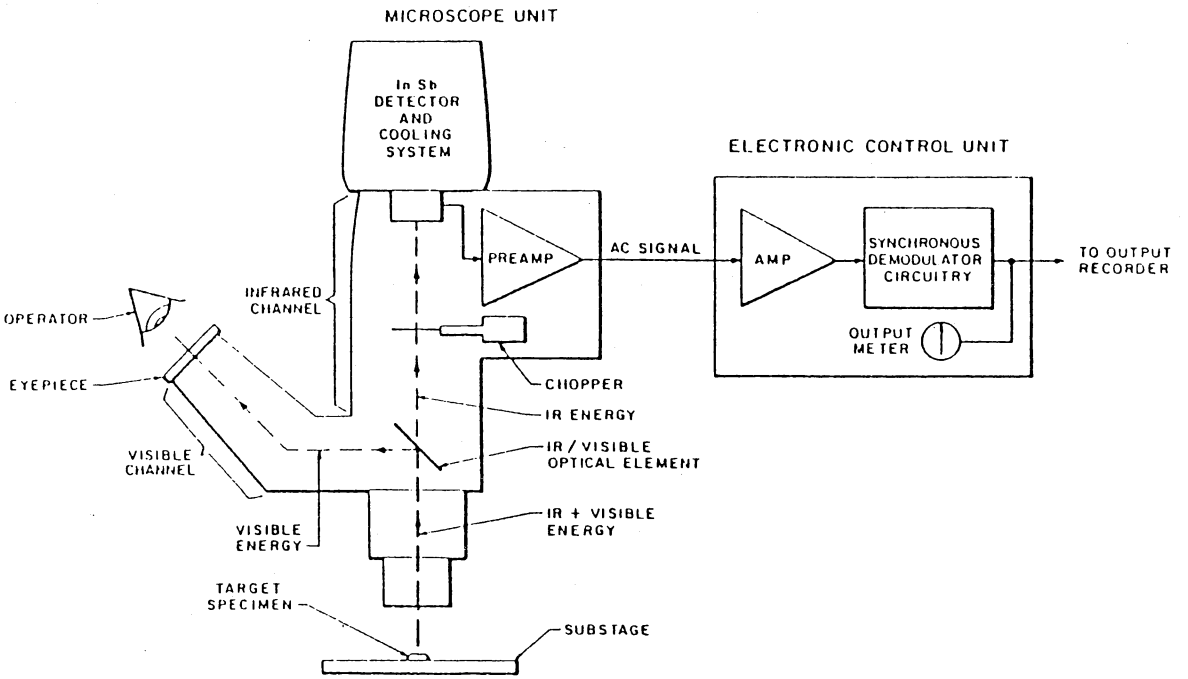

Figure 14. Functional Diagram of the RM-2A [51]

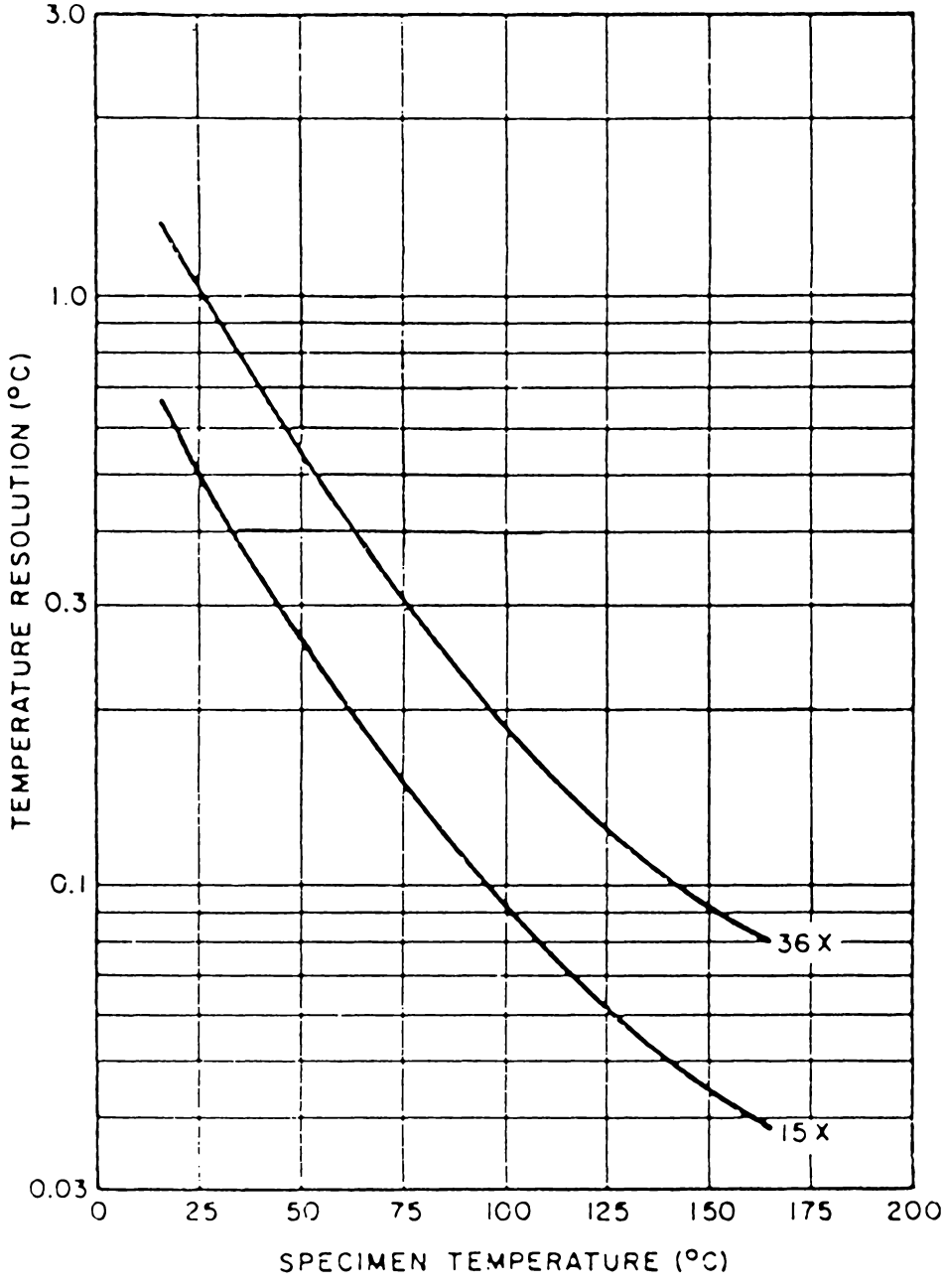

Figure 15. RM-2A Temperature Resolution, Bandwidth of 1Hz [51]

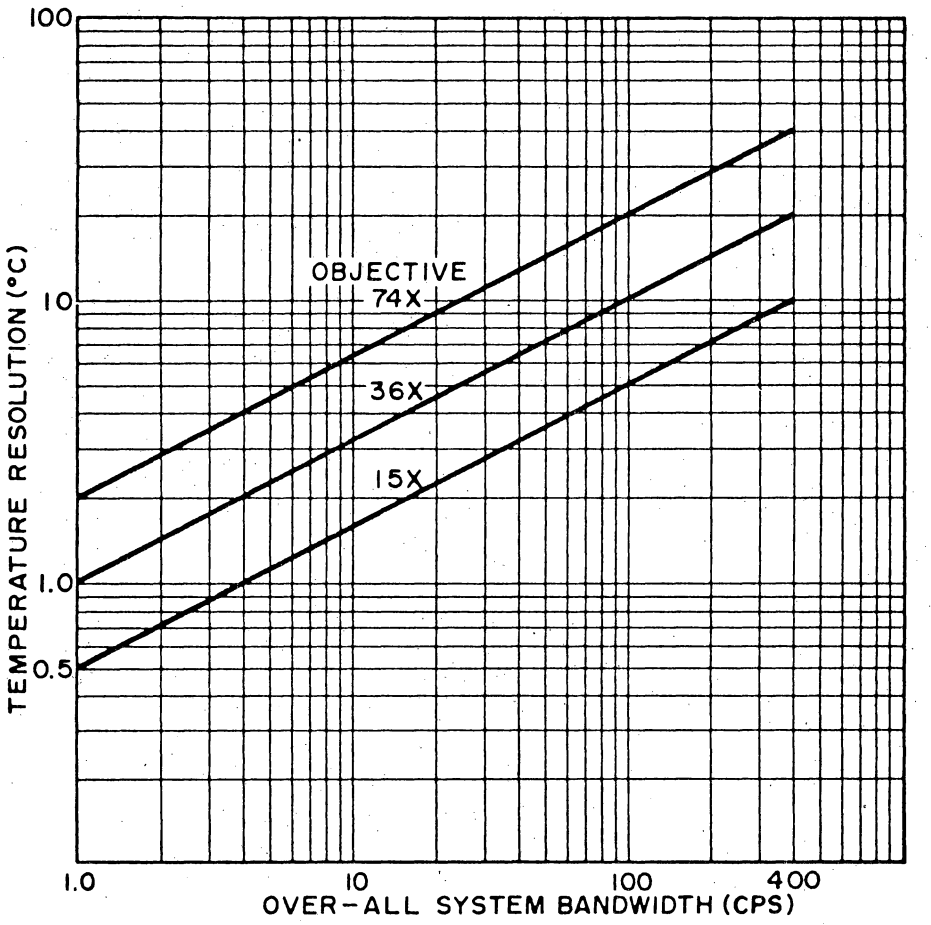

25°C SPECIMEN

Figure 16. Temperature Resolution of RM-2A for Bandwidth [51]

perature resolution varies with the system band width when measuring a 25°C specimen [48].

A Barnes Model RM121-1 Calibration Source was used to calibrate the microscope (Fig. 17). This calibration device is a self-contained, temperature controlled, infrared radiation source. It was made especially for calibrating the infrared radiometric microscopes made by Barnes Engineering Company. The calibration source consists of a source cavity and a wide range temperature controller which regulates the source cavity temperature to within ± 1°C (over a range from 60°C to 230°C).

The microscope unit is positioned on a precision X-Y table. This X-Y table enables the microscope to scan the contact. Linear variable differential transformers (LVDT's) are mounted to the table and stationary base in both the X and Y direction (Fig. 18). From the LVDT outputs, the exact position of the microscope within a contact zone can be determined.

Friction measurements were made with the aid of a Lebow miniature torque transducer (Fig. 19). The torque transducer was placed between the drive gear and the sapphire disk shaft. By knowing the radius at which the specimen was run from the center of the shaft and the normal load of the specimen against the sapphire, the coefficient of friction can be calculated.

A specimen is loaded against a sapphire disk by means of a balance beam that was designed not to produce an unbalanced moment (Fig. 20). The specimen was held at one end of the beam and the beam counter-

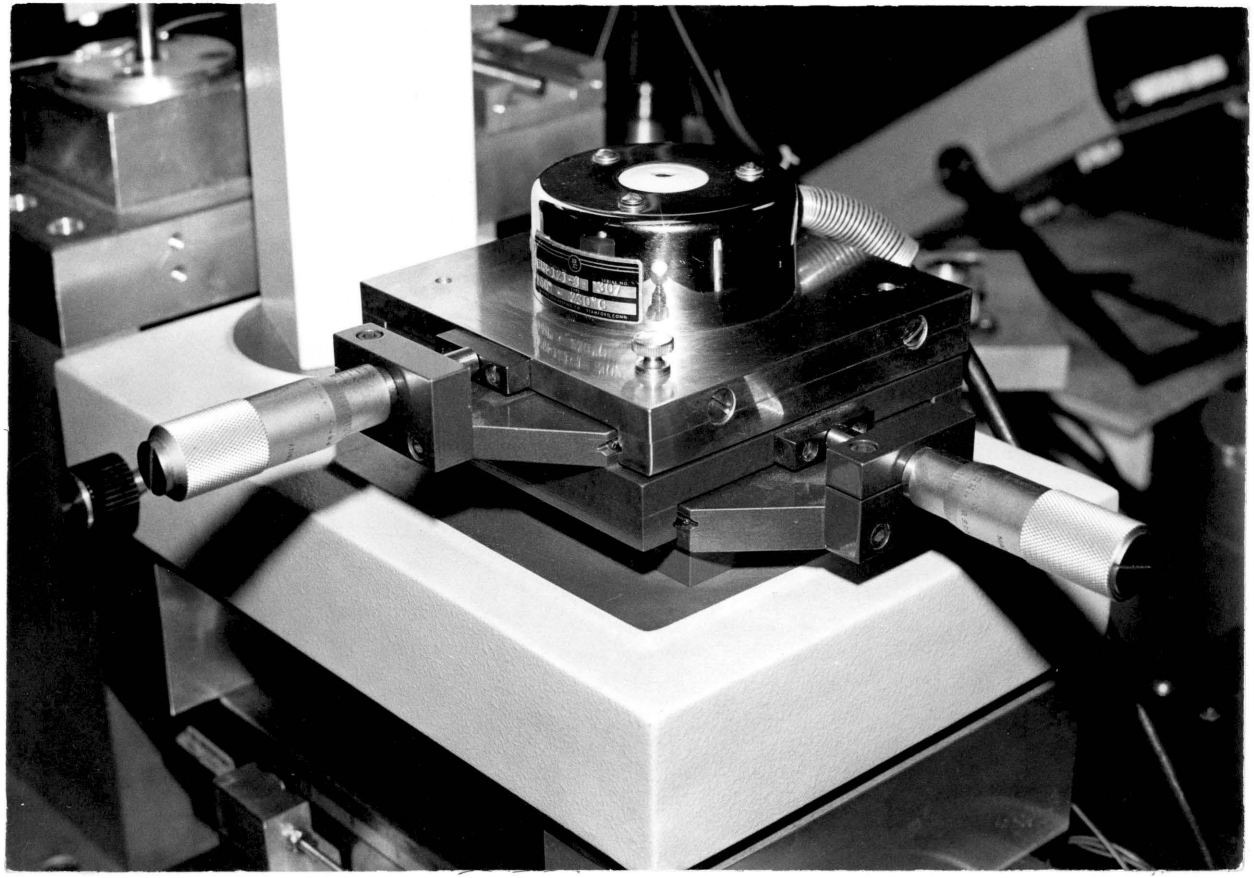

Figure 17. Model RM121-1 Calibration Source

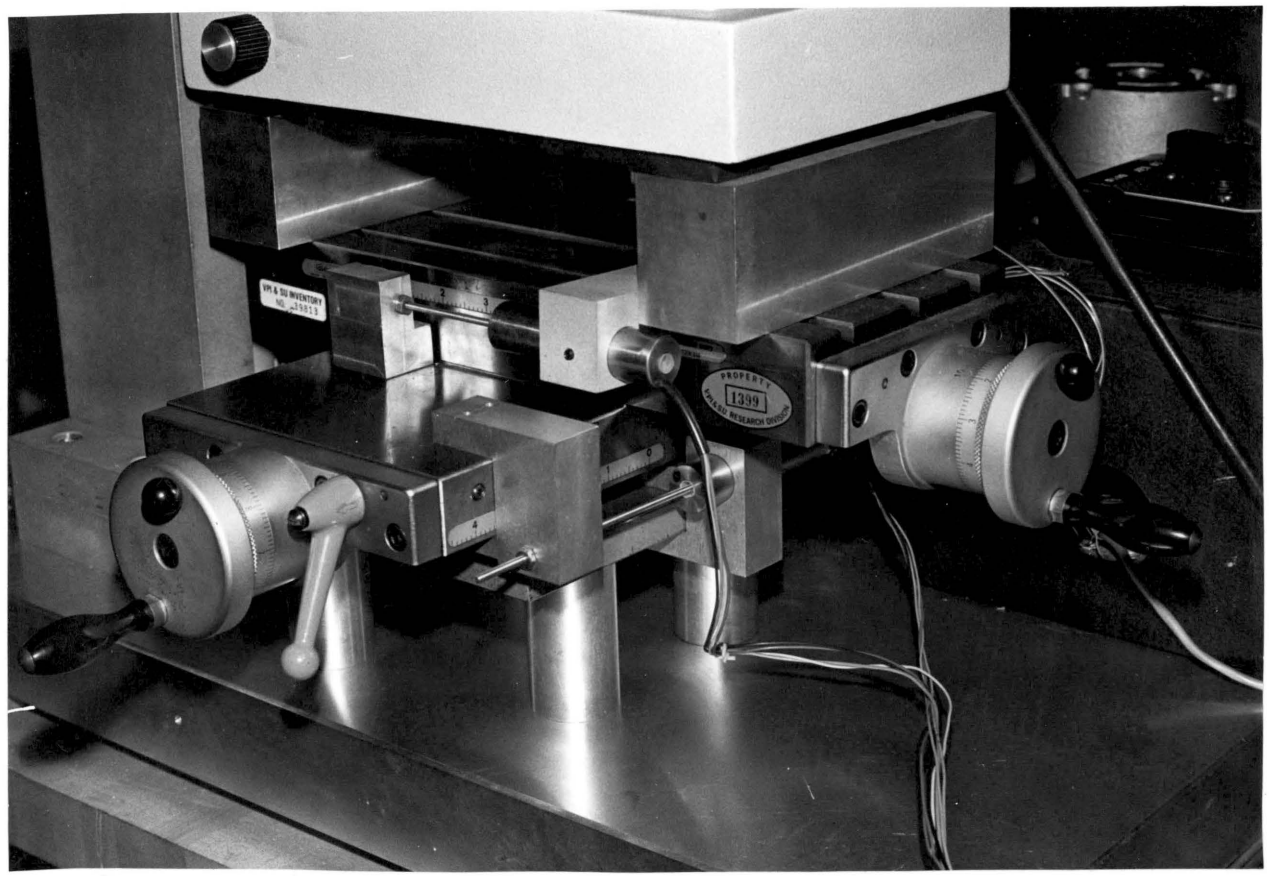

Figure 18. The Precision X-Y Table and LVDT's

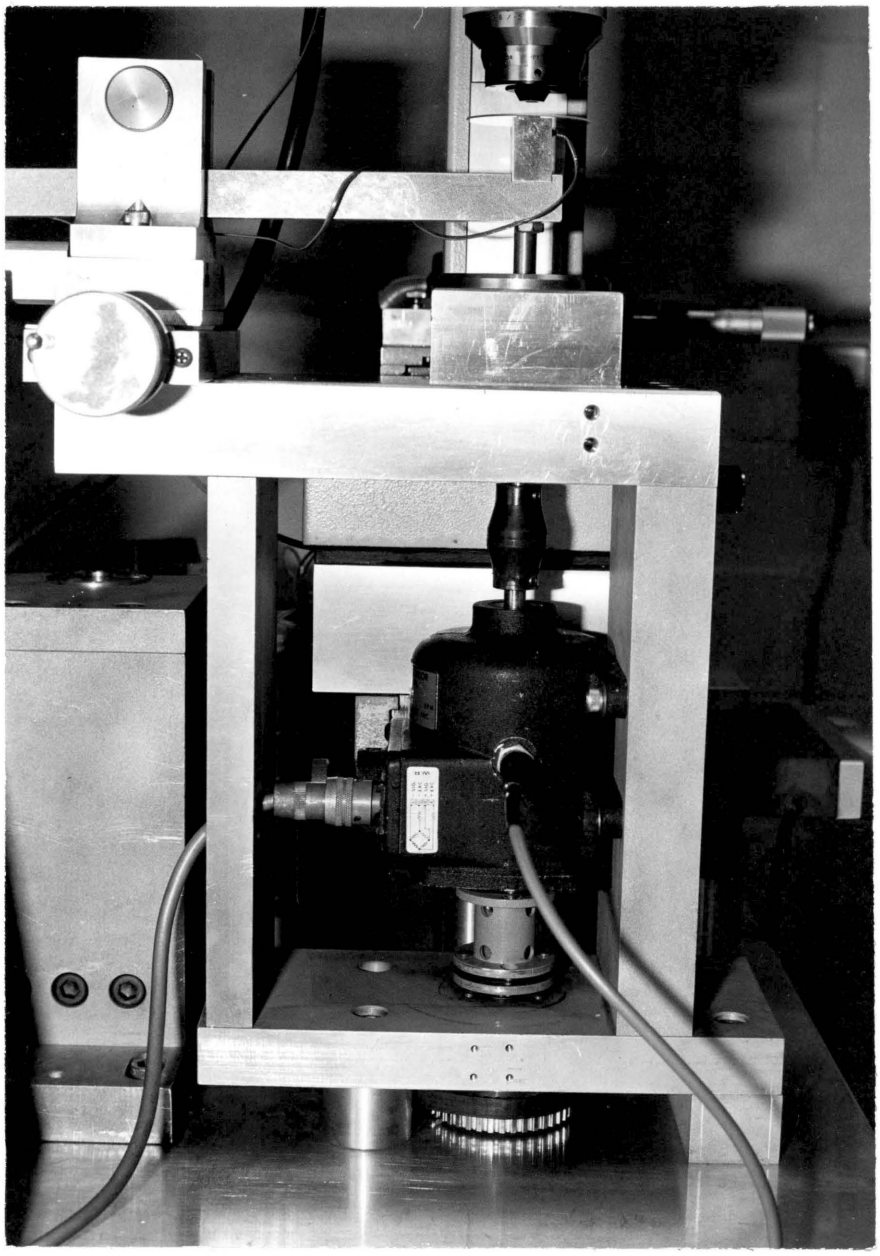

Figure 19. The Lebow Miniature Torque Transducer

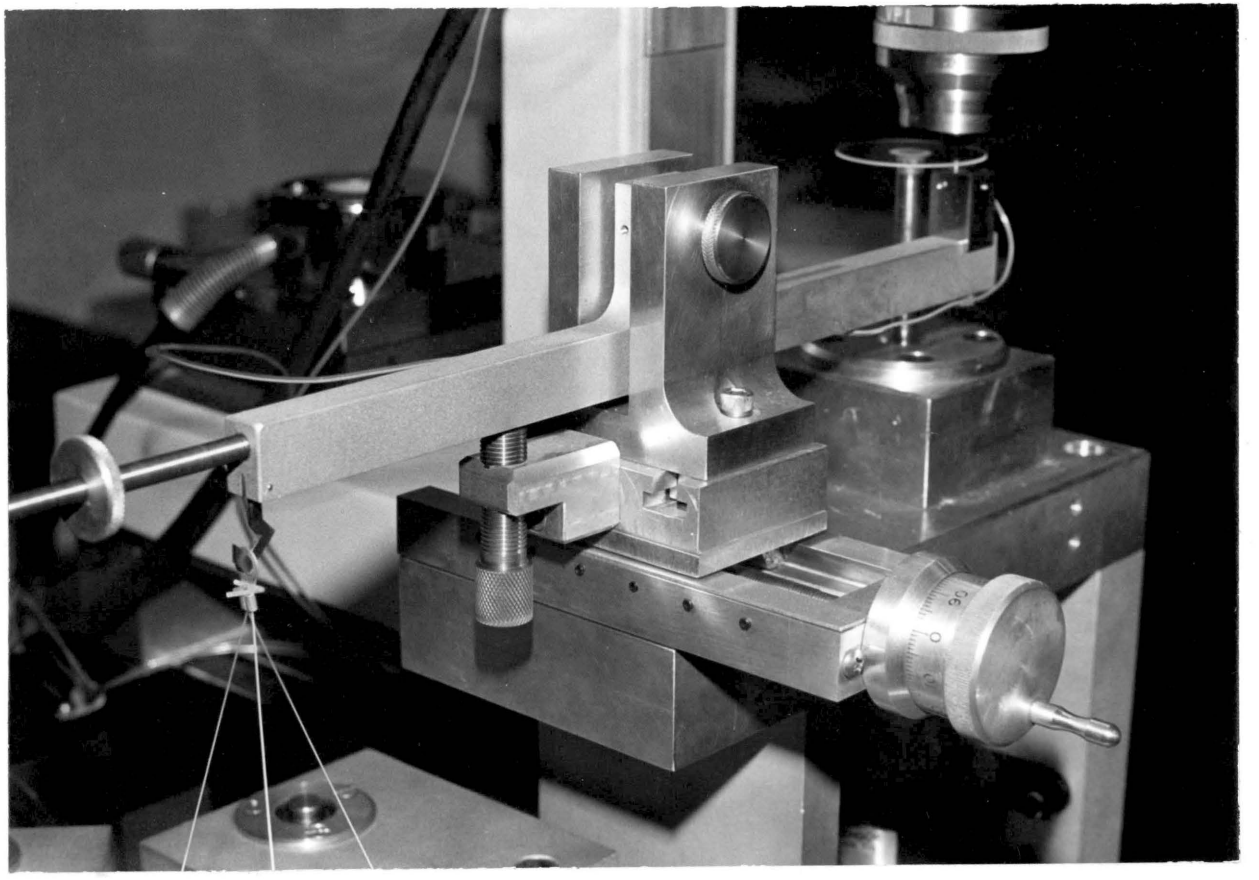

Figure 20. The Balance Beam System

balanced by means of a weight which can be moved along a threaded rod. Weights were then added to the bowpan which applies a normal load to the sapphire disk equal to the weights in the bowpan. This entire assembly was mounted on a linear displacement slide so the specimen could be positioned at any desired radial distance on the sapphire disk.

The sapphire disk is driven by a series of pulleys and belts by a hysterisis synchronous motor (Fig. 21). This arrangement allows for a large selection of speeds (from 1.125 rpm to 28800 rpm).

The selection of metals to be used in this type of study was extremely important. There are several material properties and behaviors that must be examined before a metal is selected as a medium for this type of experimental investigation. One important factor which determines most dramatically if a material can actually be used is its tendency to transfer onto the sapphire disk during sliding contact. Any metal transfer to the disk can reduce the transmittance drastically.

One of the first choices of a material in this study was aluminum. The aluminum used in preliminary tests was a 1100-alloy of 99% purity. With a normal load of 1.0 N and a sliding velocity of 2 m/sec and contact time of 15 seconds against the sapphire disk, enough transfer of the aluminum to the sapphire had occurred to reduce the external transmittance of the disk from 85 to 43%. Not only was material transfer a problem but with even a short contact time as 15 seconds, the aluminum scratched the sapphire disk. This was determined by cleaning the transferred aluminum off the disk and running a Talysurf trace across the wear track of the disk. The fact that aluminum scratches

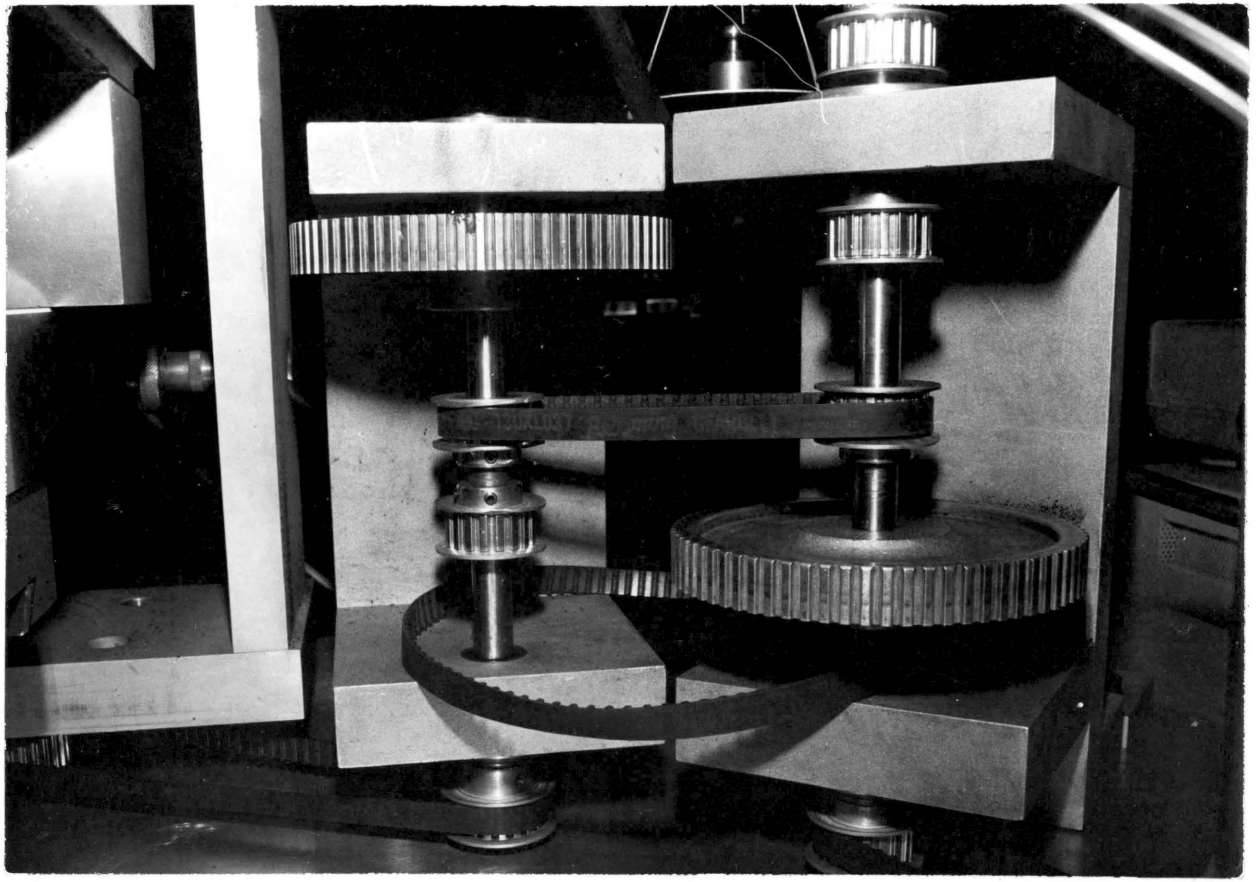

Figure 21. The Drive Belt System

sapphire is interesting to note, being that the hardness of aluminum is 2.94×10^8 N/m^2 and that of the sapphire is 1.770×10^{10} N/m^2 or 9 on the Mohs hardness scale. The fact that the aluminum scratched the sapphire disk illustrates the importance of considering not only the bulk material and its properties, but also its oxides and its physical, thermal and chemical properties and how it might react with sapphire. It has been suggested that, in the case of aluminum on sapphire, it was actually the aluminum oxide, a well known abrasive, which caused the scratching of the disk. Sapphire, being an aluminum oxide itself, may very likely have high compatibility with the aluminum and therefore high adhesion forces which cause material transfer.

The material finally selected for this study was an electrolytic copper alloy of 99.9% purity (see Table 1). This selection was made after preliminary testing which resulted in the following information. Copper, unlike aluminum, displayed no transfer to the disk and the specimen did not scratch the disk. After preliminary tests were completed, emissivity data were taken. From the emissivity data it was learned that copper exhibits a characteristic that is very advantageous for the kinds of tests which were planned. The copper specimens had two very different and distinct emissivity levels. One level was very low, approximately 0.10, and appeared to correspond visually to an area of 'clean' metal where there was no oxide formation. The other level is what was considered a 'high' level, approximately 0.55, which seemed to correspond to the areas covered by an oxide from visual observation. It is not absolutely clear that the high level emissivity corresponded to

TABLE 1

MATERIAL PROPERTIES

	Copper [52]	Sapphire [53,52]
Modulus of Elasticity (N/m^2)	1.14×10^{11}	3.65×10^{11}
Density (kg/m^3)	8.90×10^{3}	3.98×10^{3}
Specific Heat (Joules/kg.°C)	3.94×10^{2}	4.20×10^{2}
Thermal Conductivity (Joules/sec.m.°C)	3.72×10^{2}	4.18×10^{1}
Hardness (N/m^2)	7.85×10^{8}	1.77×10^{10}
Melting Point (°C)	1.08×10^{3}	2.31×10^{3}
Poisson's Ratio	3.30×10^{-1}	2.00×10^{-1}

an oxide or what type of oxide existed on the surface at all, but with visual observation through the optical channel of the radiometric microscope this conclusion seems reasonable. The reason this bi-level emissivity is so important is that, with any metals, the emissivity changes over a wide range during a test and the dynamic nature of the emissivity makes it very difficult to convert the radiance to temperature. It was hoped that the bi-level nature of the copper would be clearly evident in the radiation data and therefore make it easier to convert this radiance to surface temperature.

3.2 Radiation Analysis

Figure 22 shows the components of the radiation received by the infrared detector. There are three sources of areal radiant intensity N_o - due to reflected ambient background radiation, N_d - due to emission from the sapphire disk, and N_s - due to emission from the specimen. There is an attenuation factor associated with each of these radiation components caused by absorption of the sapphire disk and Fresnel reflection losses. To see where and how these factors operate on a sapphire disk with an air interface on the top and bottom surface of the sapphire disk we can use a ray-tracing technique. The model of an air interface on the top and bottom surface of the sapphire disk is the working system when the internal transmissivity and external transmittance is being evaluated (Fig. 23).

Referring to Figure 23, consider a unit intensity incident on the upper boundary. At contact with the first interface, an amount ρ is reflected so that $(1-\rho)$ enters the material of this, $(1-\rho)\tau$ is transmitted to the bottom surface which means that $(1-\rho)(1-\rho)$ is absorbed along the path. When the ray of intensity $(1-\rho)$ reaches the bottom surface, $\rho(1-\rho)\tau$ is reflected and consequently $(1-\rho)^2\tau$ passes out of the plate through the lower boundary. As the process continues, the fraction of incident energy reflected by the plate is the sum of the terms leaving the top surface:

$$R = \rho[1+(1-\rho)^2\tau^2(1+\rho^2\tau^2+\rho^4\tau^4\cdots)] = \rho\left[1+\frac{(1-\rho)^2\tau^2}{1-\rho^2\tau^2}\right] \qquad (43)$$

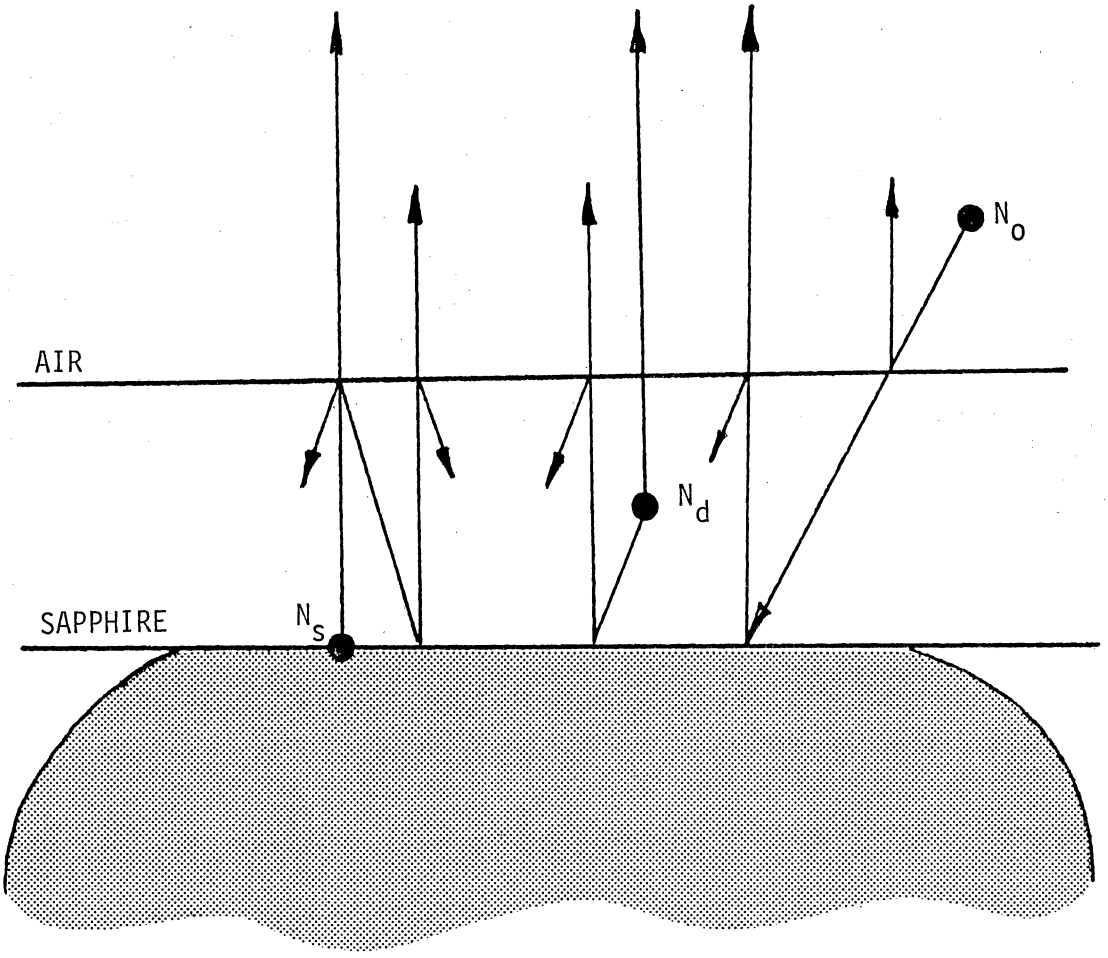

Figure 22. Components of Radiation Received by the Infrared Microscope

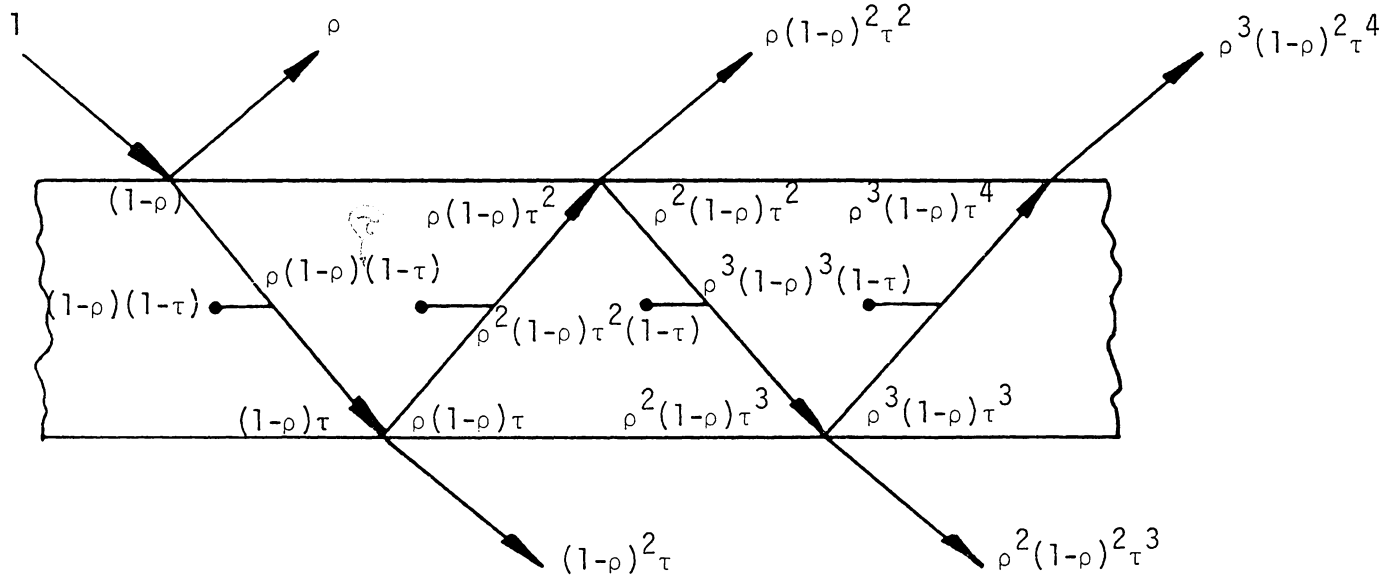

Figure 23. Ray Tracing of an Air-Sapphire-Air System

The fraction transmitted, (external transmittance), is the sum of terms leaving the bottom surface:

$$T = \tau(1-\rho)^2[1+\rho^2\tau^2+\rho^4\tau^4+\cdots] = \frac{\tau(1-\rho)^2}{1-\rho^2\tau^2} = \tau\frac{1-\rho}{1+\rho}\frac{1-\rho^2}{1-\rho^2\tau^2} \tag{44}$$

The last term on the right, $\frac{1-\rho^2}{1-\rho^2\tau^2}$, is often close to unity, which yields

$$T = \tau\frac{1-\rho}{1+\rho} \tag{45}$$

The fraction of energy absorbed is

$$A = (1-\rho)(1-\tau)[1+\rho\tau+\rho^2\tau^2+\rho^3\tau^3+\cdots] = \frac{(1-\rho)(1-\tau)}{1-\rho\tau} \tag{46}$$

In the above equations, ρ is introduced as the Fresnel reflection. For smooth surfaces Fresnel derived expressions for the reflectivity of unpolarized radiation on passing from a medium 1 with a refractive index, n, to medium 2 with a reflective index of n_2 as:

$$r_{\perp} = \frac{\sin^2(\theta_2-\theta_1)}{\sin^2(\theta_2+\theta_1)} \tag{47}$$

$$r_{\parallel} = \frac{\tan^2(\theta_2-\theta_1)}{\tan^2(\theta_2+\theta_1)} \tag{48}$$

$$r = \frac{I_{\perp}}{I_{\parallel}} = \frac{1}{2}[r_{\perp} + r_{\parallel}] \tag{49}$$

where Θ_1 and Θ_2 are the angles of incidence and refraction, as shown in Figure 24 [49]. Equation (47) represents the perpendicular component of unpolarized radiation, $r_{\perp}$, and equation (48) represents the parallel component of unpolarized radiation, r_{11}. The terms parallel and perpendicular refer to the plane defined by the incident beam and the surface normal. Equation (49) then gives the reflection of unpolarized radiation as the average of the two components. The angles Θ_1 and Θ_2 are related to the indices of refraction by Snell's law

$$\frac{n_1}{n_2} = \frac{\sin\Theta_2}{\sin\Theta_1} \tag{50}$$

Thus, if the angle of incidence and refractive indices are know, equations (47) through (50) are sufficient to calculate the reflectance of the single interface.

For radiation at normal incidence, both Θ_1 and Θ_2 are 0, then equations (49) and (50) can be combined to yield

$$r(0) = \left[\frac{(n_1 - n_2)}{(n_1 + n_2)}\right]^2 \tag{51}$$

If one medium is air, which has a refractive index of nearly unity, equation (51) becomes

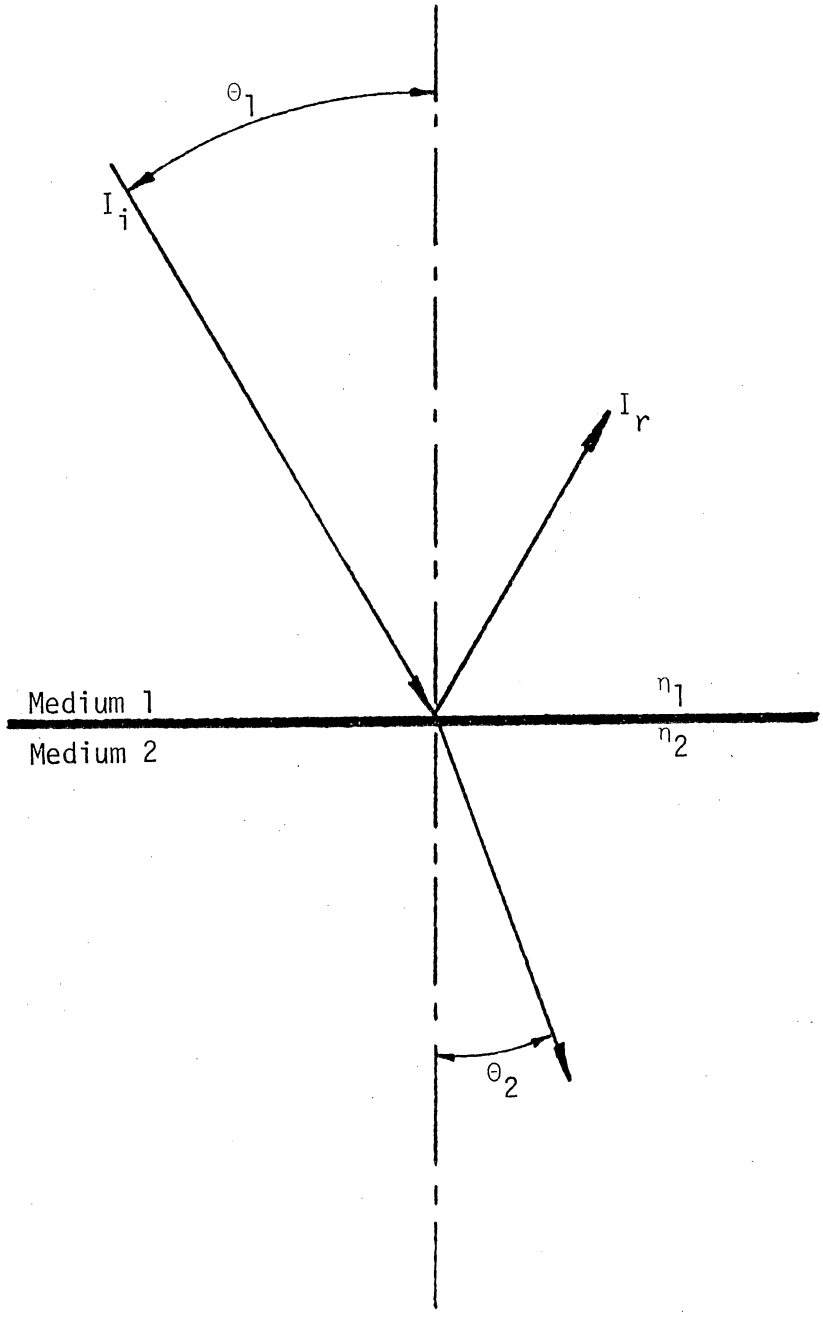

Figure 24. Angles of Incidence and Refraction in Media Having Different Refractive Indices

$$r(0) = \left[\frac{n-1}{n+1}\right]^2 \tag{52}$$

The system is changed fundamentally when the bottom air-sapphire interface is replaced with an opaque smooth metal surface against the sapphire. Referring to Figure 25, and applying the ray tracing technique to radiation being emitted from the opaque metal surface, the following equation for external transmittance appears.

$$\begin{aligned} T &= (1-\rho)\tau+(1-\rho)\rho\rho_s\tau^3+(1-\rho)\rho^2\rho_s^2\tau^5+\cdots \\ &= (1-\rho)\tau[1+\rho\rho_s\tau^2+\rho^2\rho_s^2\tau^4+\cdots] \end{aligned} \tag{53}$$

where ρ_s is the reflectivity of the specimen surface.

Most surfaces encountered in engineering applications do not behave like black bodies. To characterize the radiation properties of non-black surfaces, dimensionless quantities such as the emittance and absorptance are used to relate the emitting and absorbing capabilities of a surface to those of a black body. Designating E_λ as the monochromatic emissive power of a real (non-black) surface, the monochromatic hemispherical emittance of the surface, ε_λ, is defined by the relation

$$E_\lambda = \varepsilon_\lambda E_{b\lambda} \tag{54}$$

where $E_{b\lambda}$ is the monochromatic emissive power of a black body. Restated, ε_λ is the percentage of black body radiation emitted by the

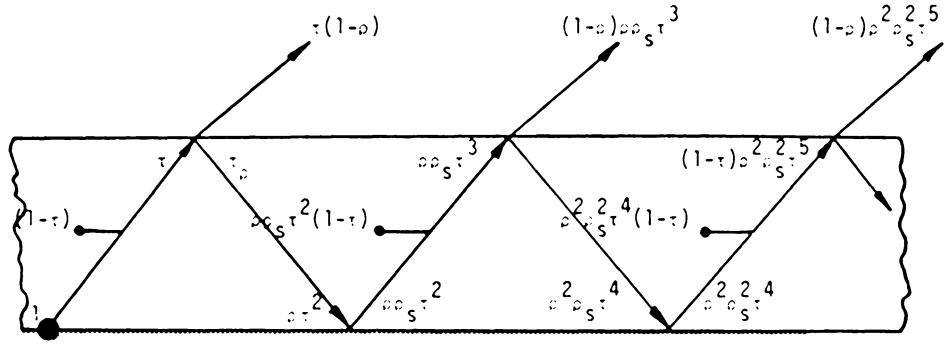

Figure 25. Ray Tracing of Specimen Radiation

surface at the wavelength, λ. The hemispherical monochromatic absorptance of a surface, $\alpha\lambda$, is defined as the percentage of the total radiation incident on the surface which is absorbed. An important relation between $\varepsilon\lambda$ and $\alpha\lambda$ can be obtained from Kirchhoff's radiation law which states in essence that the monochromatic emittance is equal to the monochromatic absorptance for any surface. However, even though the relation $\varepsilon\lambda = \alpha\lambda$ is valid, the total values of absorptance and emittance are, in general, different. They are only equal when the following condition prevails:
if $\varepsilon\lambda$ and $\alpha\lambda$ are uniform over the entire wavelength spectrum. Such surfaces are called gray bodies. Even though most real materials do not meet this specification exactly, it is often possible to choose suitable average values for the emittance and absorbance to make the gray body assumption acceptable for engineering analysis.

When a surface does not absorb all the incident radiation, the portion not absorbed will either be transmitted or reflected. Most solids, such as metal specimens, are opaque and do not transmit radiation. The portion of the irradiation which is not absorbed is, therefore, reflected back into hemispherical space. This may be expressed as the hemispherical reflectance, ρ_s, which for nontransmitting materials the following relation holds:

$$\rho = 1 - \alpha \tag{55}$$

For the most general case of a material which partly absorbs, partly reflects, and partly transmits radiation incident on its surface, the total relation between reflectance, absorptance and transmittance is:

$$\rho+\alpha+\tau = 1 \tag{56}$$

Noting that this expression is to be applied to a smooth metal surface we shall assume τ is negligible and $\alpha = \varepsilon$ which results in

$$\rho_s+\varepsilon = 1 \tag{57}$$

or

$$\rho_s = 1-\varepsilon \tag{58}$$

The same technique used to derive equation (53) for radiation being emitted from the metal surface through the sapphire disk can be used to model the system of ambient radiation being reflected from the top surface of the sapphire disk and from the smooth metal surface (Fig. 26). Applying this ray-tracing technique and summing the terms of the quantity of radiation being directed towards the microscope yields:

$$\begin{aligned} R &= \rho+\rho_s(1-\rho)^2\tau^2+\rho_s^2(1-\rho)^2\tau^4\cdots \\ &= \rho+[\rho_s(1-\rho)^2\tau^3(1+\rho_s\tau^2+\rho_s^2\tau^4+\ldots)] \end{aligned} \tag{59}$$

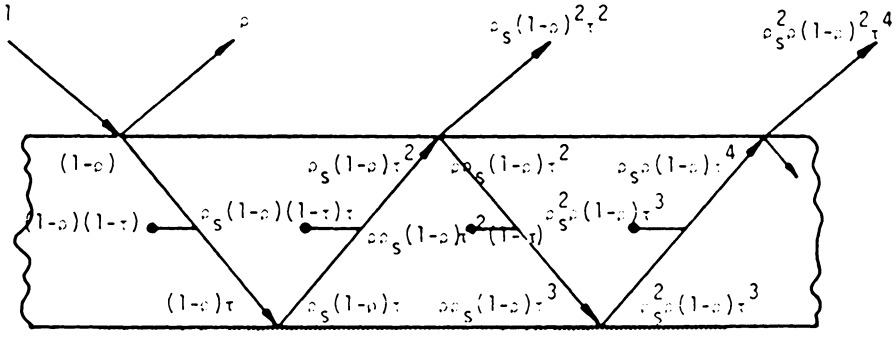

Figure 26. Ray Tracing of Ambient Radiation

Combining the above derived equations into an expression that yields the quantity of radiation that is received by the microscope results in

$$N_{TOTAL} = TN_s + RN_o \tag{60}$$

where T is defined by equation (53) and R by equation (59). N_s is the quantity of radiation emitted by the specimen and N_o is the amount of ambient radiation.

3.3 Basic Operational Theory of the Radiometric Microscope [51]

Objects at the same temperature radiate different amounts of infrared energy depending upon their emissivities. Emissivity is a term used to describe a target's radiating efficiency. A black body which is a perfect emitter and absorber of infrared energy has a emissivity of 1.0; all practical materials have an emissivity less than 1.0.

The term radiance is defined as the radiation power emitted into a unit solid angle from a surface unit area and can be expressed as

$$N = \varepsilon_t N_{BB} \tag{61}$$

where N = radiance emitted by target

ε_t = emissivity of the target

N_{BB} = radiance of a black body at the same target temperature

In order to determine exact values of target temperature, the infrared radiometric microscope must distinguish between the radiance emitted by a target and the background radiance reflected from it. The total radiance collected by the microscope is given by:

$$N_{TOTAL} = N+(1-\varepsilon_t)N_o \tag{62}$$

where:

N_{TOTAL} = total radiance collected from the target

N = radiance emitted by target

$(1-\varepsilon_t)N_o$ = radiance reflected by target

$(1-\varepsilon_t)$ = ρ, the target reflectivity

N_o = radiance emitted by ambient background

or, substituting Equation (61),

$$N_{TOTAL} = \varepsilon_t N_{BBT} + (1-\varepsilon_t)N_o \tag{63}$$

Note that if the target emissivity is unity, the total radiance collected from the target is given by N_{BBT}, the radiance of an ideal black body at the same temperature.

The Barnes Model RM-2A Radiometric Microscope contains a black body source (chopper) at ambient temperature. The mechanical chopper situated between the germanium dichroic and In-Sb detector (Figure 13) exposes the detector to the incident radiation and then to the black body cavity. Since the collected radiation is chopped with a 50% duty cycle, the detector observes the total radiance only one-half of the time. During the interval that the incoming radiation is blocked by the chopper, the detector receives ambient background radiation. The magnitude of the detector electrical output over one cycle or more is equal to the difference between the total radiance collected from the target and that of the background.

$$E = k(N_{TOTAL} - N_o) \tag{64}$$

where k is an experimentally determined instrument constant (see Appendix A).

The RM-2A infrared microscope (or any infrared detector system) does not have an ideally flat spectral response, transmission or reflection characteristics. Due to this fact, a new term is used which refers to the radiance "seen" by the detector and therefore accounts for the non-flat spectral response. The term is "effective black body radiance". As was stated earlier, the microscope unit produces an electrical output which is proportional to the radiation it "sees" or the effective black body radiance. The effective black body radiance can be described analytically as

$$N_{BBeff} = \int_0^\infty \frac{R(\lambda)}{R_{peak}} \cdot N_{BB(\lambda)} d\lambda \tag{65}$$

where $R(\lambda)$ = detector spectral response

R_{peak} = peak detector response

$N_{BB(\lambda)}$ = black body spectral radiance

N_{BBeff} = effective black body radiance

Barnes Engineering Company has computed N_{BBeff} for various temperatures using the spectral response of the microscope detector and optics. These data are plotted as Effective Black Body Radiance vs. Temperature and can be seen in Appendix E.

With the use of the microscope's spectral response curve it is possible to numerically evaluate equation (65) and, to calculate a temperature mathematically rather than using the curves in Appendix E. This method was used to convert the raw data to temperature as will be explained in the next sections. The method begins with the spectral response curve for this particular unit, which was supplied by Barnes Engineering Company (Fig. 27). This spectral response curve has already been normalized, where the highest peak is equal to 100%. From equation (65) this curve represents $R(\lambda)/R_{peak}$. $N_{BB(\lambda)}$ is the spectral radiant intensity of a black body at a given temperature and is defined as

$$N_{BB(\lambda)} = e_{\lambda b}(\lambda) = \pi i_{\lambda b}(\lambda) = \frac{2\pi C_1}{\lambda^5 (e^{c_2/\lambda T} - 1)} \qquad (66)$$

where $e_{\lambda b}(\lambda)$ = Planck's spectral distribution of emissible power

$i_{\lambda b}(\lambda)$ = Spectral Radiance intensity of a black body

T = Temperature K°

C_1 & C_2 = Constant in Planck's spectral energy distribution

$C_1 = 0.59544 \times 10^8$ W·nm^4/m^2

$C_2 = 14388$ m·K

From this $i_{\lambda b}(\lambda)$, $[N_{BB(\lambda)}]$, may be found as

$$i_{\lambda b}(\lambda) = \frac{2C_1}{\lambda^5 (e^{c_2/\lambda T} - 1)} \qquad (67)$$

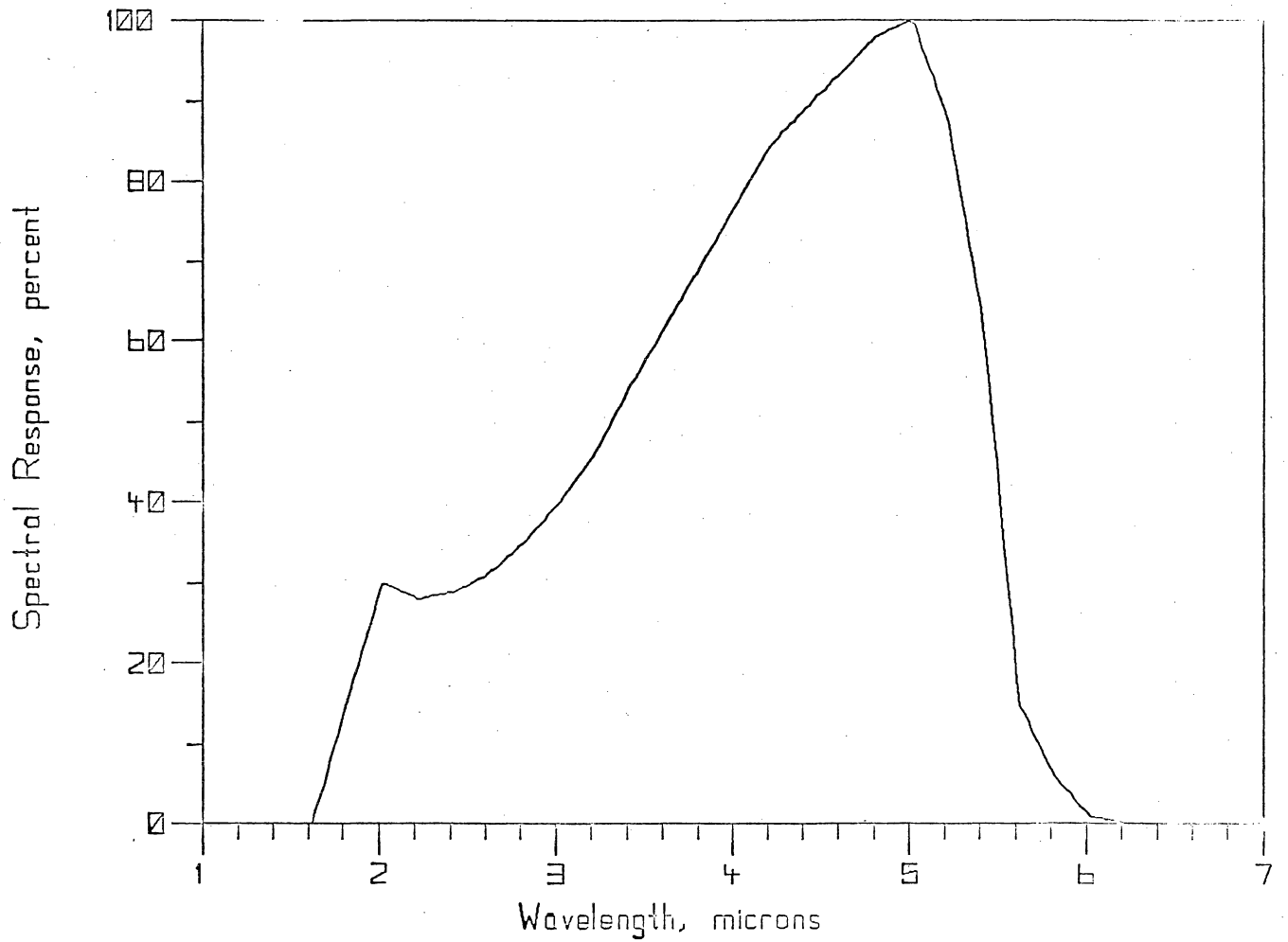

Figure 27. Normalized Spectral Response for the RM-2A Infrared Microscope

the procedure to go from equation (67) to N_{BBeff} is to calculate the black body radiant intensity for wavelengths in the bandwidth of the microscope, 1.6 to 6.2 microns, and then correct this curve by applying the spectral response curve to it (Fig. 28). Once the corrected curve is created which is equivalent analytically to

$$\frac{R(\lambda)}{R_{peak}} \; N_{BB(\lambda)} \tag{68}$$

the area under the curve is evaluated by a numerical integration technique to find N_{BBeff}.

In this study, the raw data, N_{BBeff}, must be converted to a temperature. This is accomplished by a computer program that follows the procedure described above with an interation scheme involved. The objective is to find the temperature corresponding to the radiance read by the microscope. First an initial temperature is guessed and the black body radiant intensity is calculated over the spectral range of the microscope. The radiant intensity is then corrected by multiplying these values by the spectral response at the appropriate wavelength. This new curve is then integrated by Simpson's composite rule of numerical integration. The result from this integration, multiplied by a microscope constant, is the N_{BBeff}. If this value is lower or higher than the measured radiance, then the temperature is altered accordingly until it converges to the same effective radiance. The computer program is listed in Appendix F.1.

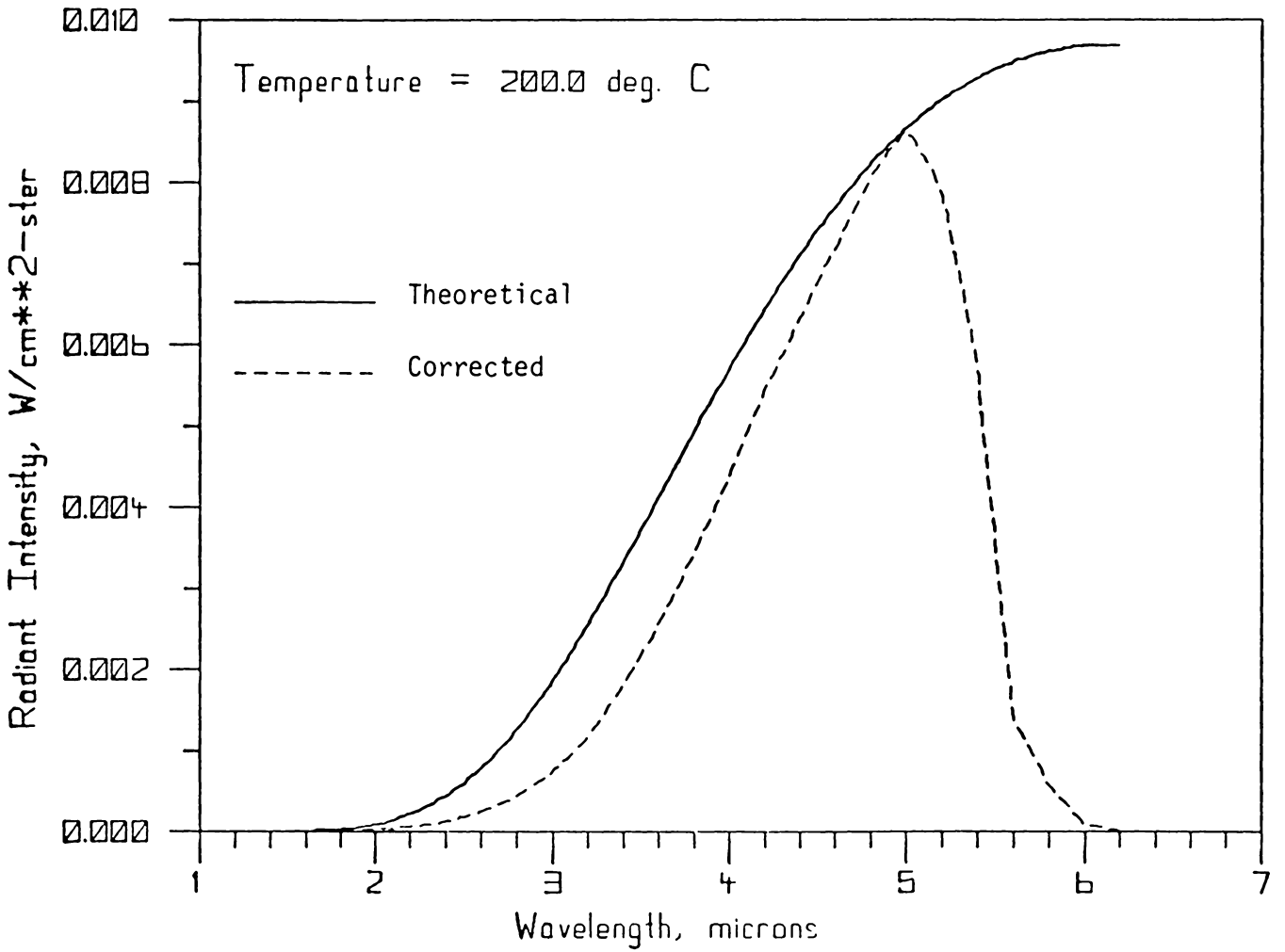

Figure 28. Theoretical and Corrected Radiant Intensity Curves for the RM-2A Bandwidth

3.4 Experimental Determination of Internal Transmissivity of the Sapphire Disk

The internal transmissivity of the sapphire disk must be determined because the external transmittance assumes that there is an air interface on both sides of the sapphire disk as in Fig. 23. When a specimen is loaded against the sapphire, the system changes where the term T of equation (53) is not the same as the external transmittance. The transmittance of the disk with a metal specimen on the bottom interface is a function of the internal transmittance as seen by equation (53).

The internal transmittance can be very easily experimentally determined. The procedure is to heat, preferably, a black body and take a radiance reading. Recalling, the infrared microscope produces a voltage output proportional to the total radiation received minus the ambient background radiation that was zeroed out prior to measurements and is expressed as

$$E = k(N_{TOTAL} - N_o) \tag{69}$$

To determine N_{TOTAL} alone, it is necessary to add N_o to the expression. N_o is obtained by using the calibration curve of effective black body radiance vs. temperature for the RM-2A microscope which accounts for its non-flat spectral response (see Appendix D). To obtain target temperatures from the radiance scale, the target emissivity must be known. The value of radiance ($N_{TOTAL} - N_o$) read on the radiance scale should first be divided by the target emissivity. To this value, the quantity N_o

must be added to obtain the value of effective radiance of a black body at the target temperature, N_{BBT}

$$N_{BBT} = \left[\frac{N_{TOTAL} - N_o}{\epsilon_t}\right] + N_o \tag{70}$$

Note that if the target is a black body, an emissivity of 1.0, then $N_{TOTAL} = N_{BBT}$. Then, to find the radiation emitted by the black body source, the ambient radiation which was zeroed out prior to the measurement is added to the converted electrical output, i.e.,

$$N_{TOTAL} = E_k + N_o \tag{71}$$

The external transmittance of the sapphire disk is the fraction of radiation which is emitted by the black body source and is able to travel through the sapphire disk and reach the infrared detector. Expressed in a different manner, it is the ratio of the radiance read by the microscope when the sapphire disk is between the black body source and the radiance read when the sapphire disk is absent.

The radiance reading used to calculate the external transmittance, by definition, is not corrected for Fresnel reflections of the emitted black body radiance. However the radiance reading must be corrected for the reflected ambient radiation (Fig. 26) and using only two reflections yields the T^2 term in

$$N_{\substack{TOTAL \\ w/DISK}} = \frac{E}{k} + [1-\rho-\rho(1-\rho)^2]N_o \qquad (72)$$

The second reflection is neglected as it has an insignificant effect on the total, less than 1%. The external transmittance is therefore expressed by the following relationship { see Pg 202 for experimental determination

$$T = \frac{N_{TOTAL\ w/DISK}}{N_{TOTAL\ w/o\ DISK}} \qquad (73)$$

Figure 29 is a spectral external transmittance curve reproduced from Optical Properties and Applications of Linde Cz Sapphire [53]. The external transmittance for high temperatures should be very close to the top of the curve within the microscope's region. As the temperature drops, the external transmittance could also fall slightly as the lower the temperature the greater the shift of the spectral radiation distribution curve to the right. With this shift to the right and the decline of the external transmittance at wavelengths greater than 4.0 microns and steep decrease in transmittance beyond 5.0 microns, the weighted or total transmittance is also bound to drop.

In the radiation analysis section of this paper, the expression for transmittance was introduced as

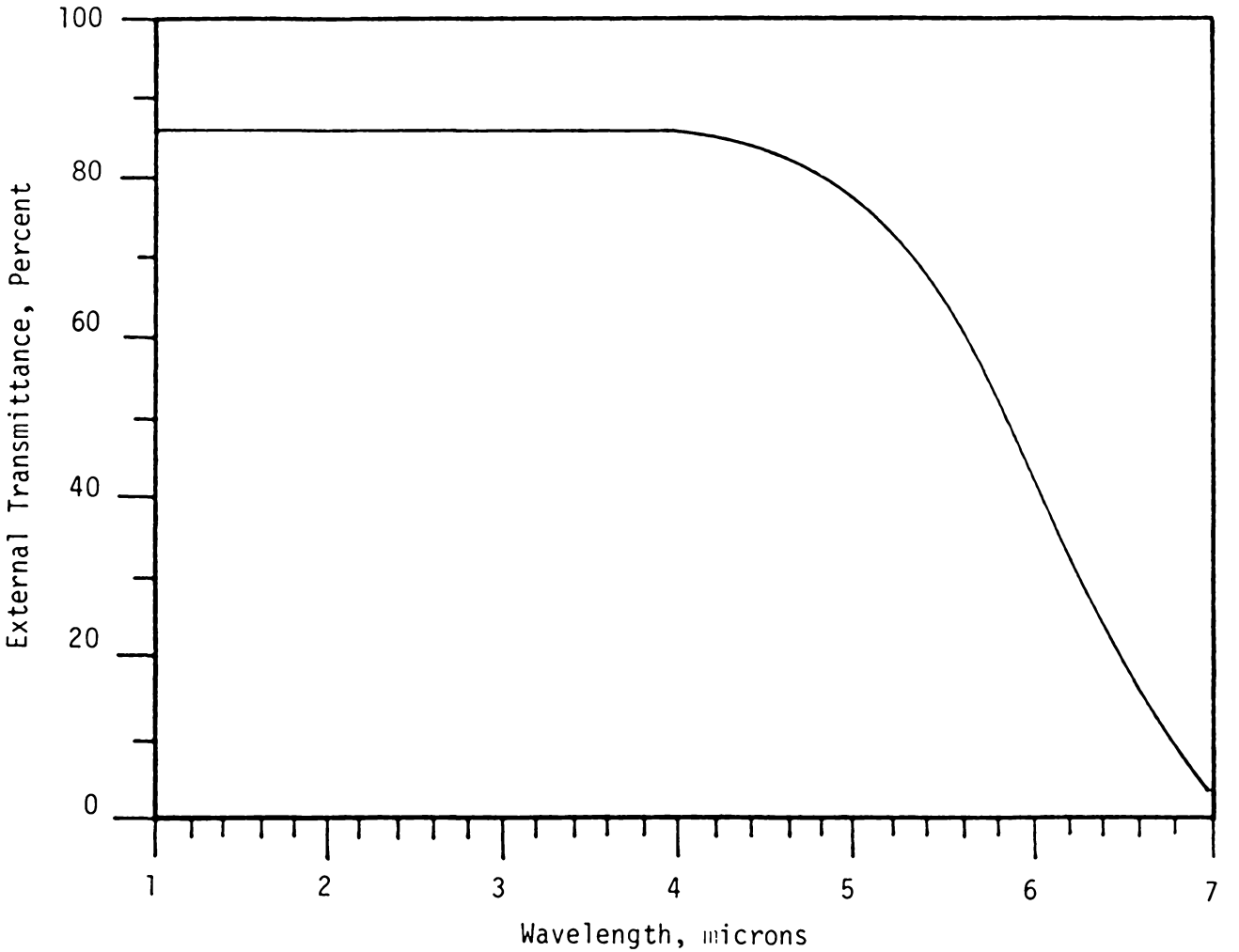

Figure 29. External Transmittance vs. Wavelength

$$T = \tau(1-\rho)^2[1+\rho^2\tau^2+\rho^4\tau^4+\cdots] = \frac{\tau(1-\rho)}{1-\rho^2\tau^2} = \tau\frac{1-\rho}{1+\rho}\,\frac{1-\rho^2}{1+\rho^2}\,\tau^2 \qquad (74)$$

where the last term on the right is close to unity which yields

$$T = \tau\frac{1-\rho}{1+\rho} \qquad (75)$$

From this expression we can calculate, τ, the internal transmissivity. However, ρ, the Fresnel reflection loss coefficient for an air-sapphire interface is not a straight forward calculation as the spectral index of refraction changes by more than 10 percent over the range of the microscope (Fig.30). Figure 31 shows how the Fresnel reflection is affected by this change in the index of refraction. Once an appropriate index of refraction has been selected, and thus the Fresnel reflection coefficient, ρ, it is a simple task to calculate the internal transmissivity.

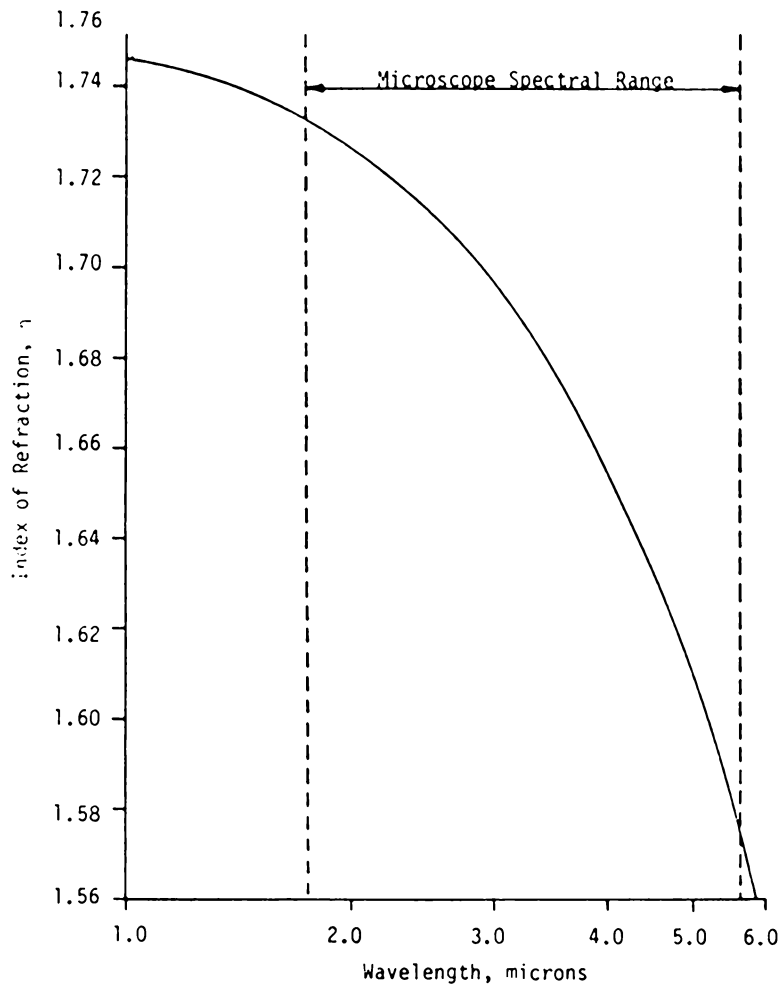

Figure 30. Index of Refraction vs. Wavelength

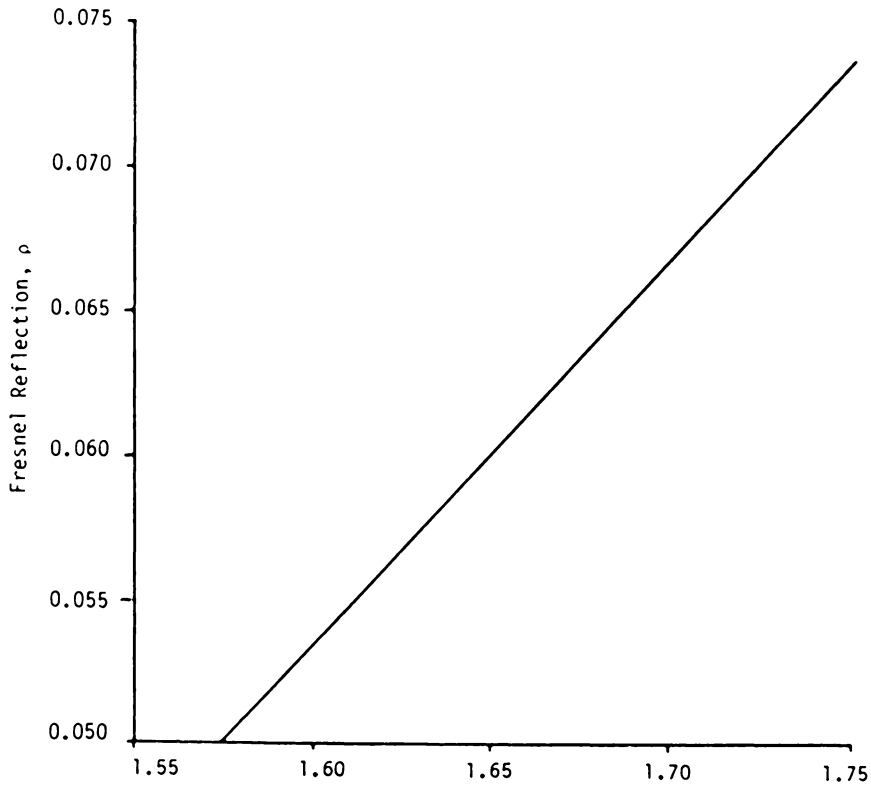

Figure 31. Fresnel Reflection vs. Refractive Index

3.5 Converting the Microscope Output to Temperature

It can be seen from Figure 16 that the total incident areal radiant intensity is given by

$$N_{TOTAL} = \eta_s N_s + \eta_d N_d + \eta_o N_o \tag{76}$$

However, the sapphire disk is expected to have a large temperature gradient throughout its thickness and therefore radiation is emitted from throughout the thickness rather than just at a surface. This is to say that it is expected or assumed that the upper surface of the sapphire disk is at ambient temperature while the lower surface is raised to some higher temperature. Even for extreme cases of high temperature gradients, it can be shown that the contribution of the sapphire radiation is very small.

As an order of magnitude approximation [31], assume that the upper surface of the sapphire disk is at ambient temperature of 25°C and the bottom surface at 115°C. These temperatures correspond to black body areal radiant intensity values of 3.5×10^{-3} and 4.0×10^{-2} watts/cm^2-ster respectively. The radiation emitted by the sapphire should be less than the average of the upper and lower surface radiation values, due to the fourth power relation between temperature and radiant intensity. For an average black body areal radiant intensity of 22×10^{-3} watts/cm^2-ster and a sapphire emissivity of 0.018, the emitted areal radiant intensity becomes 3.96×10^{-3}. This emitted areal radiant intensity is approximately 1 percent of the radiant black body intensity from the

From Figure 26 we can imagine that after some finite number of reflections each additional ray directed toward the microscope will have little effect on the total amount of radiation received by the microscope. Table 2 shows how the ambient radiation is received by the microscope per reflection and from this table it can be stated that there is little advantage in considering any effect of reflections past the third for the reflected background ambient radiation. The attenuation factor for the contribution of the reflected background ambient can be expressed as

$$\eta_o = \rho+\rho_s(1-\rho)^2\tau^2+\rho_s^2\rho(1-\rho)^2\tau^4 \tag{80}$$

Using the same argument as above it is now possible to find the attenuation factor for the emitted specimen radiation. Based on the data of Table 3, we can again state that little is achieved in considering the contribution of the reflections past the second. Therefore the attenuation factor N_s can be written

$$\eta_s = (1-\rho)\tau(1+\rho\rho_s\tau^2) \tag{81}$$

By inserting the attenuation factors into Equation (66) and solving equation (69) as a function of the radiant quantities, it becomes

TABLE 2

THE CONTRIBUTION OF EACH REFLECTION OF AMBIENT RADIATION (ASSUMING AN INTERNAL TRANSMISSIVITY OF 1.0)

η, Index of Refraction of Sapphire 1.65
Fresnel Reflection Coeffient, ρ 0.06016
ρ_s, Reflectivity of Specimen, $\rho_s = 1 - \varepsilon_s$

ρ_s	0.5	0.6	0.7	0.8	0.9
1st Reflection ρ	0.06016	0.06016	0.06016	0.06016	0.06016
2nd Reflection $\rho_s(1-\rho)^2$	0.4416	0.5300	0.6183	0.7066	0.7950
3rd Reflection $\rho^2\rho(1-\rho)^2$	0.01328	0.01913	0.02604	0.03401	0.04304
4th Reflection $\rho_s^3\rho^2(1-\rho)^2$	0.00040	0.00069	0.00110	0.00164	0.00233

TABLE 3

THE FRACTION OF EMITTED RADIATION FROM THE SPECIMEN THAT LEAVES THE TOP SURFACE OF THE SAPPHIRE (ASSUMING AN INTERNAL TRANSMISSIVITY OF 1.0)

η, Index of Refraction of Sapphire 1.65
Fresnel Reflection Coefficient, ρ 0.06016
ρ_S, Reflectivity of the Specimen, $\rho_S = 1-\varepsilon_S$

ρ_S	0.5	0.6	0.7	0.8	0.9
1st Reflection $(1-\rho)$	0.9398	0.9398	0.9398	0.9398	0.9398
2nd Reflection $(1-\rho)\rho\rho_S$	0.02827	0.02827	0.03958	0.04523	0.0508
3rd Reflection $(1-\rho)\rho^2\rho^2_S$	0.00179	0.00204	0.00238	0.00272	0.0030

$$E_k = (1-\varepsilon)\tau(1+\rho\rho_s\tau^2)\varepsilon N_s^{BB} + \{\varepsilon+\rho_s(1-\varepsilon)^2\tau^2+\rho_s^2\varepsilon(1-\varepsilon)^2\tau^4\}N_o \quad (82)$$

From the above equation the N_s^{BB} can be solved as it is the only unknown and then using the calibration curves for the RM-2A the temperature is then determined.

The above analysis is incorporated into a FORTRAN program (see Appendix F.1) which takes the electrical output of the microscope and an emissivity and then proceeds through the above analysis described in Section 3.3 to arrive at a temperature of the specimen.

3.6 Experimental Procedure

The experimental procedure used in this investigation is the single most important factor in being able to confidently and accurately convert the radiance output of the microscope to temperature. This procedure is also of extreme importance in terms of being able to reproduce any of the experimental data. The instrumentation used is a rather complex system (See Fig. 32) and the number of different pieces of information or data needed to make an experiment complete (radiance, torque, position of microscope) requires that a carefully thought out and systematic procedure be developed.

Before beginning any experiments, the specimen was cleaned using a prescribed method developed specifically for the material being used. The sapphire disk was also cleaned before a set of tests were run. Each of the specimens was first checked for any irregularities such as burrs on the surface. The specimens were then rinsed to remove any coarse debris that was on the specimen. All the specimens were soaked in a trisodium phsophate solution for approximately one hour to remove dirt, grit, and grease that the specimens could have accumulated from the machining processes. After the specimens were dried they were rinsed with acetone to remove any residue from the soaking and then rinsed with distilled water and dried with lintless towels. The disk was first scrubbed with a paper towel saturated with a detergent solution of tri-sodium phosphate. The disk was then rinsed with distilled water and immersed in nitric acid (50% concentration). A rinse with distilled

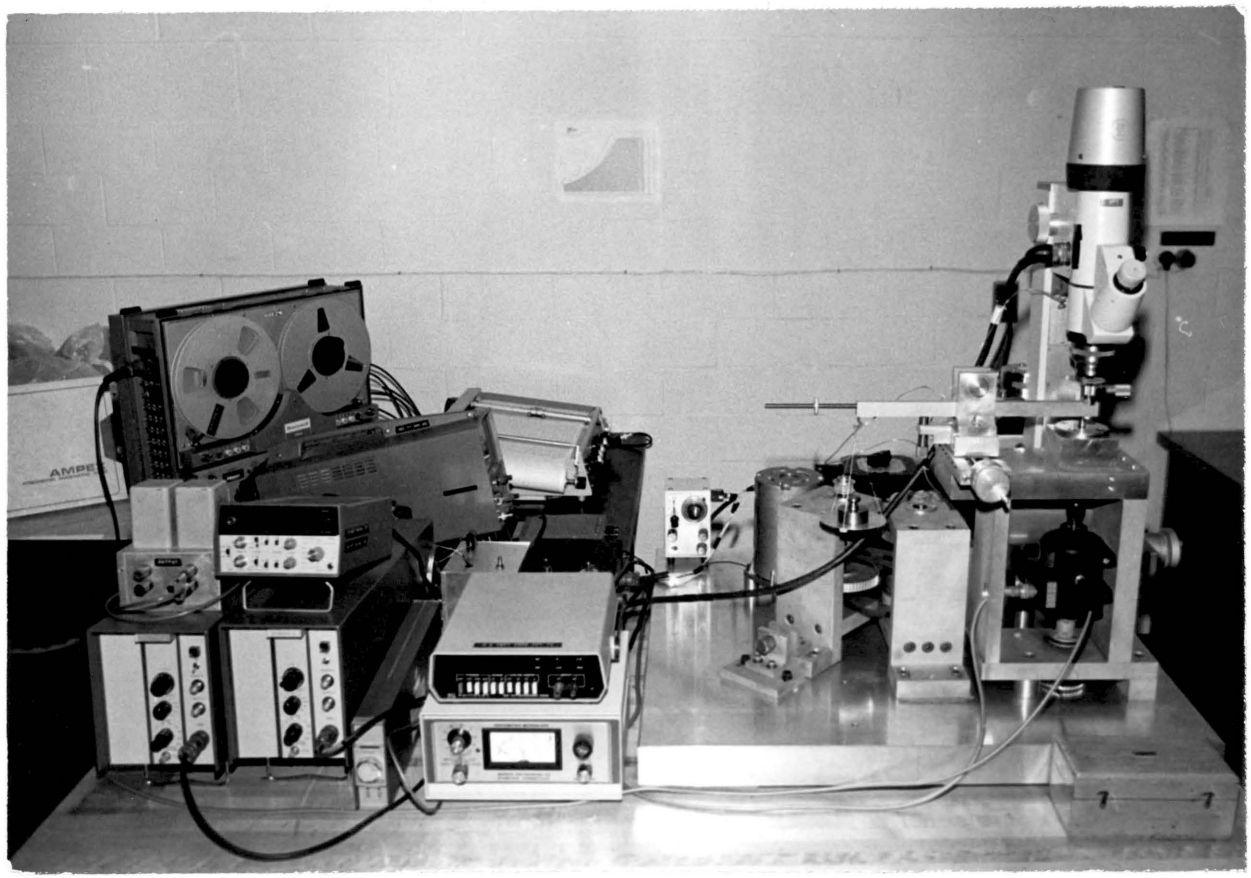

Figure 32. Overall View of Experimental Apparatus

water followed and then it was immersed in hexane, rinsed, and then immersed again in acetone and again rinsed. Methanol was poured over the disk to remove any remaining water. This disk and the specimens were then stored in a desiccator until time of use.

The instrumentation was turned on and given a warm-up period of at least one-half hour. It was found that the infrared microscope needed at least one-half hour to stabilize after the dewar flask was filled with liquid nitrogen. The switches and dials on the controller box were then checked. The emissivity knob must be turned to the value of 1.0 and the radiance level knob to 10X in order for the calibration curves in Appendix A to be correct.

The specimen was then placed into the specimen holder and the beam counterbalanced by moving the threaded counterweights along the rod at the end of the beam. The beam bearing tightness was then checked to be sure that excessive lateral movement in the beam was not allowed. The specimen was then moved to the proper radius on the disk to give the desired sliding velocity. The revolution counter was then zeroed and reset.

A number of adjustments in the instrumentation were required. The proper input voltage was applied to the LVDTs. The microscope output was then zeroed by using the Barnes Engineering calibration source at ambient temperature. The microscope was then focused onto the center of the surface of the specimen which had been loaded against the sapphire disk. When the 36X objective was used, the lens setting was checked to be sure that it was at '0' (zero). The LVDTs were then zeroed so that

an output of zero volts on both the radial and tangental LVDTs would correspond to the the center of the specimen. All the amplifiers were checked at this point to set the proper gains.

The torque transducer adjustments and settings were made at this point. A 12-volt battery was used as the voltage source of the torque transducer but the input voltage was set to 10 volts by means of a voltage divider. The specimen was unloaded or removed from contact with the disk. The motor was turned on and with the use of an oscilloscope the vibrational generated noise was reduced by adjusting the drive belt tension. The torque transducer brushes were then opened.

The instrumentation was at this point ready for an experiment. The data from all the instrumentation were stored on magnetic tape. The data stored on the magnetic tape consisted of:

1) Radiance (0-1 Hz)
2) Radiance (0 - 400 Hz)
3) Torque
4) Radial LVDT (X position of microscope)
5) Tangential LVDT (Y position of microscope)
6) Speed

The torque transducer brushes were now closed and the revolution counter started. The tape recorder was started which initialized all the inputs to a known and static value. The motor was started at the same time the tape recorder was started and allowed to run for 15 seconds. The output from the torque transducer was the torque from friction in the bearings and other system responses. This torque

reading was subtracted from the torque transducer output obtained during the running of an experiment. The tape recorder was allowed to run for 15 seconds more to initialize all of the inputs. As soon as the motor was stopped the specimen was loaded against the disk. After the 30 second initializing period the motor was turned on and the experiment run for a five (5) minute period.

After five minutes of gathering data the drive motor was turned off and another 30 second period of data gathering was used to allow for recording the cooling of the specimen.

Another important experimental procedure involved gathering all the vital data used to measure and map the emissivity of the contact area. The procedure simply involved the use of a specially-designed specimen heater which allowed comparison between the radiance emitted from a blackbody at an elevated temperature and the radiance emitted from discrete points on the contact surface at the same elevated temperature. The specimen heater and procedure used in mapping the emissivity was developed by Steven C. Moyer and a more detailed explanation of this method may be found in his Master's Thesis (January, 1983) [54].

Two other invaluable experimental techniques were used to evaluate the data, both involved photography. The first was the adaptation of a 35 mm camera to the optical channel of the infrared microscope (Fig. 33). Photographs were taken of the specimen surface after a test was completed and with the sapphire disk removed. This photographic technique allowed color pictures or slides to be taken which in some situations could help in distinguishing whether oxide films were present

Figure 33. Infrared Microscope with 35 mm Camera Attached

and even perhaps the type of oxide. This technique did not have a sufficient depth of field to show if oxides were on top of the surface or if pitting of the surface occurred. The scanning electron microscope was used for this purpose. A number of these micrographs will be presented later in this paper and used to compare emissivity maps with the topography of the surface.

3.7 Test Conditions

The main objective of this investigation was to study the effect of subdivision of the contact area on surface temperatures. To accomplish this, some very unique tests were performed. In order to experimentally determine the effect of subdivision of the contact area on surface temperatures, many different types of experiments and specimen configurations can be used. A very basic problem is the question of what magnitude of contact area should this study be dealing with, the real contact area or the apparent contact area. One answer would be the actual true contact area. The problems with this experimentally are that 1) the true area of contact can not be determined exactly by experimental techniques and therefore a theoretical assumption would have to be made, and 2) a rather complex and expensive machining procedure would have to be used such as chemical milling or laser etching because of the magnitude of the contact area. If using the real contact area is ruled out, the next question is if the same information can be learned from tests that use comparatively large geometric contact areas (5 mm dia.). Archard claims that it is reasonable to compare surface temperatures of specimens that have large geometric areas to those calculated using his theoretical model of a single cylinder in total contact with a semi-infinite body. Archard gives some conditions to this statement, 1) the bodies should be sliding at low speeds and 2) the real contact area of the larger geometric area be composed of small, closely packed contact areas [25]. Another rationale is that if we assume that subdivision merely reduces the load carried by each contact

area, then subdividing the larger geometric area should have the same effect as reducing the load supported by each microscopic contact area. The experiments which were decided on were designed to test this final hypothesis.

The specimen geometry selected was a cone (Fig. 34). The cone shape allows one to vary the angle of the cone which in turn varies the volume of material which needs to be worn away to produce a desired wear area. The subdivided geometries were produced by means of a 3.2 mm slit down the center of the specimens. Subdivisions of two and four contacts were used (Fig. 34).

A number of tests were performed to experimentally determine the effect of heat input to the system and how load and velocity influenced the surface temperatures. Table 4 lists the loads, sliding velocities and number of contacts for each test and the corresponding test numbers.

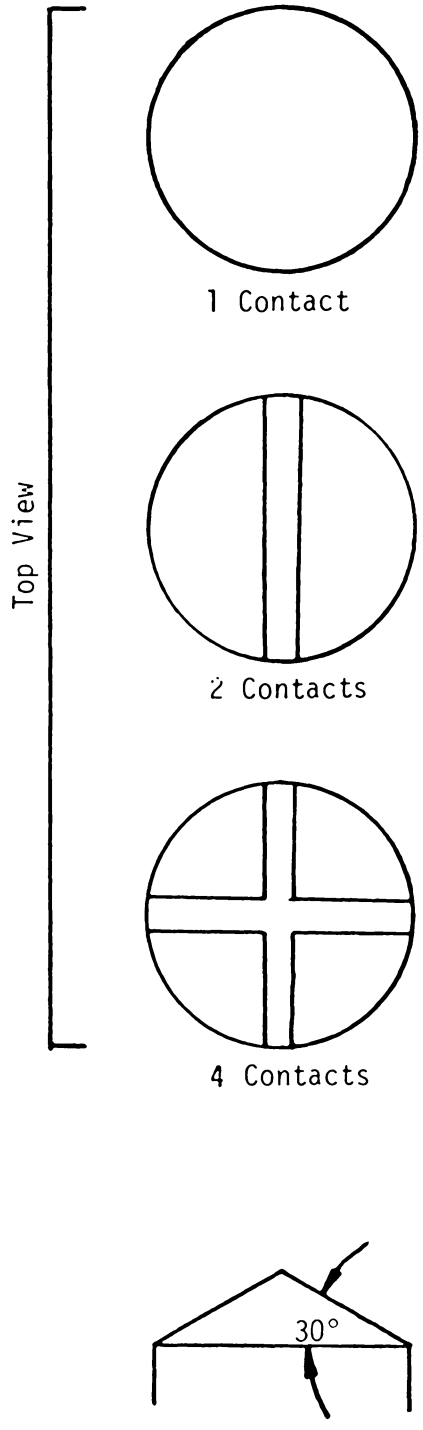

Figure 34. Specimen Geometry

TABLE 4

TEST CONDITIONS

MATERIALS: COPPER-ON-SAPPHIRE
DURATION OF TEST: 5 MINUTES

No. of Contacts	Sliding Velocity (m/sec)	Normal Load (N)	No. of Tests	Test No.
1	2	2	2	1-22
1	2	3	2	1-23
1	2	4	2	1-24
1	2	6	2	1-26
1	4	2	2	1-42
1	4	3	2	1-43
1	4	4	2	1-44
1	4	6	2	1-46
1	8	2	3	1-82
1	8	3	3	1-83
1	8	4	3	1-84
1	8	6	3	1-86
2	2	2	2	2-22
2	2	3	2	2-23
2	2	4	2	2-24
2	2	6	2	2-26
2	4	2	2	2-42
2	4	3	2	2-43
2	4	4	2	2-44
2	4	6	2	2-46
2	8	2	2	2-82
2	8	3	2	2-83
2	8	4	2	2-84
2	8	6	2	2-86
4	4	2	2	4-42
4	4	3	2	4-43
4	4	4	2	4-44
4	4	6	2	4-46

4.0 RESULTS AND DISCUSSION

4.1 Discussion of Data

This experimental study involves presenting information about the surface temperatures generated by friction in various forms. However, a number of interesting things can be found by a careful examination of the raw data itself without any regard to temperature. In this experimental study, the single most important element in generating accurate and reliable temperature data is the determination of the emissivity. The emissivity and radiance data will be discussed in this section so that the difficulty of converting radiance to temperature can be fully realized.

As stated earlier, one of the expected characteristics of copper was a bi-level emissivity. Many of the actual tests displayed this bi-level characteristic. To illustrate this, Fig. 35 shows a radiance trace of a specimen test that was a low emissivity specimen. The voltage output from the microscope was relatively low and the trace was 'clean'. It did not show a great deal of high frequency changes in the radiance which could be interpreted as emissivity fluctuations or short duration temperatures changes.

In contrast, Fig. 36 shows a relatively high radiance level, which is partly due to a higher surface temperature than the preceding case, but the character of the radiance is much different. Figure 36 shows the radiance making a very rapid increase to its maximum level. The radiance in this particular case is a relatively "noisy" signal and also

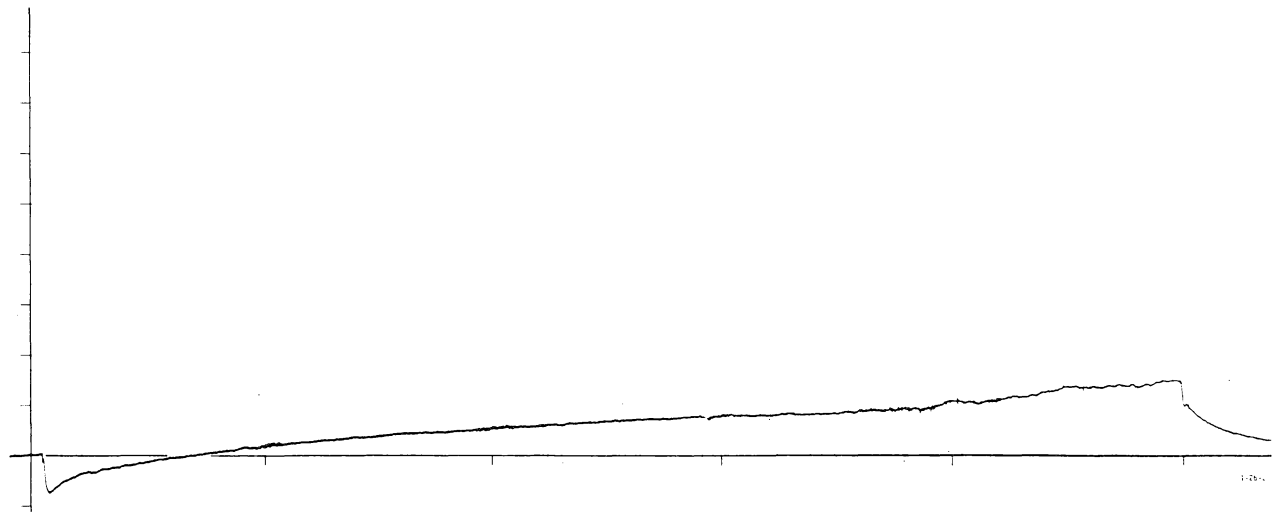

Figure 35. Radiance Trace of Test 1-26-2

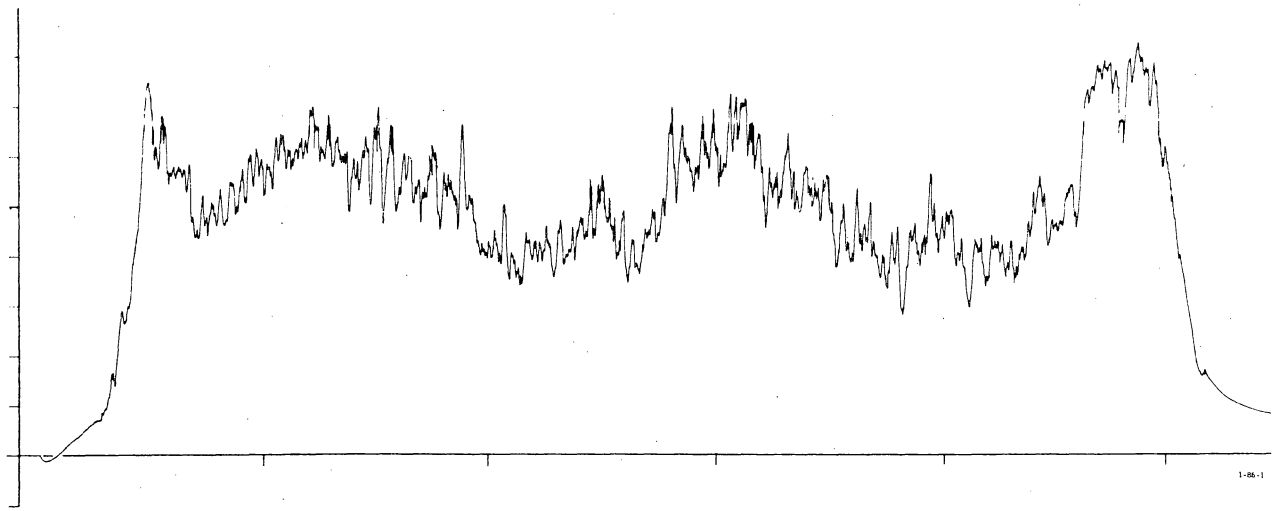

Figure 36. Radiance Trace of Test 1-86-2

has a periodic nature to it. One possible explanation is that an oxide film is created on the surface very quickly and when the oxide film reaches a critical thickness the film breaks off or is partially reduced in size and the emissivity decreases. It is not believed that the oxide film is totally removed as this would most likely be evident in the torque data; and the torque remained relatively constant in all tests. Figure 37 is a typical trace of the torque output.

Most of the tests however displayed both levels of radiance, most generally exhibiting the lower level characteristic radiance during the initial stages of a test and then very dramatically stepping up to the higher level. Examples of this can be seen in Figs. 38, 39, and 40. There are also several radiance traces which show a variation on this characteristic bi-level form. Many of the tests showed a multi-level radiance curve, in which case there was one low radiance section with a sudden jump to a second level much like those shown in Figs. 38, 39 and 40. However once the radiance reached this level, the radiance again jumped to a third and sometimes a fourth level in many cases. These additional levels were only slight variations in the initial 'high' emissivity level and therefore could possibly be explained by varying densities or types of copper oxides present on the surface.

The major difficulty in converting the radiance to temperature, is the problem of determining the emissivity of the surface. Of course the problem arises in that we would ideally like to know the emissivity at the exact time and location at which we are taking radiance data. This is not possible in a dynamic system and therefore a 'next best' tech-

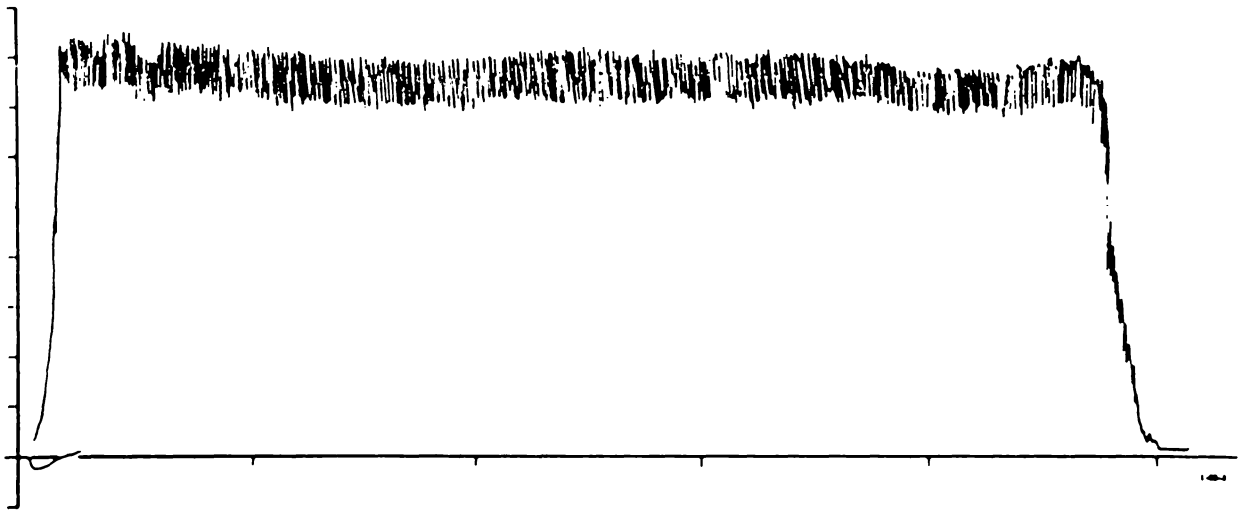

Figure 37. Typical Torque Trace

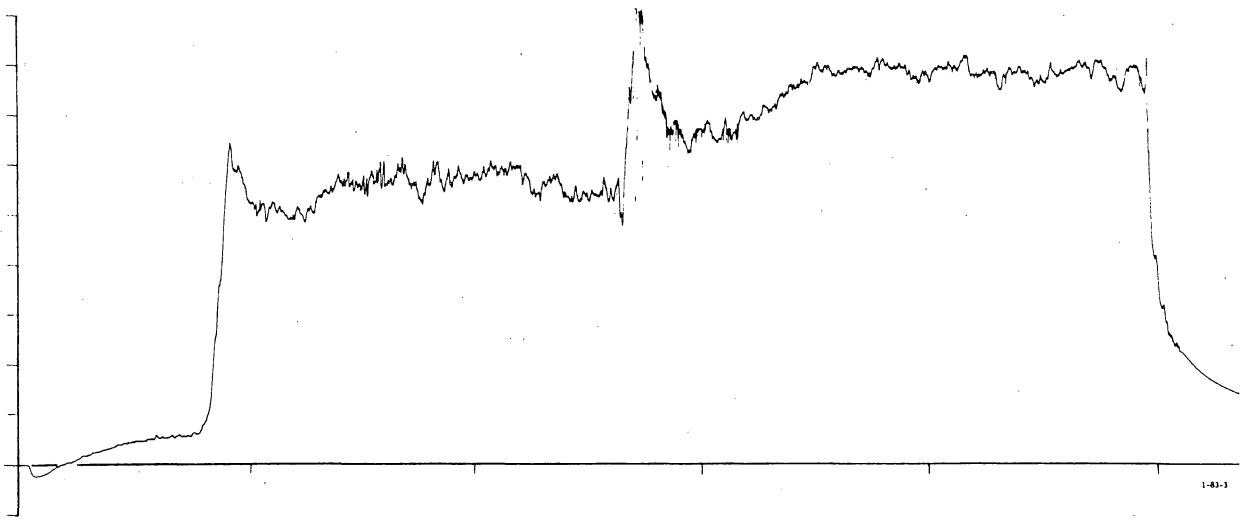

Figure 38. Radiance Trace of Test 1-83-3

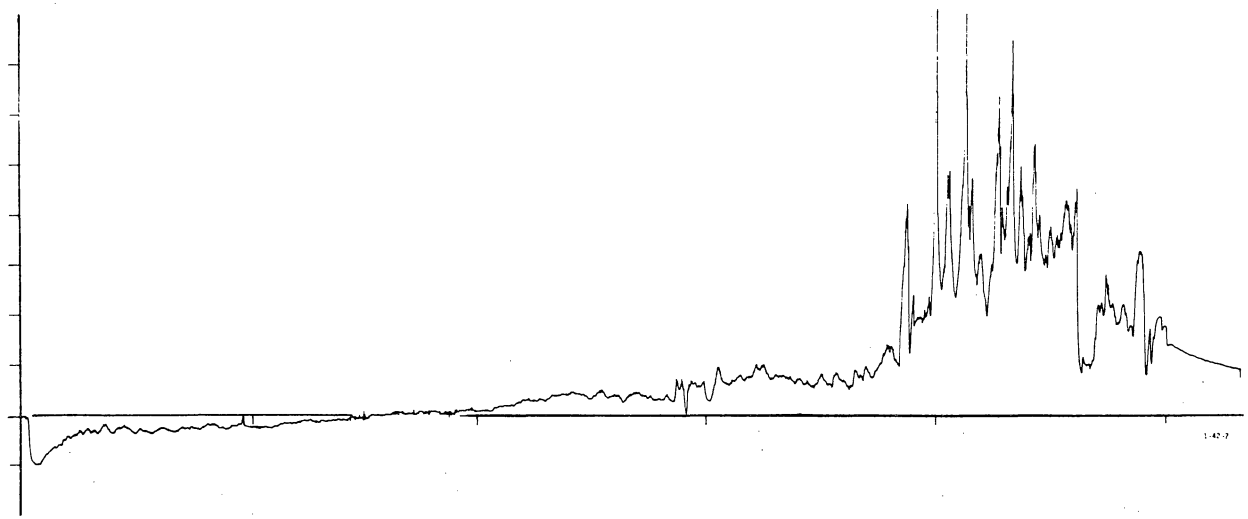

Figure 39. Radiance Trace of Test 1-42-2

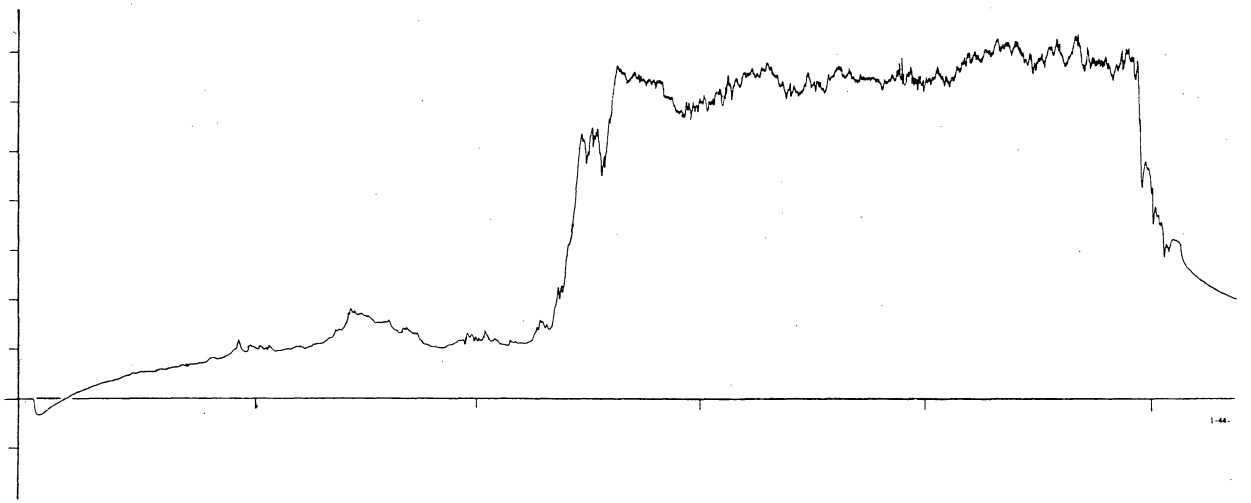

Figure 40. Radiance Trace of Test 1-44-1

nique must be developed. The emissivity of the specimen surface was mapped using an apparatus and technique developed by Steven C. Moyer (see ref. [54]). This technique which allowed high resolution produced a significant amount of information from which temperature could reliably be deduced.

Each of the experiments were run for five continuous minutes and a number of temperatures for each experiment were desired. Therefore radiance readings were recorded at 1 minute intervals for the single contact tests; for the two subdivision tests, radiance data was used of one contact at 3 minutes and of the other contact at 5 minutes, for the four subdivision tests, the data used in calculating temperatures was at the 2,3, 4 and 5 minute intervals, recording the radiance from a different contact each time. An obvious problem then arises, how is the emissivity determined at the 1, 2, 3 and 4 minute intervals? The emissivity after a test (or 5 minutes) can be measured experimentally. However, the emissivity of every specimen after a test was not measured because it was determined that only a selected number of specimens had to be measured to determine the emissivity characteristics of the copper specimens. The emissivity of a selected number of specimens after a completed test were then known. In order to fill in all of the unknown emissivities the radiance traces were then used. The radiance traces of the test for which the emissivity was experimentally determined were first used. If the radiance was fairly constant with no sudden jumps (such as Fig. 35) the emissivity was assumed constant. If sudden jumps occurred in the radiance, this was assumed to result from a sudden increase

in the surface emissivity. Working from the known emissivity at the end of an experiment and from comparison with other radiance traces for which the emissivity was known, an estimate was then made. The experimentally-determined emissivities are shown in Table 5 by an '*' placed next to the emissivity. All other emissivities are estimates based on comparisons with the actually known emissivities and then respective radiance traces.

The emissivity data was graphed as a contour plot and also as a 3-dimensional plot. The contour plots were generated by interpolating between the discrete emissivity points. Therefore, the resolution of the contour plot is greater than the 3-dimensional plot.

Scanning electron micrographs (SEM's) were taken of selected specimens and then compared to the emissivity contour and 3-dimensional plots. This comparison yields a great deal of interesting information. The first and most noticeable conclusion that can be made is that the rough sections of the surface have a considerably higher emissivity than the smoother looking surfaces. Figures 41, 42, 43, allow for a comparison between the SEM and emissivity plots of test number 1-22-1. The SEM shows a relatively smooth surface with what appears to be pitting on the right-hand side. The emissivity plots show a mean emissivity of approximately 0.4 with a section at 0.5 corresponding to the pitted regions. Many of the other tests show an even more dramatic comparison. Test 1-26-2 (Figs. 44, 45, 46 shows the high emissivity plots. Figures 47, 48, 49 show a phenomenon that occurred on many of the test specimens. The pitting occurred in a direction parallel to the direction of

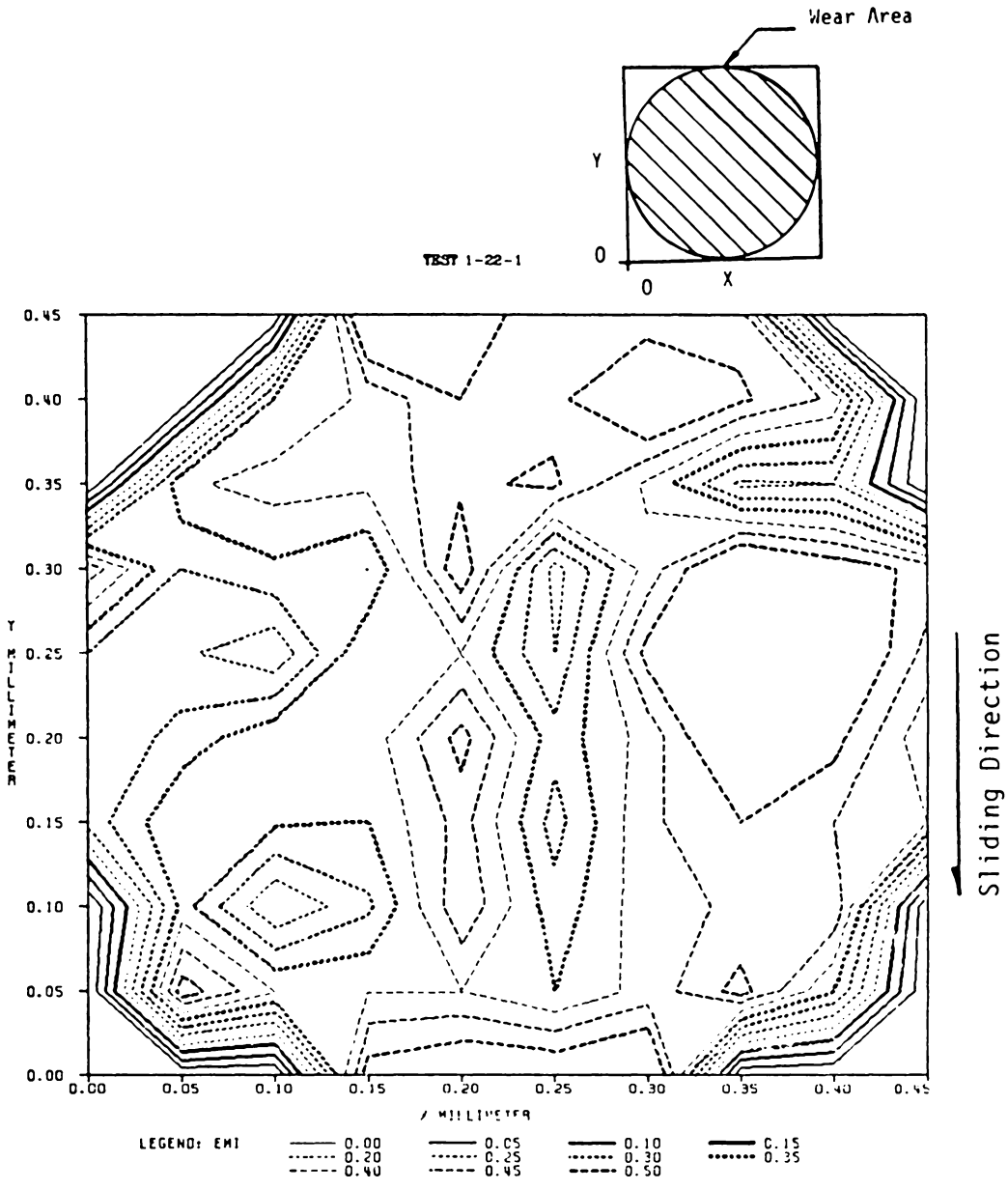

Figure 41. Emissivity Contour Plot of Specimen 1-22-1

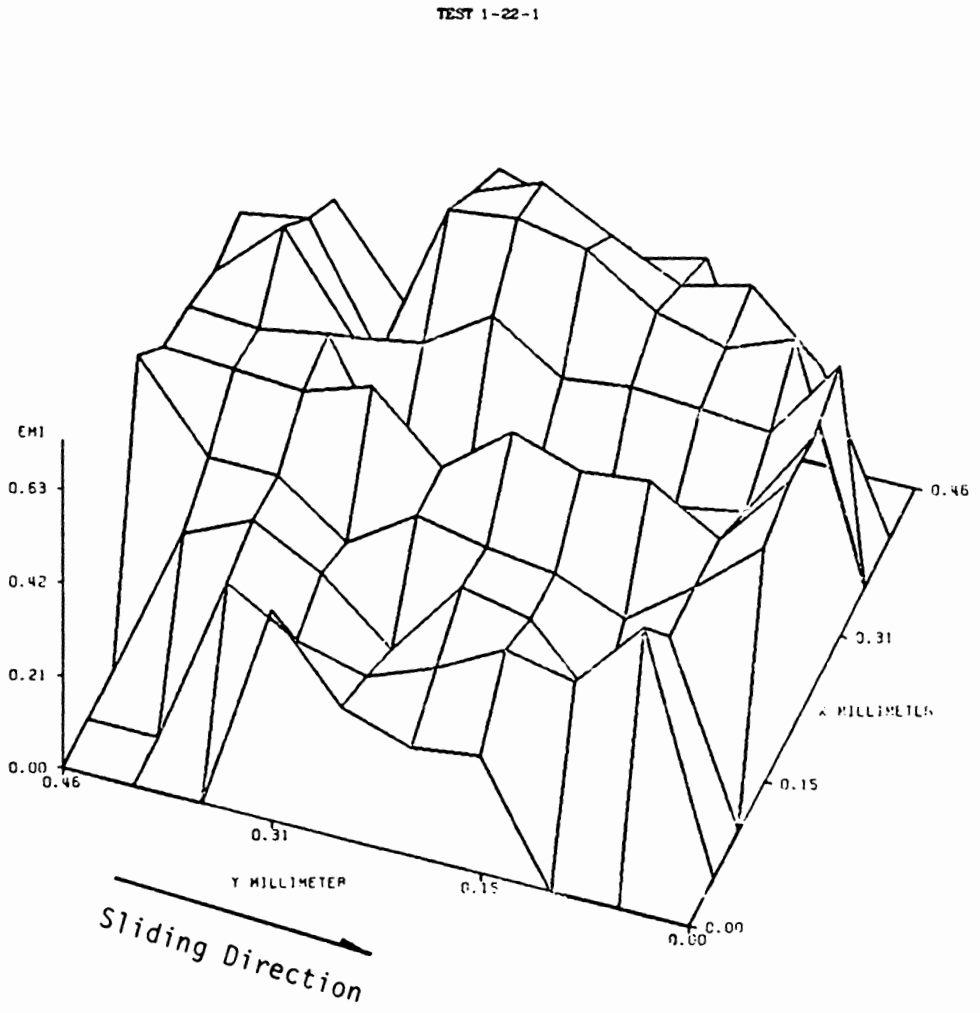

Figure 42. Emissivity 3-D Plot of Specimen 1-22-1

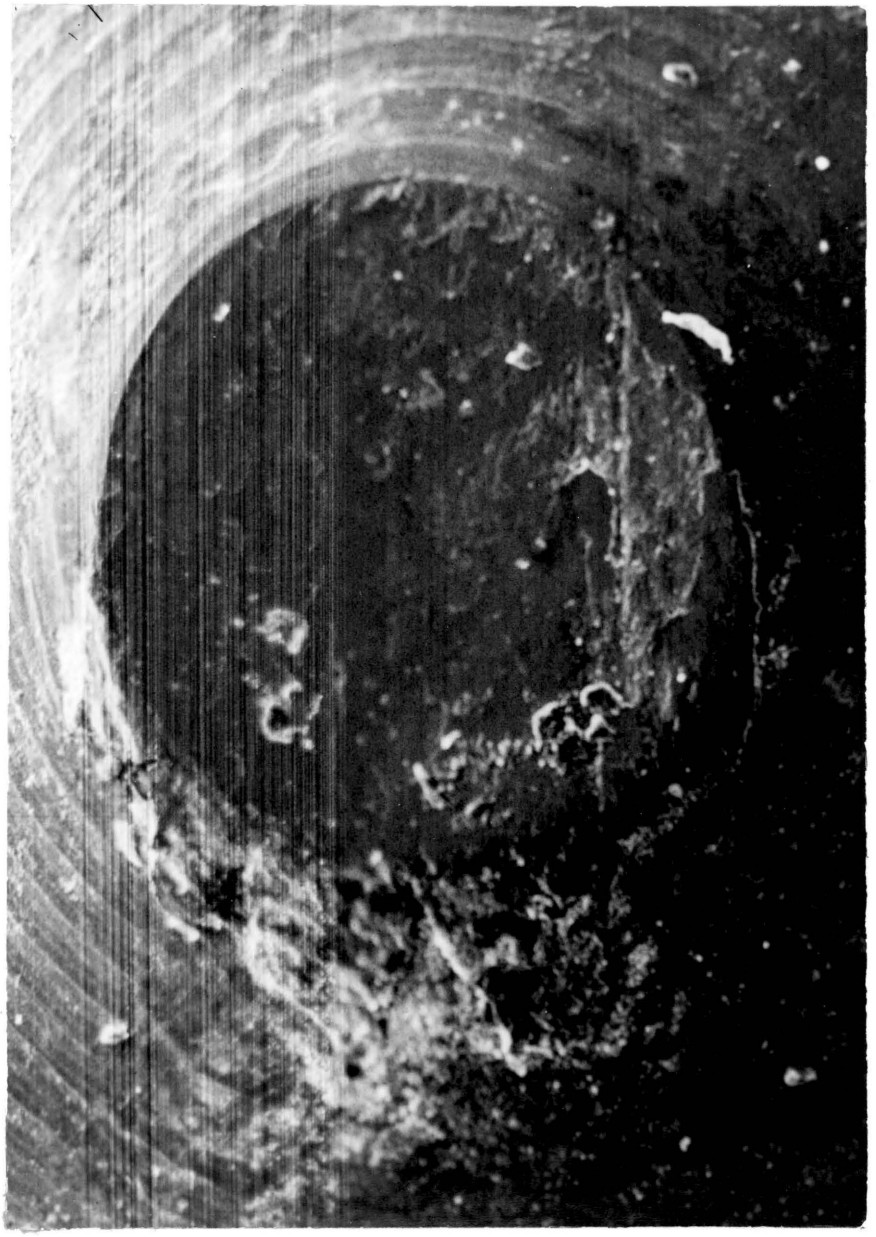

Figure 43. SEM of Specimen 1-22-1 (160 x Magnification)

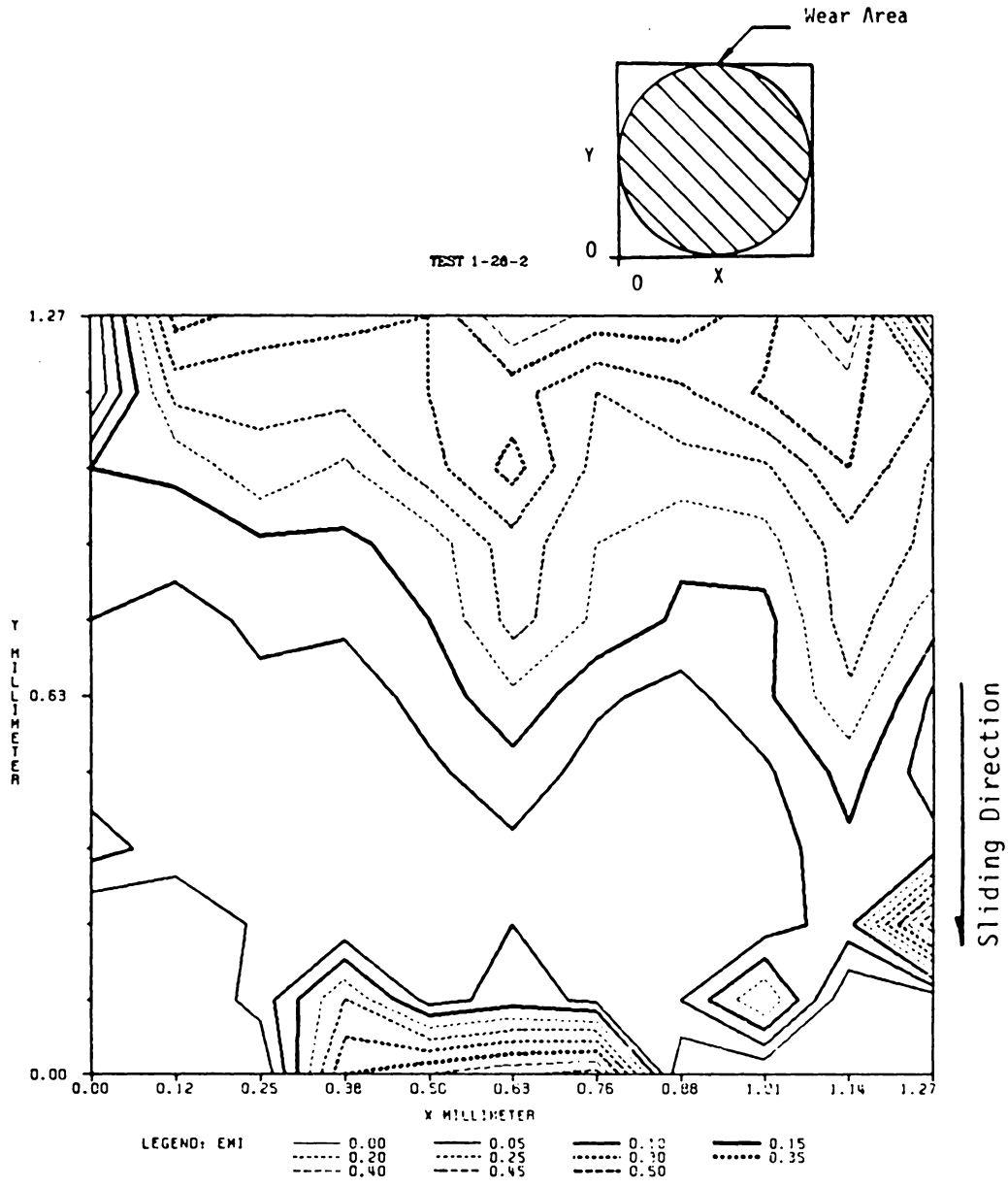

Figure 44. Emissivity Contour Plot of Specimen 1-26-2

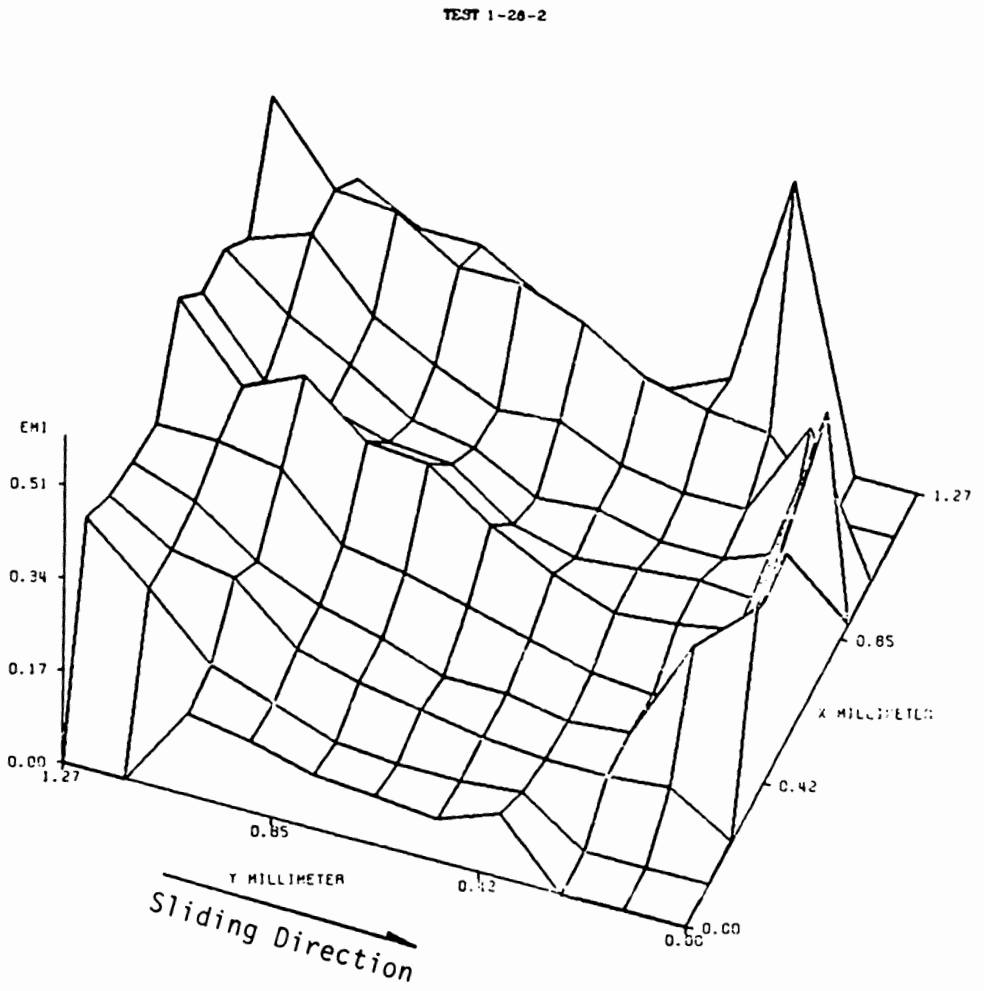

Figure 45. Emissivity 3-D Plot of Specimen 1-26-2

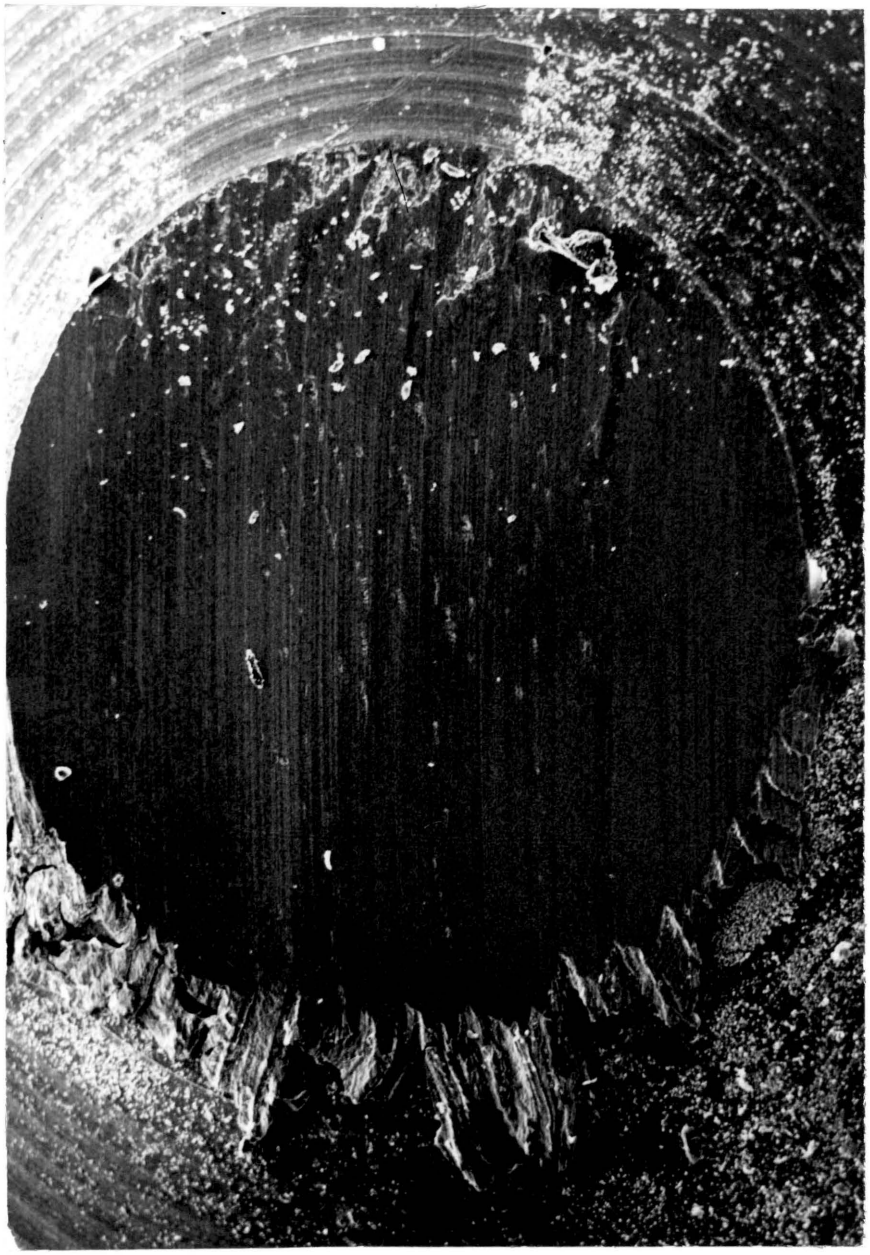

Figure 46. SEM of Specimen 1-26-2 (80 x Magnification)

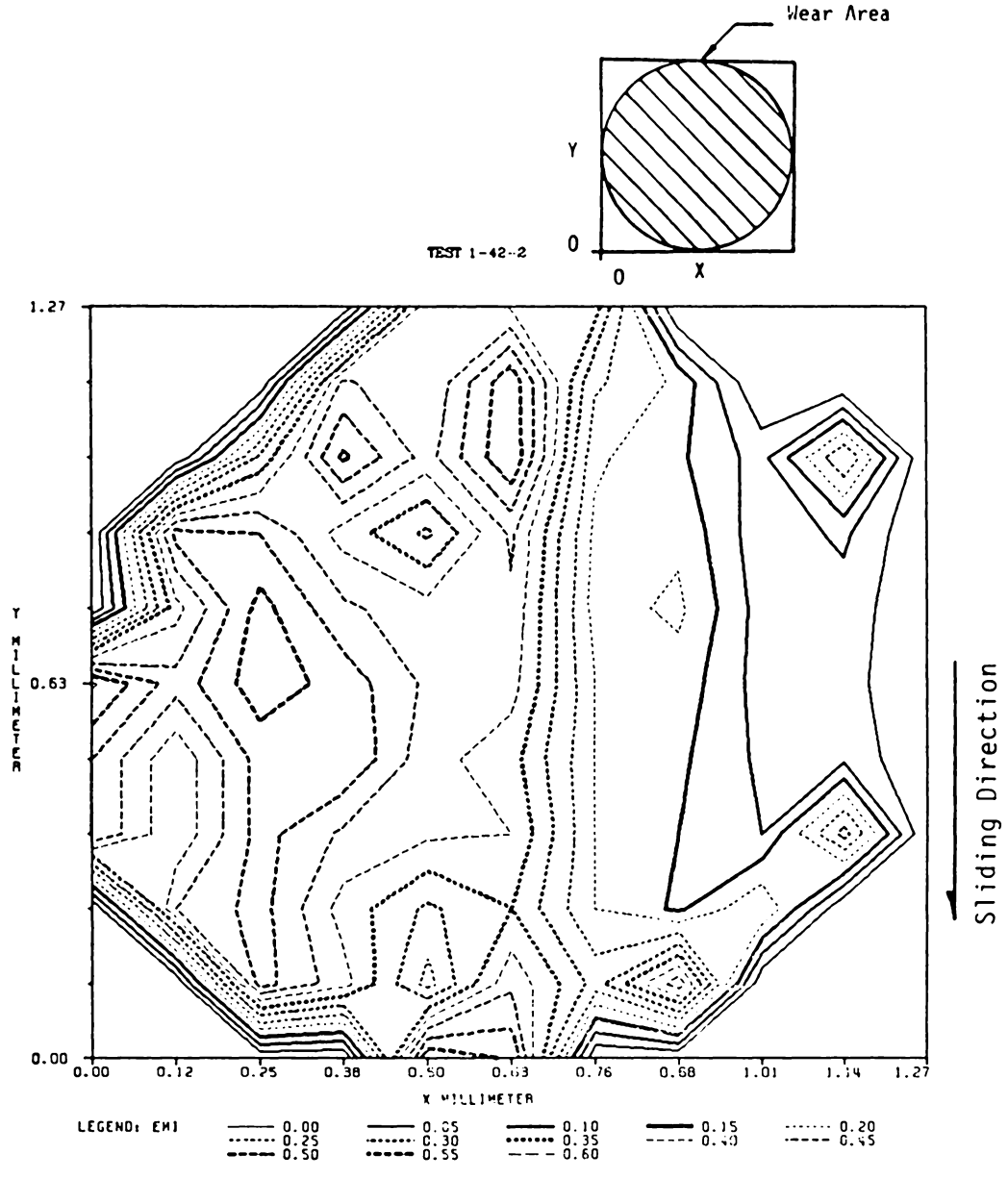

Figure 47. Emissivity Contour Plot of Specimen 1-42-2

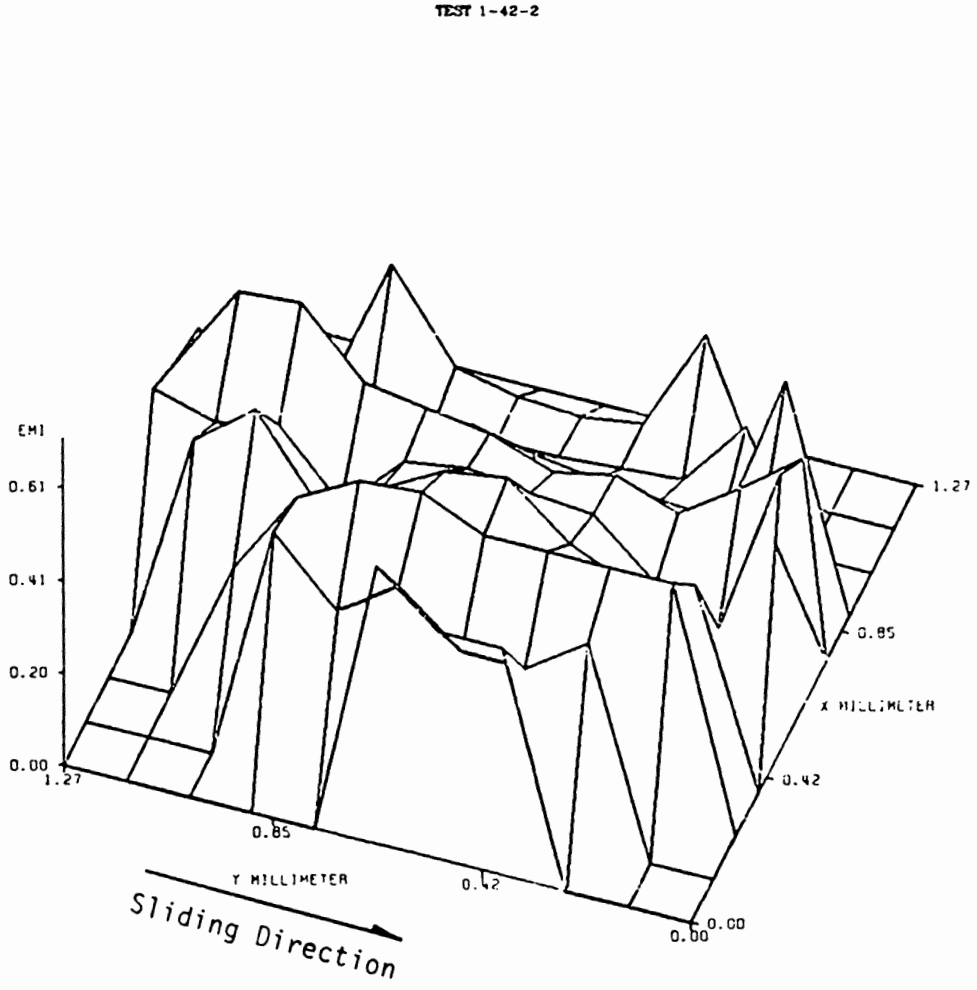

Figure 48. Emissivity 3-D Plot of Specimen 1-42-2

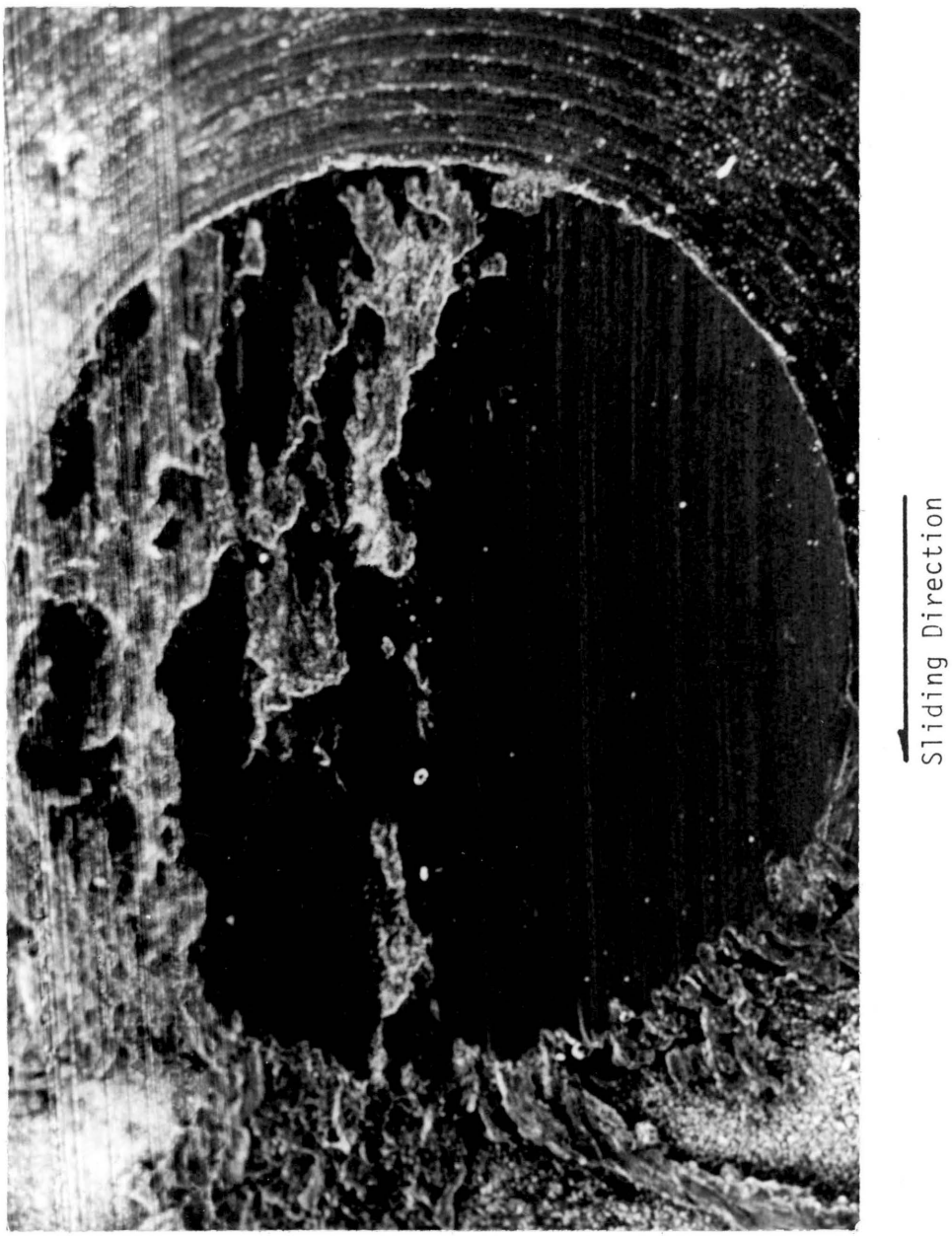

Figure 49. SEM of Specimen 1-42-2 (80 x Magnification)

sliding. Figures 50, 51, 52 show a rougher surface but still has the thin section of pitting. Test 1-84-2 (Figs. 53, 54, and 55) behaved much like that described by Steven Moyer [54] in his experimental work with iron. He found that the surface was pitted and contained more oxide near the trailing edge, with the leading edge of the specimen being fairly smooth.

It is interesting to note that inspection of the scanning electron micrographs shows that the low and high emissivities correspond to the smooth and rough sections of the surfaces respectively. In the beginning of this section it was stated that the low and high emissivity levels seemed to correspond to 'clean' metal and an oxide film, respectively. This statement was made from visual observations through the microscope in which there were jumps in the radiance when a blue colored section was in view. Based on the scanning electron micrographs it is not clear that an oxide film ever existed or if it was formed and rubbed off the surface very quickly leaving these 'pits.'

The examples of data found in this section have all been from the experiments with one geometric contact area. Many of the other experiments exhibited similar characteristics. Figures 56 and 57 are SEMs of the wear areas of specimens with two and four geometric contact areas, respectively. Comparison of these SEMs with those from singular contact specimens show that the wear and surface characteristics are similar for all tests.

There are two basic problems involved with converting the radiance data to temperature: (1) the emissivity must be known at every point in

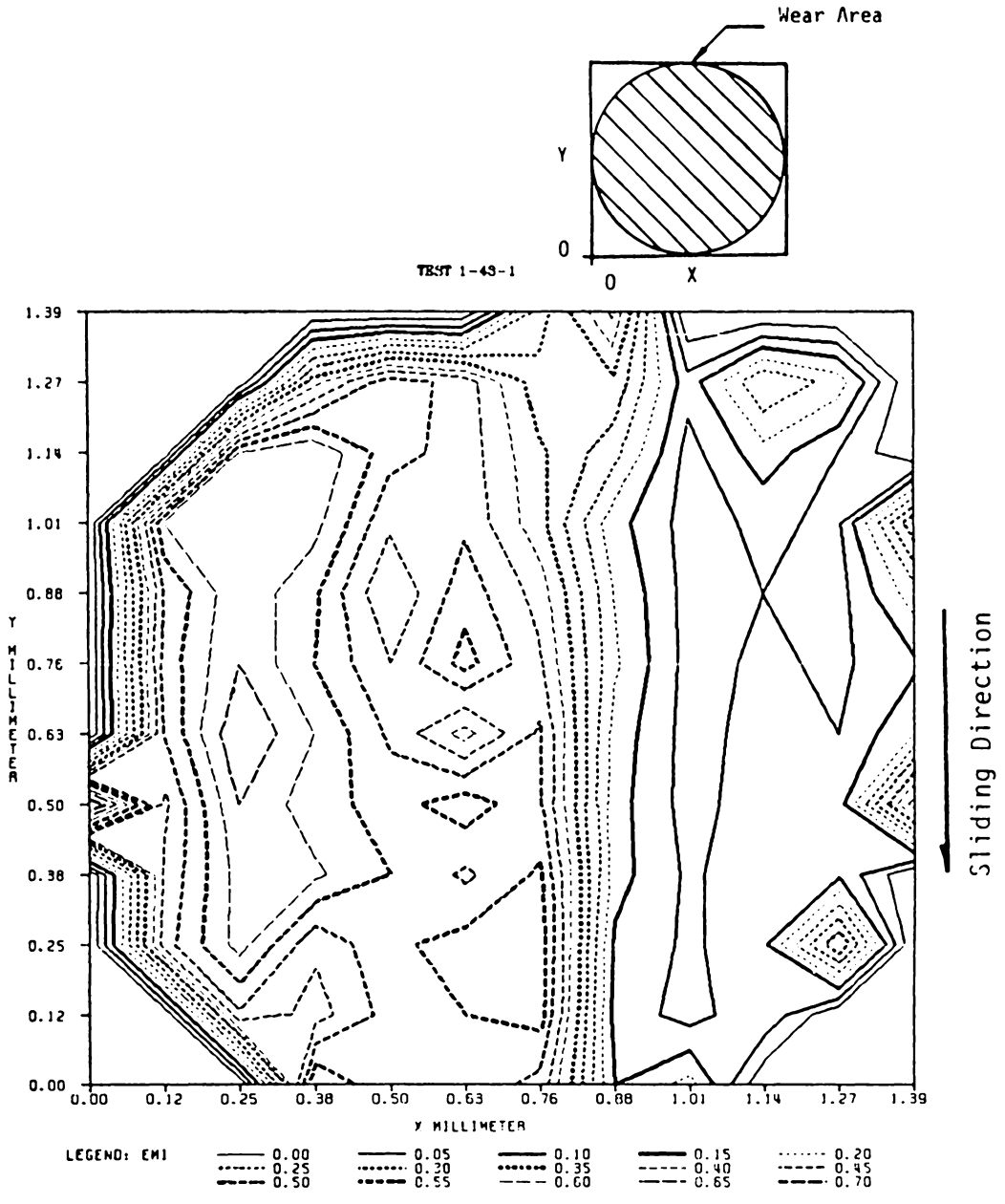

Figure 50. Emissivity Contour Plot of Specimen 1-43-1

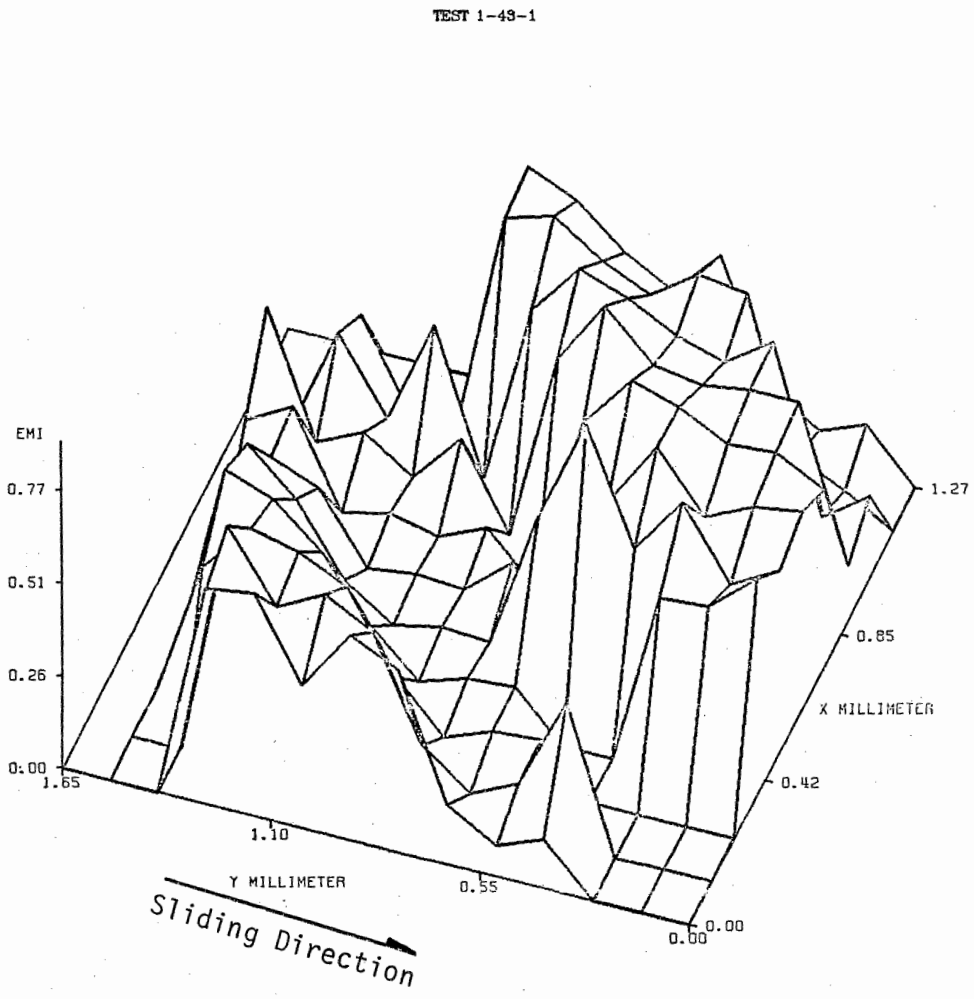

Figure 51. Emissivity 3-D Plot of Specimen 1-43-1

Figure 52. SEM of Specimen 1-43-1 (80 x Magnification)

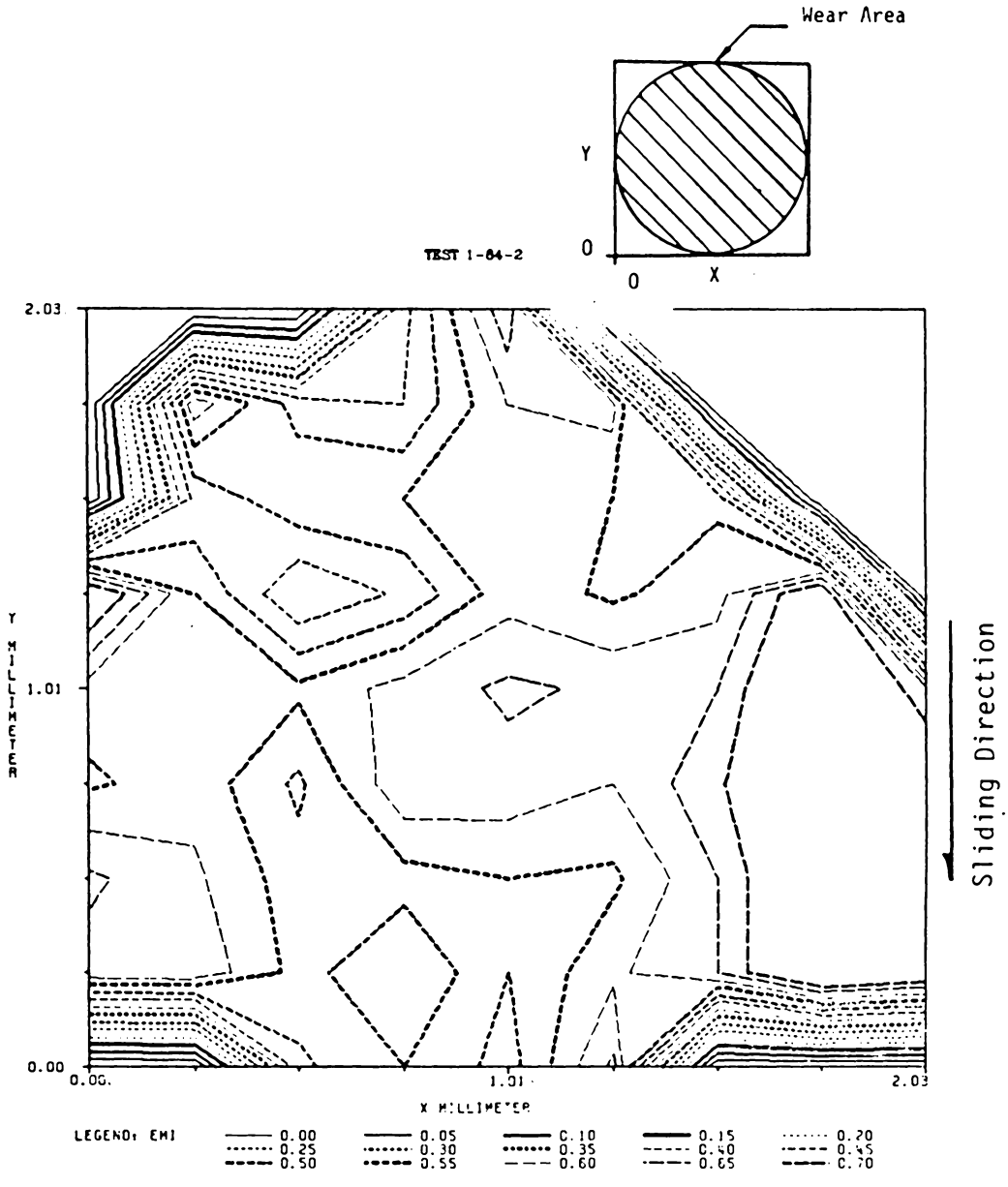

Figure 53. Emissivity Contour Plot of Specimen 1-84-2

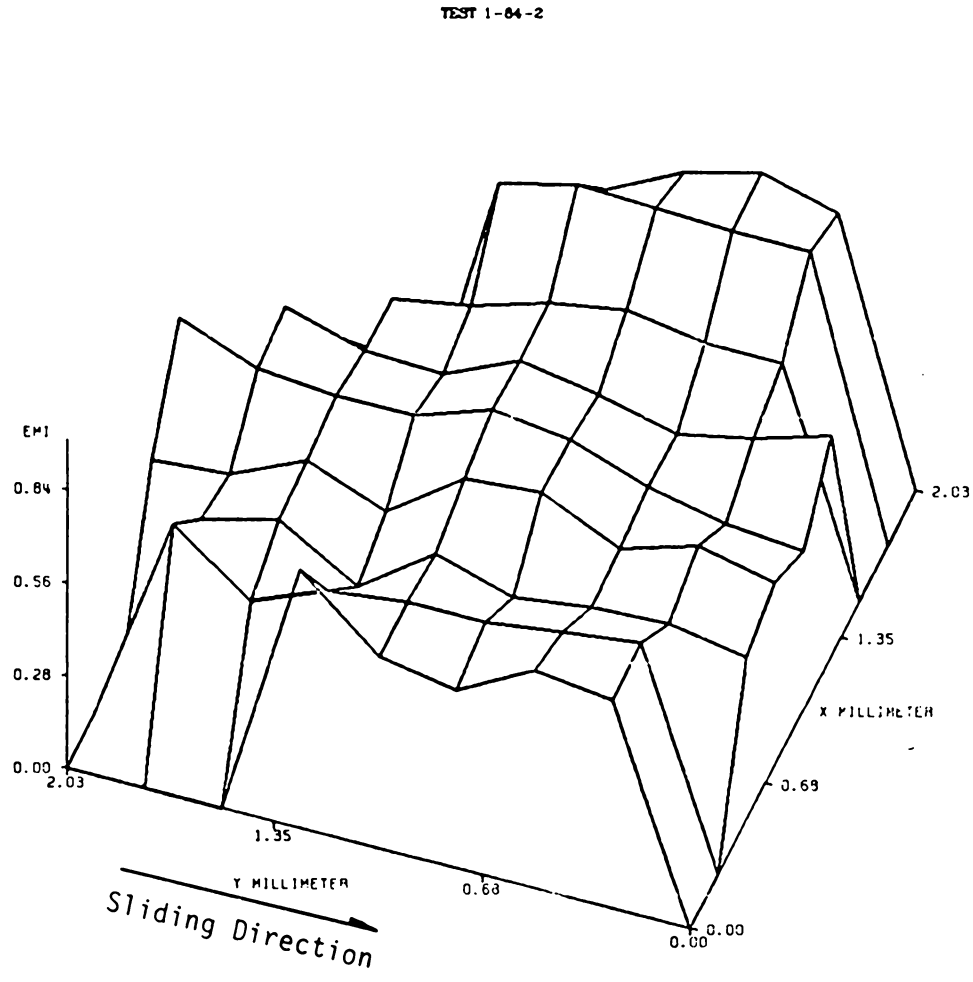

Figure 54. Emissivity 3-D Plot of Specimen 1-84-2

Figure 55. SEM of Specimen 1-84-2 (40 x Magnification)

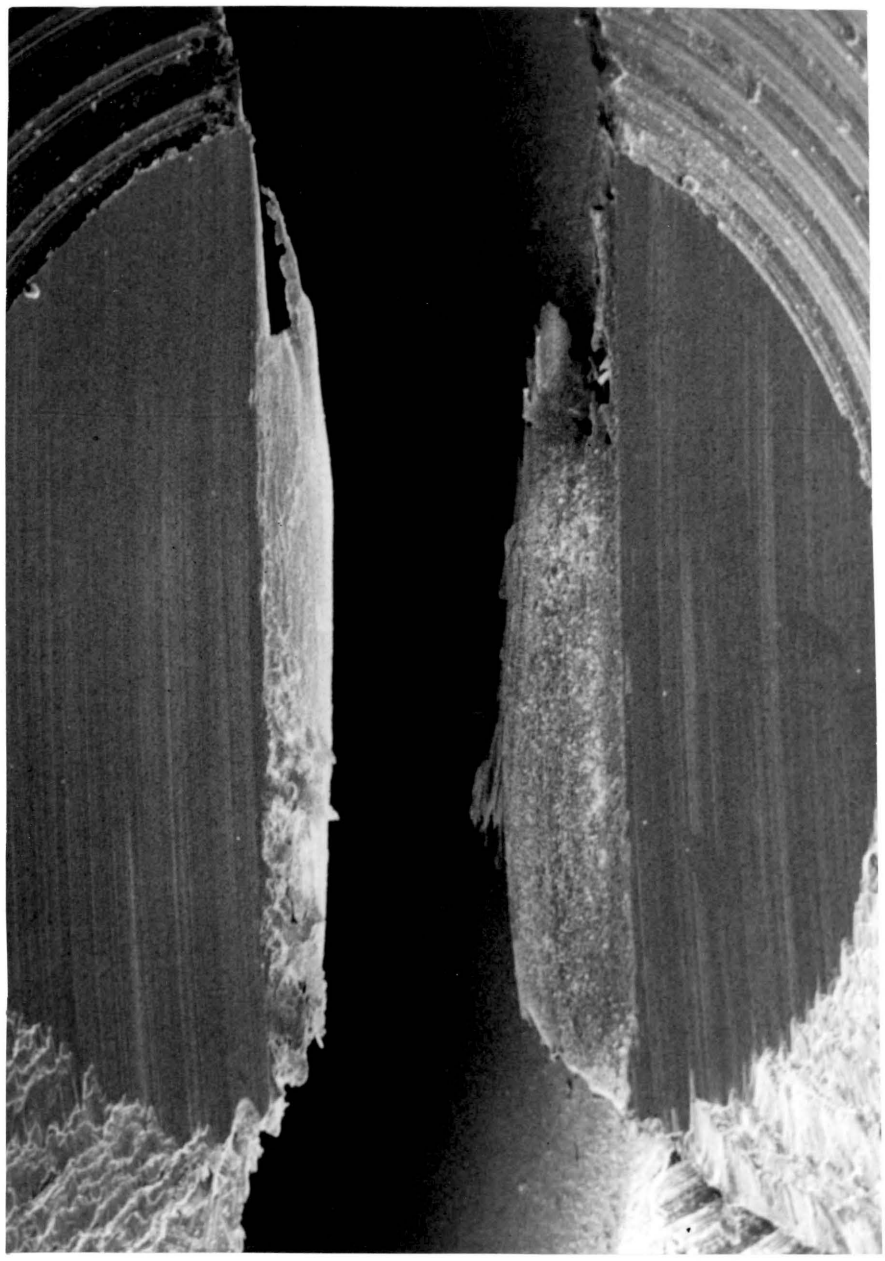

Figure 56. SEM of Specimen with 2 Contact Areas

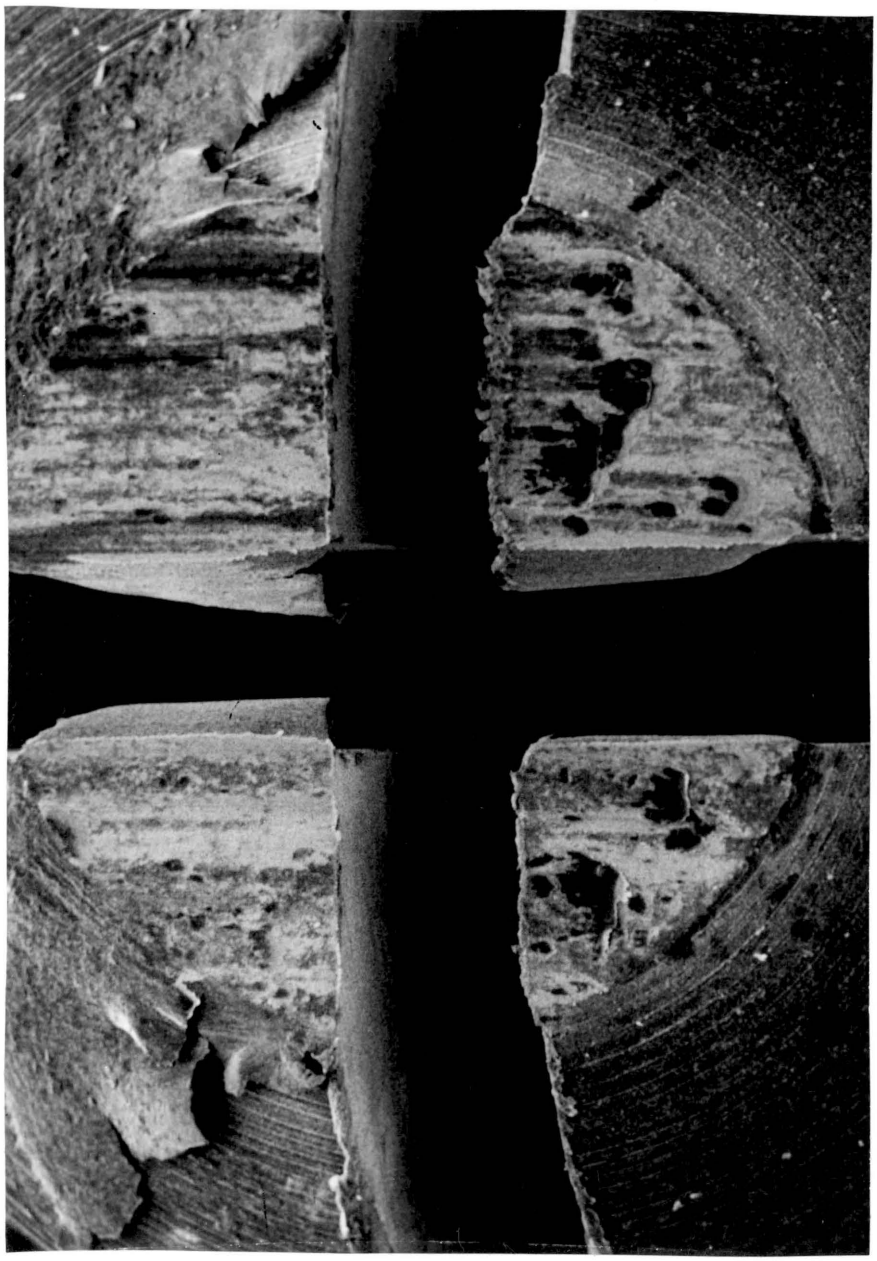

Figure 57. SEM of Specimen with 4 Contact Areas

time and at every location in contact, and (2) a reliable method to determine the true voltage of the microscope must be devised.

Problem (1) is by far the most difficult to solve and in fact is not totally solved. This problem is dealt with by taking emissivity data of unused specimens, specimens that have been in contact with the moving disk for 5 seconds and 15 seconds, and then mapping the emissivity of specimens after a completed test. All of this data along with the radiance itself is vital and evaluated to arrive at a 'best guess'.

One of the most important pieces of information that is used in determining the dynamic emissivity and the voltage output from the microscope is the emissivity after 5 seconds of contact. The reason that this is important and yields better information than the emissivity of the new specimen is that every new specimen had an unique emissivity. This was partly due to the individual nature of the machining of the specimens. Figure 58 is a scanning electron micrograph of a specimen that shows the tooling marks on a specimen. The emissivities of an unused specimen varied between 0.15 to 0.60 and therefore a more standard and uniform method had to be used. It was quickly learned from the radiance curves that every test had one common trait. As soon as the disk started to rotate the radiance dropped considerably (see Fig 59). This drop in radiance was obviously not due to temperature decrease but rather a drop in the emissivity. Emissivity tests were then performed on numerous specimens after they had been run against the disk for 5 and 15 seconds. These tests showed a very constant emissivity for all specimens, i.e., 0.10 $\pm$ 0.02. The emissivity was essentially the same

Figure 58. SEM of Specimen After 5 Seconds Contact (160 x Magnification)

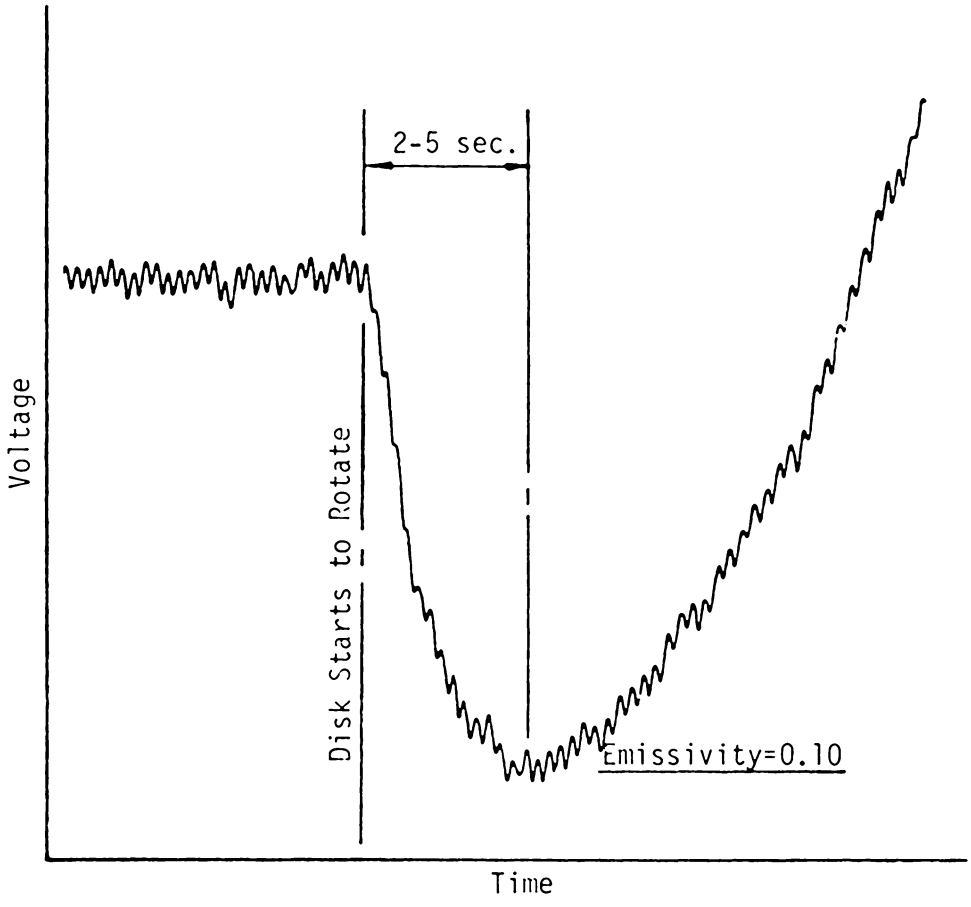

Figure 59. Typical Radiance of First 15 Seconds

for the 5 second and 15 second tests. Figure 60 is a scanning electron micrograph of the wear spot created by the sliding disk at 2 m/sec and a load of 2N. Note that the surface appears much smoother than any of the other scanning electron micrographs even under the high magnification used, 800X. Figure 61 shows the contact surface of a specimen run under the same conditions as described for Fig. 60 but for 15 seconds. In this photograph it is interesting to note the formation of the wear "chips" that occurred on every specimen.

The problem of determining the absolute voltage output of the microscope was solved with the fortunate finding of the predictable emissivity after a short time of running against the disk. A known emissivity must be used to determine the voltage output. The method used to determine the voltage output involved using the lowest point on the radiance curve as a datum point or a zero reference voltage from which all other voltages were measured. This point had a known emissivity of 0.10 and it was assumed that the surface of the specimen was still at room temperature. With the use of a computer program (see Appendix F.5) the voltage output was calculated using the method explained in Chapter 3 for a specimen with an emissivity of 0.10 and a surface temperature of 20°C or ambient temperature. Once this voltage was known, it was a standard task to find the voltage output at any other point on the radiance curve. A number of zero reference curves, zero reference voltage vs. emissivity, are contained in Appendix G.

Table 5 shows the data (radiance voltage and emissivity) and the resulting temperature rise for all of the tests. It should be noted

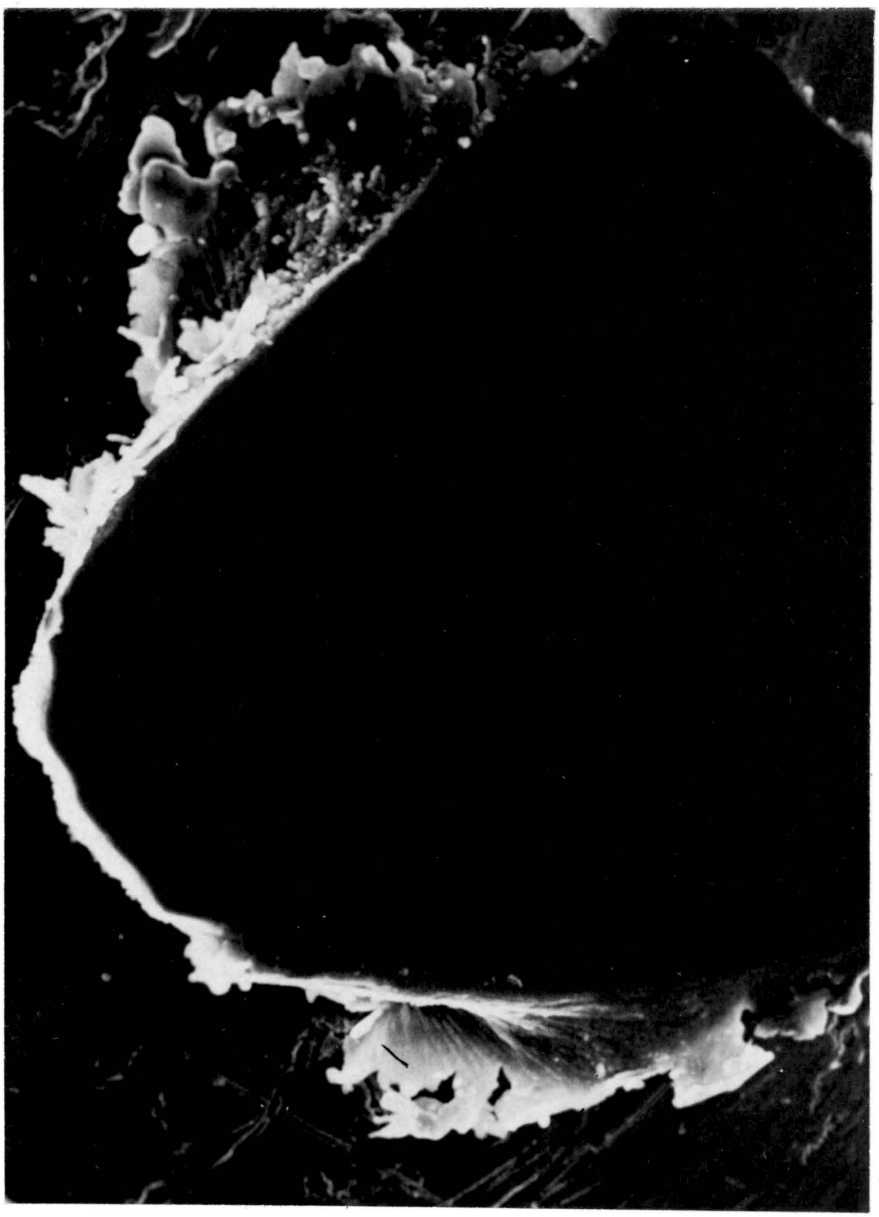

Figure 60. SEM of Contact Surface After 5 Seconds (800 x Magnification)

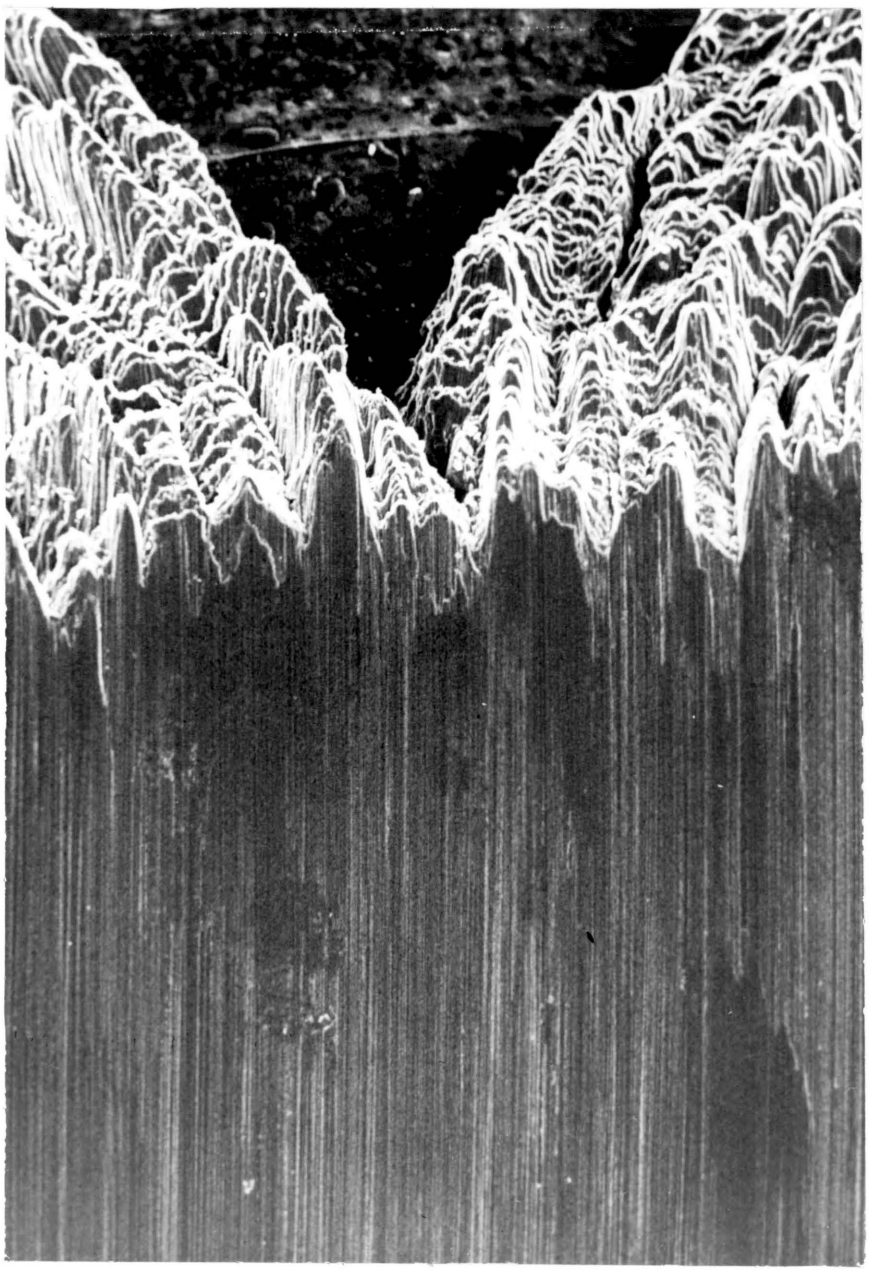

Figure 61. SEM of Trailing Edge Showing Formation of Wear 'Chip' (400 x Magnification)

TABLE 5

DATA TO CONVERT RADIANCE TO TEMPERATURE RISE
OF A COPPER ON SAPPHIRE SYSTEM
(Ambient Temp. = 20°C)

Test	Time (min)	Radiance Voltage	Emissivity	Temperature Rise (°C)	Friction Coeff.	θ/f (°C)
1-22-1	1	0.286	0.45	56	0.124	290
(Gain	2	0.411	0.45	64	0.110	400
= 20)	3	0.301	0.45	57	0.110	336
	4	0.271	0.45	54	0.110	309
	* 5	0.241	0.45	52	0.104	356
1-22-2	1	0.911	0.80	70	0.166	301
(Gain	2	0.371	0.45	61	0.152	263
= 20)	3	0.391	0.45	63	0.159	270
	4	0.391	0.45	63	0.159	270
	5	0.391	0.45	63	0.166	259
1-23-1	1	0.071	0.15	68	0.133	361
(Gain	2	0.081	0.15	71	0.143	357
= 10)	3	0.171	0.30	70	0.153	327
	4	0.141	0.25	70	0.156	321
	5	0.241	0.40	72	0.152	342
1-23-2	1	0.181	0.35	68	0.143	336
(Gain	2	0.146	0.25	72	0.152	342
= 10)	3	0.146	0.25	72	0.156	333
	4	0.141	0.20	78	0.152	382
	5	0.126	0.20	74	0.161	335
1-24-1	1	0.211	0.35	72	0.131	397
(Gain	2	0.231	0.35	74	0.143	372
= 10)	3	0.239	0.35	75	0.145	379
	4	0.239	0.35	75	0.145	379
	5	0.236	0.35	75	0.148	372
1-24-2	1	0.236	0.30	80	0.133	451
(Gain	2	0.216	0.30	77	0.127	449
= 10)	3	0.216	0.30	77	0.124	460
	4	0.266	0.35	79	0.129	457
	5	0.296	0.40	78	0.131	443

TABLE 5

DATA TO CONVERT RADIANCE TO TEMPERATURE RISE
OF A COPPER ON SAPPHIRE SYSTEM
(Ambient Temp. = 20°C)

Test	Time (min)	Radiance Voltage	Emissivity	Temperature Rise (°C)	Friction Coeff.	θ/f (°C)
1-22-1	1	0.286	0.45	56	0.124	290
(Gain	2	0.411	0.45	64	0.110	400
= 20)	3	0.301	0.45	57	0.110	336
	4	0.271	0.45	54	0.110	309
	* 5	0.241	0.45	52	0.104	356
1-22-2	1	0.911	0.80	70	0.166	301
(Gain	2	0.371	0.45	61	0.152	263
= 20)	3	0.391	0.45	63	0.159	270
	4	0.391	0.45	63	0.159	270
	5	0.391	0.45	63	0.166	259
1-23-1	1	0.071	0.15	68	0.133	361
(Gain	2	0.081	0.15	71	0.143	357
= 10)	3	0.171	0.30	70	0.153	327
	4	0.141	0.25	70	0.156	321
	5	0.241	0.40	72	0.152	342
1-23-2	1	0.181	0.35	68	0.143	336
(Gain	2	0.146	0.25	72	0.152	342
= 10)	3	0.146	0.25	72	0.156	333
	4	0.141	0.20	78	0.152	382
	5	0.126	0.20	74	0.161	335
1-24-1	1	0.211	0.35	72	0.131	397
(Gain	2	0.231	0.35	74	0.143	372
= 10)	3	0.239	0.35	75	0.145	379
	4	0.239	0.35	75	0.145	379
	5	0.236	0.35	75	0.148	372
1-24-2	1	0.236	0.30	80	0.133	451
(Gain	2	0.216	0.30	77	0.127	449
= 10)	3	0.216	0.30	77	0.124	460
	4	0.266	0.35	79	0.129	457
	5	0.296	0.40	78	0.131	443

* Denotes experimentally determined emissivity

TABLE 5 (Continued)

Test	Time (min)	Radiance Voltage	Emissivity	Temperature Rise (°C)	Friction Coeff.	θ/f (°C)
1-26-1	1	0.236	0.30	80	0.133	451
(Gain	2	0.216	0.30	77	0.127	449
= 10)	3	0.216	0.30	77	0.124	460
	4	0.266	0.35	79	0.129	457
	5	0.296	0.40	78	0.131	443
1-26-2	1	0.031	0.15	52	0.097	330
(Gain	2	0.046	0.15	59	0.099	394
= 10)	3	0.061	0.15	65	0.104	433
	4	0.076	0.15	70	0.106	472
	* 5	0.096	0.15	75	0.108	528
1-42-1	1	0.032	0.10	52	0.097	330
(Gain	2	0.066	0.10	63	0.093	462
= 20)	3	0.080	0.10	67	0.093	505
	4	0.094	0.10	70	0.090	556
	5	0.100	0.10	72	0.097	536
1-42-2	1	0.098	0.10	55	0.090	389
(Gain	2	0.148	0.10	61	0.086	477
= 30)	3	0.188	0.10	66	0.090	511
	4	0.298	0.15	64	0.093	473
	* 5	0.458	0.20	66	0.107	430
1-43-1	1	0.041	0.10	67	0.124	379
(Gain	2	0.076	0.15	70	0.117	427
= 10)	3	0.286	0.40	77	0.124	460
	4	0.306	0.40	79	0.124	476
	* 5	0.301	0.40	78	0.124	468
1-43-2	1	0.052	0.10	59	0.129	302
(Gain	2	0.082	0.10	67	0.120	392
= 20)	3	0.322	0.35	65	0.127	354
	4	0.252	0.20	74	0.133	406
	5	0.222	0.20	70	0.133	376

TABLE 5 (Continued)

Test	Time (min)	Radiance Voltage	Emissivity	Temperature Rise (°C)	Friction Coeff.	θ/f (°C)
1-44-1	1	0.156	0.15	90	0.124	565
(Gain	2	0.176	0.15	95	0.121	620
= 10)	3	0.656	0.50	97	0.117	658
	4	0.656	0.50	97	0.117	658
	5	0.736	0.50	102	0.117	701
1-44-2	1	0.096	0.10	90	0.124	565
(Gain	2	0.336	0.30	92	0.124	581
= 10)	3	0.646	0.50	97	0.128	602
	4	0.646	0.50	97	0.128	602
	5	0.686	0.50	99	0.131	603
1-46-1	1	0.420	0.30	116	0.124	702
(Gain	2	0.400	0.50	120	0.120	717
= 10)	3	1.120	0.50	119	0.115	870
	4	1.180	0.50	122	0.110	927
	* 5	1.180	0.50	122	0.110	927
1-46-2	1	0.406	0.30	116	0.117	821
(Gain	2	1.146	0.60	120	0.122	820
= 10)	3	1.106	0.50	119	0.120	825
	4	1.186	0.50	122	0.120	850
	5	1.186	0.50	122	0.115	887
1-82-1	1	1.002	0.50	88	0.124	548
(Gain	2	1.242	0.50	95	0.117	641
= 20)	3	1.062	0.50	90	0.110	636
	4	1.042	0.50	89	0.117	590
	5	0.222	0.10	94	0.117	632
1-82-2	1	0.240	0.15	82	0.101	614
(Gain	2	0.300	0.15	89	0.106	651
= 20)	3	0.360	0.15	96	0.110	691
	4	0.740	0.15	95	0.110	682
	5	0.560	0.15	113	0.117	795

TABLE 5 (Continued)

Test	Time (min)	Radiance Voltage	Emissivity	Temperature Rise (°C)	Friction Coeff.	°/f (°C)
1-82-3 (Gain = 20)	1	0.736	0.40	85	0.114	570
	2	0.876	0.40	90	0.114	614
	3	1.176	0.45	97	0.110	700
	4	1.176	0.45	97	0.110	700
	5	1.156	0.45	97	0.114	675
1-83-1 (Gain = 20)	1	0.702	0.20	110	0.106	849
	2	1.502	0.45	107	0.101	861
	3	1.361	0.45	103	0.092	902
	4	1.262	0.45	100	0.097	825
	5	1.422	0.45	105	0.097	876
1-83-2 (Gain = 20)	1	1.882	0.25	109	0.106	840
	2	1.520	0.45	108	0.092	957
	3	1.562	0.45	109	0.092	967
	4	1.602	0.45	110	0.092	978
	* 5	1.322	0.45	102	0.092	1000
1-83-3 (Gain = 10)	1	1.056	0.60	109	0.106	840
	2	1.216	0.60	115	0.106	896
	3	1.356	0.65	117	0.124	782
	4	1.616	0.65	125	0.129	814
	5	1.576	0.65	124	0.129	806
1-84-1 (Gain = 10)	1	0.686	0.30	120	0.117	855
	2	1.166	0.50	122	0.110	927
	3	1.206	0.50	123	0.090	1144
	4	0.826	0.40	116	0.083	1157
	5	0.706	0.40	109	0.072	1236
1-84-2 (Gain = 5)	1	0.758	0.60	125	0.114	921
	2	0.738	0.60	124	0.114	912
	3	0.618	0.55	120	0.114	877
	4	0.638	0.55	120	0.114	877
	* 5	0.538	0.55	114	0.114	842

TABLE 5 (Continued)

Test	Time (min)	Radiance Voltage	Emissivity	Temperature Rise (°C)	Friction Coeff.	θ/f (°C)
1-84-3	1	0.240	0.30	105	0.124	685
(Gain	2	0.360	0.40	110	0.124	726
= 2)	3	0.960	0.55	140	0.135	889
	4	1.200	0.65	144	0.131	947
	5	1.140	0.65	142	0.128	953
1-86-1	1	1.087	0.50	150	0.106	1226
(Gain	2	1.067	0.50	149	0.106	1217
= 5)	3	0.967	0.50	144	0.106	1170
	4	0.907	0.50	140	0.106	1132
	5	0.987	0.50	145	0.106	1179
1-86-2	1	1.348	0.50	162	0.110	1291
(Gain	2	1.168	0.50	154	0.110	1264
= 5)	3	1.088	0.50	150	0.110	1182
	4	1.328	0.50	161	0.104	1356
	* 5	1.348	0.50	162	0.104	1365
1-86-3	1	0.203	0.30	139	0.115	1035
(Gain	2	0.333	0.40	150	0.110	1182
= 2)	3	0.463	0.50	156	0.110	1236
	4	0.483	0.50	159	0.108	1287
	5	0.403	0.50	149	0.104	1240

TABLE 5 (Continued)

Test	Time (min)	Radiance Voltage	Emissivity	Temperature Rise (°C)	Friction Coeff.	θ/f (°C)
2-22-1 (Gain = 50)	3	0.070	0.20	19	0.122	156
	5	0.100	0.10	21	0.118	178
2-22-2 (Gain = 50)	3	0.045	0.15	20	0.105	190
	* 5	0.030	0.15	18	0.105	191
2-23-1 (Gain = 50)	3	0.085	0.20	20	0.107	187
	5	0.160	0.30	20	0.112	179
2-23-2 (Gain = 50)	3	0.095	0.15	26	0.118	220
	5	0.100	0.15	27	0.122	221
2-24-1 (Gain = 50)	3	0.191	0.30	36	0.110	327
	5	0.246	0.30	25	0.119	214
2-24-2 (Gain = 50)	3	0.171	0.15	34	0.108	315
	5	0.171	0.15	34	0.110	309
2-26-1 (Gain = 50)	3	0.410	0.25	38	0.120	317
	5	0.390	0.25	37	0.126	294
2-26-2 (Gain = 20)	3	0.480	0.25	41	0.114	360
	5	0.480	0.25	42	0.119	345
2-42-1 (Gain = 20	3	0.044	0.10	36	0.114	313
	5	0.284	0.50	33	0.115	287
2-42-2 (Gain = 20)	3	0.274	0.50	32	0.115	278
	5	0.144	0.30	31	0.115	270

TABLE 5 (Continued)

Test	Time (min)	Radiance Voltage	Emissivity	Temperature Rise (°C)	Friction Coeff.	$\Delta T/f$ (°C)
2-43-1 (Gain = 10)	3	0.112	0.30	42	0.123	341
	* 5	0.192	0.30	54	0.120	450
2-43-2 (Gain = 10)	3	0.164	0.30	49	0.116	422
	5	0.434	0.30	57	0.116	491
2-44-1 (Gain = 10	3	0.562	0.60	65	0.108	602
	5	0.402	0.50	60	0.115	522
2-44-2 (Gain = 10	3	0.292	0.40	57	0.114	500
	5	0.532	0.60	63	0.114	553
2-46-1 (Gain = 20)	3	1.284	0.50	85	0.119	714
	5	1.084	0.40	79	0.119	664
2-46-2 (Gain = 5)	3	1.106	0.15	82	0.128	641
	5	1.126	0.15	88	0.124	710
2-82-1 (Gain = 5)	3	1.050	0.20	48	0.103	466
	5	1.116	0.60	40	0.103	388
2-82-2 (Gain = 5)	3	1.014	0.10	40	0.099	404
	5	1.120	0.60	40	0.099	404
2-83-1 (Gain = 2)	3	1.153	0.65	73	0.110	664
	* 5	1.178	0.65	79	0.110	718
2-83-2 (Gain = 2)	3	1.278	0.80	89	0.104	856
	5	1.028	0.10	82	0.104	788

TABLE 5 (Continued)

Test	Time (min)	Radiance Voltage	Emissivity	Temperature Rise (°C)	Friction Coeff.	θ/f (°C)
2-84-1 (Gain = 2)	3	0.183	0.80	95	0.106	849
	5	0.318	0.80	95	0.106	896
2-84-2 (Gain = 2)	3	0.328	0.80	96	0.108	889
	5	0.328	0.80	95	0.108	889
2-86-1 (Gain = 2)	3	0.508	0.80	117	0.118	992
	5	0.598	0.80	125	0.118	1059
2-86-2 (Gain = 2)	3	0.538	0.80	120	0.109	1101
	* 5	0.598	0.80	125	0.109	1147
4-42-1 (Gain = 50)	2	0.860	0.50	37	0.112	286
	3	0.780	0.50	35	0.112	313
	4	0.780	0.50	35	0.112	313
	5	0.780	0.50	35	0.112	313
4-42-2 (Gain = 50)	2	0.440	0.30	35	0.115	304
	3	0.440	0.30	35	0.115	304
	4	0.680	0.50	32	0.115	278
	5	0.480	0.30	37	0.115	322
4-43-1 (Gain = 20)	2	0.514	0.60	42	0.110	382
	3	0.514	0.60	42	0.110	382
	4	0.464	0.60	40	0.110	364
	* 5	0.464	0.60	40	0.110	364
4-43-2 (Gain = 20)	2	0.438	0.60	38	0.117	325
	3	0.328	0.60	32	0.117	274
	4	0.468	0.60	40	0.117	342
	5	0.398	0.60	36	0.117	303
4-44-1 (Gain = 20)	2	0.864	0.60	57	0.103	553
	3	0.766	0.60	53	0.103	515
	4	0.804	0.60	54	0.103	524
	5	0.764	0.60	53	0.103	515

TABLE 5 (Continued)

Test	Time (min)	Radiance Voltage	Emissivity	Temperature Rise (°C)	Friction Coeff.	ΔT/f (°C)
4-44-2	2	0.684	0.60	50	0.117	427
(Gain	3	0.684	0.60	50	0.117	427
= 20)	4	0.684	0.60	60	0.117	427
	5	0.684	0.60	50	0.117	427
4-46-1	2	0.772	0.60	50	0.105	733
(Gain	3	0.772	0.60	77	0.105	733
= 10)	4	0.592	0.60	67	0.105	638
	5	0.772	0.60	77	0.105	733
4-46-2	2	0.732	0.60	75	0.125	600
(Gain	3	0.732	0.60	75	0.125	600
= 10)	4	0.852	0.60	80	0.125	640
	* 5	0.732	0.60	75	0.125	600

that for most tests there are generally two emissivities which correspond to the bi-level emissivity nature of copper. In a few cases, 10 out of 60, it was felt that three emissivities should be used.

One of the primary objectives of the research was to investigate the effect of subdivisions numerically. The temperatures listed in Table 6 are averages of all the temperatures experimentally determined for each test condition and therefore this table is a summary of 260 actual temperatures. These results show a very important trend, in all but one test, the temperature increases with load for a given sliding velocity. The effect of subdivision is shown in Table 7. This effect is demonstrated by listing the percent decrease in surface temperature due to subdividing the apparent contact area from 1 to 2 and 2 to 4. Subdividing the contact from 1 area to 2 results in an average percent decrease in the surface temperature of 24.7 percent. In general the percent decrease in temperature with subdivision also follows an interesting trend. The percent decrease in temperature is reduced with higher loads or higher heat input.

In order to more accurately and quantitatively determine the factors that affect surface temperatures, a statistical analysis was performed on the experimental results. A three-factor two-level analysis designed to indicate whether subdivision, load, velocity, and their first and second-order interactions were at all significant, displayed important results. Table 8 shows that all of the single factors (subdivision, load and velocity) have significant effects on surface temperatures at the 99% confidence level. Figure 62 illustrates

TABLE 6

EXPERIMENTALLY DETERMINED TEMPERATURES OF COPPER-ON-SAPPHIRE

Test Conditions		Temperature Rise (°C)		
Sliding Velocity (m/s)	Normal Load (N)	1 Contact	2 Contacts	4 Contacts
2	2	41	20	
2	3	51	23	
2	4	53	32	
2	6	51	39	
4	2	44	33	35
4	3	51	51	39
4	4	75	61	52
4	6	98	84	75
8	2	73	42	
8	3	90	81	
8	4	102	94	
8	6	132	122	

TABLE 7

PERCENT DECREASE IN SURFACE TEMPERATURE RISE

DUE TO SUBDIVISION OF THE CONTACT

Test Conditions		Percent Decrease in Surface Temperature due to to subdivision		
Sliding Velocity (m/s)	Normal Load (N)	2:1 contacts	4:1 contacts	4:2 contacts
2	2	51		
2	3	55		
2	4	40		
2	6	24		
4	2	25	20	-6
4	3	0	24	24
4	4	19	31	15
4	6	14	23	11
8	2	42		
8	3	10		
8	4	8		
8	6	8		

TABLE 8

FACTORS THAT AFFECT SURFACE TEMPERATURES

Factor	Levels	Signicant	(Confi-dence Level)	Avg. Temp. Rise
Subdivision	1-2	Yes	99%	71.1 - 56.8
Load	2N-6N	Yes	99%	55.3 - 99.0
Velocity	2m/s-8m/s	Yes	99%	48.9 - 97.9
Sub x Load		Yes	98%	
Sub x Velocity		No		
Load x Velocity		Yes	98%	
Sub x Load x Velocity		No		

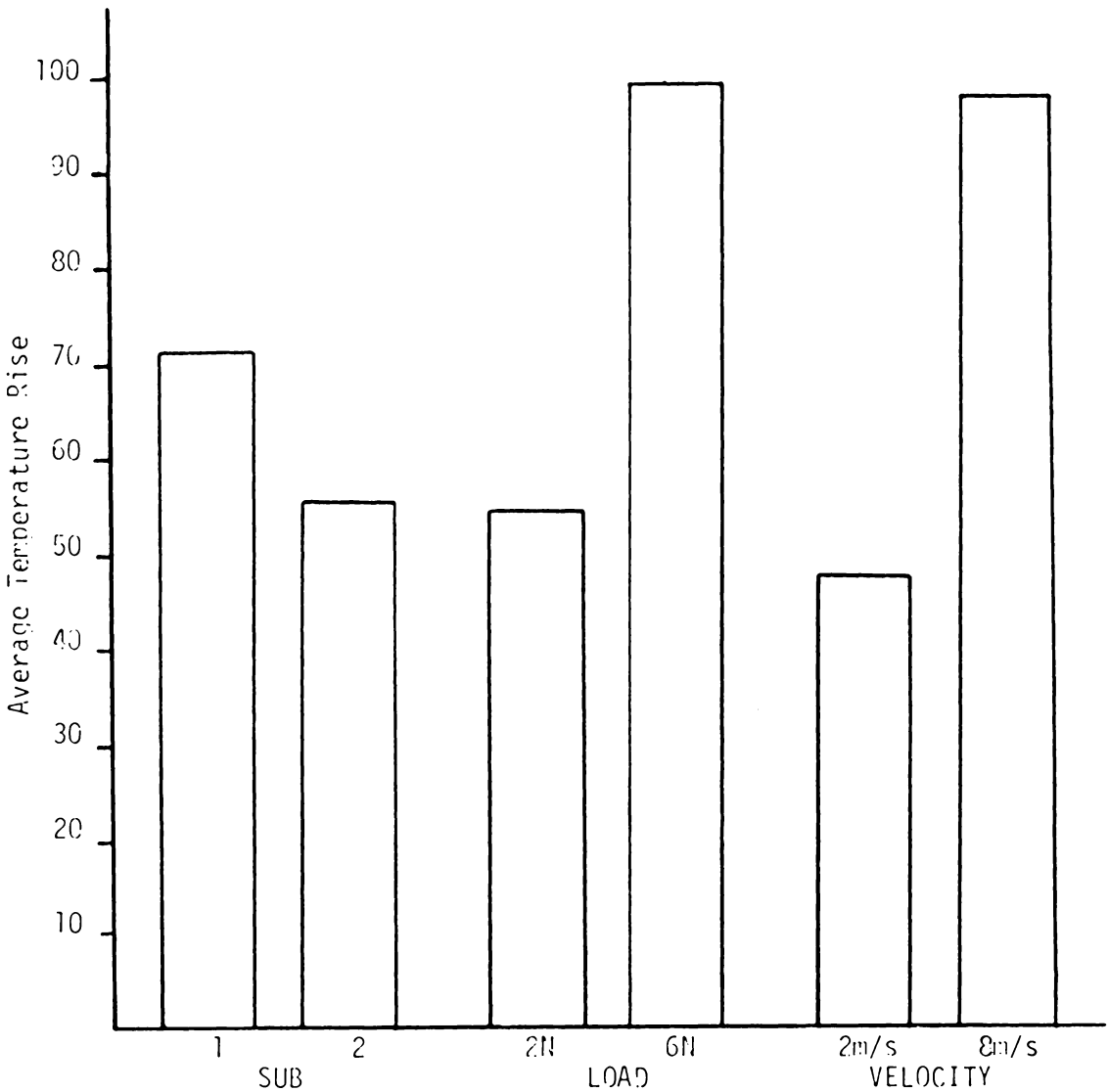

Figure 62. The Significance of the Factors that Affect Surface Temperature

the magnitude of the effect of each of the factors. This figure shows that not only is the effect of subdivision significant on surface temperatures but also the magnitude of its effect to reduce surface temperatures appear to be sizeable.

4.2 Discussion of Results

There are a number of interesting ways to evaluate and explain the temperature results. In this study, the effect of the subdivision of the contact area is of primary importance and, thus, a comparison of surface temperatures for like conditions and the various number of subdivisions will be made. Comparisons between experiment and theory will also be made.

Before presenting comparisons of the experimental results with the theoretical temperatures, another look at the theory is in order. To make a true comparison, where the objective is to see how well the theory predicts the physical process, we must be sure that the theory considers all the elements present in the real system. This would include the temperature dependence of the physical and thermal properties, and does the theoretical model properly describe the real system? Also important is the question of whether the physical and thermal properties used in theory actually define the material.

Taking a look at this last problem is vital to a study with copper. Copper is a material which is characterized by its work-hardening tendency. In both the Archard and Jaeger theories the real area of contact must be known. In this study, plastic deformation theory was used because the specimen geometry did not yield itself to elastic theory. This then means that the surface hardness of the specimen is important as it determines the contact area. It is difficult to know exactly how the hardness changes during the course of a test. An even more basic question would be: does plastic deformation theory come

close to determining what the true contact area is? It is at this point where some assumptions must be made. As some of the literature explains in great detail, the Archard and Jaeger theories are to some extent quite basic and simple in that they do not attempt to describe physical systems. The philosophy that is used in this paper is that the Archard and Jaeger equations may describe the trends very well but they do not describe a real dynamic system. Even where the theories may accurately determine the temperature, the user cannot accurately supply them with real contact area data. This alone causes an uncertainty in the theoretical results. Therefore, experimental that will be presented are meant to see how the theories may be used in real systems or how they might be altered to more accurately describe the dynamic system.

In order to compare experimental data results with theoretical predictions of temperatures, it would be interesting to know how the hardness alone affects the theoretical temperatures. The hardness used in all the theoretical calculations was 7.85×10^8 N/m^2. If work hardening of the copper specimen occurred, then the theory would predict higher temperatures than those with the initial hardness because the contact area would be smaller and thus the heat flux would be greater. Table 9 shows the theoretical temperatures of Archard and Jaeger for all the test conditions used in this study. To see the effect of changes in hardness, the theoretical temperatures were again calculated using hardnesses based on percent increases of 5,10, 15, and 25. The relative increase in temperature was plotted against the percent increase in hardness (Fig. 63) and a statistical regression performed which deter-

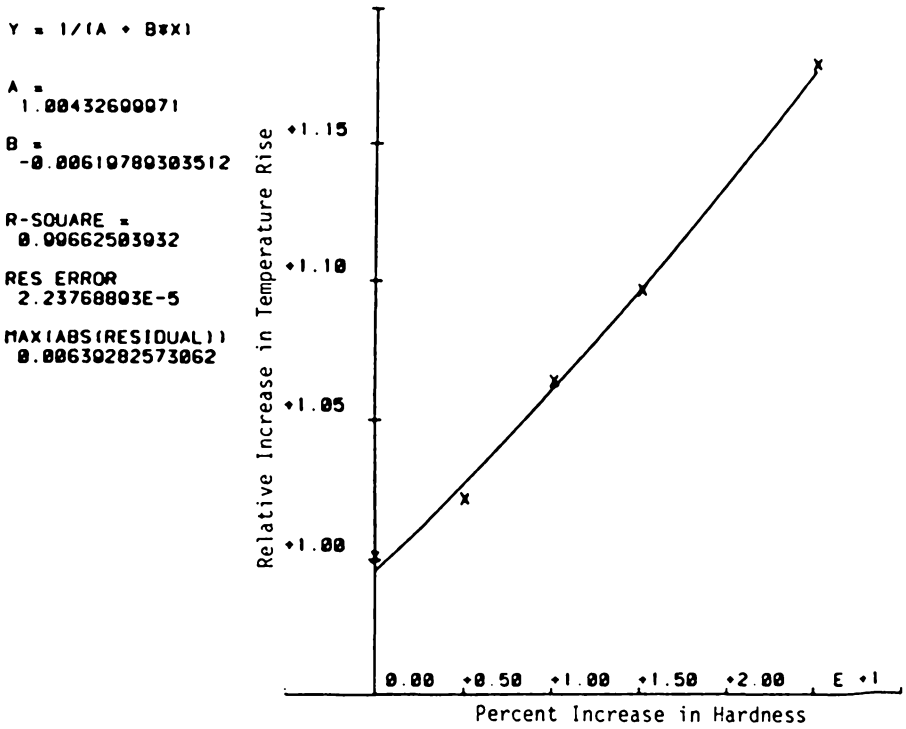

Figure G3. The Effect of Increased Hardness on Surface Temperatures

TABLE 9

The Effect of Hardness on Caculated Theoretical

Temperature Rise

	Archard Temp/Jaeger Temp (°C/f)				
	(Initial Value)	(5% Increase)	(10% Increase)	(15% Increase)	(25% Increase)
Load (N)	$P_m=7.85\times10^8 N/m^2$	$P_m=8.26\times10^8 N/m^2$	$P_m=8.72\times10^8 N/m^2$	$P_m=9.25\times10^8 N/m^2$	$P_m=1.05\times10^9 N/m^2$
Sliding Velocity = 2.0 m/sec					
2.0	240/96	247/98	255/101	263/104	283/111
3.0	284/116	293/119	302/122	312/126	336/135
4.0	322/132	331/136	341/140	353/144	380/154
6.0	384/160	395/165	407/170	420/175	452/187
Sliding Velocity = 4.0 m/sec					
2.0	431/183	444/188	459/194	475/200	512/214
3.0	508/220	524/227	541/233	560/241	604/258
4.0	569/251	588/258	608/266	630/275	679/294
6.0	664/301	686/310	709/319	734/392	795/353
Sliding Velocity - 8.0 m/sec					
2.0	743/342	766/352	792/363	820/375	887/402
3.0	1528/417	1587/430	1653/443	1726/457	1039/482
4.0	1642/473	1705/487	1776/502	1855/519	2041/558
6.0	1817/564	1888/580	1966/599	2053/619	2260/665

mined the best equation to define the data. Table H-1 of Appendix H has temperature rise data plus the average heat input to the system is also listed. An interesting comparison between temperature rise and heat input was first shown by M. J. Furey [55]. In his experimental study using a ball on cylinder device, he showed there was a power function correlation between heat input and surface temperature. Figure 64 is a plot of average heat input vs. normalized temperature rise. With the use of a statistical regression analysis the 'best-fit' function was determined from a library of eight functions. The function that was determined to best describe the data was

$$Y = AB^{X}$$

which is the power function first shown by Furey. Even though the data appears a bit scattered it is interesting that the power function correlation still exists.

The key results that are now to be presented are those showing the relationship between the number of subdivided contact areas and the surface temperatures generated by friction. Before looking directly at the effect of subdivision, it would be nice to know just how well the specimens resemble the theoretical model. This is best seen by looking at the experimental data plotted alongside the Archard and Jaeger theories. Figures 65 - 67 show the mean temperature divided by friction plotted against normal contact load for the three sliding velocities used in this investigation. The mean temperature rise for a friction coefficient of 1.0 or as it is referred to in the tables, normalized temperature rise, can also be expressed as mean temperature rise divided

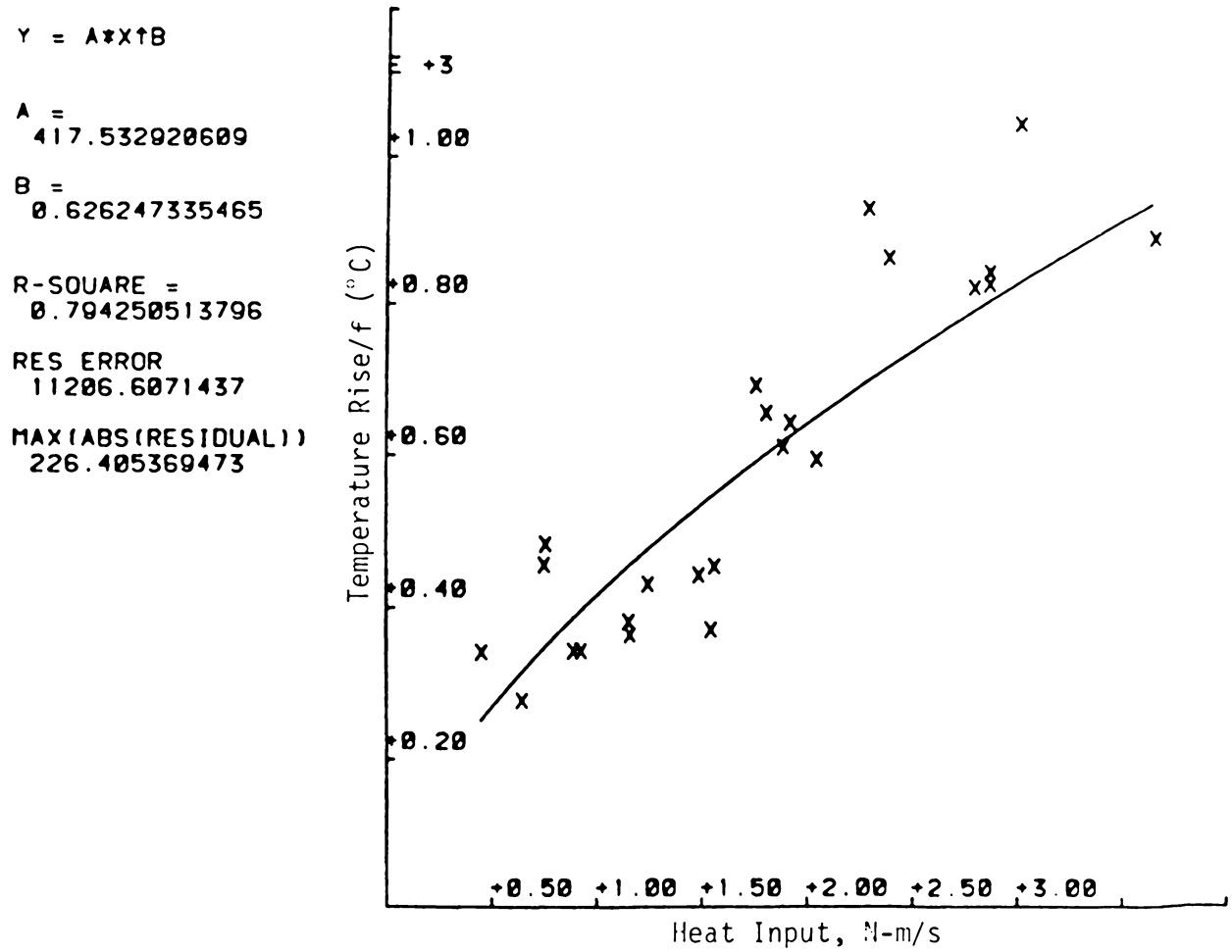

Figure G4. The Effect of Heat Input on Temperature Rise

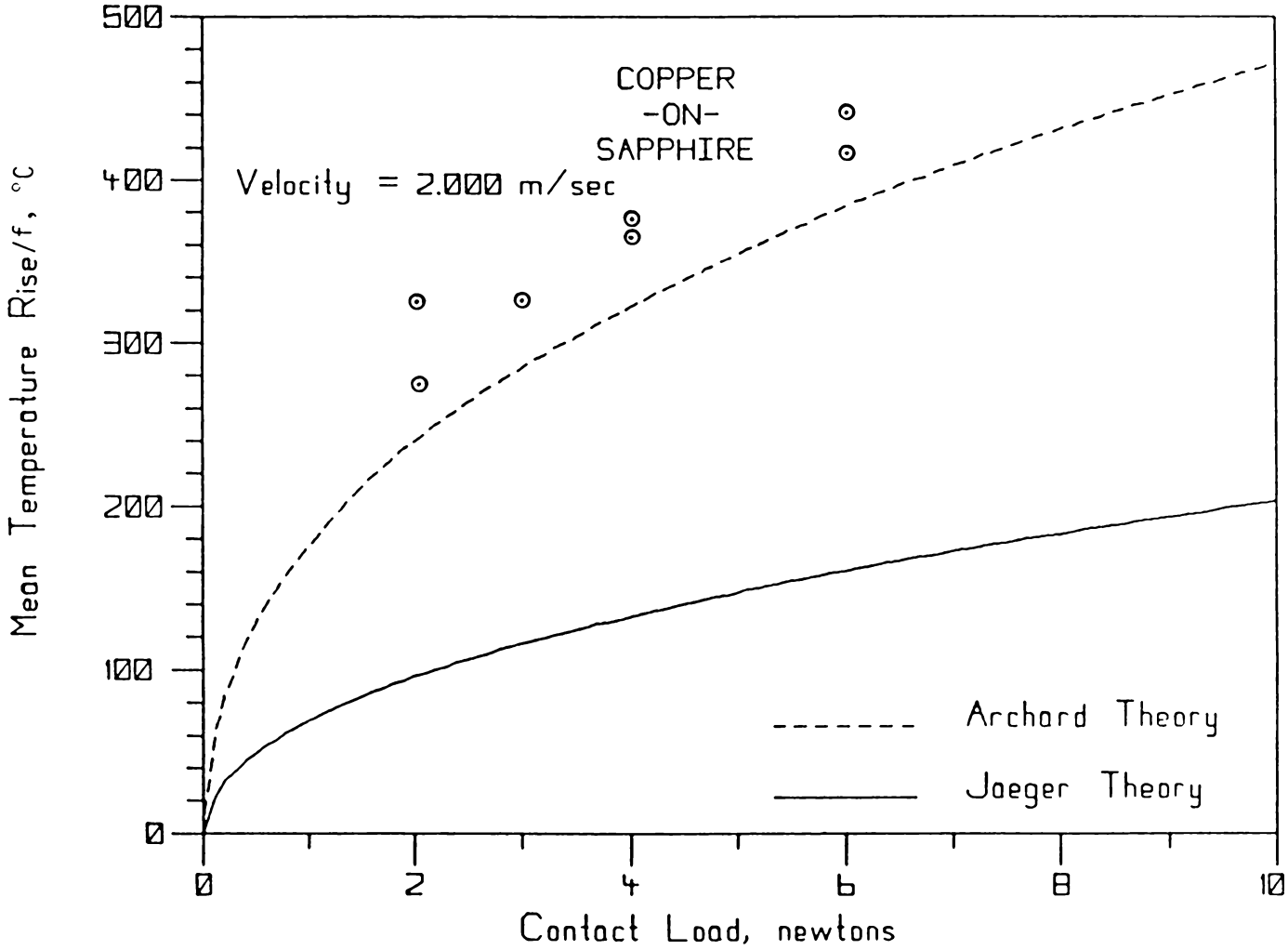

Figure 65. The Effect of Load on Surface Temperature, Velocity=2.0m/s

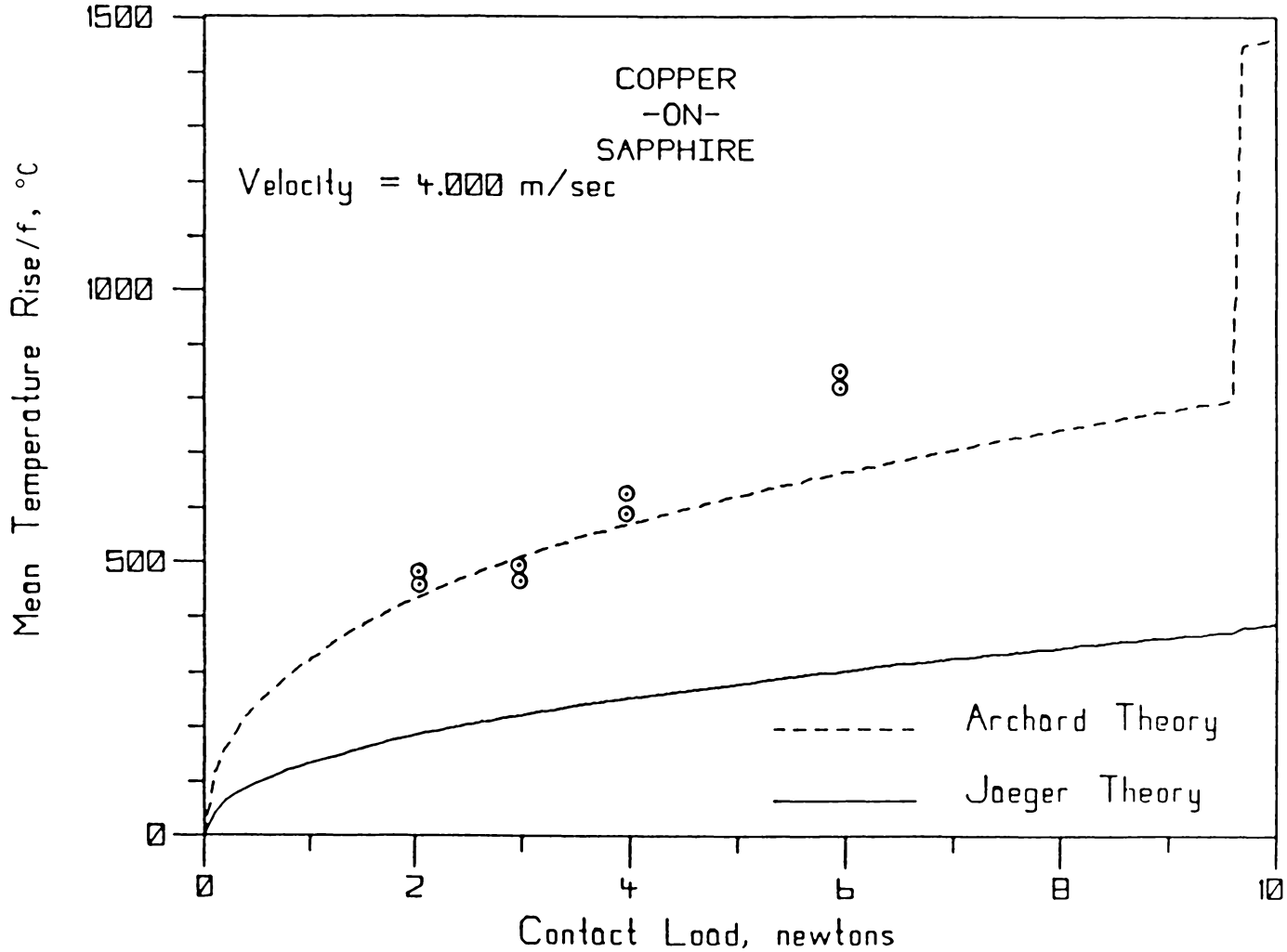

Figure 66. The Effect of Load on Surface Temperature, Velocity=4.0m/s

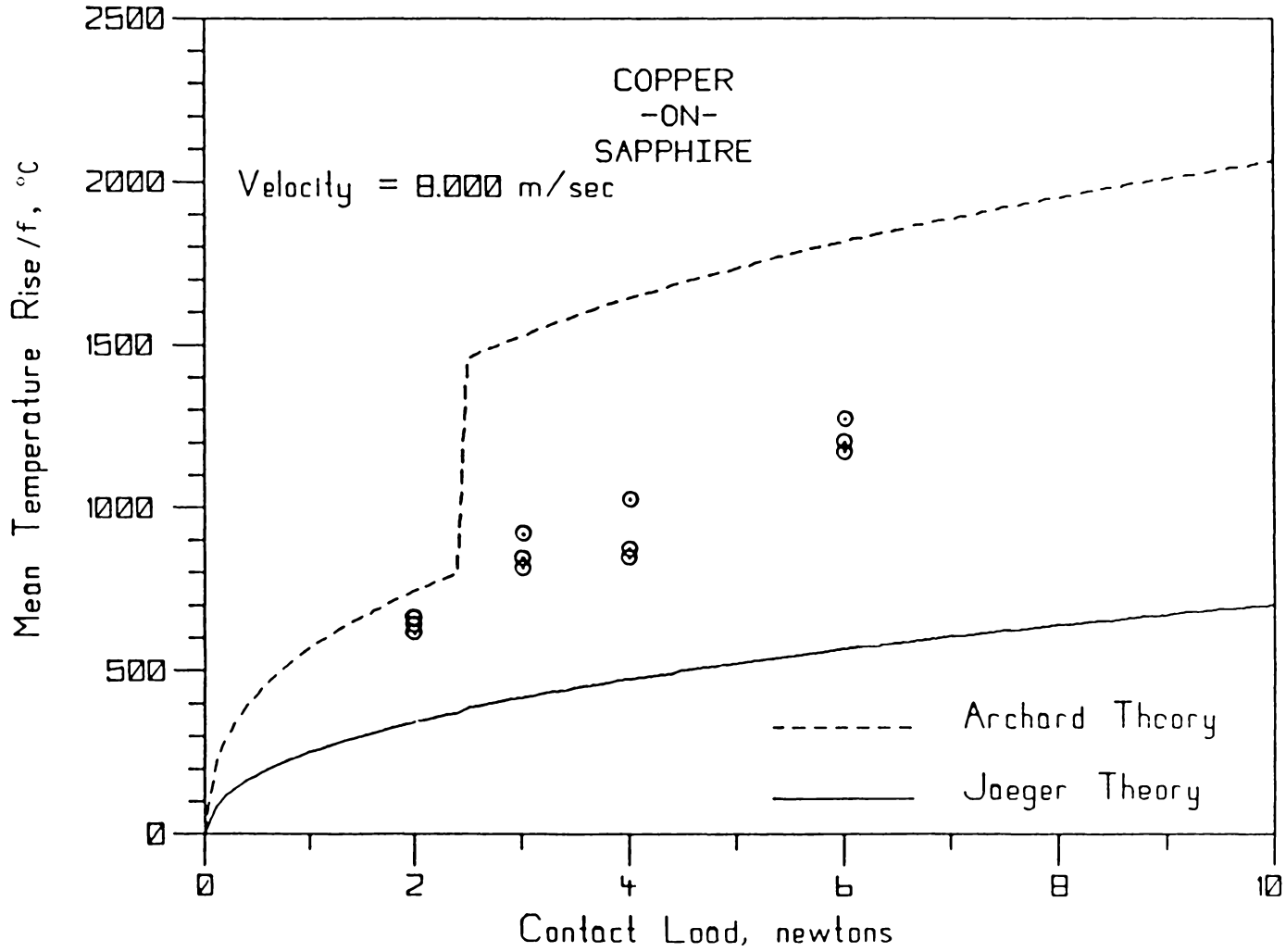

Figure 67. The Effect of Load on Surface Temperatures, Velocity=8.0m/s

by the coefficient of friction. The data is presented in this manner as the friction coefficient varies from test to test and even within a single test itself. Figures 68 - 71 show the same data plotted on theoretical curves that relate the normalized temperature for a given load against sliding speed. From these figures it is quite evident that the experimental data for a single geometric area is in fair agreement with the Archard theory. It is important to note a few characteristics of the theoretical data. First, the tests were in the most part, in the so called intermediate range of the theory. It is in this range of Archard's theory that his treatment with the use of Jaeger's "Figure 7" is questioned. In many of these figures, a step increase in the theoretical temperature is seen. This is due to the discontinuity in Archard's theory when going from the intermediate range to the high speed range. Figure 67 illustrates that the experimental data is obviously not affected by going from the intermediate region to the high speed region. This figure also shows that the trend defined by the theoretical curves does in fact exist in the experimental data. It also seems that the same trends are defined by both theories, that is the difference between Archard and Jaeger is really the magnitude of the temperatures. This is to be expected to some degree as Archard's theory is a simplification of Jaeger's theory. It is reasonable that one could possibly justify drawing the conclusion that either Archard or Jaeger's theory would accurately predict the surface temperature if the proper contact area was used. The most important message found in these plots is that the specimen geometry in this experimental study is fairly

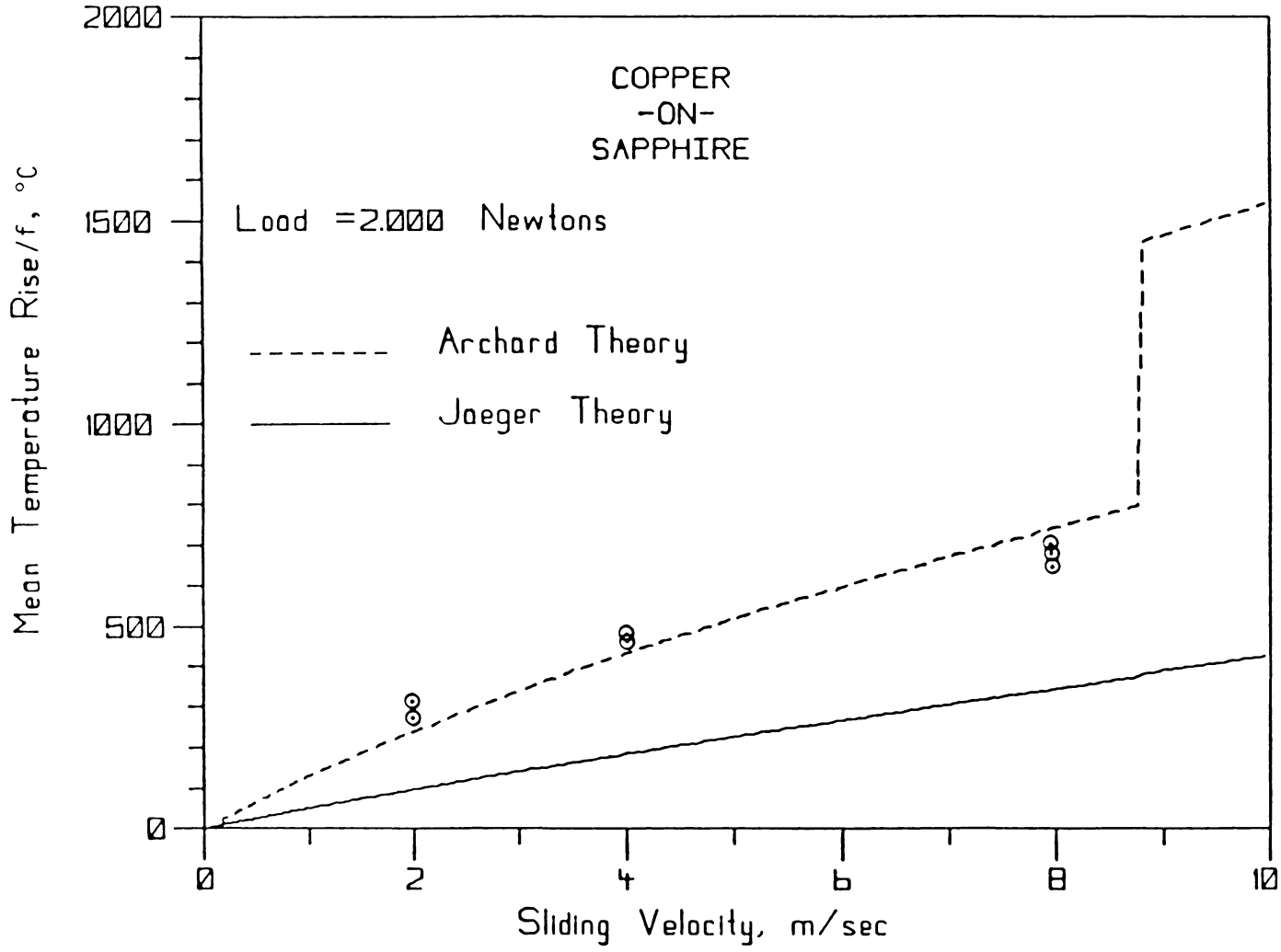

Figure 68. The Effect of Velocity on Surface Temperature, Load=2.0N

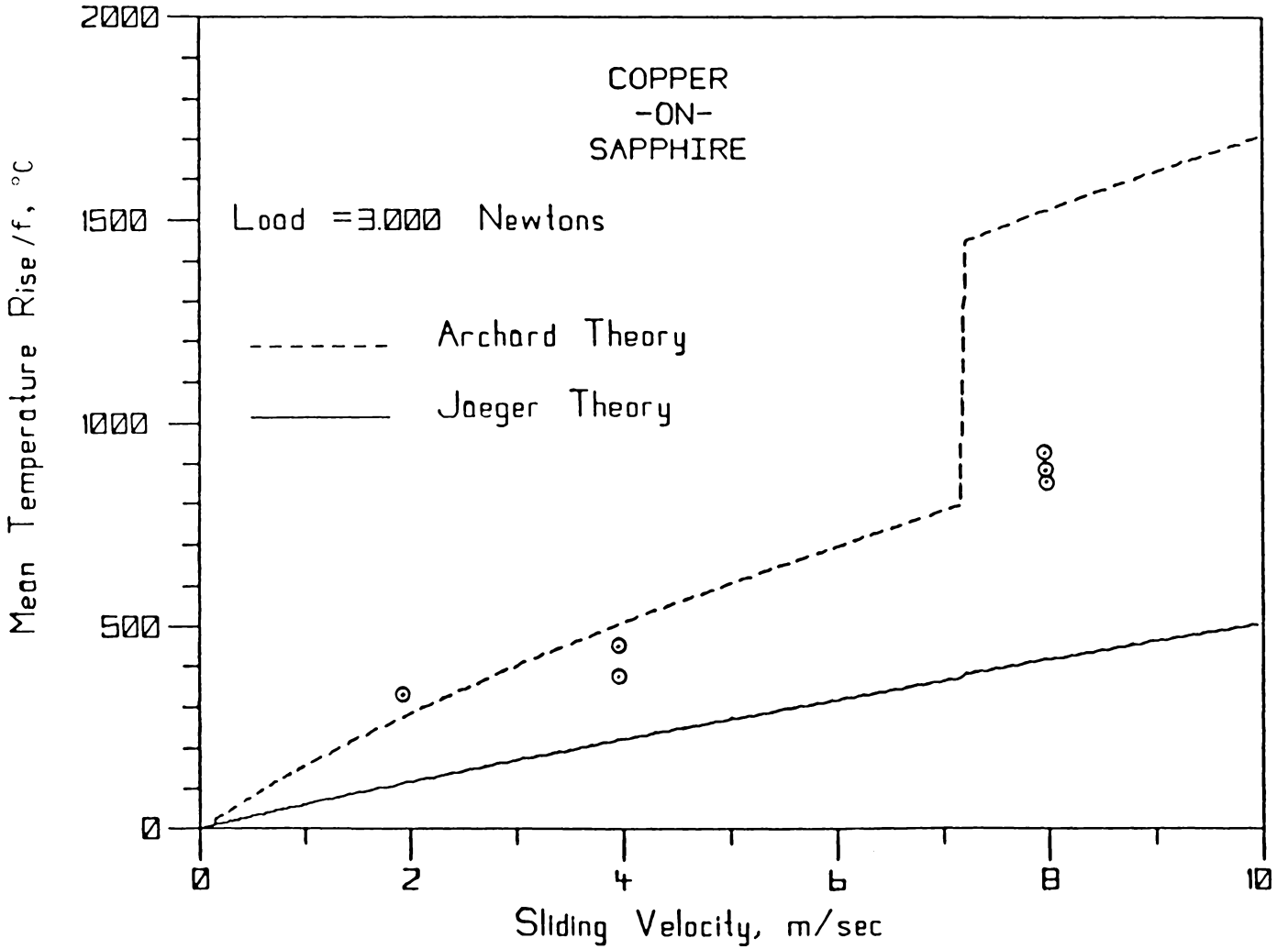

Figure 69. The Effect of Velocity on Surface Temperature, Load=3.0N

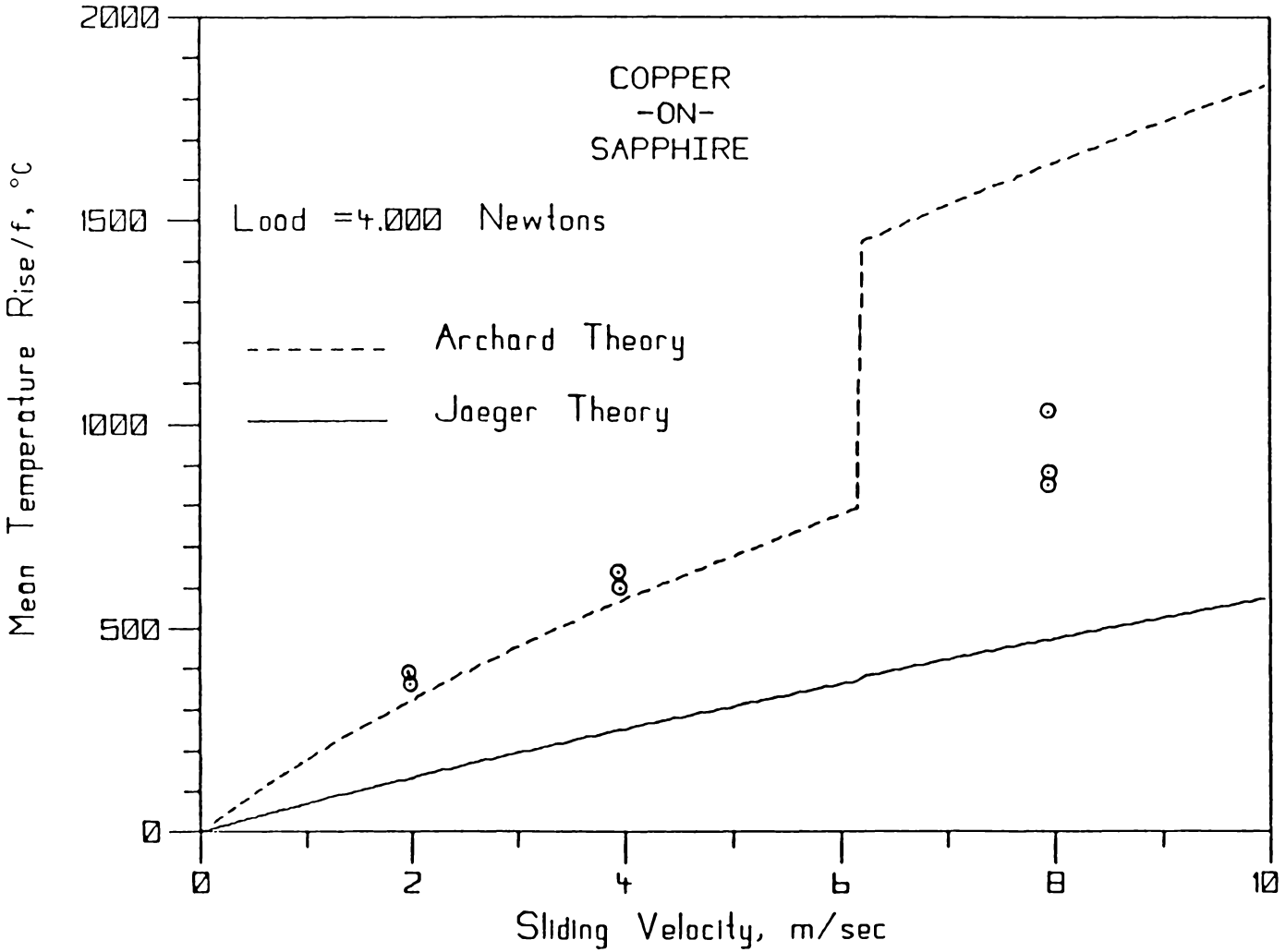

Figure 70. The Effect of Velocity on Surface Temperature, Load=4.0N

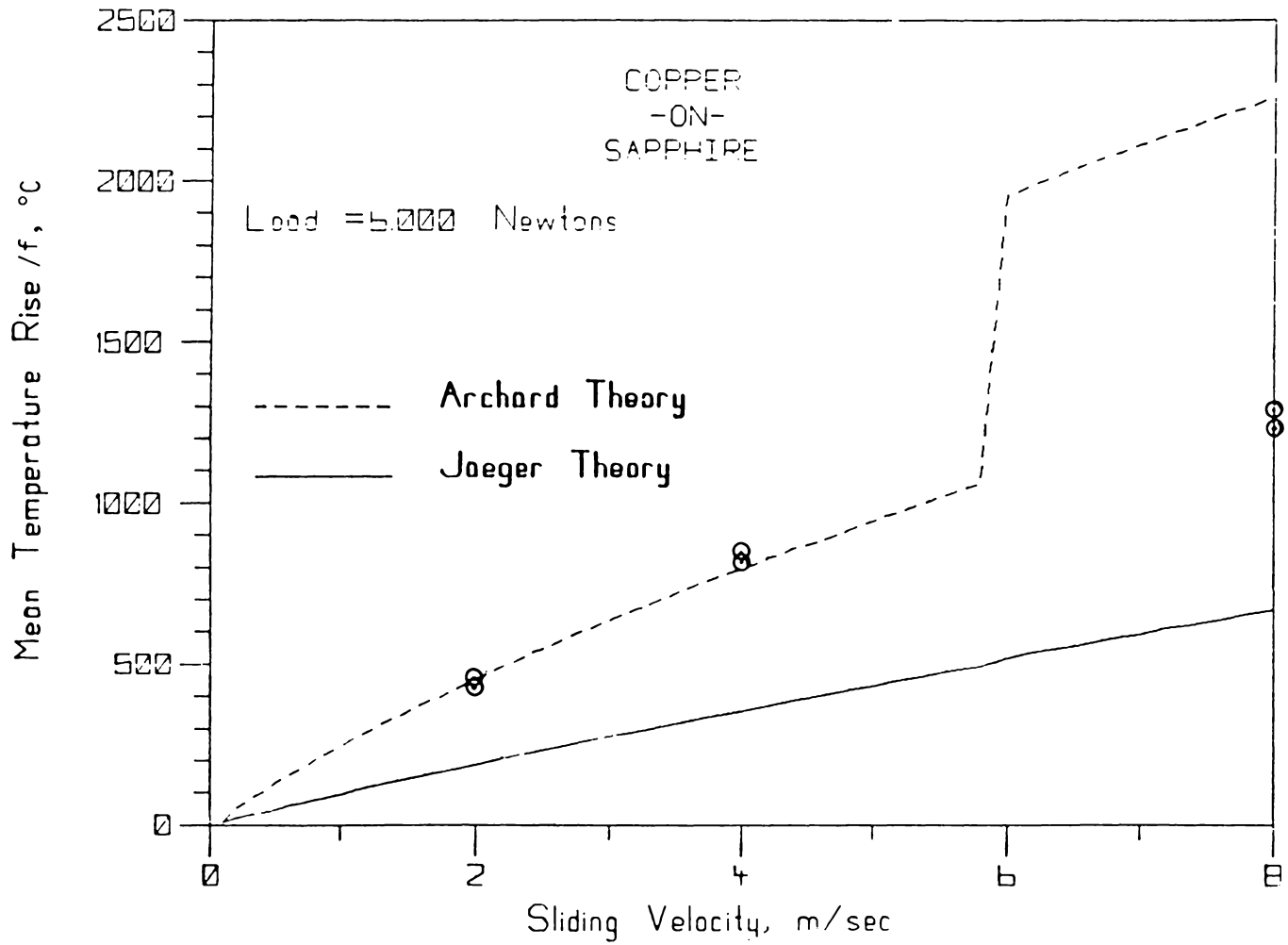

Figure 71. The Effect of Velocity on Surface Temperature, Load = 6.0 N

closely approximated by the theoretical models. This is a rather significant finding in as much as this implies that the individual microscopic contact areas are not as important as the basic geometry of the specimen.

Figure 63 shows that a 25 percent increase in hardness results in an approximately 18 percent increase in the theoretical surface temperature rise. It is therefore evident that the theoretical temperatures can be adjusted over a fairly large range by simply changing the hardness. Confidence in the theoretical temperatures can be achieved only with confidence in the manner in which the contact area is calculated and the assumptions used.

Based on the findings that the specimen geometry used was a close approximation to the theoretical model, it would seem reasonable to expect that the macroscopic subdivision of the contact may reduce the surface temperatures as predicted by theory. The effect of subdivision is shown numerically in Table 7. The temperatures listed are averages of all the temperatures experimentally determined for each test condition and therefore this table is a summary of 260 actual temperatures. The effect of subdivision is shown pictorially in Figs. 72 - 83. These figures were generated with the use of the computer program listed in Appendix F.2. Again these figures plot the normalized temperature to the number of contacts for both the Archard and Jaeger theories. In the Archard theory, a sharp decrease in the temperature from one contact to two followed by a much more gradual decrease is caused by the discontinuity from the high speed equation to the intermediate equation.

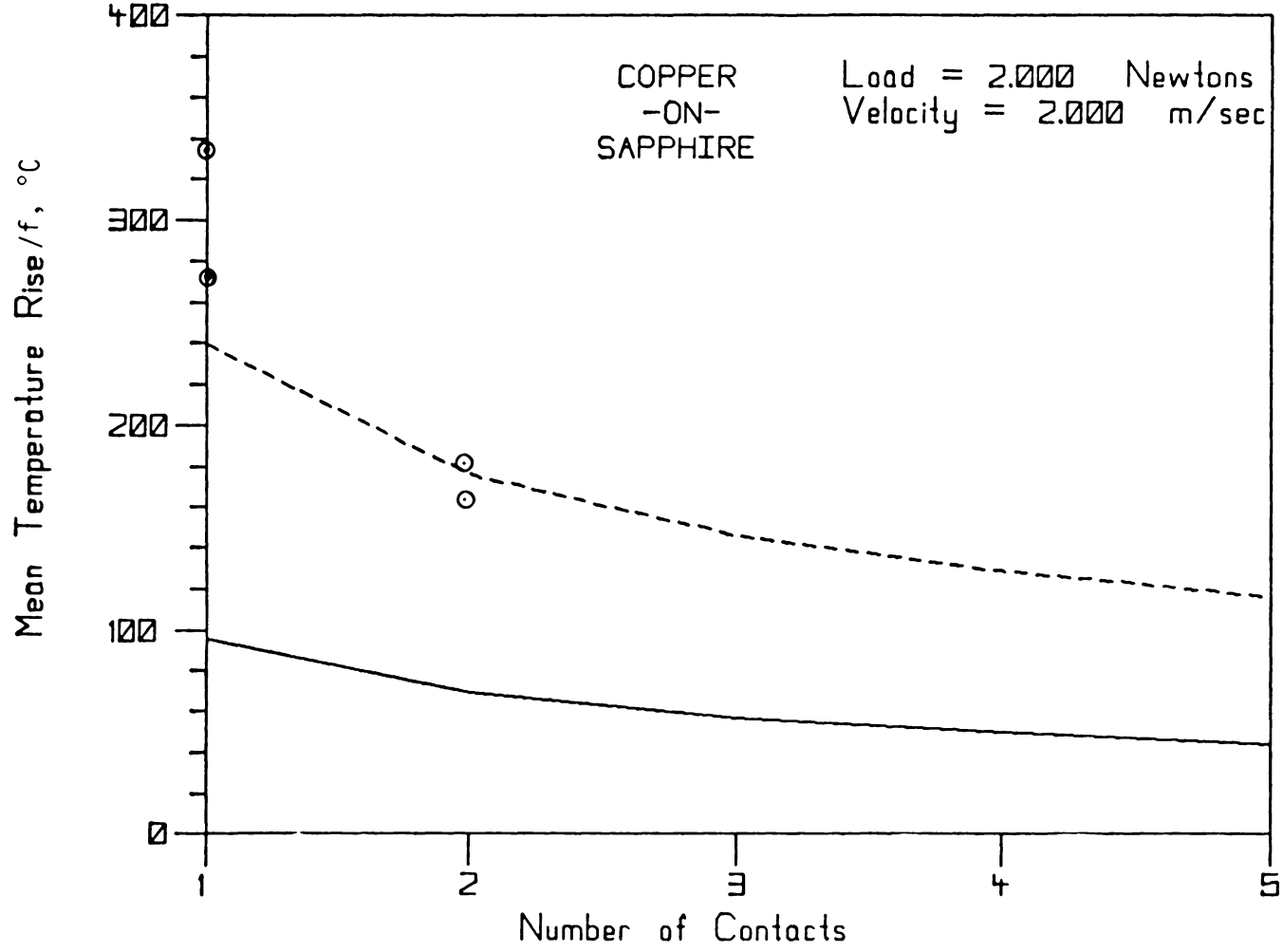

Figure 72. The Effect of Subdivision - Load=2N, Velocity=2m/s

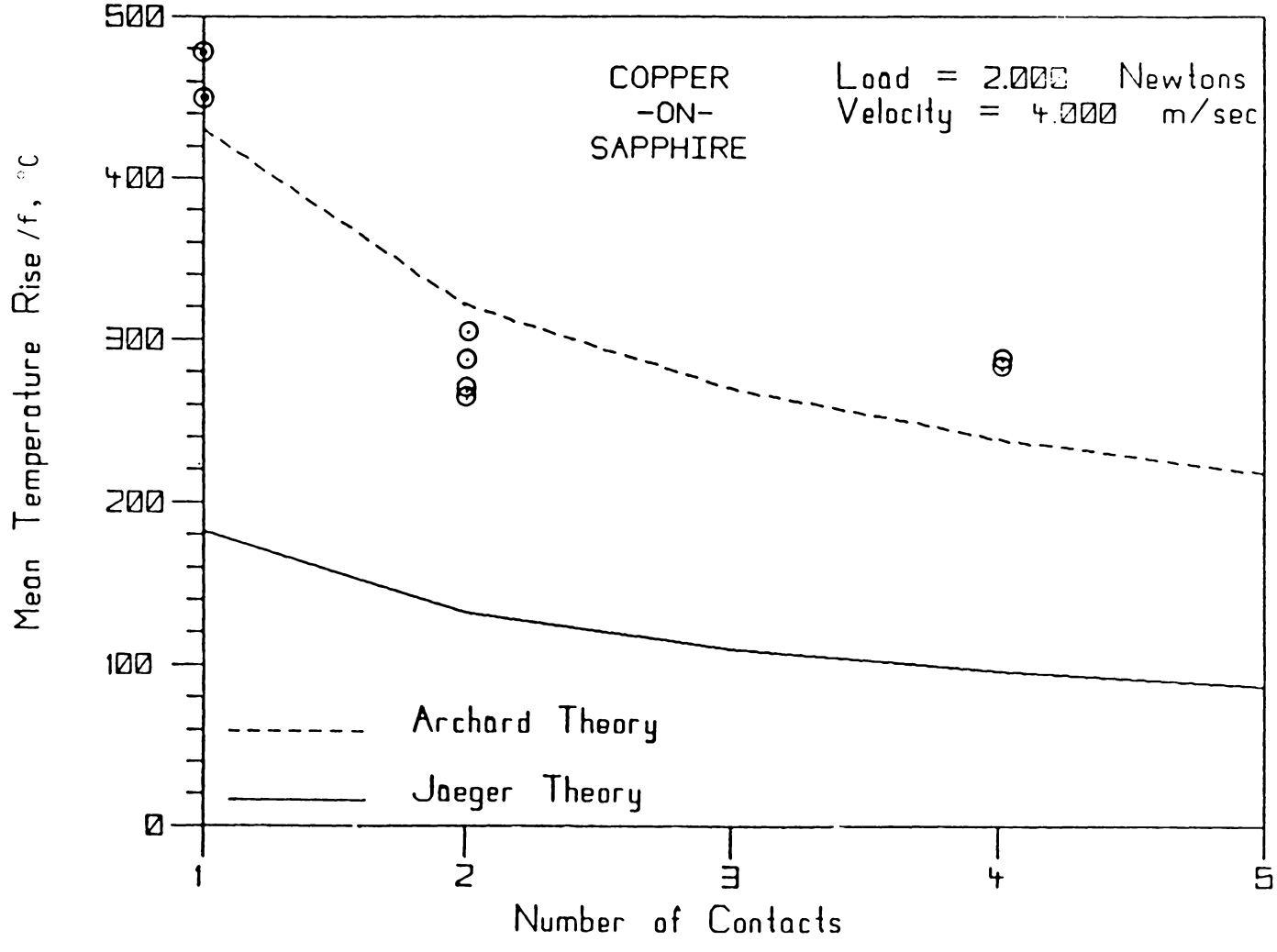

Figure 73. The Effect of Subdivision - Load=2N, Velocity=4m/s

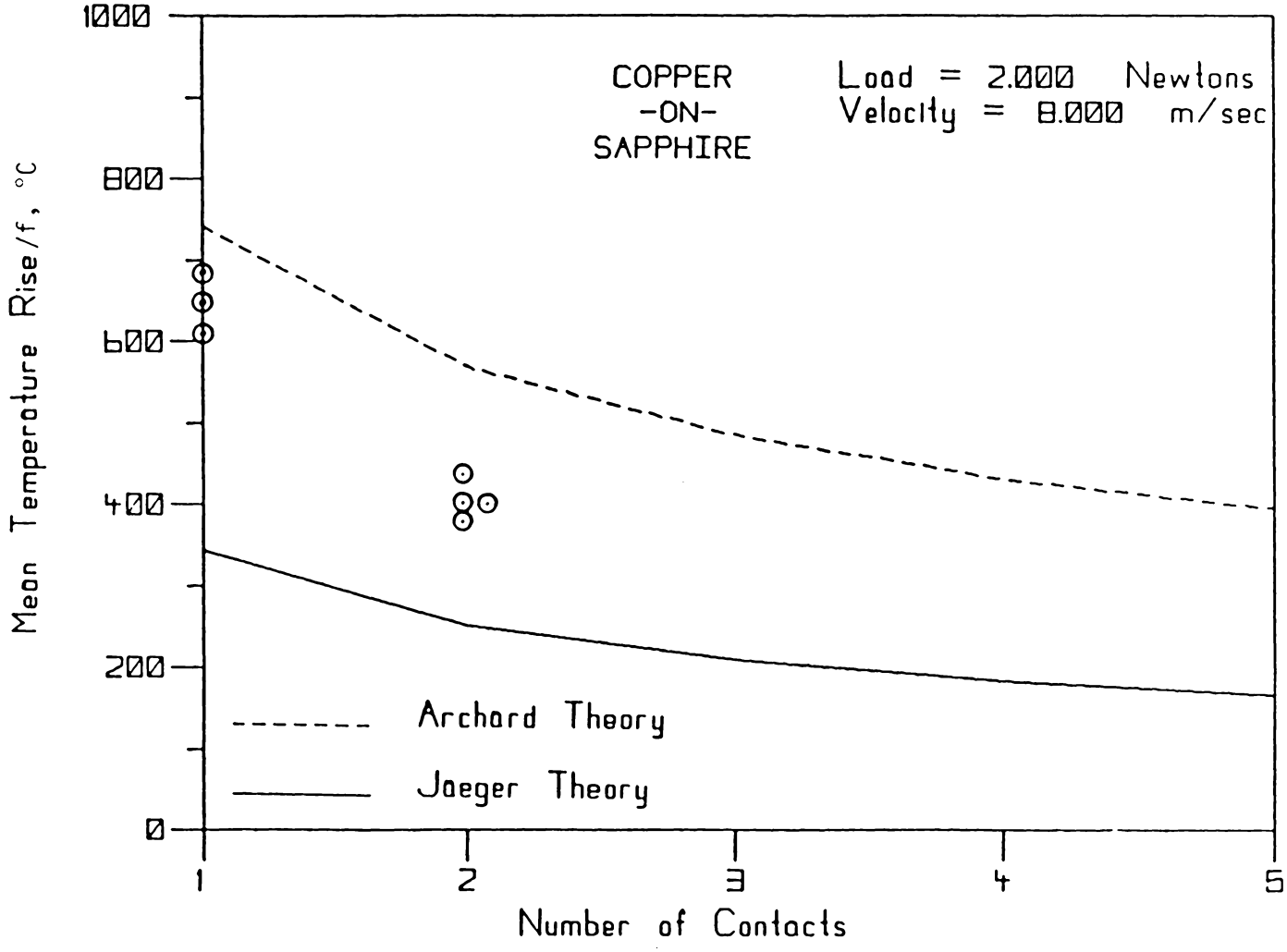

Figure 74. Effect of Subdivision - Load=2N, Velocity=8m/s

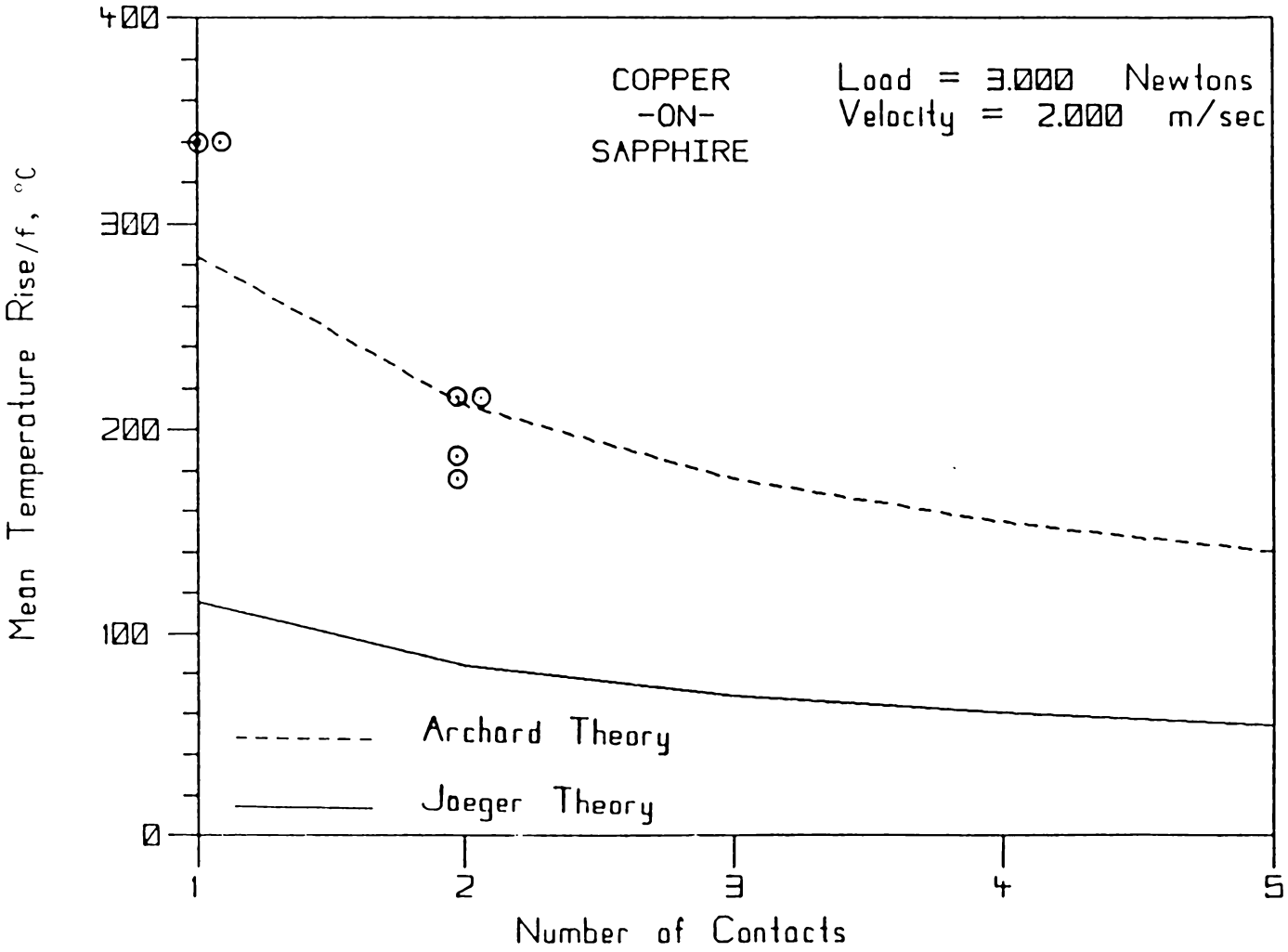

Figure 75. Effect of Subdivision - Load=3N, Velocity=2m/s

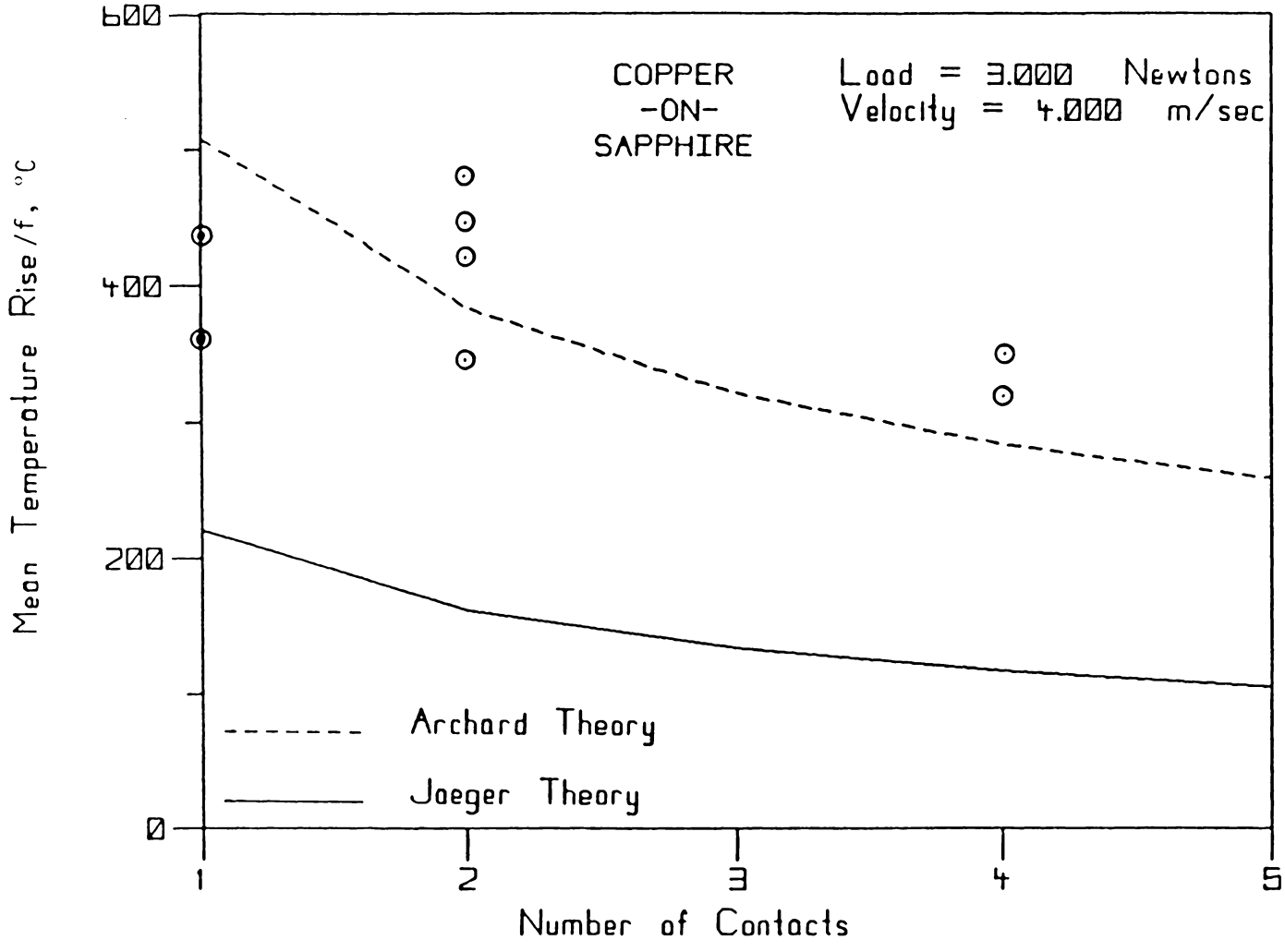

Figure 76. The Effect of Subdivision - Load=3N, Velocity=4m/s

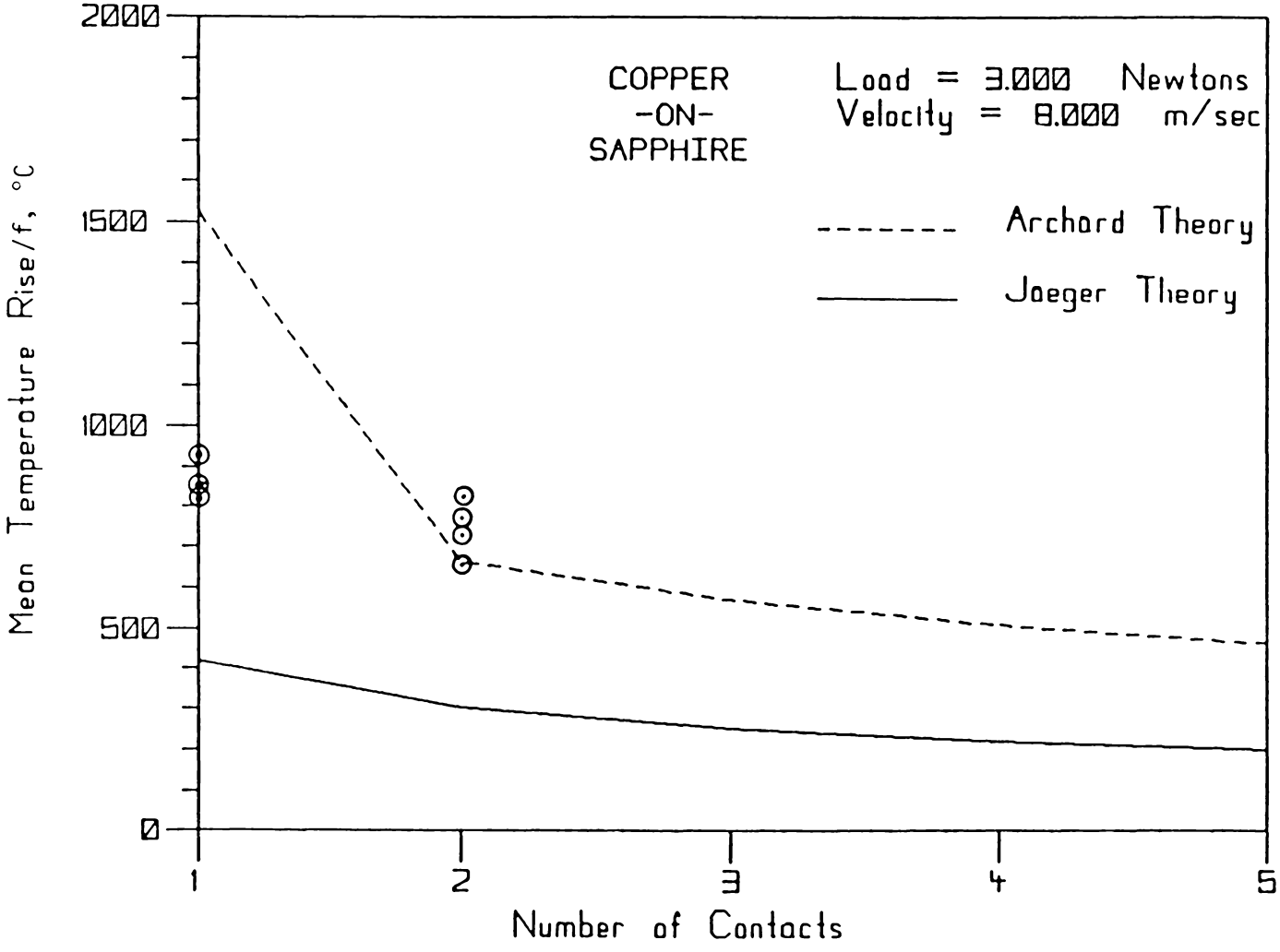

Figure 77. Effect of Subdivision - Load=3N, Velocity=8m/s

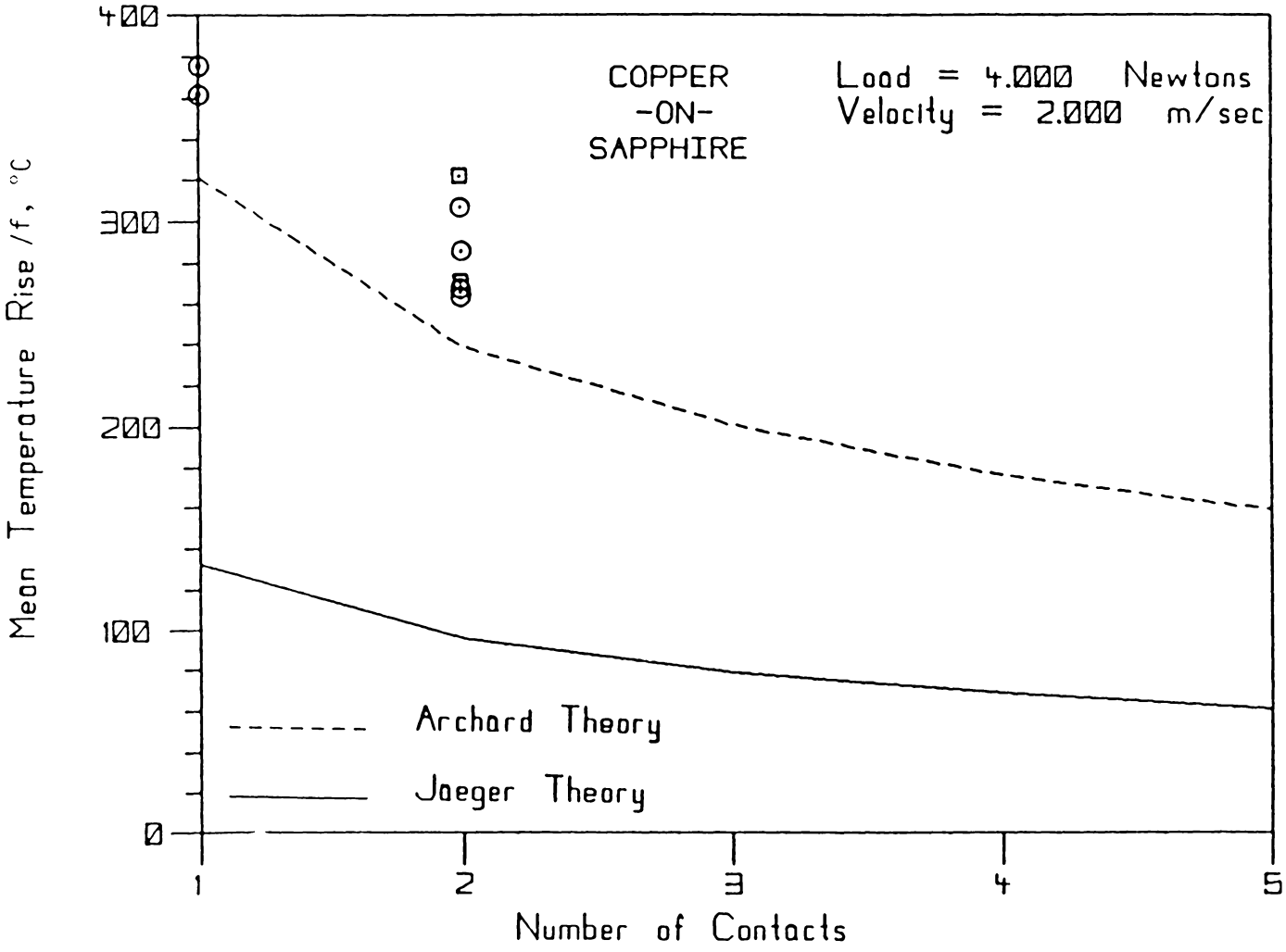

Figure 78. The Effect of Subdivision - Load=4N, Velocity=2m/s

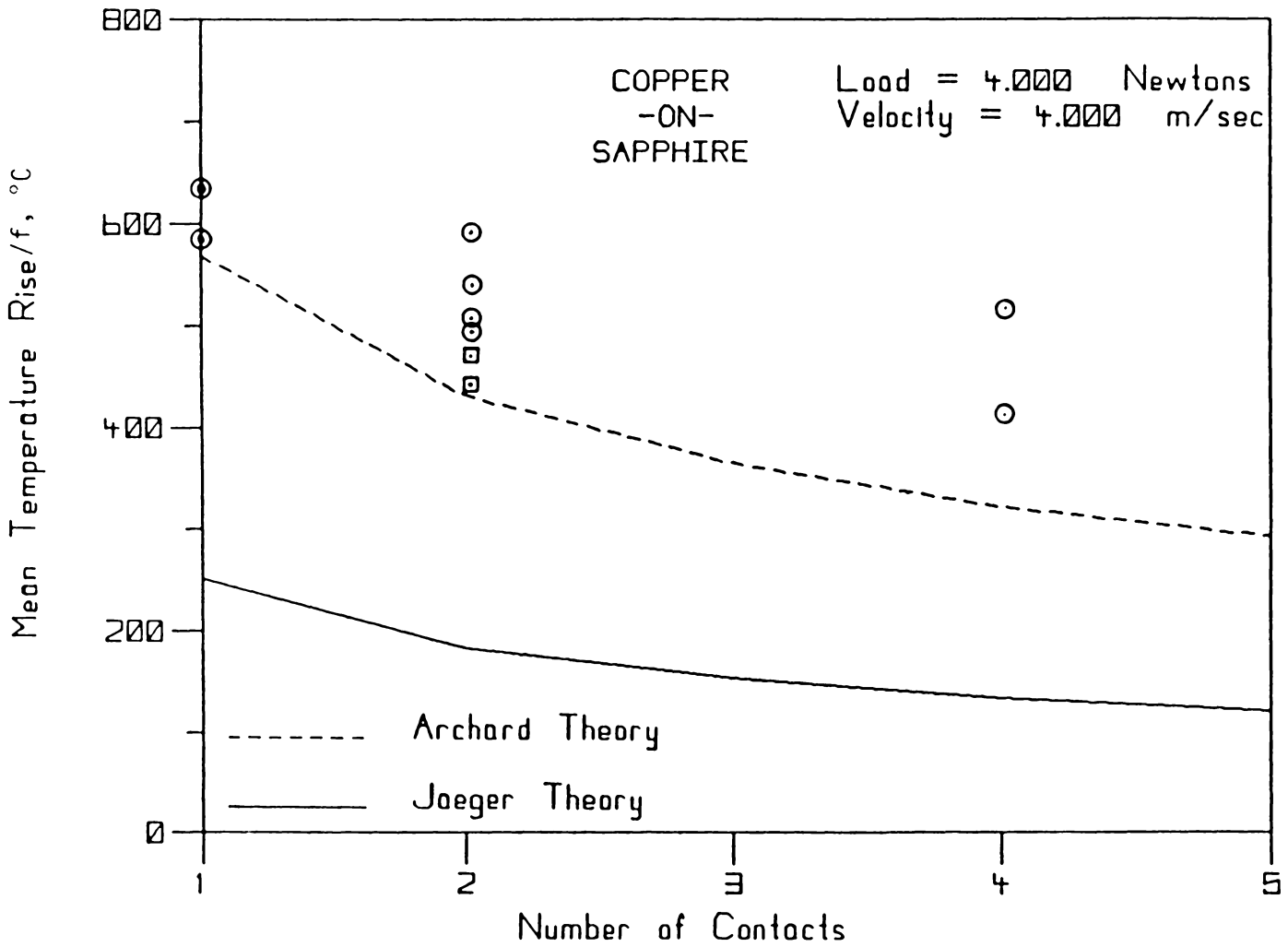

Figure 79. Effect of Subdivision - Load=4N, Velocity=4m/s

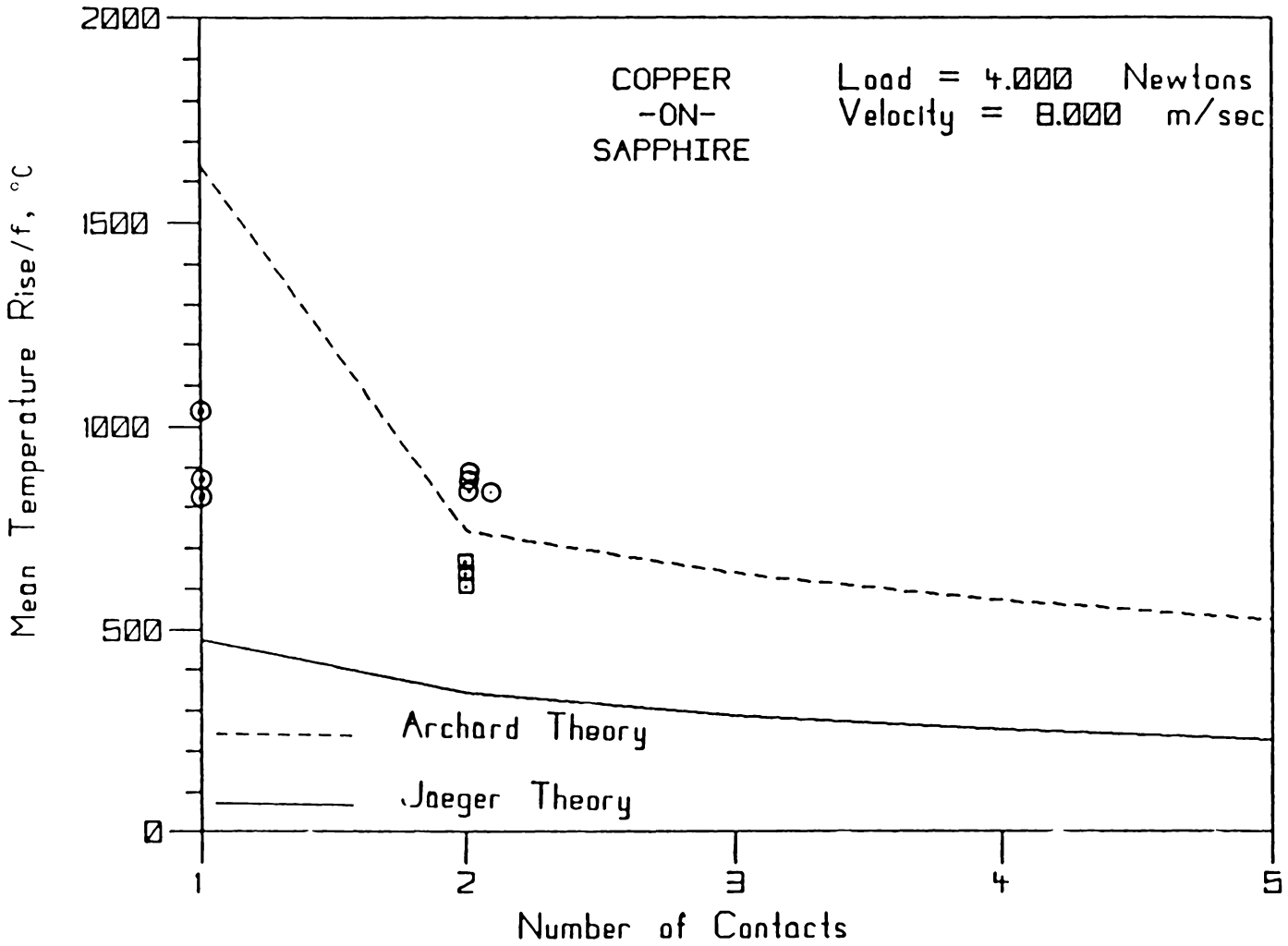

Figure 80. The Effect of Subdivision - Load=4N, Velocity=8m/s

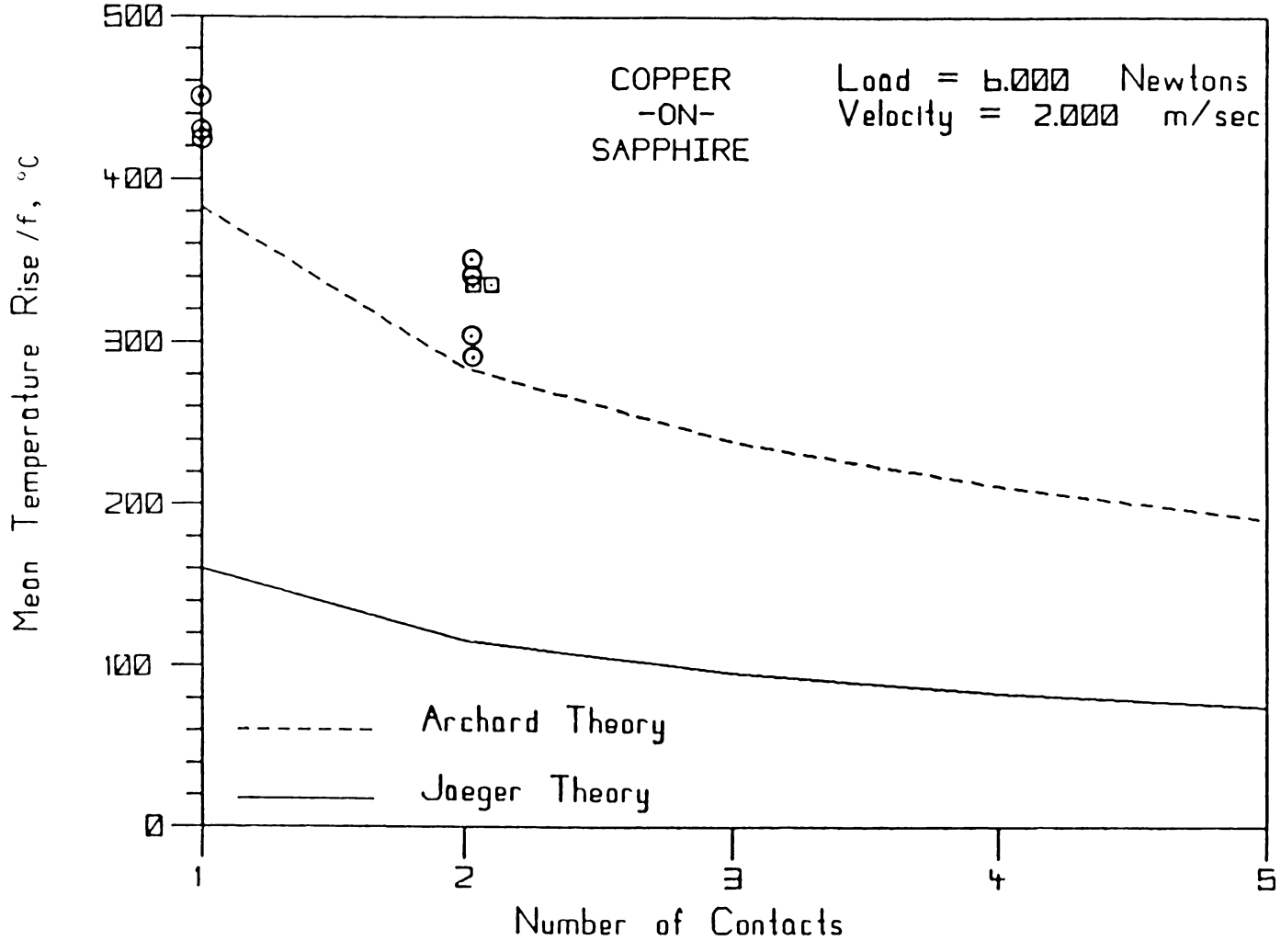

Figure 81. Effect of Subdivision - Load=6N, Velocity=2m/s

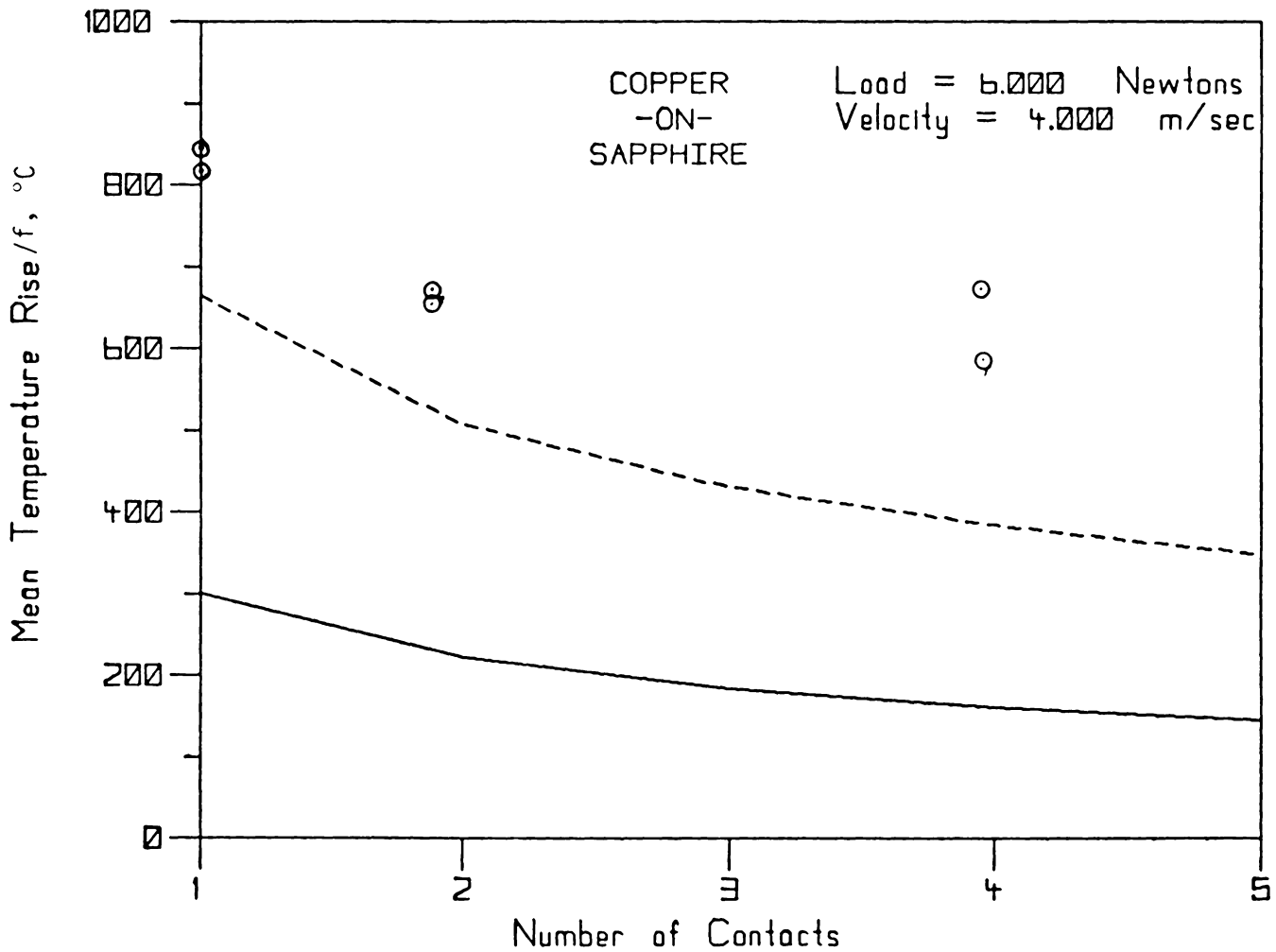

Figure 82. The Effect of Subdivision - Load=6.0N, Velocity=4m/s

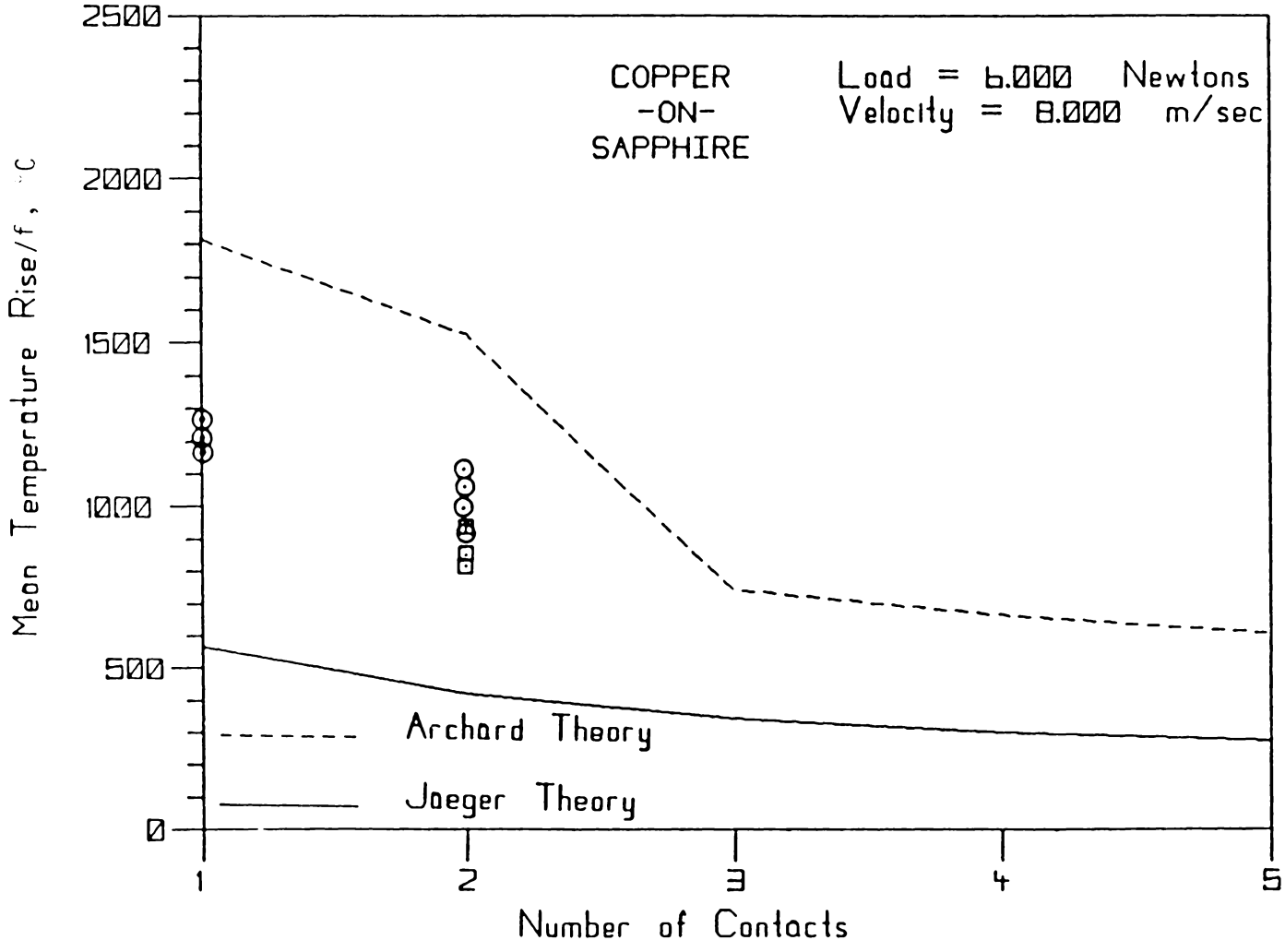

Figure 83. Effect of Subdivision - Load=6N, Velocity=8m/s

A graph has been generated for each experimental condition and the experimental data plotted on each. The data for two contacts consists of results from the subdivided specimens plus results from the single contact experiment with one half the load. These single contact tests which are used as subdivided data points are to some extent the 'experimental model.' Using the rationale that developed the theoretical curve, a single contact with one half the load should generate the same surface temperature as a subdivided specimen with the reference load. The graphs in general indicate that this statement is true as the data points are scattered within a reasonable experimental error range. Differences between the subdivided specimens and the 'single contact - one half' load temperatures may be explained in some cases as being caused by an interaction of the two subdivided halves and therefore creating higher temperatures. Again, the data are well represented by Archard's theory with the trends being consistent between theory and experiment.

5.0 CONCLUSIONS

1) The infrared microscope system was successfully adapted to measure, and store on magnetic tape, all the necessary data needed to complete a detailed experimental study of surface temperatures of copper-on-sapphire in dry-sliding contact.

2) A statistical analysis of the experimental results showed that the main effects of subdivision, load and sliding velocity had a significant effect on surface temperatures with a confidence level of 98% or higher.

3) The copper specimens displayed a consistent bi-level emissivity characteristic. The lower level emissivity was approximatey 0.10 and the higher level at about 0.55.

4) The Archard and Jaeger theories describe the influence that load, sliding velocity and subdivision have on surface temperatures.

5) As a result of comparison between the experimental results with theory, it was determined that the Archard or Jaeger models of contact should be used when applying the theory to a real system in which the apparent contact area is much larger than the real contact area. The theoretical predictions of surface temperatures using the singular real contact area model were in close agreement with the experimental results. The contact area and load to be used in the theory would be equal to the initial real contact area and load divided by the number of subdivided apparent contact areas.

6) Three computer programs were successfully completed. The programs written were:
   a) Theoretical effect of load on surface temperature.
   b) Theoretical effect of sliding velocity on surface temperatures using both the Archard and Jaeger theories.
   c) Determination of surface temperature from the electrical output of the infrared microscope.
7) A detailed infrared radiation analysis was completed and experimentally confirmed for its accuracy.

REFERENCES

1. Blok, H., "Theoretical Study of Temperature Rise at Surface of Actual Contact Under Oiliness Lubricating Conditions," Proc. General Discussion, Lubrication and Lubricants, Inst. Mech. Eng., London, Vol. 2, pp. 222-35, 1937.

2. Blok, H., "The Postulate about the Constancy of Scoring Temperature, NASA Symp. Interdisciplinary Approach to the Lubrication of Concentrated Contacts," Troy, N.Y., 15-17 July 1969; NASA Document SP-237, pp. 153-248, 1970.

3. Al-Rubeye, H. S., "Friction, Wear, and Temperature in Sliding Contact." J. of Lubrication Technology, Vol. 102, pp. 107-112, 1980.

4. Fein, R. S., "Effects of Lubricants on Transition Temperatures." Preprint No. 64 LC-7, ASLE/ASME Lubrication Conf., Washington, D.C., 13-16 Oct. 1964.

5. Fohl, J., Vetz, H., "Failure Criteria in Thin Film Lubrication - influence of Temperature on Seizing, Wear and Reaction Layer Formation." Wear, Vol. 36, pp. 25-36, 1976.

6. Kelley, B. W., Leach, E. F., "Temperature - The Key to Lubricant Capacity." Preprint No. 64 LC-13, ASLE/ASME Lubrication Conf., Washington, D.C., 13-16 Oct. 1964.

7. Matveevskii, R. M. "The Critical Temperature of Oil with Point and Line Contact Machines," Paper No. 64-Lub-7, ASME/ASLE International Lubrication Conf., Washington, D.C., 13-16 Oct. 1964; see also "Stability of Temperature of Viscous Layers in the Case of Friction of Metals and Alloys" by the same author (in Russian), 212 pages, 218 references, published by "NAUKA" (Science), Moscow, 1971.

8. Quinn, T. F. J., "The Division of Heat and Surface Temperatures at Sliding Steel Interfaces and Their Relations to Oxidational Wear." Preprint No. 76-LC-2B-1, ASLE/ASME Lubrication Conf., Boston, Mass., 5-7 Oct. 1976.

9. Rozeanu, L., Pneli, D., "Two Temperature Gradient Model for Friction Failure." J. of Lubrication Technology, Vol. 100, pp. 479-485, 1978.

10. Burton, R. A., "Thermal Deformation in Frictionally Heated Contact." Wear, Vol. 59, pp. 1-20, 1980.

11. Ezzat, H. A., and Ronde, S. M., "Thermal Transients in Finite Slider Bearings," ASLE/ASME Joint Lubrication Conf., Paper No. 73-Lub-9, Atlanta, Ga., 14-18 Oct. 1973.

12. Cameron, A., "Principles of Lubrication," Longmans Green & Co. Ltd., London, pp. 397-410, 1966.

13. Furey, M. J., "Thermal Aspects of Film Formation by Antiwear Additives." Lecture, Fourth Limits of Lubrication Conference, Imperial College, London, 7-11 July 1975.

14. Furey, M. J. "Surface Temperatures and the Limit of Lubrication." Lecture, Sixth Limits of Lubrication Conference, Imperial College, London, 9-13 July 1979.

15. Furey, M. J., "Friction, Wear, and Lubrication." Chapter 11, pp. 133-151 in Chemistry and Physics of Interfaces - II, published by the American Chemical Society, Washington, D.C., 1971.

16. Furey, M. J., "Infrared Measurements of Surface Temperatures Produced in Tribological Processes," 3rd International Tribology Congress ("EUROTRIB 81"), Warsaw, Poland, Vol. I, pp. 118-139, 21-24 September 1981.

17. Furey, M. J., "The Formation of Polymeric Films Directly on Rubbing Surfaces to Reduce Wear." Conf. on Physico-Chemical Mechanics of Friction and Wear, Kiev, USSR, 25-29 June 1973; Wear, Vol. 26, pp. 369-392, 1973.

18. Furey, M. J., "The 'in situ' Formation of Polymeric Films on Rubbing Surfaces." Proceedings of International Conference on Polymers and Lubrication (Brest), published by Centre National de la Recherche Scientificque, Paris, No. 233, pp. 393-404, 1975.

19. Jaeger, J. C., "Moving Sources of Heat and the Temperature at Sliding Contacts." Proc. Royal Soc. New South Wales, Vol. 56, pp. 204-24, 1942.

20. Holm, R., "Calculation of Temperature Development in a Contact Heated in the Contact Surface, and the Application to the Problem of the Temperature Rise in a Sliding Contact." J. Appl. Phys., Vol. 19, pp. 361-6, 1948.

21. Bowden, F. P., Tabor, D., "The Friction and Lubrication of Solids." Chap. II, pp. 33-57, Oxford Univ. Press, London, 1950.

22. Cook, N. H., Bhushan, B., "Sliding Surface Interface Temperatures." Trans. ASME J. of Lubrication Technology, pp. 59-64, January 1973.

23. Francis, H. A., "Interfacial Temperature Distribution Within a Sliding Hertzian Contact." Transactions 14, pp. 41-54, 25th ASLE Annual Meeting, Chicago, 4-8 May 1970.

24. Ling, F. F., Ng., C. W., "On Temperatures at the Interfaces of Bodies in Sliding Contact." Proc., Fourth U.S. National Congress of Applied Mechanics, pp. 1343-9, 1962.

25. Archard, J. F., "The Temperature of Rubbing Surfaces." Wear, Vol. 2, pp. 438-55, 1959.

26. Winer, W., Cheng, H. S., Wear Control Handbook, pp. 133-138.

27. Powell, D. G., Earles, S. W. E., "An Assessment of Surface Temperature Predictions in the High Speed Sliding of Unlubricated SAE 1113 Steel Surfaces," ASME Transactions, Vol. 15, pp. 103-112, 1971.

28. Ling, F. F., Surface Mechanics Chaps. 2 and 3, pp. 12-81, John Wiley and Sons, Inc., New York, 1973.

29. Furey, M. J., "Surface Temperatures in Sliding Contact," Trans. ASLE, Vol. 6, pp. 133-146 (1964)

30. Godet, M., Deyber, P., "Contact Temperature in Mixed Friction," Tribology, pp. 150-154, August 1971

31. Winer, W. O., Sanborn, D. M., Nagaroj, H. S., "Direct Surface Temperature Measurement by Infrared Radiation in Elastohydrodynamic Contacts and the Correlation with the Blok Flash Temperature Theory." Wear, Vol. 40, pp. 43-59, 1978.

32. Jones, M., "The determination of surface temperatures," European Space Research and Technology Center, Technical Notes, ESRO TN-78, February 1969.

34. Kannel, J. W., Zugaro, F. F., Down, T. A., "A Method for Measuring Surface Temperature Between Rolling/Sliding Steel Cylinders." Trans. ASME, J. of Lubrication Technology, Vol. 100, pp. 110-114, Jan. 1978.

35. Omori, D. I., "Infrared Measurements of Surface Temperatures Generated by Friction." Master of Science Thesis, Mechanical Engineering, Virginia Polytechnic Institute and State University, Blacksburg, Va., August 1975.

36. Wiggins, J. M., "An Experimental Method for Measuring Surface Temperatures Generated by Friction." Master of Science Thesis, Mechanical Engineering, Virginia Polytechnic Institute and State University, Blacksburg, Va., December 1974.

37. Richardson, M. H. "Experimental Investigation of the Surface Temperature of Graphite in a Sliding System Using an Infrared Microscope." Master of Science Thesis, Mechanical Engineering, Virginia Polytechnic Institute and State University, Blacksburg, Va., August 1976

38. Li, S. H., "Experimental Investigation of Surface Temperatures of Some Polymers in Unlubricated Sliding." Master of Science Thesis, Mechanical Engineering, Virginia Polytechnic Institute and State University, Blacksburg, Va., August 1976

39. Blok, H., "The Flash Temperature Concept." Wear, 6, pg. 483-494, 1963.

40. Carslaw, Conduction of Heat, 2nd Ed., 1921, page 150.

41. Ling, F. F., "On Temperature Transients at Sliding Interface." Trans. ASME J. of Lubrication Technology, pp. 397-405, July 1969

42. Niemann, G., Lechner, G., "The Measurement of Surface Temperatures on Gear Teeth," Transactions of ASME, Journal of Basic Engineering, pp. 641-654, Sept. 1965.

43. Bramson, M. A., "Infrared Radiation: A Handbook for Applications," trans. from Russian by R. R. Rodman, Plenum Press, New York, 1968.

44. Bowden, F. P., Stone, M. A., and Tudor, G. K., "Hot Spots on Rubbing Surfaces and the Detonation of Explosives by Friction," Proc. Roy. Soc. Vol. A188, pp. 329-349, 1947.

45. Bowden, F. P., and Ridler, K. E. W., "Physical Properties of Surfaces III - The Surface Temperature of Sliding Metals, The Temperature of Lubricated Surfaces," Proc. Roy. Soc. Vol. A 154, 1936, pp. 648-656.

46. Bowden, F. P., and Thomas, P. H. "The Surface Temperature of Sliding Solids," Proc. Roy. Soc. A273, 1954, pp. 29-40.

47. Cocks, M., Ph.D. Thesis, Reading University, 1953.

48. Furey, M. J., "An Experimental Study of Surface Temperatures Generated at the Solid-Solid Interface." VPI&SU Research Proposal Submitted to National Science Foundation, 1981.

49. Ling, F. F., Simkins, T.E., "Measurement of Pointwise Junction Condition of Temperature at the Interface of Two Bodies in Sliding Contact." Trans ASME J. of Basic Engineering, 62-Lub-14, 1962.

APPENDIX A

Calibration of the Barnes Infrared Microscope

The procedure used to calibrate the Barnes Infrared Microscope is as follows:

1. The infrared microscope was placed over the radiometric calibration source and focused onto the edge of the blackbody source.

2. With the calibration source at ambient temperature the microscope was moved to the center of the blackbody source.

3. The microscope output was then zeroed with the use of the ambient control and the zero control on the front of the control box as directed in the Barnes Operating manual. Page 4-11, Example 1.

4. The microscope was then rotated away from the calibration source while it was heated to a known temperature so that the microscope itself would not be heated.

5. After the calibration source had reached an equilibrium temperature (approximately 10 min.) the microscope was rotated to the center of the blackbody source and the voltage output of the microscope recorded.

6. The above procedure (steps 4 and 5) were repeated for numerous temperatures and the voltage output recorded.

7. The calibration procedure was performed for both the 36X objective and the 15X objective.

8. To obtain the radiance-per-volt factor, the voltage output of the microscope was plotted against the effective blackbody radiance of the temperatures of the calibration source.

9. The calibration constant or the radiance-per-volt factor was statistically determined and corresponds to the slope of the effective blackbody radiance vs. voltage curve.

TABLE A-1

Microscope Calibration Data

Blackbody Calibration Source Temp (°C)	Effective Blackbody Radiation (W/m^2-ster)	Voltage Output Objective 36X	Voltage Output Objective 15X
70	1.45×10^{-2}	0.035	0.063
80	1.85×10^{-2}	0.048	0.088
90	2.35×10^{-2}	0.066	0.118
100	3.00×10^{-2}	0.086	0.155
110	3.75×10^{-2}	0.110	0.120
120	4.60×10^{-2}	0.138	0.250
130	5.55×10^{-2}	0.167	0.210
140	6.80×10^{-2}	0.206	0.379
150	8.10×10^{-2}	0.235	0.464
160	9.70×10^{-1}	0.301	0.556
170	1.16×10^{-1}	0.366	0.670
180	1.38×10^{-1}	0.430	0.792
190	1.60×10^{-1}	0.508	0.948
200	1.85×10^{-1}	0.600	1.112
210	2.15×10^{-1}	0.696	1.290
220	2.50×10^{-1}	0.815	1.484
230	2.80×10^{-1}	0.916	1.710

INSTRUMENTATION

1. Barnes Infrared Radiometric Microscope
   Model RM-2A
   Serial Number 412

2. Beck Reflecting Objective - 36x
   Model RM-163
   Serial Number 255

3. Barnes Reflecting Objective - 15x
   Model X15/.28
   Serial Number 363

4. Barnes Radiometric Calibration Source
   Model RM 121-1
   Serial Number 307

5. Hewlett Packard Amplifier
   Model 2470A
   Serial Number 605-00106

6. Keithley Digital Voltmeter
   Model 168
   Serial Number 36873

APPENDIX B

Calibration of the Torque Transducer

The procedure used to calibrate the Lebow Miniature Rotary Torque Transducer is as follows:

1. To calibrate the torque transducer, the power input shaft, the end driven by the belt system, was clamped so that no movement could occur. The clamp is specially designed to attach to the input shaft once the gear is removed and then secured with screws to the microscope base.

2. The sapphire disk, which is mounted on the upper shaft of the torque transducer, was replaced by an aluminum disk 0.0508 m in diameter. On the side of the disk is a screw from which a wire can be secured in the manner described below.

3. A thin wire was wrapped around the edge of the aluminum disk and then over a set of pulleys. The wire was wrapped around the disk so that even with a rotation of the disk caused by an applied torque, the force along the wire would always be tangent to the disk.

4. A bowpan was attached to one end of the wire that went over a ball bearing support. A counterweight was attached to the other end of

the wire that went over another ball bearing support. The counterweight was to assure that no torque was being applied to the shaft from the weight of the bowpan. This was checked by passing the signal output of the torque transducer through a HP 2470A Amplifier and then to a digital voltmeter where the voltage should be zero.

5. Known weights were placed on the bowpan to produce a known torque.

6. Voltage readings were taken for each weight applied which was then converted into a voltage output-to-torque applied factor.

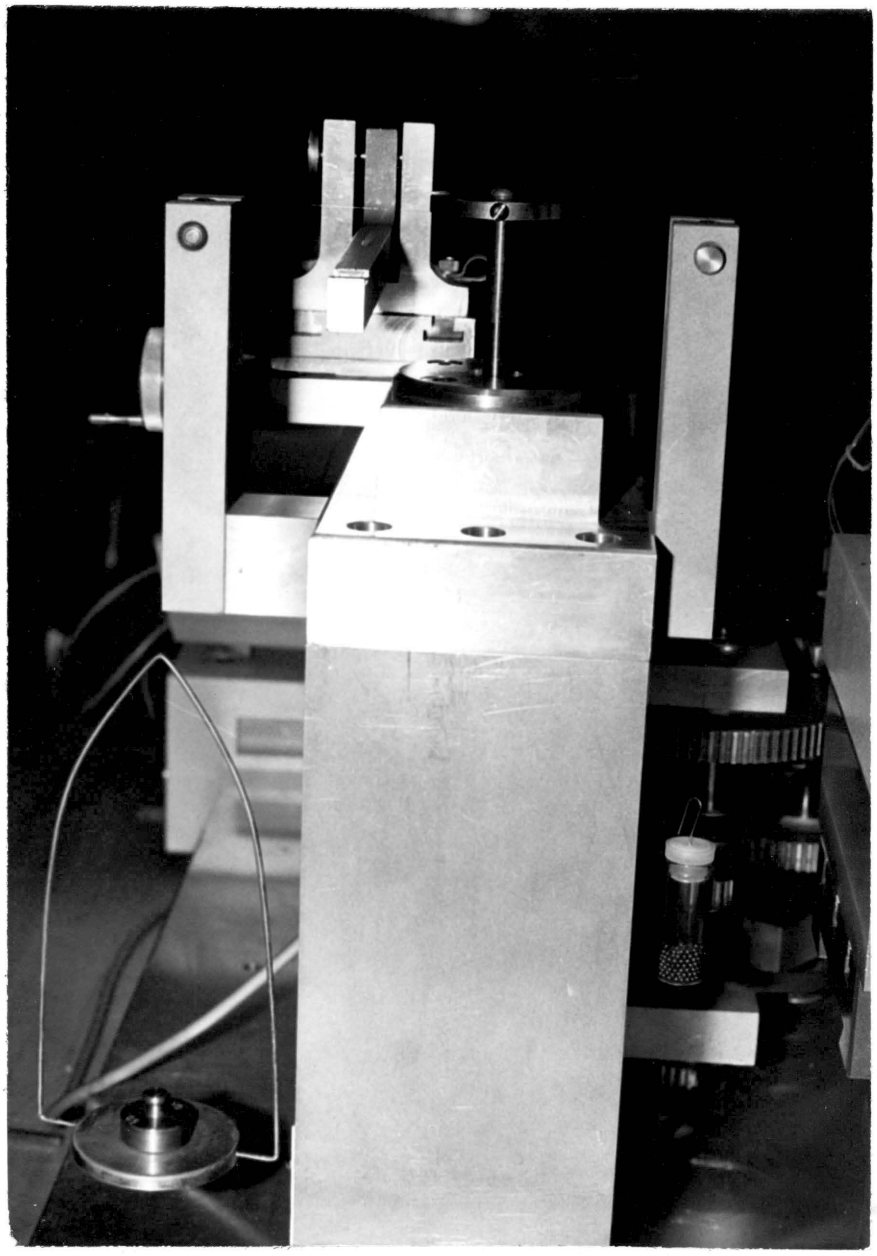

Figure B-1. Calibration Setup of the Torque Transducer

TABLE B-1

Rotary Torque Transducer Calibration

Mass (Gm)	Torque (Gm-Cm)	Voltage Output (mV)
0.000	0.000	0.000
10.0	25.40	0.174
20.0	50.80	0.357
30.0	76.20	0.536
40.0	101.60	0.717
50.0	127.00	0.902
60.0	152.4	1.078
70.0	177.8	1.258
80.0	203.2	1.441
90.0	228.6	1.620
100.0	254.0	1.804
120.0	304.8	2.17
140.0	355.6	2.53
160.0	406.4	2.89
180.0	457.2	3.26
200.0	508.0	3.61
250.0	635.0	4.52
300.0	762.0	5.42
350.0	889.0	6.32
400.0	1016.0	7.22

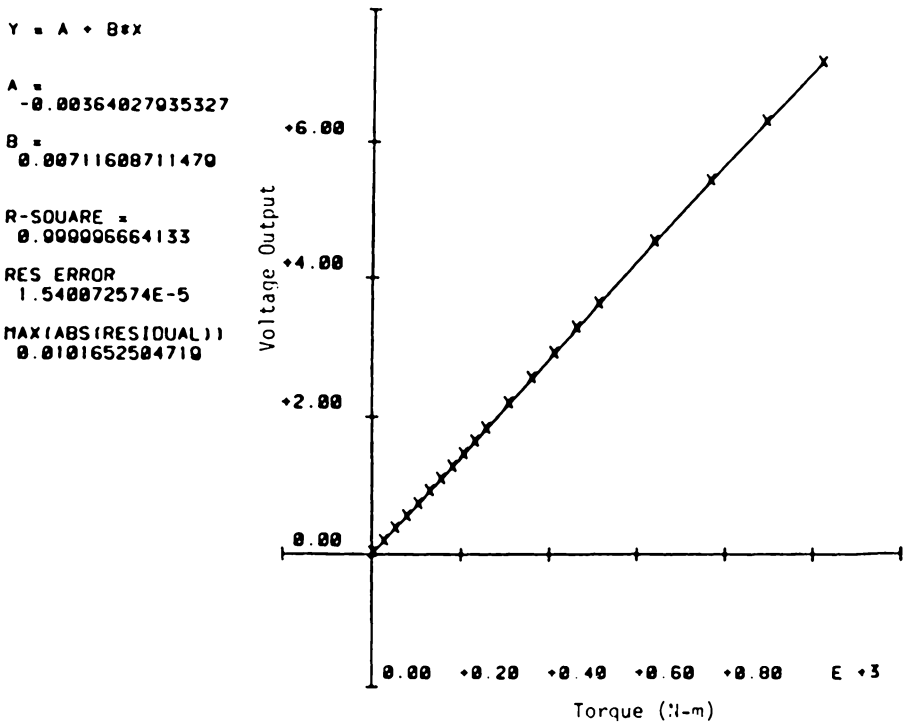

Figure 3-2. Calibration Curve of the Torque Transducer

INSTRUMENTATION

1. Lebow Miniature Rotary Torque Transducer
   Model 1102-50
   Serial Number 752

2. Hewlett Packard DC Power Supply
   Model HP 6218A
   Serial Number 1148404942

3. Hewlett Packard Amplifier
   Model 2470
   Serial Number 605-00106

4. Keithley Digital Voltmeter
   Model 168
   Serial Number 36873

APPENDIX C

Calibration of the Linear Variable Differential Transformer

Linear variable differential transformers (LVDT) are attached to the precision X-Y table which allows accurate location and positioning of the microscope within a contact zone. The LVDTs accept a fixed DC voltage input for which the signal produced is proportional to the relative displacement of the LVDT. An input voltage of 13.0 volts was supplied to both LVDTs. This voltage was selected because of the requirements that the maximum DC voltage that the tape recorder will accept is 1.4 volts and the maximum displacement of the LVDTs during an experiment is 0.24 cm. An input of 13.0 volts creates an output signal of approximately 1.0 volts for the maximum expected displacement. The following procedure was used to calibrate the LVDTs:

1. The LVDTs were adjusted so that their output was zero volts. This is the point from which all displacements are measured.

2. The X-Y table was then moved at 0.025 cm (0.01 in) intervals as measured by the micrometer gauges that are attached to the X-Y table.

3. The voltage output for each micrometer setting was recorded as the X-Y table was moved at +0.025 cm (0.01 in) intervals and then -0.025 cm (0.01 in) intervals.

4. This data was then plotted and the voltage-to-displacement factor determined statistically.

TABLE C-1

LVDT Calibration Input Voltage: 13V

Relative Displacement (inches)	Voltage Output	
	Radial LVDT	Tangential LVDT
0.10	0.961	0.751
0.09	0.861	0.681
0.08	0.762	0.609
0.07	0.664	0.537
0.06	0.567	0.465
0.05	0.471	0.391
0.04	0.375	0.316
0.03	0.281	0.240
0.02	0.187	0.162
0.01	0.093	0.083
0.00	0.000	0.000
-0.01	-0.094	-0.084
-0.02	-0.188	-0.171
-0.03	-0.284	-0.262
-0.04	-0.381	-0.356
-0.05	-0.478	-0.453
-0.06	-0.579	-0.553
-0.07	-0.680	-0.655
-0.08	-0.784	-0.760
-0.09	-0.890	-0.869
-0.10	-0.996	-0.982

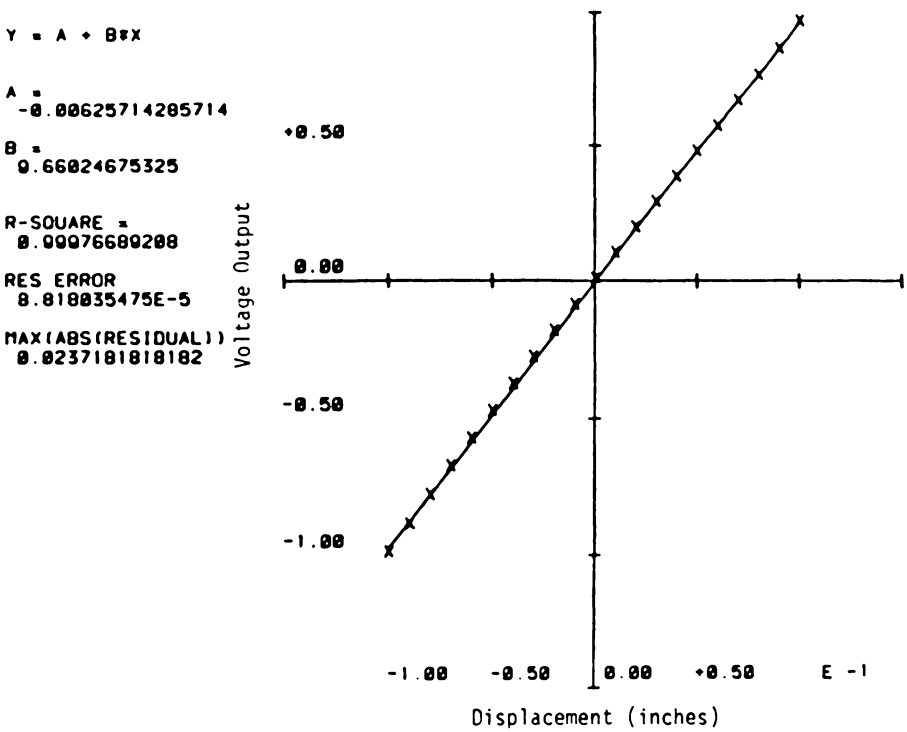

Figure C-1. Calibration Curve of the Radial LVDT - Input Voltage=13V

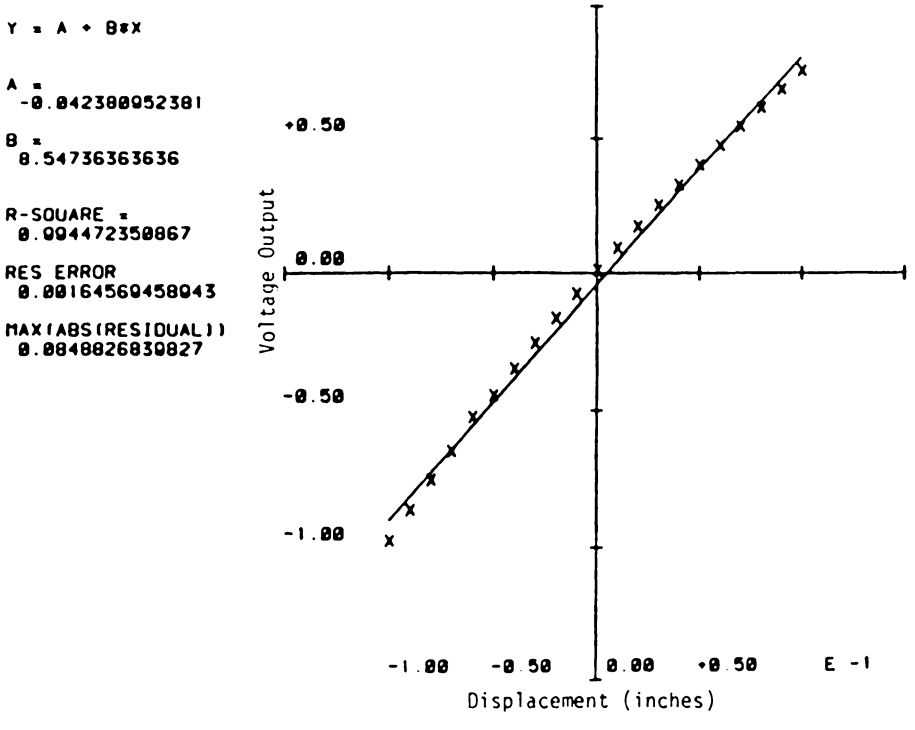

Figure C-2. Calibration Curve of the Tangential LVDT - Input Voltage=13V

TABLE C-2

LVDT Calibration Input Voltage: 20V

Relative Displacement (inches)	Voltage Output	
	Radial LVDT	Tangential LVDT
0.020	0.775	0.656
0.018	0.697	0.589
0.016	0.619	0.525
0.014	0.514	0.458
0.012	0.464	0.392
0.010	0.386	0.326
0.008	0.309	0.262
0.006	0.232	0.195
0.004	0.151	0.129
0.002	0.026	0.065
0.000	0.000	0.000
-0.002	-0.070	-0.063
-0.004	-0.146	-0.127
-0.006	-0.224	-0.195
-0.008	-0.303	-0.263
-0.010	-0.380	-0.328
-0.012	-0.457	-0.395
-0.014	-0.535	-0.459
-0.016	-0.613	-0.523
-0.018	-0.690	-0.590
-0.020	-0.769	-0.657

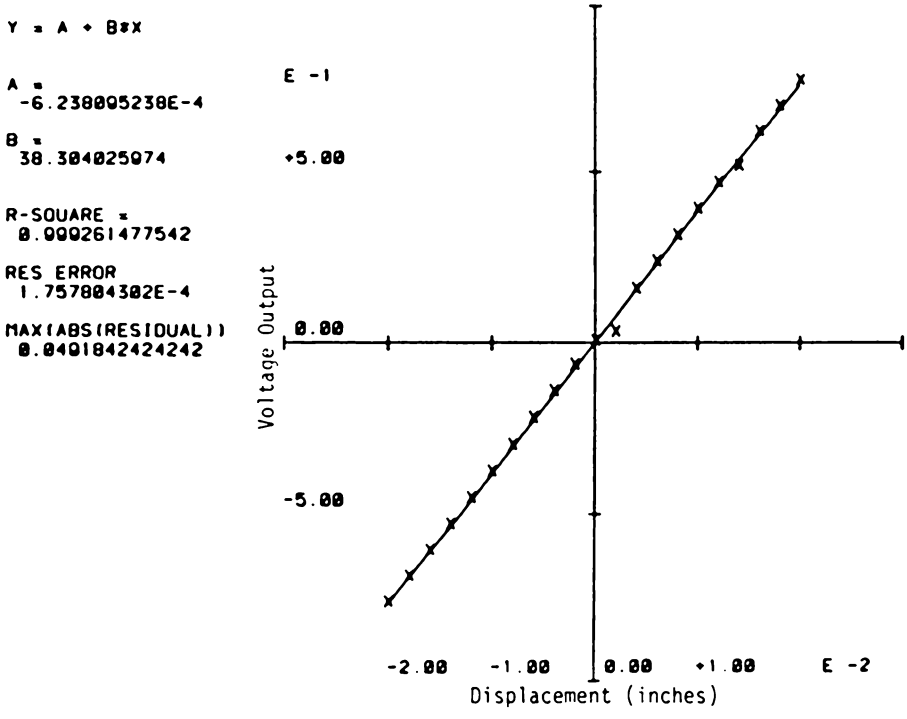

Figure C-3. Calibration Curve of the Radial LVDT - Input Voltage=20V

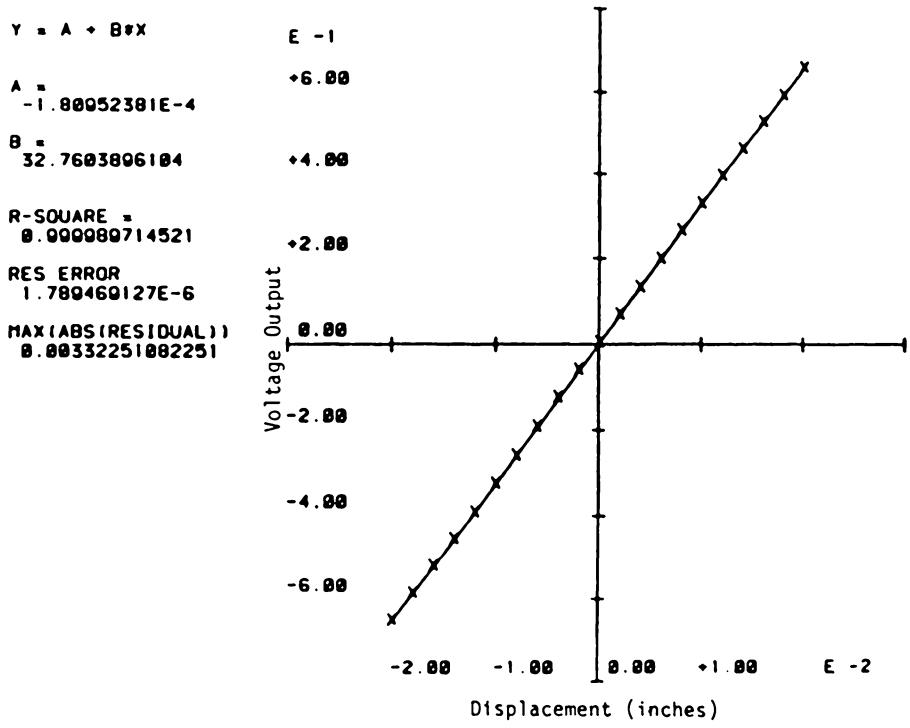

Figure C-4. Calibration Curve of the Tangential LVDT - Input Voltage=20V

APPENDIX D

Procedure for Determining the External Transmittance of the Sapphire Disk

The procedure used to determine the transmissivity of the sapphire disk is as follows:

1. The Barnes Radiometric Calibration Source was placed on the microscope substage and set to a desired temperature setting.

2. The calibration source was allowed to reach its equilibrium temperature (approximately 10 minutes).

3. The microscope was focused onto the edge of the blackbody hole of the calibration source. Once the microscope was focused, it was then moved to the center of the hole and a voltage or radiance reading taken.

4. The sapphire disk was then placed directly on the blackbody source and another voltage or radiance reading taken.

5. The disk and microscope were then moved away from the calibration source while the source was being heated to a new temperature.

6. The external transmittance was measured again to see what effect temperature had on the transmissivity.

TABLE D-1

Experimental Determination of External Transmissivity

Temp °C	External Transmittance 1	2	3	4	5	Average Transmittance
70	0.8524	0.8456	0.8498	0.8542	0.8542	0.8512
100	0.8522	0.8554	0.8534	0.8594	0.8569	0.8555
120	0.8551	0.8556	0.8527	0.8561	0.8567	0.8552
150	0.8571	0.8580	0.8558	0.8596	0.8541	0.8569
210	0.8492	0.8544	0.8507	0.8519	0.8492	0.8511
230	0.8530	0.8528	0.8548	0.8527	0.8550	0.8537
				Total Average		0.8539

INSTRUMENTATION

1. Barnes Infrared Radiometric Microscope
   Model RM-24
   Serial Number 412

2. Beck Reflecting Objective (36x)
   Model RM-163
   Serial Number 255

3. Barnes Radiometric Calibration Source
   Model Number RM14-1
   Serial Number 307

APPENDIX E

EFFECTIVE BLACKBODY RADIANCE VS. TEMPERATURE

(Reproduced from Barnes Engineering Operating Manual of the RM-2A Radiometric Microscope)

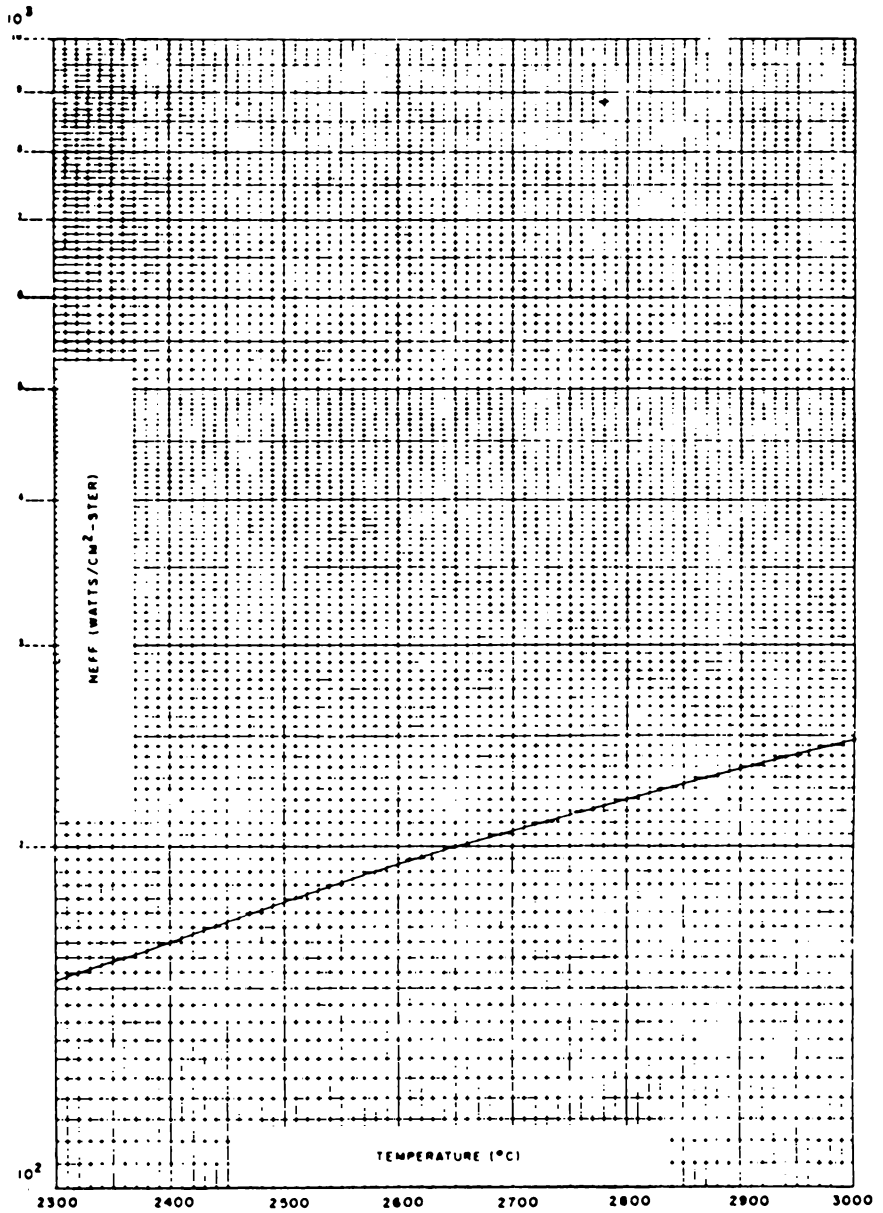

Figure 3-1. Effective Radiance vs. Temperature (0-350°C)

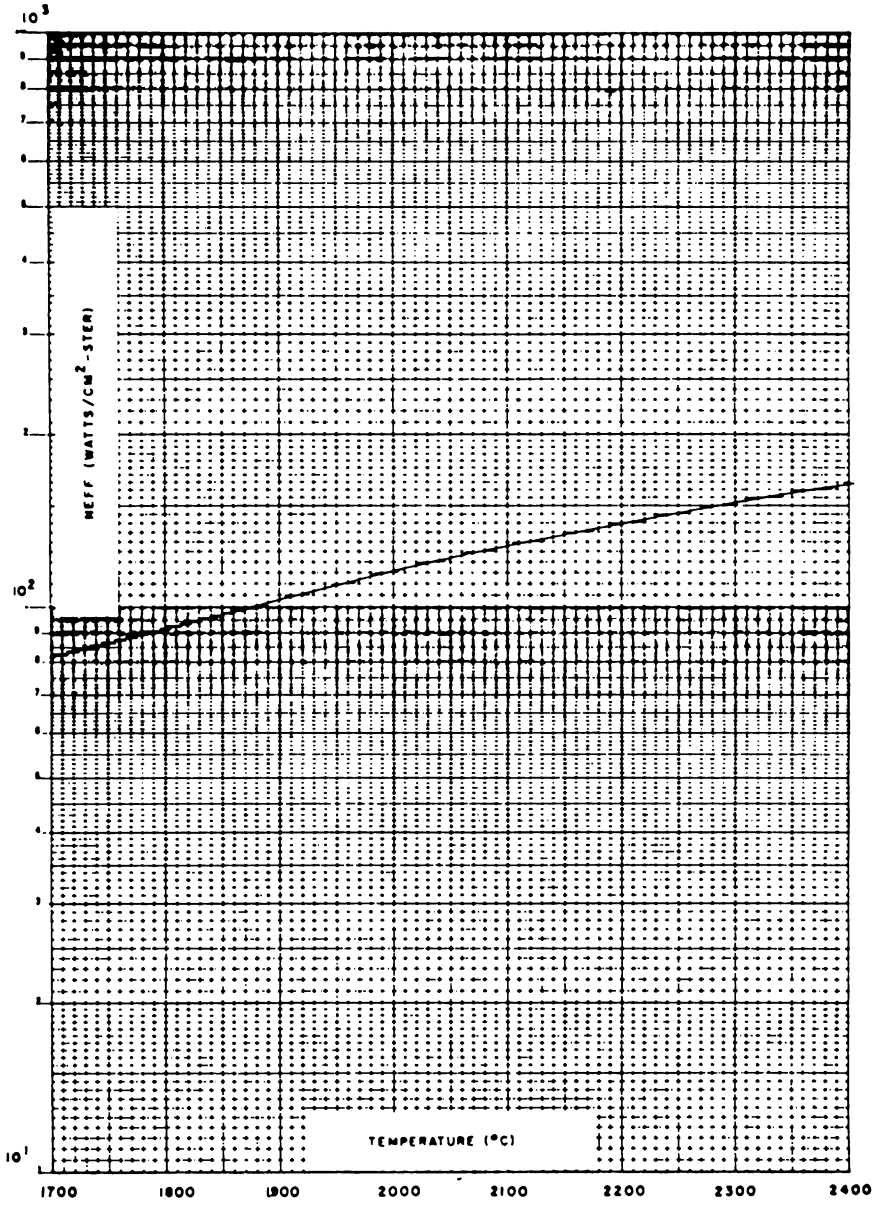

Figure E-2. Effective Radiance vs. Temperature (300-1000°C)

APPENDIX F

COMPUTER PROGRAMS

APPENDIX F.1

COMPUTER PROGRAM:

Conversion of infrared microscope voltage output to effective blackbody radiance emitted from the specimen and its temperature.

```
      REAL IR,NS,NO
C
C ***********************************************************************
C ***********************************************************************
C
C                ***CONVERSION OF INFRARED MICROSCOPE'S
C           .      VOLTAGE OUTPUT TO BLACKBODY RADIANCE
C              EMITTED FROM THE SPECIMEN AND TEMPERATURE ***
C
C ***********************************************************************
C
C   THIS PROGRAM CONVERTS THE VOLTAGE OUTPUT FROM
C   THE BARNES MODEL RM-2A INFRARED RADIAMETRIC
C   MICROSCOPE TO EFFECTIVE BLACKBODY RADIANCE
C   EMITTED FROM THE SPECIMEN AND ITS TEMPERATURE
C   NEEEDS THE EXPERIMENTALLY DETERMINED EMISSIVITY, THE
C   VOLTAGE OUTPUT OF THE MICROSCOPE  AND THE GAIN SETTING,
C   OF ANY EXTERNAL AMPLIFIERS. THE OUTPUT CONTAINS THE
C   FRESNEL REFLECTION COEFFICIENT, THE EMISIVITY OF THE
C   SPECIMEN, THE SURFACE REFLECTIVITY OF THE SPECIMEN,
C   THE ATTENUATION FACTORS OF THE AMBIENT AND SPECIMEN
C   RADIATION EMITTED FROM THE SPECIMEN. DESCRIPTION
C   OF THE FOLLOWING EQUATIONS AND THE ATTENUATION FACTORS
C   CAN BE FOUND IN CHAPTER 3 OF CRAIG A. ROGERS' MASTERS
C   THESIS (NOVEMBER 1982).
C
C ***********************************************************************
C
      DIMENSION ANAME(10),VOLT(20),EMISS(20),RADINT(250),TAU(250)
C
C ***********************************************************************
C
C   READS THE POWER OF THE MICROSCOPE
C   OBJECTIVE USED WHERE:
C      OBJ = MICROSCOPE OBJECTIVE
C            (36X OR 15X)
C
C ***********************************************************************
C
      READ (5,5) OBJ
5     FORMAT(F3.0)
C
C ***********************************************************************
C
C   READS THE DATA FROM DATA CARD
C   NUMBER 2 WHERE:
C        ANAME = SPECIMEN MATERIAL
C        GAIN  = EXTERNAL AMPLIFIER GAIN
C        AMB   = AMBIENT RADIATION (W/CM**2-STER)
C
C ***********************************************************************
```

```
C
      READ (5,10) (ANAME(I),I=1,10),GAIN,AMB
10    FORMAT (10A1,F6.1,F9.7,F5.3)
C
C ***************************************************************
C
C   READS THE DATA FROM DATA CARD
C   NUMBER 3 WHERE:
C          NE = NUMBER OF EMISSIVITIES TO BE EVALUATED
C          NV = NUMBER OF VOLTAGES TO BE EVALUATED
C
C ***************************************************************
C
      READ (5,20) NE,NV
20    FORMAT (2I3)
      WRITE (6,30)
      WRITE (6,40)
      WRITE (6,50)
      WRITE (6,30)
30    FORMAT('*****************************************************')
40    FORMAT(1H1,10X,'CALCULATION OF THE EMITTED BLACKBODY')
50    FORMAT(15X,'RADIATION FROM THE SPECIMEN'/)
C
C ***************************************************************
C
C   READS THE DATA FROM CARD
C   NUMBER 4 WHERE:
C       EMISS = EMISSIVITY OF THE SPECIMEN SURFACE
C
C ***************************************************************
C
      READ (5,60) (EMISS(I),I=1,NE)
C
C ***************************************************************
C
C   READS THE DATA FROM DATA
C   CARD NUMBER 5 WHERE:
C       VOLT = VOLTAGE OUTPUT FROM MICROSCOPE AND ANY
C              EXTERNAL AMPLIFIER
C
C ***************************************************************
C
      READ (5,60) (VOLT(I),I=1,NV)
60    FORMAT (20F6.3)
C
C ***************************************************************
C
C   THIS DO-LOOP EVALUATES EACH EMISSIVITY
C   FOR EVERY VOLTAGE OUTPUT IN THE DATA
C
C ***************************************************************
C
      DO 120 I=1,NE
      WRITE (6,70)
70    FORMAT (///)
```

```
      IHARD=IVET(1,2,IE)
      IF(IHARD.EQ.2) GO TO 5
      CALL PLSAVE
5     CONTINUE
      CALL FINITT(0,700)
      RETURN
      END
C
C
C
C
C **********************************************************************
C **********************************************************************
C **********************************************************************
C
C
C                     SUBROUTINE INTENT
C
C  SUBROUTINE ITENT PLOTS A CURVE OF THE
C  MONOCHROMATIC BLACKBODY RADIANT INTENSITY
C  OVER THE MICROSCOPE'S SENSITIVITY REGION.
C  THE PLOT ALSO SHOWS HOW THE NORMALIZED
C  SPECTRAL RESPONSE CHARACTERISTIC OF THE
C  INFRARED MICROSCOPE ACTS ON THE RADIANT
C  INTENSITY CURVE.
C
C **********************************************************************
C **********************************************************************
C **********************************************************************
C
C
      SUBROUTINE INTENT(WAVE,RADY,RADI,ICOUN,TEMPC)
      DIMENSION WAVE(250),RADY(250),RADI(250),X(250),Y1(250),Y2(250)
      ICP1=ICOUN+1
      DO 1 I=2,ICP1
      X(I)=WAVE(I-1)
      Y1(I)=RADY(I-1)
      Y2(I)=RADI(I-1)
1     CONTINUE
      X(1)=ICOUN
      Y1(1)=ICOUN
      Y2(1)=ICOUN
      CALL INITT(120)
      CALL BINITT
      CALL XFRM(2)
      CALL YFRM(2)
      CALL CHECK(X,Y2)
      CALL DSPLAY(X,Y2)
      CALL LINE(3)
      CALL CPLOT(X,Y1)
      CALL FRAME
      CALL LABLE3(375,50,1.25,0.,19,'Wavelength, microns')
      CALL LABLE3(35,200,1.25,90.,31,'Radiant Intensity, W/cm**2-ster')
      CALL LABLE3(175,650,1.25,0.,14,'Temperature = ')
      CALL RLOUT(350,650,TEMPC,5,1)
```

```
C
C ***************************************************************
C
C   THIS EXPRESSION EVALUATES THE SURFACE
C   REFLECTIVITY OF THE SPECIMEN AS
C   (1-EMISSIVITY) WHERE:
C        SURF = SURFACE REFLECTIVITY
C
C ***************************************************************
C
      SURF=1.0-EMISS(I)
C
C ***************************************************************
C
C   THE NEXT DECLARATION SETS THE INDEX
C   OF REFRACTION TO A GIVEN VALUE WHERE:
C        IR = INDEX OR REFRACTION OF THE SAPPHIRE
C
C ***************************************************************
C
      IR=1.65
C
C
C ***************************************************************
C
C   THE NEXT EXPRESSION CALCULATES THE
C   FRESNEL REFLECTION COEFFICIENT FROM
C   THE INDEX OF REFRACTION GIVEN ABOVE
C
C ***************************************************************
C
      FRES=(IR-1.0)**2/((IR*1.0)**2)
C
C ***************************************************************
C
C   THE NEXT SECTION CALCULATES THE
C   INTERNAL TRANSMISSIVITY BASED ON THE
C   DECLARED INDEX OF REFRACTION AND THE
C   EXPERIMENTALLY DETERMINED EXTERNAL
C   TRANSMITTANCE WHERE:
C        EXTER = EXTERNAL TRANSMITTANCE
C        TRANS = INTERNAL TRANSMISSIVITY
C
C ***************************************************************
C
      EXTER=0.8539
      TRANS=EXTER/((1-FRES)/(1*FRES))
C
C ***************************************************************
C
C   THIS SECTION CREATES A TABLE OF IMPORTANT
C   DATA FOR EACH NEW EMISSIVITY EVALUATED
C
C ***************************************************************
C
```

```
      WRITE (6,80) EMISS(I),IR,SURF,FRES,TRANS,GAIN,OBJ
80    FORMAT (1X,'EMISSIVITY OF THE SPECIMEN     ',F6.4/1X,
     2          'INDEX OF REFRACTION            ',F6.4/1X,
     3          'SPECIMENT REFLECTIVITY         ',F6.4/1X,
     4          'FRESNEL REFLECTION             ',F6.4/1X,
     5          'INTERNAL TRANSMISSIVITY        ',F6.4/1X,
     6          'AMPLIFIER GAIN                 ',F4.0/1X,
     7          'MICROSCOPE OBJECTIVE           ',F3.0,'X'///)
      WRITE (6,90)
90    FORMAT(1X,'VOLTAGE',4X,'SPECIMEN',8X,'AMBIENT',6X,'AMBIENT',
     1 8X,'SPECIMEN',6X,'SPECIMEN'/1X
     2'OUTPUT',4X,'ATTENUATION',4X,'ATTENUATION',3X,'RADIATION',7X,
     3'BLACKBODY',3X,'TEMPERATURE',/13X,
     3'FACTOR',9X,'FACTOR',22X,'RADIATION',6X,'DEG. C',/1X
     4'-------------------------------------------------------------
     5-----------'/)
C
C *********************************************************************
C
C   THIS DO-LOOP CONVERTS EVERY VOLTAGE
C   OUTPUT TO BLACKBODY RADIANCE OF THE
C   SPECIMEN WITH THE EMISSIVITY
C   DETERMINED BY THE OUTSIDE DO-LOOP
C
C *********************************************************************
C
      DO 110 J=1,NV
C
C *********************************************************************
C
C   CONVERTS THE VOLTAGE OUTPUT TO
C   RADIANCE WHERE:
C        0.312 = THE CALIBRATION CONSTANT FOR THE
C                    MICROSCOPE WITH A 36X OBJECTIVE
C        0.171 = THE CALIBRATION CONSTANT FOR THE
C                    MICROSCOPE WITH A 15X OBJECTIVE
C
C *********************************************************************
C
      IF(OBJ.EQ.15.)CAL=.171
      IF(OBJ.EQ.36.)CAL=.312
      VOUT=VOLT(J)*CAL/GAIN
C
C *********************************************************************
C
C   THE NEXT SECTION CALCULATES THE FRACTION
C   OF SPECIMEN AND AMBIENT RADIATION THAT
C   IMPINGES ON THE INFRARED DETECTOR;I.E.
C        REFLS1 = FRACTION OF SPECIMEN RADIATION DUE
C                    TO REFLECTION NUMBER 1
C        REFLA3 = FRACTION OF AMBIENT RADIATION DUE
C                    TO REFLECTION NUMBER 3
C
C *********************************************************************
C
```

```
      REFLS1=(1-FRES)*TRANS
      REFLS2=(1-FRES)*SURF*FRES*(TRANS**3)
      REFLA1=FRES
      REFLA2=(1-FRES)**2*SURF*(TRANS**2)
      REFLA3=(1-FRES)**2*(SURF**2)*FRES*(TRANS**4)
C
C ***************************************************************
C
C   THE ATTENUATION FACTORS ARE THE SUM OF
C   THE APPROPRIATE REFLECTION FRACTIONS WHERE:
C       NO = AMBIENT ATTENUATION FACTOR
C       NS = SPECIMEN ATTENUATION FACTOR
C
C ***************************************************************
C
      NS=REFLS1*REFLS2
      NO=REFLA1*REFLA2*REFLA3
C
C ***************************************************************
C
C   THE NEXT EXPRESSION CALCULATES THE BLACK-
C   BODY RADIANCE EMITTED FROM THE
C   SPECIMEN WHERE:
C        RAD = BLACKBODY RADIANCE
C
C ***************************************************************
C
      RAD=(VOUT*AMB-(NO*AMB))/(EMISS(I)*NS)
C
C ***************************************************************
C
C   THE NEXT STATEMENT GIVES THE FOLLOWING
C   SUBROUTINE TEMPER, AN INITIAL GUESS OF
C   THE TEMPERATURE OF THE SPECIMENS.
C
C ***************************************************************
C
      TEMP=10.
C
C ***************************************************************
C
C   SUBROUTINE TEMPER CALCULATES THE
C   SPECIMEN TEMPERATURE
C
C ***************************************************************
C
      CALL TEMPER(RAD,TEMP,TEMPC,DLMDA,TAU,ICOUN)
      WRITE(6,100) VOLT(J),NS,NO,AMB,RAD,TEMPC
100   FORMAT (2X,F6.3,5X,F7.3,8X,F7.3,3X,2(E12.4,5X),F7.2)
110   CONTINUE
120   CONTINUE
      WRITE (6,130)
130   FORMAT (1H1)
C
C ***************************************************************
```

```
C
C   SUBROUTINE RESPON PLOTS THE SPECTRAL
C   RESPONSE CURVE USED IN THE CALCULATION
C   OF TEMPERATURE
C
C ***********************************************************************
C
C     CALL RESPON(TAU,DLMDA,ICOUN)
      STOP
      END
C
C
C
C
C ***********************************************************************
C ***********************************************************************
C ***********************************************************************
C
C                    SUBROUTINE TEMPER
C
C   SUBROUTINE TEMPER TAKES THE EXPERIMENTAL SPECIMEN EFFECTIVE
C   BLACKBODY RADIANCE AND THEN CALCULATES THE CORRESPONDING
C   TEMPERATURE. THIS IS DONE BY GUESSING A TEMPERATURE AND THEN
C   CALCULATING THE MONOCHROMATIC BLACKBODY RADIANT INTENSITY FOR
C   THE BANDWIDTH OF THE MICROSCOPE. THE RADIANT INTENSITIES ARE
C   THEN MULTIPLIED BY THE SPECTRAL RESPONSE OF THE MICROSCOPE.
C   BY NUMERICAL INTEGRATION THE AREA UNDER THIS CURVE IS CALCULATED
C   AND REPRESENTS THE ACTUAL RADIATION RECEIVED BY THE MICROSCOPE.
C   THIS VALUE IS CORRECTED FOR THE ELECTRICAL CONSTANTS AFFECTING
C   THE OUTPUT AND THEN COMPARED WITH EXPERIMENTAL VALUE. AN
C   ITERATIVE PROCESS IS USED TO CONVERGE TO THE PROPER TEMPERATURE.
C
C
C ***********************************************************************
C ***********************************************************************
C ***********************************************************************
C
C
      SUBROUTINE TEMPER(RAD,TEMP,TEMPC,DLMDA,TAU,ICOUN)
      DIMENSION RADINT(250),TAU(250),X(250),Y1(250),Y2(250),WAVE(250)
      DIMENSION RADI(250),RADY(250)
      TEMPK=TEMP+273.
1     DLMDA=0.022
      WAV=1.6-DLMDA
      ICOUN=0
C
C ***********************************************************************
C
C   THE NEXT SECTION CALCULATES THE NORMALIZED
C   SPECTRAL RESPONSE OF THE MICROSCOPE FOR A GIVEN
C   WAVELENGTH, WHERE:
C        TTAU=NORMALIZED SPECTRAL RESPONSE
C        TAU=MATRIX CONTAINING TTAU
C
C ***********************************************************************
```

```
C
2     ICOUN=ICOUN+1
      WAV=WAV+DLMDA
      IF(WAV.GT.6.2) GO TO 3
      IF(WAV.GE.1.6.AND.WAV.LT.2.0) TTAU=.75*WAV-1.2
      IF(WAV.GE.2.0.AND.WAV.LT.2.2) TTAU=-.10*WAV+.50
      IF(WAV.GE.2.2.AND.WAV.LT.2.4) TTAU=0.0375*WAV+.1975
      IF(WAV.GE.2.4.AND.WAV.LT.2.6) TTAU=.1125*WAV+0.0175
      IF(WAV.GE.2.6.AND.WAV.LT.2.8) TTAU=.20*WAV-.21
      IF(WAV.GE.2.8.AND.WAV.LT.3.0) TTAU=.25*WAV-.35
      IF(WAV.GE.3.0.AND.WAV.LT.3.2) TTAU=.30*WAV-.50
      IF(WAV.GE.3.2.AND.WAV.LT.3.4) TTAU=.425*WAV-.90
      IF(WAV.GE.3.4.AND.WAV.LT.4.2) TTAU=.375*WAV-.73
      IF(WAV.GE.4.2.AND.WAV.LT.4.8) TTAU=.225*WAV-.10
      IF(WAV.GE.4.8.AND.WAV.LT.5.0) TTAU=.10*WAV+.50
      IF(WAV.GE.5.0.AND.WAV.LT.5.2) TTAU=-.60*WAV+4
      IF(WAV.GE.5.2.AND.WAV.LT.5.4) TTAU=-1.30*WAV+7.64
      IF(WAV.GE.5.4.AND.WAV.LT.5.6) TTAU=-2.35*WAV+13.31
      IF(WAV.GE.5.6.AND.WAV.LT.5.8) TTAU=-.45*WAV+2.67
      IF(WAV.GE.5.8.AND.WAV.LT.6.0) TTAU=-.25*WAV+1.51
      IF(WAV.GE.6.0.AND.WAV.LT.6.2) TTAU=-.05*WAV+.31
      TAU(ICOUN)=TTAU
      WAVE(ICOUN)=WAV
      GO TO 2
C
C ***************************************************************
C
C   THE FOLLOWING SECTION CALCULATES THE
C   MONOCHROMATIC BLACKBODY RADIANT INTENSITY
C   IN WATTS/CM**2-STER
C
C ***************************************************************
C
3     CONTINUE
      ICOUN=ICOUN-1
      WAV=1.6-DLMDA
      DO 7 I=1,ICOUN
      A=14388/(WAV*TEMPK)
      IF(A-86.)4,4,5
4     RADI(I)=((11909/WAV**5)*(1./(EXP(A)-1.)))
      RADINT(I)=((11909/WAV**5)*(1/(EXP(A)-1.)))*TAU(I)
      RADY(I)=RADINT(I)
      GO TO 6
C
C ***************************************************************
C
C   THE FOLLOWING SECTION CALCULATES THE TOTAL
C   BLACKBODY RADIANT INTENSITY BY USING
C   SIMPSON'S RULE OF NUMERICAL INTEGRATION
C
C ***************************************************************
C
5     RADINT(I)=0.0
      RADY(I)=0.0
      RADI(I)=0.0
```

```
6     WAV=WAV+DLMDA
7     CONTINUE
      RADF=RADINT(1)+RADINT(ICOUN)
      EVEN=0.0
      ODD=0.0
      M=ICOUN-1
      DO 8 K=2,M,2
      ODD=RADINT(K)+ODD
8     CONTINUE
      L=ICOUN-2
      DO 9 K=3,L,2
      EVEN=RADINT(K)+EVEN
9     CONTINUE
      EFRAD=(DLMDA/3.0)*(RADF+4.0*ODD+2.0*EVEN)
C
C ***************************************************************
C
C   THE NEXT STATEMENT CONVERTS THE ACTUAL RADIANCE
C   TO THAT READ BY THE MICROSCOPE DUE TO THE
C   MICROSCOPE'S ELECTRICAL SYSTEM (PER CONVERSATION
C   WITH NELSON ENGBORG OF BARNES ENGINEERING CO.)
C
C ***************************************************************
C
      EFFRAD=EFRAD*13.50
      TEMPC=TEMPK-273.
C
C ***************************************************************
C
C   THIS SECTION PERFORMS THE ITERATION OF THE
C   TEMPERATURE TO CONVERGENCE. CONVERGENCE IS
C   ACHEIVED WHEN THE CALCULATED RADIANCE EQUALS
C   THE EXPERIMENTAL RADIANCE + OR - 1.5 PERCENT.
C   AN ERROR RANGE LESS THAN THIS CAUSES NO
C   CONVERGENCE FOR SOME TEMPERATURES BECAUSE THE
C   TEMPERATURE IS INCREMENTED IN WHOLE NUMBERS AND
C   THE RADIANCE CHANGES LESS THAN THE ERROR
C
C ***************************************************************
C
      IF(TEMPC.LT.160.) GO TO 13
      ERROR=RAD*0.0075
      GO TO 14
13    ERROR=RAD*.0200
14    CONTINUE
      HIGH=EFFRAD-RAD
      ELOW=RAD-EFFRAD
      IF(HIGH.GT.ERROR) GO TO 10
      IF(ELOW.GT.ERROR) GO TO 11
      GO TO 12
10    TEMPK=TEMPK-1.
      GO TO 1
11    TEMPK=TEMPK+10.
      GO TO 1
12    CONTINUE
```

```
C     CALL INTENT(WAVE,RADY,RADI,ICOUN,TEMPC)
      RETURN
      END
C
C
C
C
C ***********************************************************************
C ***********************************************************************
C ***********************************************************************
C
C
C                       SUBROUTINE RESPON
C
C   SUBROUTINE RESPON PLOTS THE SPECTRAL RESPONSE CURVE USED IN
C   THE NUMERICAL INTEGRATION OF THE BLACKBODY RADIANT INTENSITY.
C   THE PLOTTING COMMANDS ARE FROM THE AGII TEKTRONIX PACKAGE AND
C   SOME CUSTOM SUBROUTINES.
C
C ***********************************************************************
C ***********************************************************************
C ***********************************************************************
C
C
      SUBROUTINE RESPON(TAU,DLMDA,ICOUN)
      DIMENSION TAU(250),WAVE(250),Y(250)
      ICP1=ICOUN+1
      DO 2 I=2,ICP1
      Y(I)=TAU(I-1)*100
2     CONTINUE
      Y(1)=ICOUN
      WAV=1.6
      DO 3 I=1,ICOUN
      L=I+1
      WAVE(L)=WAV+DLMDA
      WAV=WAVE(L)
3     CONTINUE
      WAVE(1)=ICOUN
      CALL INITT(120)
      CALL BINITT
      CALL XFRM(2)
      CALL YFRM(2)
      CALL CHECK(WAVE,Y)
      CALL DSPLAY(WAVE,Y)
      CALL FRAME
      CALL LABLE3(35,265,1.25,90.,26,'Spectral Response, percent')
      CALL LABLE3(375,50,1.25,0.,19,'Wavelength, microns')
      CALL LABLE3(350,765,1.0,0.,28,'NORMALIZED SPECTRAL RESPONSE')
      CALL LABLE3(350,740,1.0,0.,28,'CURVE FOR THE RM-2A INFRARED')
      CALL LABLE3(350,715,1.0,0.,28,'        MICROSCOPE          ')
      CALL MOVABS(0,780)
      CALL ANMODE
      WRITE(3,4)
4     FORMAT(10X,'DO YOU WISH TO GET A HARDCOPY OF THIS PLOT?',
     +/,10X'TYPE 1 TO GET A HARDCOPY OR 2 FOR NO HARDCOPY.')
```

```
      CALL LABLE3(440,650,1.25,0.,6,'deg. C')
      CALL MOVABS(175,500)
      CALL DRWABS(275,500)
      CALL LABLE3(275,500,1.25,0.,13,'  Theretical')
      CALL MOVABS(175,450)
      CALL DSHABS(275,450,3)
      CALL LABLE3(275,450,1.25,0.,11,'  Corrected')
      CALL MOVABS(0,780)
      CALL ANMODE
      WRITE(3,2)
2     FORMAT(10X,'DO YOU WISH TO GET A HARDCOPY OF THIS PLOT?',
     +/10X,'TYPE 1 TO GET A HARDCOPY OR 2 FOR NO HARDCOPY.')
      IHARD=IVET(1,2,IE)
      IF(IHARD.EQ.2) GO TO 3
      CALL PLSAVE
      CALL ERASE
3     CONTINUE
      RETURN
      END
```

APPENDIX F.2

COMPUTER PROGRAM:

Surface temperature calculations with subdivision of the contact area.

```
      REAL KB,KC,MU,LE,LP,N,L,JE,JP,JAVG,NUM
C
C ***********************************************************************
C ***********************************************************************
C
C            ***SURFACE TEMPERATURE CALCULATION
C
C               PROGRAM WITH SUBDIVISION OF THE
C
C                     CONTACT AREA***
C
C ***********************************************************************
C
C      THIS PROGRAM CALCULATES SURFACE TEMPERATURES
C      GENERATED BY FRICTION USING ARCHARD'S THEORY
C      AND WHEN THE CONTACT AREA IS SUBDIVIDED.
C      THE TEMPERATURES ARE CALCULATED FOR A GIVEN
C      VELOCITY AND LOAD AND BY ASSUMING BOTH
C      PLASTIC AND ELASTIC DEFORMATION THEORY. THE
C      ONLY VARIABLE IN EACH RUN IS THE NUMBER
C      OF CONTACT AREAS WHICH INCREMENTS ITSELF FROM
C      1 TO 200 TO ALLOW ONE TO SEE THE RAPID DECREASE
C      IN THE CALCULATED TEMPERATURES WITH AN
C      INCREASE IN NUMBER OF CONTACTS.
C
C ***********************************************************************
C
      DIMENSION BNAME(5), CNAME(5),X(225),Y1(225),Y2(225)
      READ(5,10) (BNAME(I),I=1,3),EB,RHOB,CB,KB,PMB,TMB,POISB
      READ(5,10) (CNAME(I),I=1,3),EC,RHOC,CC,KC,PMC,TMC,POISC
10    FORMAT(3A4,7F9.7)
C
C ***********************************************************************
C
C     THE FOLLOWING SECTION CREATES THE TITLE
C     AND MATERIAL PROPERTY TABLE WHERE:
C        EB,EC= MODULUS OF ELASTICITY
C        RHOB,RHOC= DENSITY
C        CB,CC= SPECIFIC HEAT
C        KB,KC= THERMAL CONDUCTIVITY
C        PMB,PMC= HARDNESS OR FLOW STRENGTH
C        TMB,TMC= MELTING POINT OF THE SOLIDS
C        POISB,POISC= POISSON'S RATIO
C
C ***********************************************************************
C
      WRITE(6,20)
20    FORMAT(1H1,'CALCULATION OF SURFACE TEMPERATURES'//)
      WRITE(6,40)
      WRITE(6,30)
30    FORMAT(1H*,30X,'_________',5X,'_________'/)
```

```
40    FORMAT(1H ,28X,'    SPHERE',5X,'     PLANE')
      WRITE(6,50) (BNAME(I),I=1,3),(CNAME(I),I=1,3),EB,EC,RHOB,
     2 RHOC,CB,CC,KB,KC,PMB,PMC,TMB,TMC,POISB,POISC
50    FORMAT(1X,'MATERIAL                          ',3A4,5X,3A4/1X,
     2         'MODULUS OF ELASTICITY(N/M**2) ',1PE10.4,5X,1PE10.4/1X,
     3         'DENSITY(KG/M**3)              ',1PE10.4,5X,1PE10.4/1X,
     4         'SPECIFIC HEAT(JOULES/KG-C)    ',1PE10.4,5X,1PE10.4/1X,
     5         'CONDUCTIVITY(JOULES/SEC-M-C)  ',1PE10.4,5X,1PE10.4/1X,
     6         'HARDNESS(N/M**2)              ',1PE10.4,5X,1PE10.4/1X,
     7         'MELTING POINT(C)              ',1PE10.4,5X,1PE10.4/1X,
     8         'POISSONS RATIO                ',1PE10.4,5X,1PE10.4/)
C
C ********************************************************************
C
C    FROM THE DATA THE LOAD,W (NEWTONS),THE
C    VELOCITY,V (METERS/SEC), THE COEFFICIENT OF
C    FRICTION,MU , AND THE RADIUS OF THE SPECIMEN
C    BALL, R (METERS), IS READ.
C
C ********************************************************************
C
60    READ(5,70) W,V,MU,R
70    FORMAT(4F10.5)
      K=1
      IF (W.EQ.0.) GO TO 260
      WRITE(6,80)W,V,MU,R
80    FORMAT(//' LOAD=',F6.3,' N',5X,' SPEED=',F6.3,' M/S',5X,' COEFF
     2OF FRICTION=',F6.3//,1X,' RADIUS OF SPHERE=',F8.5,' M'//)
C
C ********************************************************************
C
C    INCREMENTS THE NUMBER OF SUBDIVIDED
C    CONTACT AREAS FROM 1 TO 200
C
C ********************************************************************
C
      AN=0.
90    IF (AN.GE.50.) AN=AN*10
      IF (AN.GE.10.AND.AN.LT.50.) AN=AN*5.
      IF (AN.LT.10.) AN=AN*1.
      IF (AN.GT.200.) GO TO 280
C
C ********************************************************************
C
C    CALCULATES THE RADIUS OF A
C    SINGLE CONTACT FROM
C    ELASTIC DEFORMATION THEORY
C
C ********************************************************************
C
100   AE=((((1.-POISB**2)/EB)+((1.-POISC**2)/EC))*.75*W*R)**.333333
     C/SQRT(AN)
C
C ********************************************************************
C
```

```
C    DETERMINES THE MATERIAL WITH THE LOWEST
C    HARDNESS AND THEN USES THIS VALUE OF 'PM'
C    IN THE ELASTIC DEFORMATION THEORY
C
C ***************************************************************
C
      PM=PMC
      IF(PMC.GT.PMB) PM=PMB
C
C ***************************************************************
C
C   CALCULATES THE RADIUS OF THE PLASTIC
C   AREA OF CONTACT
C
C ***************************************************************
C
      AP=SQRT(W/(3.14159*PM*AN))
      AP2=W/(PM*AN)
C
C ***************************************************************
C
C    CALCULATES THE AREA OF A SINGLE CONTACT
C    USING BOTH ELASTIC AND PLASTIC DEFORMATION
C    THEORY
C
C ***************************************************************
C
      AE2=3.14159*AE**2
      IF(AN.GT.1.) GO TO 120
      WRITE(6,110) AE2,AP2
110   FORMAT(1X,'ELASTIC AREA OF CONTACT =',1PE10.4,' M**2'//1X,
     2          'PLASTIC AREA OF CONTACT =',1PE10.4,' M**2'/)
C
C ***************************************************************
C
C    DETERMINES THE MATERIAL WITH THE
C    LOWEST MELTING POINT SO THAT
C    TEMPERATURES WILL NOT BE CALCULATED
C    ABOVE THE MELTING POINT OF ONE OF
C    THE MATERIALS
C
C ***************************************************************
C
120   IF(TMB.GT.TMC)TM=TMC
      IF(TMC.GE.TMB)TM=TMB
C
C ***************************************************************
C
C    DIF EQUALS THERMAL DIFFUSIVITY
C
C ***************************************************************
C
      DIF=KC/(RHOC*CC)
      IF(AN.GT.1.) GO TO 140
      WRITE(6,130)
```

```
130   FORMAT(43X,'ARCHARDS THEORY',5X,'JAEGERS THEORY'/23X,
     2'PECLET NUMBER',15X,'TEMPERATURE RISE (C)'//1X,
     3'NUMBER OF CONTACTS',3(3X,'ELASTIC',3X,'PLASTIC')/)
C
C ***************************************************************
C
C    CALCULATES THE PECLET NUMBER FOR
C    THE ELASTIC AND PLASTIC AREAS OF CONTACT
C
C ***************************************************************
C
140   LE=V*AE/(2.*DIF)
      LP=V*AP/(2.*DIF)
C
C ***************************************************************
C
C    CALCULATES THE HEAT INPUT TO A
C    SINGLE CONTACT REGION
C
C ***************************************************************
C
      Q=MU*W*V/AN
C
C ***************************************************************
C
C     DETERMINES WHICH OF THE THREE EQUATIONS
C     SHOULD BE USED BASED ON THE SPEED CRITERION
C     OR THE PECLET NUMBER.
C
C ***************************************************************
C
150   IFLAG=1
      IF (LP.LT..1) GO TO 190
      IF (LP.GT.5.) GO TO 220
      IF (LP.GE..1.AND.LP.LE.5.) GO TO 250
160   IFLAG=2
      IF (LE.LT..1) GO TO 190
      IF (LE.GT.5.) GO TO 220
      IF (LE.GE..1.AND.LE.LE.5.) GO TO 250
170   WRITE(6,180) AN,LE,LP,TME,TMP,JE,JP
180   FORMAT(6X,F7.0,7X,F8.4,3X,F7.4,4(4X,F6.1))
      K=K+1
      X(K)=AN
      Y1(K)=JP
      Y2(K)=TMP
      GO TO 90
C
C ***************************************************************
C
C     CALCULATES THE SURFACE TEMPERATURE WHEN
C     L IS LESS THAN 0.1 USING THE SLOW SPEED
C     ARCHARD EQUATION
C
C ***************************************************************
C
```

```
190   IF (IFLAG.EQ.1) RAD=AP
      IF (IFLAG.EQ.2) RAD=AE
      TAVG=(1./(KB*KC))*Q/(4*RAD)
      JAVG=0.946*Q/(4*RAD*(KB*KC))
      IF (IFLAG.NE.1) GO TO 200
      TMP=TAVG
      JP=JAVG
      GO TO 160
200   IF (IFLAG.NE.2) GO TO 210
      TME=TAVG
      JE=TAVG
210   IF (TME.GE.TM) GO TO 170
      GO TO 170
C
C ***************************************************************************
C
C     CALCULATES THE SURFACE TEMPERATURE
C     WHEN L IS GREATER THAN 5 USING THE
C     HIGH SPEED EQUATION
C
C ***************************************************************************
C
220   IF (IFLAG.EQ.1) RAD=AP
      IF (IFLAG.EQ.2) RAD=AE
      TAVG=0.31*Q*SQRT(DIF/(V*RAD))/(KC*RAD)
      NUM=1.064*(Q/(3.1417*RAD))*(DIF**0.5)
      DEN=(1.125*KB*DIF**0.5)*(KC*(RAD*V)**0.5)
      JAVG=NUM/DEN
      IF (IFLAG.NE.1) GO TO 230
      TMP=TAVG
      JP=JAVG
      GO TO 160
230   IF (IFLAG.NE.2) GO TO 240
      TME=TAVG
      JE=JAVG
240   IF (TME.GE.TM) GO TO 170
      GO TO 170
C
C ***************************************************************************
C
C     CALCULATES THE SURFACE TEMPERATURE
C     WHEN L IS BETWEEN 0.1 AND 5. USING
C     THE INTERMEDIATE SPEED-ARCHARD EQUATION
C     WITH ALPHA DERIVED FROM FIGURE 7 OF
C     JAEGER'S PAPER
C
C ***************************************************************************
C
250   IF (IFLAG.EQ.1) L=LP
      IF (IFLAG.EQ.2) L=LE
C
C   THESE NEXT FIVE EQUATIONS REPRESENT
C   THE CURVE OF FIGURE 7 OF JAEGER'S PAPER
C   BY APPROXIMATING THE CURVE AS
C   FIVE DIFFERENT STRAIGHT LINE SEGMENTS
```

```
C
      IF (L.GE.0.1.AND.L.LE..5) Y=2.25*L-0.025
      IF (L.GT.0.5.AND.L.LE.1.0) Y=1.50*L+0.35
      IF (L.GT.1.0.AND.L.LE.2.0) Y=1.05*L+0.80
      IF (L.GT.2.0.AND.L.LE.3.0) Y=0.80*L+1.30
      IF (L.GT.3.0.AND.L.LE.5.0) Y=0.60*L+1.90
      ALPHA=(4*Y)/(3.14159**2*L)
      IF (IFLAG.EQ.1) RAD=AP
      IF (IFLAG.EQ.2) RAD=AE
      NB=Q/(RAD**2*RHOB*CB*V)
      NC=Q/(RAD**2*RHOC*CC*V)
C
C     TEMPB IS CALCULATED USING THE STATIONARY
C     HEAT SOURCE EQUATION
C
      TEMPB=0.5*NB*L
C
C     TEMPC IS CALCULATED USING THE INTERMEDIATE
C     SPEED EQUATION
C
      TEMPC=0.5*ALPHA*NC*L
C
C     THE AVERAGE TEMPERATURE ACROSS THE
C     HEAT SOURCE IS FOUND BY:
C
C           1/TAVG=(1/TEMPB)+(1/TEMPC)
C
C     .
      TAVG=1/((1/TEMPB)+(1/TEMPC))
      NUM=0.946*DIF*Y*Q/(3.1417*RAD)
      DEN=(1.486*RAD*KC*V)+(DIF*KB*Y)
      JAVG=NUM/DEN
      IF (IFLAG.NE.1) GO TO 260
      TMP=TAVG
      JP=JAVG
      GO TO 160
260   IF (IFLAG.NE.2) GO TO 270
      TME=TAVG
      JE=JAVG
270   IF (TME.GE.TM) GO TO 170
      GO TO 170
280   X(1)=K-1
      Y1(1)=K-1
      Y2(1)=K-1
      CALL INITT(120)
      CALL BINITT
      CALL XFRM(2)
      CALL YFRM(2)
      CALL LINE(3)
      CALL CHECK(X,Y2)
      CALL DSPLAY(X,Y2)
      CALL LINE(0)
      CALL CPLOT(X,Y1)
      CALL FRAME
      CALL LABLE3(35,265,1.25,90.,29,'Mean Temperature Rise, deg. C')
```

```
      CALL LABLE3(375,50,1.25,0.,18,'Number of Contacts')
      CALL LABLE3(400,650,1.0,0.,12,BNAME)
      CALL LABLE3(460,625,1.0,0.,4,'-ON-')
      CALL LABLE3(400,600,1.0,0.,12,CNAME)
      CALL LABLE3(600,650,1.25,0.,6,'Load =')
      CALL LABLE3(600,600,1.25,0.,16,'Friction Coef. =')
      CALL RLOUT(800,600,MU,4,3)
      CALL LABLE3(600,625,1.25,0.,10,'Velocity =')
      CALL RLOUT(675,650,W,6,3)
      CALL RLOUT(710,625,V,6,3)
      CALL LABLE3(800,650,1.25,0.,7,'Newtons')
      CALL LABLE3(830,625,1.25,0.,5,'m/sec')
      CALL MOVABS(550,450)
      CALL DSHABS(650,450,3)
      CALL LABLE3(650,450,1.25,0.,16,'  Archard Theory')
      CALL MOVABS(550,400)
      CALL DRWABS(650,400)
      CALL LABLE3(650,400,1.25,0.,15,'  Jaeger Theory')
      CALL MOVABS(0,780)
      CALL ANMODE
      WRITE(3,290)
  290 FORMAT(10X,'DO YOU WISH TO GET A HARDCOPY OF THIS PLOT?',
     *'/,10X,'TYPE 1 TO GET A HARDCOPY OR 2 FOR NO HARDCOPY.')
      IHARD = IVET(1,2,IE)
      IF(IHARD .EQ. 2) GO TO 300
      CALL PLSAVE
      CALL ERASE
  300 CONTINUE
      GO TO 60
  310 WRITE(6,320)
  320 FORMAT(1H1)
      CALL FINITT(0,700)
      STOP
      END
```

APPENDIX F.3

COMPUTER PROGRAM:

Surface temperature calculation program
using Archand and Jaeger theories.
Calculates temperatures with a given velocity
constant and incrementing the load.

```
      REAL KB,KC,MU,LE,LP,L,N,JE,JP,JAVG,NUM
C
C ***************************************************************
C ***************************************************************
C
C
C          ***SURFACE TEMPERATURE CALCULATION PROGRAM***
C
C            THIS PROGRAM CALCULATES SURFACE TEMPERATURES
C            GENERATED BY FRICTION USING BOTH ARCHARD'S
C            AND JAEGERS'S MEAN TEMPERATURE THEORIES.
C            THE TEMPERATURES ARE CALCULATED BY ASSUMING
C            PLASTIC DEFORMATION AND ALSO ELASTIC DEFOR-
C            MATION, ALLOWING FOR COMPARISON OF THE TWO
C            METHODS WHICH DETERMINE CONTACT AREA AND THE
C            TWO DIFFERENT THEORIES. THIS PROGRAM SETS A
C            GIVEN VELOCITY CONSTANT AND THEN INCREMENTS THE
C            LOAD TO CREATE A CURVE OF TEMPERATURE RISE VS. LOAD.
C
C
C            THIS PROGRAM WAS WRITTEN BY CRAIG A. ROGERS.
C            EXPLANATION OF THE PROGRAM AND THE MANNER
C            IN WHICH FIGURE 7 OF JAEGERS PAPER IS
C            INCORPORATED IN THE PROGRAM CAN BE FOUND
C            IN C. A. ROGERS' MASTERS THESIS (NOV. 1982).
C
C
C
C
C ***************************************************************
C ***************************************************************
C
C
C
C ***************************************************************
C
C            THE FOLLOWING STATEMENT CREATES A MATRIX
C            WHICH HOLDS THE NAMES OF THE MATERIALS
C            WHICH ARE TO BE READ FROM THE DATA
C
C ***************************************************************
C
      DIMENSION X(1000),Y1(1000),Y2(1000),BNAME(10), CNAME(10)
      READ(5,10) (BNAME(I),I=1,3),EB,RHOB,CB,KB,PMB,TMB,POISB
      READ(5,10) (CNAME(I),I=1,3),EC,RHOC,CC,KC,PMC,TMC,POISC
10    FORMAT(3A4,7F9.7)
C
C ***************************************************************
C
C     THE FOLLOWING SECTION CREATES THE TITLE
C     AND MATERIAL PROPERTY TABLE WHERE:
```

```
C          EB,EC=MODULUS OF ELASTICITY OF THE TWO BODIES
C          RHOB,RHOC=DENSITY OF THE TWO BODIES
C          CB,CC=SPECIFIC HEAT OF THE TWO BODIES
C          KB,KC=THERMAL CONDUCTIVITY OF THE TWO BODIES
C          PMB,PMC=HARDNESS OR FLOW STRENGTH (3XY.S)
C          TMB,TMC=MELTING POINT OF THE TWO BODIES
C          POISB,POISC=POISSON'S RATIO OF THE TWO BODIES
C
C ***************************************************************************
C
      WRITE (6,350)
      WRITE(6,25)
      WRITE(6,20)
      WRITE(6,25)
20    FORMAT(20X,'CALCULATION OF SURFACE TEMPERATURES'//)
25    FORMAT(14X,'************************************************'/)
      I=0
      WRITE(6,40)
      WRITE(6,30)
30    FORMAT(1H*,30X,'_________',5X,'_________'/)
40    FORMAT(1H ,28X,'    SPHERE',5X,'     PLANE')
      WRITE(6,50)(BNAME(I),I=1,3),(CNAME(I),I=1,3),EB,EC,RHOB,RHOC,CB,
     2  CC,KB,KC,PMB,PMC,TMB,TMC,POISB,POISC
50    FORMAT(1X,'MATERIAL                              ',3A4,5X,3A4/1X,
     2          'MODULUS OF ELASTICITY(N/M**2) ',1PE10.4,5X,1PE10.4/1X,
     3          'DENSITY(KG/M**3)              ',1PE10.4,5X,1PE10.4/1X,
     4          'SPECIFIC HEAT(JOULES/KG-C)    ',1PE10.4,5X,1PE10.4/1X,
     5          'CONDUCTIVITY(JOULES/SEC-M-C)  ',1PE10.4,5X,1PE10.4/1X,
     6          'HARDNESS(N/M**2)              ',1PE10.4,5X,1PE10.4/1X,
     7          'MELTING POINT(C)              ',1PE10.4,5X,1PE10.4/1X,
     8          'POISSONS RATIO                ',1PE10.4,5X,1PE10.4/)
C
C ***************************************************************************
C
C     FROM THE DATA THE VELOCITY (M/SEC),THE
C     COEFFICIENT OF FRICTION, MU, AND THE
C     RADIUS OF THE SPECIMEN BALLS,R (METERS),IS READ.
C
C ***************************************************************************
C
60    READ(5,70) V,MU,R
      K=1
      IF (V.EQ.0.0) GO TO 340
      I=0
70    FORMAT(3F10.5)
      WRITE(6,80)V,MU,R
80    FORMAT(//' VELOCITY =',F6.2,' M',5X,'COEFF. OF FRICTION =',F5.3,
     2   5X,' RADIUS = ',1PE12.6,'  M'//)
C
C ***************************************************************************
C
C    DETERMINES THE MATERIAL WITH THE
C    LOWEST MELTING POINT. THE PROGRAM
C    WILL STOP WHEN IT CALCULATES A
C    TEMPERATURE GREATER THAN THIS MELTING
```

```
C    POINT
C
C ***************************************************************
C
     IF(TMB.GT.TMC)TM=TMC
     IF(TMC.GE.TMB)TM=TMB
C
C ***************************************************************
C
C     DIF EQUALS THE THERMAL DIFFUSIVITY
C
C ***************************************************************
C
     DIF=KC/(RHOC*CC)
     WT=-0.749999
     WRITE(6,100)
100  FORMAT(43X,'ARCHARDS THEORY',5X,'JAEGERS THEORY'/23X,
    2'PECLET NUMBER',15X,'TEMPERATURE RISE (C)'//1X,
    3' LOAD (NEWTONS)   ',3X,'ELASTIC',3X,'PLASTIC',3X,'ELASTIC',
    43X,'PLASTIC',3X,'ELASTIC',3X,'PLASTIC'/)
C
C ***************************************************************
C
C     INCREMENTS THE LOAD BY
C
C     0.75 NEWTONS
C ***************************************************************
C
110   WT=WT+0.75
C
C ***************************************************************
C
C     DETERMINES THE Softest MATERIAL AND THEN USES
C     ITS HARDNESS IN THE PLASTIC DEFORMATION THEORY
C
C ***************************************************************
C
     AE=((((1.-POISB**2)/EB)+((1.-POISC**2)/EC))*.75*WT*R)**.33333
C
C ***************************************************************
C
C     CALCULATES THE RADIUS OF THE ELASTIC AREA
C     OF CONTACT, AE.
C
C          AP2=PLASTIC AREA OF CONTACT
C          AE2=ELASTIC AREA OF CONTACT
C
C ***************************************************************
C
     PM=PMC
     IF(PMC.GT.PMB) PM=PMB
     AP=SQRT(WT/(3.14159*PM))
     AP2=WT/PM
     AE2=3.14159*AE*AE
C
```

```
C ***********************************************************************
C
C     CALCULATES THE PECLET NUMBER FOR THE ELASTIC
C     AND PLASTIC AREA OF CONTACT.
C
C           LE=PECLET NUMBER USING ELASTIC DEFORMATION
C           LP=PECLET NUMBER USING PLASTIC DEFORMATION
C
C ***********************************************************************
C
170   LE=V*AE/(2.*DIF)
      LP=V*AP/(2.*DIF)
C
C ***********************************************************************
C
C     CALCULATES THE HEAT INPUT TO THE SYSTEM
C
C          Q=HEAT INPUT
C
C ***********************************************************************
C
      Q=MU*WT*V
C
C ***********************************************************************
C
C    DETERMINES WHICH OF THE THREE EQUATIONS
C    SHOULD BE USED BASED ON THE SPEED CRITERION
C    OR THE PECLET NUMBER.
C
C ***********************************************************************
C
180   IFLAG=1
      IF (LP.LT..1) GO TO 220
      IF (LP.GT.5.) GO TO 250
      IF (LP.GE..1.AND.LP.LE.5.) GO TO 280
190   IFLAG=2
      IF (LE.LT..1) GO TO 220
      IF (LE.GT.5.) GO TO 250
      IF (LE.GE..1.AND.LE.LE.5.) GO TO 280
200   WRITE(6,210) WT,LE,LP,TME,TMP,JE,JP
210   FORMAT(6X,F7.3,7X,F8.4,3X,F7.4,4(4X,F6.1))
      K=K+1
      X(K)=WT
      Y1(K)=JP
      Y2(K)=TMP
      GO TO 110
C
C ***********************************************************************
C
C     CALCULATES THE SURFACE TEMPERATURE WHEN
C     L IS LESS THAN 0.1 USING THE SLOW SPEED
C     EQUATIONS
C
C ***********************************************************************
C
```

```
220   IF(IFLAG.EQ.1) RAD=AP
      IF(IFLAG.EQ.2) RAD=AE
C
C ***************************************************************************
C
C      TAVG IS THE MEAN TEMPERATURE ACROSS
C        THE HEAT SOURCE USING ARCHARD'S EQUATION
C      JAVG IS THE MEAN TEMPERATURE USING
C        JAEGER'S THEORY
C
C ***************************************************************************
C
      TAVG=(1./(KB*KC))*Q/(4*RAD)
      JAVG=0.946*Q/(4*RAD*(KB*KC))
      IF (IFLAG.NE.1) GO TO 230
      TMP=TAVG
      JP=JAVG
      GO TO 190
230   IF (IFLAG.NE.2) GO TO 240
      TME=TAVG
      JE=JAVG
240   IF (JP.GE.TM) GO TO 310
      GO TO 200
C
C ***************************************************************************
C
C     CALCULATES THE SURFACE TEMPERATURE
C     WHEN L IS GREATER THAN 5 USING THE
C     HIGH SPEED ARCHARD EQUATION
C
C ***************************************************************************
250   IF (IFLAG.EQ.1) RAD=AP
      IF (IFLAG.EQ.2) RAD=AE
      TAVG=.31*Q*SQRT(DIF/(V*RAD))/(KC*RAD)
C
C ***************************************************************************
C
C      NUM IS THE NUMERATOR AND DEN IS
C      THE DENOMINATOR OF THE JAEGER
C      EQUATIONS.
C
C ***************************************************************************
C
      NUM=1.064*(Q/(3.1417*RAD))*(DIF**0.5)
      DEN=(1.125*KB*DIF**0.5)+(KC*(RAD*V)**0.5)
      JAVG=NUM/DEN
      IF (IFLAG.NE.1) GO TO 260
      TMP=TAVG
      JP=JAVG
      GO TO 190
260   IF (IFLAG.NE.2) GO TO 270
      TME=TAVG
      JE=JAVG
270   IF (JP.GE.TM) GO TO 310
      GO TO 200
```

```
C ***************************************************************
C
C     CALCULATES THE SURFACE TEMPERATURE
C     WHEN L IS BETWEEN 0.1 AND 5, USING
C     THE INTERMEDIATE SPEED-ARCHARD EQUATION
C     WITH ALPHA DERIVED FROM FIGURE 7 OF
C     JAEGER'S PAPER
C
C ***************************************************************
C
280   IF (IFLAG.EQ.1) L=LP
      IF (IFLAG.EQ.2) L=LE
C
C   THESE NEXT FIVE EQUATIONS REPRESENT
C   THE CURVE OF FIGURE 7 OF JAEGER'S
C   PAPER BY APPROXIMATING THE CURVE
C   AS 5 DIFFERENT STRAIGHT LINE SEGMENTS
C
      IF (L.GE.0.1.AND.L.LE..5) Y=2.25*L-0.025
      IF (L.GT.0.5.AND.L.LE.1.0) Y=1.50*L+0.35
      IF (L.GT.1.0.AND.L.LE.2.0) Y=1.05*L+0.80
      IF (L.GT.2.0.AND.L.LE.3.0) Y=0.80*L+1.30
      IF (L.GT.3.0.AND.L.LE.5.0) Y=0.60*L+1.90
      ALPHA=(4*Y)/(3.14159**2*L)
      IF (IFLAG.EQ.1) RAD=AP
      IF (IFLAG.EQ.2) RAD=AE
      NB=Q/(RAD**2*RHOB*CB*V)
      NC=Q/(RAD**2*RHOC*CC*V)
C
C   TEMPB IS CALCULATED USING THE ARCHARD STATIONARY
C   HEAT SOURCE EQUATION
C
      TEMPB=0.5*NB*L
C
C   TEMPC IS CALCULATED USING THE ARCHARD INTERMEDIATE
C   SPEED EQUATION
C
      TEMPC=0.5*ALPHA*NC*L
C
C   THE AVERAGE TEMPERATURE ACROSS THE
C   HEAT SOURCE IS FOUND BY
C     1/TAVG=(1/TEMPB)+(1/TEMPC)
C
      TAVG=1/((1/TEMPB)+(1/TEMPC))
      NUM=0.946*DIF*Y*Q/(3.1417*RAD)
      DEN=(1.486*RAD*KC*V)+(DIF*KB*Y)
      JAVG=NUM/DEN
      IF (IFLAG.NE.1) GO TO 290
      TMP=TAVG
      JP=JAVG
      GO TO 190
290   IF (IFLAG.NE.2) GO TO 300
      TME=TAVG
      JE=JAVG
300   IF (JP.GE.TM) GO TO 310
```

```
      GO TO 200
C
C ******************************************************
C
C   THE FOLLOWING SECTION PLOTS A CURVE OF
C   THE THEORETICAL TEMPERATURE RISE VS. LOAD.
C   THE PLOTTING COMMANDS ARE FROM THE TEKTRONIX
C   AGII PACKAGE WITH SOME CUSTOM SUBROUTINES.
C
C ************************************************************
C
310   X(1)=K-1
      Y1(1)=K-1
      Y2(1)=K-1
      CALL INITT(120)
      CALL BINITT
      CALL XTYPE(1)
      CALL YTYPE(1)
      CALL XFRM(2)
      CALL YFRM(2)
      CALL LINE(3)
      CALL CHECK(X,Y2)
      CALL DSPLAY(X,Y2)
      CALL LINE(0)
      CALL CPLOT(X,Y1)
      CALL FRAME
      CALL LABLE3(35,265,1.25,90.,29,'Mean Temperature Rise, deg. C')
      CALL LABLE3(375,50,1.25,0.,21,'Contact Load, newtons')
      CALL LABLE3(175,575,1.25,0.,10,'Velocity =')
      CALL LABLE3(175,550,1.25,0.,16,'Friction Coef. =')
      CALL RLOUT(275,575,V,6,3)
      CALL RLOUT(375,550,MU,4,3)
      CALL LABLE3(375,575,1.25,0.,5,'m/sec')
      CALL LABLE3(400,650,1.0,0.,12,BNAME)
      CALL LABLE3(460,625,1.0,0,4,'-ON-')
      CALL LABLE3(400,600,1.0,0.,12,CNAME)
      CALL MOVABS(550,200)
      CALL DSHABS(650,200,3)
      CALL LABLE3(650,200,1.25,0.,16,'  Archard Theory')
      CALL MOVABS(550,150)
      CALL DRWABS(650,150)
      CALL LABLE3(650,150,1.25,0.,15,'  Jaeger Theory')
      CALL MOVABS(0,780)
      CALL ANMODE
      WRITE(3,320)
 320  FORMAT(10X,'DO YOU WISH TO GET A HARDCOPY OF THIS PLOT?',
     *,/,10X,'TYPE 1 TO GET A HARDCOPY OR 2 FOR NO HARDCOPY.')
      IHARD = IVET(1,2,IE)
      IF(IHARD .EQ. 2) GO TO 330
      CALL PLSAVE
      CALL ERASE
330   CONTINUE
340   IF (V.NE.0.0) GO TO 60
      WRITE(6,350)
350   FORMAT(1H1)
```

```
CALL FINITT(0,700)
STOP
END
```

APPENDIX F.4

COMPUTER PROGRAM:

Surface temperature calculation program using Archand and Jaeger theories. Calculates temperatures with a given load constant and incrementing the velocity.

```
      REAL KB,KC,MU,LE,LP,L,N,JE,JP,JAVG,NUM
C
C ***********************************************************************
C ***********************************************************************
C
C
C          ***SURFACE TEMPERATURE CALCULATION PROGRAM***
C
C            THIS PROGRAM CALCULATES SURFACE TEMPERATURES
C            GENERATED BY FRICTION USING BOTH ARCHARD'S
C            AND JAEGERS'S MEAN TEMPERATURE THEORIES.
C            THE TEMPERATURES ARE CALCULATED BY ASSUMING
C            PLASTIC DEFORMATION AND ALSO ELASTIC DEFOR-
C            MATION, ALLOWING FOR COMPARISON OF THE TWO
C            METHODS WHICH DETERMINE CONTACT AREA AND THE
C            TWO DIFFERENT THEORIES. THIS PROGRAM SETS A
C            GIVEN LOAD CONSTANT AND THEN INCREMENTS THE
C            LOAD TO CREATE A CURVE OF TEMPERATURE RISE
C            VS. VELOCITY.
C
C
C            THIS PROGRAM WAS WRITTEN BY CRAIG A. ROGERS.
C            EXPLANATION OF THE PROGRAM AND THE MANNER
C            IN WHICH FIGURE 7 OF JAEGERS PAPER IS
C            INCORPORATED IN THE PROGRAM CAN BE FOUND
C            IN C. A. ROGERS' MASTERS THESIS (NOV. 1982).
C
C
C
C
C ***********************************************************************
C ***********************************************************************
C
C
C
C ***********************************************************************
C
C            THE FOLLOWING STATEMENT CREATES A MATRIX
C            WHICH HOLDS THE NAMES OF THE MATERIALS
C            WHICH ARE TO BE READ FROM THE DATA
C
C ***********************************************************************
C
      DIMENSION X(500),Y1(500),Y2(500),BNAME(10), CNAME(10)
      READ(5,10) (BNAME(I),I=1,3),EB,RHOB,CB,KB,PMB,TMB,POISB
      READ(5,10) (CNAME(I),I=1,3),EC,RHOC,CC,KC,PMC,TMC,POISC
10    FORMAT(3A4,7F9.7)
C
C ***********************************************************************
C
C     THE FOLLOWING SECTION CREATES THE TITLE
```

```
C     AND MATERIAL PROPERTY TABLE WHERE:
C          EB,EC=MODULUS OF ELASTICITY OF THE TWO BODIES
C          RHOB,RHOC=DENSITY OF THE TWO BODIES
C          CB,CC=SPECIFIC HEAT OF THE TWO BODIES
C          KB,KC=THERMAL CONDUCTIVITY OF THE TWO BODIES
C          PMB,PMC=HARDNESS OR FLOW STRENGTH (3XY.S)
C          TMB,TMC=MELTING POINT OF THE TWO BODIES
C          POISB,POISC=POISSON'S RATIO OF THE TWO BODIES
C
C ***********************************************************************
C
      WRITE (6,350)
      WRITE(6,25)
      WRITE(6,20)
      WRITE(6,25)
20    FORMAT(20X,'CALCULATION OF SURFACE TEMPERATURES'//)
25    FORMAT(14X,'************************************************'/)
      I=0
      WRITE(6,40)
      WRITE(6,30)
30    FORMAT(1H+,30X,'_________',5X,'_________'/)
40    FORMAT(1H ,28X,'    SPHERE',5X,'     PLANE')
      WRITE(6,50)(BNAME(I),I=1,3),(CNAME(I),I=1,3),EB,EC,RHOB,RHOC,CB,
     2  CC,KB,KC,PMB,PMC,TMB,TMC,POISB,POISC
50    FORMAT(1X,'MATERIAL                              ',3A4,5X,3A4/1X,
     2         'MODULUS OF ELASTICITY(N/M**2) ',1PE10.4,5X,1PE10.4/1X,
     3         'DENSITY(KG/M**3)              ',1PE10.4,5X,1PE10.4/1X,
     4         'SPECIFIC HEAT(JOULES/KG-C)    ',1PE10.4,5X,1PE10.4/1X,
     5         'CONDUCTIVITY(JOULES/SEC-M-C)  ',1PE10.4,5X,1PE10.4/1X,
     6         'HARDNESS(N/M**2)              ',1PE10.4,5X,1PE10.4/1X,
     7         'MELTING POINT(C)              ',1PE10.4,5X,1PE10.4/1X,
     8         'POISSONS RATIO                ',1PE10.4,5X,1PE10.4/)
C
C ***********************************************************************
C
C     FROM THE DATA THE LOAD,WT (NEWTONS),THE
C     COEFFICIENT OF FRICTION, MU, AND THE
C     RADIUS OF THE SPECIMEN BALLS,R (METERS),IS READ.
C
C ***********************************************************************
C
60    READ(5,70) WT,MU,R
      K=1
      IF (WT.EQ.0.0) GO TO 340
      I=0
70    FORMAT(3F10.5)
      WRITE(6,80)WT,MU,R
80    FORMAT(//' LOAD =',F6.2,' N',5X,'COEFF. OF FRICTION =',F5.3,
     2   5X,' RADIUS = ',1PE12.6,'  M'//)
C
C ***********************************************************************
C
C     CALCULATES THE RADIUS OF THE ELASTIC AREA
C     OF CONTACT, AE.
C
```

```
C           AP2=PLASTIC AREA OF CONTACT
C           AE2=ELASTIC AREA OF CONTACT
C
C ***************************************************************
C
      AE=((((1.-POISB*POISB)/EB)+((1.-POISC*POISC)/EC))*.75*WT*R)**.33333
C
C ***************************************************************
C
C     DETERMINES THE HARDEST MATERIAL AND THEN USES
C     ITS HARDNESS IN THE PLASTIC DEFORMATION THEORY
C
C ***************************************************************
C
      PM=PMC
      IF(PMC.GT.PMB) PM=PMB
      AP=SQRT(WT/(3.14159*PM))
      AP2=WT/PM
      AE2=3.14159*AE*AE
      WRITE(6,90) AE2,AP2
90    FORMAT(1X,'ELASTIC AREA OF CONTACT =',1PE12.4,' M**2'//1X,
     2          'PLASTIC AREA OF CONTACT =',1PE12.4,' M**2'/)
C
C ***************************************************************
C
C    DETERMINES THE MATERIAL WITH THE
C    LOWEST MELTING POINT. THE PROGRAM
C    WILL STOP WHEN IT CALCULATES A
C    TEMPERATURE GREATER THAN THIS MELTING
C    POINT
C
C ***************************************************************
C
      IF(TMB.GT.TMC)TM=TMC
      IF(TMC.GE.TMB)TM=TMB
C
C ***************************************************************
C
C     DIF EQUALS THE THERMAL DIFFUSIVITY
C
C ***************************************************************
C
      DIF=KC/(RHOC*CC)
      V=0.
      WRITE(6,100)
100   FORMAT(43X,'ARCHARDS THEORY',5X,'JAEGERS THEORY'/23X,
     2'PECLET NUMBER',15X,'TEMPERATURE RISE (C)'//1X,
     3'SLIDING SPEED(M/S)',3X,'ELASTIC',3X,'PLASTIC',3X,'ELASTIC',
     43X,'PLASTIC',3X,'ELASTIC',3X,'PLASTIC'/)
C
C ***************************************************************
C
C     INCREMENTS THE VELOCITY BY
C     0.1, 0.2, 1, 10, AND THEN 25 M/SEC
C
```

```
C ***********************************************************************
C
110   IF(V.GE.100..AND.V.LT.500.) V=V*25
      IF(V.GE.50..AND.V.LT.100.) V=V*10.
      IF(V.GE.10..AND.V.LT.50.) V=V*.5
      IF(V.GE.1..AND.V.LT.10.) V=V*0.05
      IF(V.GE.0..AND.V.LT.1.) V=V*0.01
C
C ***********************************************************************
C
C     CALCULATES THE PECLET NUMBER FOR THE ELASTIC
C     AND PLASTIC AREA OF CONTACT.
C
C           LE=PECLET NUMBER USING ELASTIC DEFORMATION
C           LP=PECLET NUMBER USING PLASTIC DEFORMATION
C
C ***********************************************************************
C
170   LE=V*AE/(2.*DIF)
      LP=V*AP/(2.*DIF)
C
C ***********************************************************************
C
C     CALCULATES THE HEAT INPUT TO THE SYSTEM
C
C          Q=HEAT INPUT
C
C ***********************************************************************
C
      Q=MU*WT*V
C
C ***********************************************************************
C
C    DETERMINES WHICH OF THE THREE EQUATIONS
C    SHOULD BE USED BASED ON THE SPEED CRITERION
C    OR THE PECLET NUMBER.
C
C ***********************************************************************
C
180   IFLAG=1
      IF (LP.LT..1) GO TO 220
      IF (LP.GT.5.) GO TO 250
      IF (LP.GE..1.AND.LP.LE.5.) GO TO 280
190   IFLAG=2
      IF (LE.LT..1) GO TO 220
      IF (LE.GT.5.) GO TO 250
      IF (LE.GE..1.AND.LE.LE.5.) GO TO 280
200   WRITE(6,210) V,LE,LP,TME,TMP,JE,JP
210   FORMAT(6X,F7.3,7X,F8.4,3X,F7.4,4(4X,F6.1))
      K=K*1
      X(K)=V
      Y1(K)=JP
      Y2(K)=TMP
      GO TO 110
C
```

```
C ***************************************************************
C
C     CALCULATES THE SURFACE TEMPERATURE WHEN
C     L IS LESS THAN 0.1 USING THE SLOW SPEED
C     EQUATIONS
C
C ***************************************************************
C
220   IF(IFLAG.EQ.1) RAD=AP
      IF(IFLAG.EQ.2) RAD=AE
C
C ***************************************************************
C
C      TAVG IS THE MEAN TEMPERATURE ACROSS
C        THE HEAT SOURCE USING ARCHARD'S EQUATION
C      JAVG IS THE MEAN TEMPERATURE USING
C        JAEGER'S THEORY
C
C ***************************************************************
C
      TAVG=(1./(KB*KC))*Q/(4*RAD)
      JAVG=0.946*Q/(4*RAD*(KB*KC))
      IF (IFLAG.NE.1) GO TO 230
      TMP=TAVG
      JP=JAVG
      GO TO 190
230   IF (IFLAG.NE.2) GO TO 280
      TME=TAVG
      JE=JAVG
240   IF (JP.GE.TM) GO TO 310
      GO TO 200
C
C ***************************************************************
C
C     CALCULATES THE SURFACE TEMPERATURE
C     WHEN L IS GREATER THAN 5 USING THE
C     HIGH SPEED ARCHARD EQUATION
C
C ***************************************************************
250   IF (IFLAG.EQ.1) RAD=AP
      IF (IFLAG.EQ.2) RAD=AE
      TAVG=.31*Q*SQRT(DIF/(V*RAD))/(KC*RAD)
C
C ***************************************************************
C
C      NUM IS THE NUMERATOR AND DEN IS
C      THE DENOMINATOR OF THE JAEGER
C      EQUATIONS.
C
C ***************************************************************
C
      NUM=1.064*(Q/(3.1417*RAD))*(DIF**0.5)
      DEN=(1.125*KB*DIF**0.5)*(KC*(RAD*V)**0.5)
      JAVG=NUM/DEN
      IF (IFLAG.NE.1) GO TO 260
```

```
      TMP=TAVG
      JP=JAVG
      GO TO 190
260   IF (IFLAG.NE.2) GO TO 270
      TME=TAVG
      JE=JAVG
270   IF (JP.GE.TM) GO TO 310
      GO TO 200
C ***************************************************************************
C
C     CALCULATES THE SURFACE TEMPERATURE
C     WHEN L IS BETWEEN 0.1 AND 5, USING
C     THE INTERMEDIATE SPEED-ARCHARD EQUATION
C     WITH ALPHA DERIVED FROM FIGURE 7 OF
C     JAEGER'S PAPER
C
C ***************************************************************************
C
280   IF (IFLAG.EQ.1) L=LP
      IF (IFLAG.EQ.2) L=LE
C
C   THESE NEXT FIVE EQUATIONS REPRESENT
C   THE CURVE OF FIGURE 7 OF JAEGER'S
C   PAPER BY APPROXIMATING THE CURVE
C   AS 5 DIFFERENT STRAIGHT LINE SEGMENTS
C
      IF (L.GE.0.1.AND.L.LE..5) Y=2.25*L-0.025
      IF (L.GT.0.5.AND.L.LE.1.0) Y=1.50*L+0.35
      IF (L.GT.1.0.AND.L.LE.2.0) Y=1.05*L+0.80
      IF (L.GT.2.0.AND.L.LE.3.0) Y=0.80*L+1.30
      IF (L.GT.3.0.AND.L.LE.5.0) Y=0.60*L+1.90
      ALPHA=(4*Y)/(3.14159**2*L)
      IF (IFLAG.EQ.1) RAD=AP
      IF (IFLAG.EQ.2) RAD=AE
      NB=Q/(RAD**2*RHOB*CB*V)
      NC=Q/(RAD**2*RHOC*CC*V)
C
C   TEMPB IS CALCULATED USING THE ARCHARD STATIONARY
C   HEAT SOURCE EQUATION
C
      TEMPB=0.5*NB*L
C
C   TEMPC IS CALCULATED USING THE ARCHARD INTERMEDIATE
C   SPEED EQUATION
C
      TEMPC=0.5*ALPHA*NC*L
C
C   THE AVERAGE TEMPERATURE ACROSS THE
C   HEAT SOURCE IS FOUND BY
C     1/TAVG=(1/TEMPB)+(1/TEMPC)
C
      TAVG=1/((1/TEMPB)+(1/TEMPC))
      NUM=0.946*DIF*Y*Q/(3.1417*RAD)
      DEN=(1.486*RAD*KC*V)+(DIF*KB*Y)
      JAVG=NUM/DEN
```

```
      IF (IFLAG.NE.1) GO TO 290
      TMP=TAVG
      JP=JAVG
      GO TO 190
290   IF (IFLAG.NE.2) GO TO 300
      TME=TAVG
      JE=JAVG
300   IF (JP.GE.TM) GO TO 310
      GO TO 200
310   X(1)=K-1
      Y1(1)=K-1
      Y2(1)=K-1
      CALL INITT(120)
      CALL BINITT
      CALL XTYPE(1)
      CALL YTYPE(1)
      CALL XFRM(2)
      CALL YFRM(2)
      CALL LINE(3)
      CALL CHECK(X,Y2)
      CALL DSPLAY(X,Y2)
      CALL LINE(0)
      CALL CPLOT(X,Y1)
      CALL FRAME
      CALL LABLE3(35,265,1.25,90.,29,'Mean Temperature Rise, deg. C')
      CALL LABLE3(375,50,1.25,0.,23,'Sliding Velocity, m/sec')
      CALL LABLE3(175,550,1.25,0.,6,'Load =')
      CALL LABLE3(175,525,1.25,0.,16,'Friction Coef. =')
      CALL RLOUT(235,550,WT,6,3)
      CALL RLOUT(375,525,MU,4,3)
      CALL LABLE3(350,550,1.25,0.,7,'Newtons')
      CALL LABLE3(400,650,1.0,0.,12,BNAME)
      CALL LABLE3(460,625,1.0,0,4,'-ON-')
      CALL LABLE3(400,600,1.0,0.,12,CNAME)
      CALL MOVABS(550,200)
      CALL DSHABS(650,200,3)
      CALL LABLE3(650,200,1.25,0.,16,'  Archard Theory')
      CALL MOVABS(550,150)
      CALL DRWABS(650,150)
      CALL LABLE3(650,150,1.25,0.,15,'  Jaeger Theory')
      CALL MOVABS(0,780)
      CALL ANMODE
      WRITE(3,320)
320   FORMAT(10X,'DO YOU WISH TO GET A HARDCOPY OF THIS PLOT?',
     *,10X,'TYPE 1 TO GET A HARDCOPY OR 2 FOR NO HARDCOPY.')
      IHARD = IVET(1,2,IE)
      IF(IHARD .EQ. 2) GO TO 330
      CALL PLSAVE
      CALL ERASE
330   CONTINUE
340   IF (WT.NE.0.0) GO TO 60
      WRITE(6,350)
350   FORMAT(1H1)
      CALL FINITT(0,700)
      STOP
```

APPENDIX F.5

COMPUTER PROGRAM:

Calculation of Reference Voltage Output
of a specimen at room temperature.

```
      REAL IR,NS,NO
C
C ********************************************************************
C ********************************************************************
C
C           ***CALCULATION OF REFERENCE
C            VOLTAGE OUTPUT OF A SPECIMEN
C              AT ROOM TEMPERATURE***
C
C ********************************************************************
C
C   THIS PROGRAM CALCULATES THE REFERENCE VOLTAGE
C   FORM THE INFRARED MICROSCOPE OF A SPECIMEN
C   AT ROOM TEMPERATURE. THIS VALUE ALLOWS ONE
C   TO REFERENCE ALL OTHER RADIANCE OUTPUT FROM
C   THE MICROSCOPE WITHOUT THE NEED OF TRYING
C   TO ZERO THE MICROSCOPE BY SOME EXTERNAL MEANS.
C   THE EQUATIONS USED IN THIS PROGRAM ARE IDENTICAL
C   TO THOSE USED IN THE CONVERSION OF INFRARED
C   MICROSCOPE'S VOLTAGE OUTPUT TO BLACKBODY RADIANCE
C   EMITTED FROM THE SPECIMEN AND ITS TEMPERATURE.
C   DESCRIPTION OF THE FOLLOWING EQUATIONS AND THE
C   ATTENUATION FACTORS USED IN THIS PROGRAM MAY BE
C   FOUND IN CHAPTER 3 OF CRAIG A. ROGERS' MASTERS
C   THESIS (NOVEMBER 1982).
C
C ********************************************************************
C
      DIMENSION EMISS(200),ZERO(200)
C
C ********************************************************************
C
C   READS THE POWER OF THE MICROSCOPE'S OBJECTIVE
C   FROM THE FIRST DATA CARD WHERE
C      OBJ = MICROSCOPE'S OBJECTIVE (15X OR 36X)
C
C ********************************************************************
C
      READ(5,5) OBJ
5     FORMAT(F3.0)
C
C ********************************************************************
C
C  READS THE DATA FROM THE SECOND DATA CARD
C  WHERE:
C        GAIN = EXTERNAL AMPLIFIER GAIN
C        AMB = EFFECTIVE BLACKBODY RADIANCE OF
C                ROOM TEMPERATURE (FROM CHART IN
C                BARNES OPERATING MANUAL)
C
C ********************************************************************
```

```
      READ(5,10) GAIN,AMB
10    FORMAT(F6.1,F9.7)
      WRITE(6,20)
      WRITE(6,30)
      WRITE(6,40)
      WRITE(6,20)
      WRITE(6,50)GAIN, AMB
      WRITE(6,55)OBJ
      WRITE(6,60)
      WRITE(6,70)
20    FORMAT('**************************************************')
30    FORMAT(10X,'CALCULATION OF REFERENCE VOLTAGE OF')
40    FORMAT(12X,'THE SPECIMEN AT ROOM TEMPERATURE'/)
50    FORMAT(1X,'AMPLIFIER GAIN =',F4.1,3X,'AMBIENT RADIATION =',F8.6/)
55    FORMAT(12X,'MICROSCOPE OBJECTIVE =',F4.0,'X'//)
60    FORMAT(10X,'EMISSIVITY',20X,'VOLTAGE')
70    FORMAT('-----------------------------------------')
C
C ***************************************************************
C
C   THE FOLLOWING IS THE BEGINING OF THE CALCULATION
C   LOOP WHERE THE REFERNCE VOLTAGE IS CALCULATED
C   FOR A NUMBEFR OF EMISSIVITIES RANGING FROM 0.0 TO
C   1.0 BY INCREMENTS OF 0.05.
C
C         EMIS = EMISSIVITY
C         J = COUNTER USED IN THE PLOT SUBROUTINE
C         EMISS = MATRIX WITH THE STORED EMIS VALUES
C
C ***************************************************************
C
      EMIS=-0.05
      J=1
80    EMIS=EMIS+0.05
      IF(EMIS.GT.1.0) GO TO 100
      J=J+1
      EMISS(J)=EMIS
C
C ***************************************************************
C
C   THIS EXPRESSION EVALUATES THE SURFACE
C   REFLECTIVITY OF THE SPECIMEN AS
C   (1-EMISSIVITY) WHERE:
C         SURF = SURFACE REFLECTIVITY
C
C ***************************************************************
C
      SURF=1.0-EMISS(J)
C
C ***************************************************************
C
C   IR = INDEX OF REDRACTION OF THE SAPPHIRE
C        DISK
C
```

```
C ***************************************************************
C
      IR=1.65
C
C ***************************************************************
C
C  THE NEXT EXPRESSION CALCULATES THE
C  FRESNEL REFLECTION COEFFICIENT FROM
C  THE INDEX OF REFRACTION GIVEN ABOVE.
C
C ***************************************************************
C
      FRES=(IR-1.0)**2/((IR+1.0)**2)
C
C ***************************************************************
C
C   THE NEXT SECTION CALCULATES THE INTERNAL
C   TRANSMISSIVITY BASED ON THE DECLARED INDEX
C   OF REFRACTION AND THE EXPERIMENTALLY DETERMINED
C   EXTRERNAL TRANSMITTANCE WHERE:
C        EXTER = EXTERNAL TRANSMITTANCE
C        TRANS = INTERNAL TRANSMISSIVITY
C
C ***************************************************************
C
      EXTER=0.8539
      TRANS=EXTER/((1-FRES)/(1+FRES))
C
C ***************************************************************
C
C   THE NEXT SECTION CALCULATES THE FRACTION
C   OF THE SPECIMEN AND AMBIENT RADIATION THAT
C   IMPINGES UPON THE INFRARED DETECTOR;I.E.
C        REFLS1 = FRACTION OF SPECIMEN RADIATION DUE
C                 TO REFLECTION NUMBER 1
C        REFLA3 = FRACTION OF AMBIENT RADIATION DUE
C                 TO REFLECTION NUMBER 3
C
C ***************************************************************
C
      REFLS1=(1-FRES)*TRANS
      REFLS2=(1-FRES)*SURF*FRES*(TRANS**3)
      REFLA1=FRES
      REFLA2=(1-FRES)**2*SURF*(TRANS**2)
      REFLA3=(1-FRES)**2*(SURF**2)*FRES*(TRANS**4)
C
C ***************************************************************
C
C   THE ATTENUATION FACTORS ARE THE SUM OF
C   THE APPROPRIATE REFLECTION FRACTIONS WHERE
C        NO = AMBIENT ATTENUATION FACTOR
C        NS = SPECIMEN ATTENUATION FACTOR
C
C ***************************************************************
C
```

```
      NS=REFLS1*REFLS2
      NO=REFLA1*REFLA2*REFLA3
C
C ***************************************************************************
C
C   THE NEXT TWO STATEMENTS CALCULATE THE REFERENCE
C   VOLTAGE BY FIRST CALCULATING AN ELECTRICAL
C   OUTPUT CONSTANT AND THEN USING IT IN THE FINAL
C   EQUATION TO CALCULATE THE REFERENCE VOLTAGE.
C       EK = ELECTRICAL OUTPUT CONSTANT
C       VOLT = REFERENCE VOLTAGE
C       ZERO = MATRIX WITH THE STORED VALUES OF VOLT
C              TO BE USED IN THE PLOT SUBROUTINE
C
C ***************************************************************************
C
      IF(OBJ.EQ.15.) CAL=0.171
      IF(OBJ.EQ.36.) CAL=0.312
      EK=CAL/GAIN
      VOLT=AMB*((EMISS(J)*NS)*NO-1.0)/EK
      ZERO(J)=VOLT
      WRITE(6,90)EMISS(J),VOLT
90    FORMAT(12X,F5.3,23X,F6.4)
      GO TO 80
100   CONTINUE
       CALL REF(J,ZERO,EMISS,GAIN)
      STOP
      END
C
C
C
      SUBROUTINE REF(J,ZERO,EMISS,GAIN)
      DIMENSION ZERO(200),EMISS(200)
      CALL INITT(120)
      CALL BINITT
      JP1=J-1
      EMISS(1)=JP1
      ZERO(1)=JP1
      CALL XFRM(2)
      CALL YFRM(2)
      CALL CHECK(EMISS,ZERO)
      CALL DSPLAY(EMISS,ZERO)
      CALL LABLE3(35,300,1.25,90.,14,'Voltage Output')
      CALL LABLE3(375,50,1.25,0.,19,'Specimen Emissivity')
      CALL LABLE3(200,650,1.25,0.,6,'Gain =')
      CALL RLOUT(265,650,GAIN,5,1)
      CALL KBWAIT
      CALL PLSAVE
      CALL FINITT(0,700)
      RETURN
      END
```

APPENDIX G

REFERENCE VOLTAGE GRAPHS

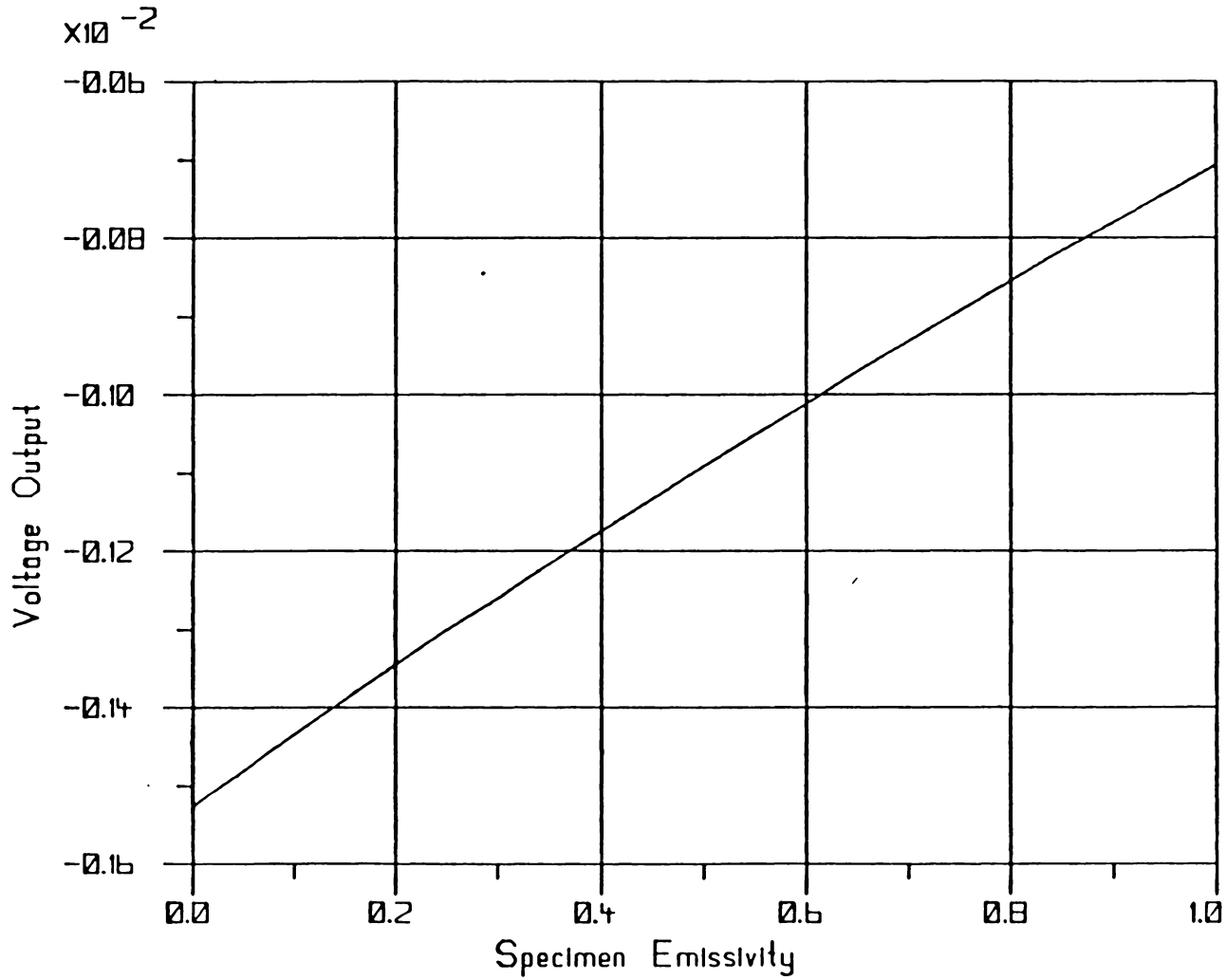

Figure G-1. Zero Reference Voltage, 15 x Objective, Gain = 1

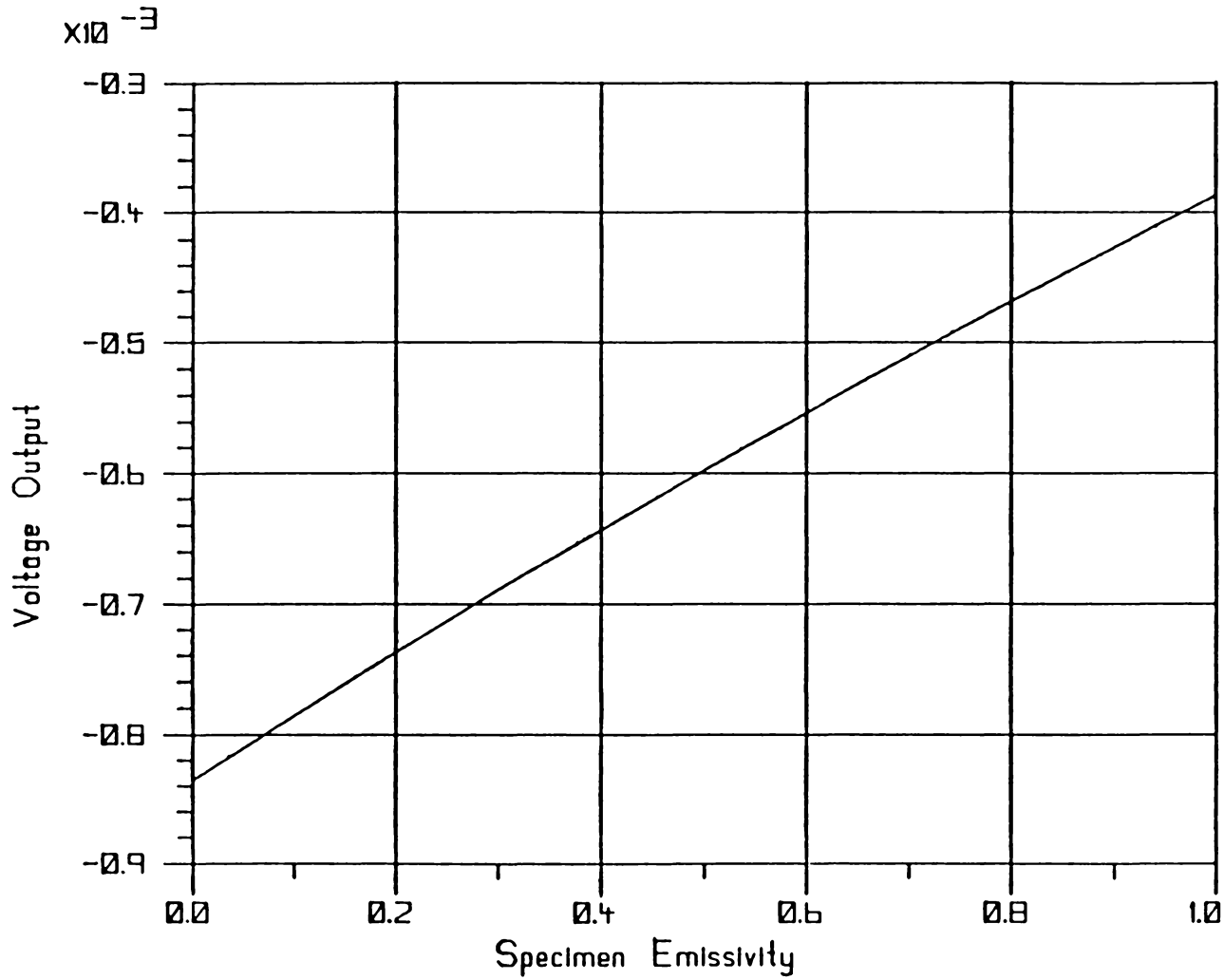

Figure G-2. Zero Reference Voltage, 36 x Objective, Gain = 1

APPENDIX H

NUMERICAL DATA

TABLE H-1

EXPERIMENTAL TEMPERATURE RISE AND HEAT INPUT

Test No.	1-22-1	1-22-2	1-23-1	1-23-2	1-24-1	1-24-2
Sliding Velocity (m/sec)	2.0	2.0	2.0	2.0	2.0	2.0
Load (N)	2.0	2.0	3.0	3.0	4.0	4.0
Friction Coeff						
1 min.	0.124	0.166	0.133	0.143	0.131	0.141
2 min.	0.110	0.152	0.143	0.152	0.145	0.145
3 min.	0.110	0.159	0.153	0.156	0.145	0.145
4 min.	0.110	0.159	0.156	0.152	0.145	0.145
5 min.	0.104	0.166	0.152	0.161	0.148	0.145
Avg.	0.112	0.160	0.147	0.153	0.143	0.144
Temperature Rise (°C)						
1 min.	36	50	48	48	52	62
2 min.	44	41	51	52	54	53
3 min.	37	43	50	52	55	49
4 min.	34	43	50	58	55	48
5 min.	32	43	52	54	55	48
Avg.	37	44	50	52	54	52
Normalized Temp. Rise						
1 min.	290	301	361	336	397	440
2 min.	400	263	357	342	372	368
3 min.	336	270	327	333	379	338
4 min.	309	270	321	382	379	338
5 min.	356	259	342	335	372	331
Avg.	338	275	340	340	378	361
Avg Heat Input ($N\text{-}^{m}/s$)	0.448	0.640	0.882	0.918	1.144	1.152

TABLE H-1 (Continued)

Test No.	1-26-1	1-26-2	1-42-1	1-42-2	1-43-1	1-43-2
Sliding Velocity (m/sec)	2.0	2.0	4.0	4.0	4.0	4.0
Load (N)	6.0	6.0	2.0	2.0	3.0	3.0
Friction Coeff						
1 min.	0.133	0.097	0.097	0.090	0.124	0.129
2 min.	0.127	0.099	0.093	0.086	0.117	0.120
3 min.	0.124	0.104	0.093	0.090	0.124	0.127
4 min.	0.129	0.106	0.090	0.093	0.124	0.133
5 min.	0.131	0.108	0.097	0.107	0.124	0.133
Avg.	0.129	0.103	0.094	0.093	0.123	0.128
Temperature Rise (°C)						
1 min.	60	32	32	35	47	39
2 min.	57	39	43	41	50	47
3 min.	57	45	47	46	57	45
4 min.	59	50	50	44	59	54
5 min.	58	57	52	46	58	50
Avg.	58	44	45	42	54	47
Normalized Temp. Rise						
1 min.	451	330	330	389	379	302
2 min.	449	394	462	477	427	392
3 min.	460	433	505	511	460	354
4 min.	457	472	556	473	476	406
5 min.	443	528	536	430	468	376
Avg.	450	427	479	452	439	367
Avg. Heat Input ($N\text{-}^{m}/s$)	1.548	1.236	0.752	0.744	0.476	0.536

TABLE H-1 (Continued)

Test No.	1-44-1	1-44-2	1-46-1	1-46-2
Sliding Velocity (m/sec)	4.0	4.0	4.0	4.0
Load (N)	4.0	4.0	6.0	6.0
Friction Coeff				
1 min.	0.124	0.124	0.124	0.117
2 min.	0.121	0.124	0.120	0.122
3 min.	0.117	0.128	0.115	0.120
4 min.	0.117	0.128	0.110	0.120
5 min.	0.117	0.131	0.110	0.115
Avg.	0.119	0.127	0.116	0.119
Temperature Rise (°C)				
1 min.	70	70	87	96
2 min.	75	72	86	100
3 min.	77	77	100	99
4 min.	77	77	102	102
5 min.	82	79	102	102
Avg.	76	75	95	100
Normalized Temp Rise				
1 min.	565	565	702	821
2 min.	620	581	717	820
3 min.	658	602	870	825
4 min.	658	602	927	850
5 min.	701	603	927	887
Avg.	639	591	819	840
Avg. Heat Input ($N\text{-}^{m}/s$)	1.904	2.032	2.784	2.856

TABLE H-1 (Continued)

Test No.	1-82-1	1-82-2	1-82-3	1-83-1	1-83-2	1-83-3
Sliding Velocity (m/sec)	8.0	8.0	8.0	8.0	8.0	8.0
Load (N)	2.0	2.0	2.0	3.0	3.0	3.0
Friction Coeff						
1 min.	0.124	0.101	0.114	0.106	0.106	0.106
2 min.	0.117	0.106	0.114	0.101	0.092	0.106
3 min.	0.110	0.110	0.110	0.092	0.092	0.124
4 min.	0.117	0.110	0.110	0.097	0.092	0.129
5 min.	0.117	0.117	0.114	0.097	0.092	0.129
Avg.	0.117	0.109	0.112	0.099	0.095	0.119
Temperature Rise (°C)						
1 min.	68	62	65	90	89	89
2 min.	75	69	70	87	88	95
3 min.	70	76	77	83	89	97
4 min.	69	75	77	80	90	105
5 min.	74	93	77	85	92	104
Avg.	71	75	73	85	88	98
Normalized Temp. Rise						
1 min.	548	614	570	849	840	840
2 min.	641	651	614	861	957	896
3 min.	636	691	700	902	967	782
4 min.	590	682	700	825	978	814
5 min.	632	795	675	876	1000	806
Avg.	607	688	652	859	926	824
Avg. Heat Input ($N\text{-}^{m}/s$)	1.872	1.744	1.792	2.376	2.280	2.856

TABLE H-1 (Continued)

Test No.	1-84-1	1-84-2	1-84-3	1-86-1	1-86-2	1-86-3
Sliding Velocity (m/sec)	8.0	8.0	8.0	8.0	8.0	8.0
Load (N)	4.0	4.0	4.0	6.0	6.0	6.0
Friction Coeff						
1 min.	0.117	0.114	0.124	0.106	0.110	0.115
2 min.	0.110	0.114	0.124	0.106	0.110	0.110
3 min.	0.090	0.114	0.135	0.106	0.110	0.110
4 min.	0.083	0.114	0.131	0.106	0.104	0.108
5 min.	0.072	0.114	0.128	0.106	0.104	0.104
Avg.	0.094	0.114	0.128	0.106	0.108	0.109
Temperature Rise (°C)						
1 min.	100	105	85	130	142	119
2 min.	102	104	90	129	134	130
3 min.	103	100	120	124	130	136
4 min.	96	100	124	120	141	139
5 min.	89	96	122	125	142	129
Avg.	98	101	108	126	139	131
Normalized Temp. Rise						
1 min.	855	921	685	1226	1291	1035
2 min.	927	912	726	1217	1264	1182
3 min.	1144	877	889	1170	1182	1236
4 min.	1157	877	947	1132	1356	1287
5 min.	1236	842	953	1179	1365	1240
Avg.	1043	886	844	1189	1287	1202
Avg. Heat Input ($N\text{-}^{m}/s$)	3.008	3.648	4.096	5.088	5.184	5.232

TABLE H-1 (Continued)

Test No.	2-22-1	2-22-1	2-23-1	2-23-2	2-24-1	2-24-2
Sliding Velocity (m/sec)	2.0	2.0	2.0	2.0	2.0	2.0
Load (N)	2.0	2.0	3.0	3.0	4.0	4.0
No. of Contacts	2	2	2	2	2	2
Friction Coeff						
2 min.	0.122	0.105	0.107	0.118	0.110	0.108
4 min.	0.118	0.105	0.112	0.122	0.117	0.110
Temperature Rise (°C)						
Contact 1	19	20	20	26	36	34
Contact 2	21	18	20	27	25	34
Avg.	20	19	20	26	30	34
Normalized Temp. Rise (°C)						
Contact 1	156	190	187	220	327	315
Contact 2	178	171	179	221	214	309
Avg.	167	181	183	220	271	312
Avg. Heat Input ($N\text{-}^{m}/s$)	0.400	0.420	0.657	0.720	0.908	0.872

TABLE H-1 (Continued)

Test No.	2-44-1	2-44-2	2-46-1	2-46-2	2-82-1	2-82-2
Sliding Velocity (m/sec)	4.0	4.0	4.0	4.0	8.0	8.0
Load (N)	4.0	4.0	6.0	6.0	2.0	2.0
No. of Contacts	2	2	2	2	2	2
Friction Coeff						
2 min.	0.108	0.114	0.119	0.128	0.103	0.099
4 min.	0.115	0.114	0.119	0.124	0.103	0.099
Temperature Rise (°C)						
Contact 1	65	57	85	82	48	40
Contact 2	60	63	79	88	40	40
Avg.	62	60	82	85	44	40
Normalized Temp. Rise (°C)						
Contact 1	602	500	714	641	466	404
Contact 2	522	553	664	710	388	404
Avg.	562	527	689	676	427	404
Avg. Heat Input ($N\text{-}^{m}/s$)	1.784	1.824	2.856	3.024	1.648	1.584

TABLE H-1 (Continued)

Test No.	2-26-1	2-26-2	2-42-1	2-42-2	2-43-1	2-43-2
Sliding Velocity (m/sec)	2.0	2.0	4.0	4.0	4.0	4.0
Load (N)	6.0	6.0	2.0	2.0	3.0	3.0
No. of Contacts	2	2	2	2	2	2
Friction Coeff						
2 min.	0.120	0.114	0.115	0.115	0.123	0.116
4 min.	0.126	0.119	0.115	0.115	0.120	0.116
Temperature Rise (°C)						
Contact 1	38	41	36	32	42	49
Contact 2	37	41	33	31	54	57
Avg.	38	41	34	32	48	53
Normalized Temp. Rise (°C)						
Contact 1	317	360	313	278	341	422
Contact 2	294	345	287	270	450	491
Avg.	306	353	300	274	396	457
Avg. Heat Input ($N\text{-}^{m}/s$)	1.476	1.392	0.920	0.920	1.464	1.392

TABLE H-1 (Continued)

Test No.	2-83-1	2-83-2	2-84-1	2-84-2	2-86-1	2-86-2
Sliding Velocity (m/sec)	8.0	8.0	8.0	8.0	8.0	8.0
Load (N)	3.0	3.0	4.0	4.0	6.0	6.0
No. of Contacts	2	2	2	2	2	2
Friction Coeff						
2 min.	0.110	0.104	0.106	0.108	0.118	0.109
4 min.	0.110	0.104	0.106	0.108	0.118	0.109
Temperature Rise (°C)						
Contact 1	73	89	90	96	117	120
Contact 2	79	82	95	96	125	125
Avg.	76	86	93	96	121	123
Normalized Temp. Rise (°C)						
Contact 1	664	856	849	889	992	1101
Contact 2	718	788	896	899	1059	1147
Avg.	691	822	873	889	1026	1124
Avg. Heat Input ($N-^{m}/s$)	2.640	2.496	3.392	3.456	3.776	5.232

TABLE H-1 (Continued)

Test No.	4-42-1	4-42-2	4-43-1	4-43-2
Sliding Velocity (m/sec)	4.0	4.0	4.0	4.0
Load (N)	2.0	2.0	3.0	3.0
No. of Contacts	4	4	4	4
Friction Coeff	.112	.115	.110	.117
Temperature Rise (°C)				
Contact 1	37	35	42	38
Contact 2	35	35	42	32
Contact 3	35	32	40	40
Contact 4	35	37	40	36
Avg.	36	35	41	37
Normalized Temp. Rise (°C)				
Contact 1	286	304	382	325
Contact 2	313	304	382	274
Contact 3	313	278	364	342
Contact 4	313	322	364	308
Avg.	306	302	373	337
Avg. Heat Input ($N\text{-}^{m}/s$)	0.896	0.920	1.320	1.404

TABLE H-1 (Continued)

Test No.	4-44-1	4-44-2	4-46-1	4-46-2
Sliding Velocity (m/sec)	4.0	4.0	4.0	4.0
Load (N)	4.0	4.0	6.0	6.0
No. of Contacts	4	4	4	4
Friction Coeff	.103	.117	.105	.125
Temperature Rise (°C)				
Contact 1	57	50	77	75
Contact 2	53	50	77	75
Contact 3	54	50	67	80
Contact 4	53	50	77	75
Avg.	54	50	75	76
Normalized Temp. Rise (°C)				
Contact 1	553	427	733	600
Contact 2	515	427	733	600
Contact 3	524	427	738	640
Contact 4	515	427	733	600
Avg.	527	427	709	610
Avg. Heat Input ($N\text{-}^{m}/s$)	1.648	1.872	2.520	3.000

TABLE H-2

TORQUE DATA

Test No.	Torque Output (mV)					Friction Coefficient					
	1 min	2 min	3 min	4 min	5 min	1 min	2 min	3 min	4 min	5 min	Avg.
1-22-1	.24	.22	.22	.22	.21	.124	.110	.110	.110	.104	.112
1-22-2	.30	.28	.29	.29	.30	.166	.152	.159	.159	.166	.160
1-23-1	.35	.37	.40	.40	.39	.133	.143	.153	.156	.152	.147
1-23-2	.37	.39	.40	.39	.41	.143	.152	.156	.152	.161	.153
1-24-1	.44	.48	.48	.48	.49	.131	.145	.145	.145	.148	.143
1-24-2	.47	.48	.48	.48	.48	.141	.145	.145	.145	.145	.144
1-26-1	.64	.61	.60	.62	.63	.133	.127	.124	.129	.131	.129
1-26-2	.48	.49	.51	.52	.53	.097	.099	.104	.105	.108	.103
1-42-1	.34	.33	.33	.32	.34	.097	.093	.093	.090	.097	.094
1-42-2	.32	.31	.32	.33	.37	.090	.086	.090	.093	.107	.123
1-43-1	.60	.57	.60	.60	.60	.124	.117	.124	.124	.124	.123
1-43-2	.62	.58	.61	.64	.64	.129	.120	.127	.133	.133	.128
1-44-1	.78	.76	.74	.74	.74	.124	.121	.117	.117	.117	.119
1-44-2	.78	.81	.80	.80	.82	.124	.124	.128	.128	.131	.127
1-46-1	1.14	1.10	1.06	1.02	1.02	.124	.120	.115	.110	.110	.116
1-46-2	1.08	1.12	1.10	1.10	1.06	.117	.122	.120	.120	.115	.119
1-82-1	.37	.35	.33	.35	.35	.124	.117	.110	.117	.117	.117
1-82-2	.31	.32	.33	.33	.34	.101	.106	.110	.110	.117	.119
1-82-3	.34	.34	.33	.33	.34	.114	.114	.110	.110	.114	.112
1-83-1	.40	.39	.37	.38	.38	.106	.101	.092	.097	.097	.099
1-83-2	.40	.37	.37	.37	.37	.106	.092	.092	.092	.092	.095
1-83-3	.40	.40	.44	.45	.45	.106	.106	.124	.129	.129	.119
1-84-1	.51	.49	.43	.41	.38	.117	.110	.090	.083	.072	.094
1-84-2	.50	.50	.50	.50	.50	.114	.114	.114	.114	.114	.144
1-84-3	.53	.53	.56	.55	.54	.124	.124	.135	.131	.128	.128
1-86-1	.63	.63	.63	.63	.63	.106	.106	.106	.106	.106	.106
1-86-2	.65	.65	.65	.62	.62	.110	.110	.110	.104	.104	.108
1-86-3	.67	.65	.65	.64	.62	.115	.110	.110	.108	.104	.109

The vita has been removed from the scanned document